



Environmental Effects Monitoring Program

Quarterly Report: January-March 2020

March 31, 2020

Fundy Ocean Research Center for Energy
PO Box 2573, Halifax, Nova Scotia, B3J 3N5
902-406-1166
fundyforce.ca

Executive Summary

Tidal stream energy devices are an emerging renewable energy technology that use the ebb and flow of the tides to generate electricity. These devices are in various stages of research, development, operation and testing in countries around the world.

FORCE was established in 2009 after undergoing a joint federal-provincial environmental assessment with the mandate to enable the testing and demonstration of tidal stream devices. Since that time, more than 100 related research studies have been completed or are underway with funding from FORCE, the Offshore Energy Research Association of Nova Scotia (OERA), and others. These studies have considered physical, biological, socioeconomic and other research areas.

The latest monitoring programs at the FORCE site were initiated in 2016 in anticipation of turbine deployments by one of FORCE's berth holders, Cape Sharp Tidal Venture (CSTV) in 2016. These efforts are divided into two components: mid-field monitoring activities led by FORCE (>100 metres from a turbine), and near-field or 'turbine-specific' monitoring led by project developers (≤100 metres from a turbine) at the FORCE site. All plans are reviewed by FORCE's independent Environmental Monitoring Advisory Committee (EMAC) and federal and provincial regulators prior to implementation.

Mid-field monitoring at the FORCE site presently consists of monitoring for fish, marine mammals, seabirds, lobster, and marine sound. Since the start of this latest monitoring effort in 2016, FORCE has completed:

- ~408 hours of hydroacoustic fish surveys;
- more than 4,385 'C-POD' marine mammal monitoring days;
- bi-weekly shoreline observations;
- 49 observational seabird surveys;
- four drifting marine sound surveys and additional sound monitoring; and
- 11 days of lobster surveys

Sea Mammal Research Unit (SMRU) Consulting Ltd. provided their 3rd year report of harbour porpoise monitoring at the FORCE test site using C-PODs. The report describes the results of C-POD deployments #7-10 (May 2018 – August 2019), and places the results in the broader context of the overall marine mammal monitoring program implemented as part of FORCE's multiyear Environmental Effects Monitoring Program (EEMP). This ongoing monitoring program continues to show the prevalence of harbour porpoise at FORCE, with the species being detected on 98.8% of the 1,626 calendar days since monitoring with C-PODs commenced in 2011. Harbour porpoise detections at FORCE varies seasonally, with peak activity occurring during May – August, and lowest detections during December – March. Harbour porpoise detections also vary spatially, with C-PODs deployed at locations W2 and S2 recording the greatest detection rates, and D1 values typically low. Mean lost time across C-PODs, due to ambient flow noise saturating the detection buffer on the C-POD, averaged 22.6%. Interestingly, an analysis against past datasets that controlled for time of year, indicated that the effects of a non-operational turbine structure (see below) had no detectable effect on the rate of harbour porpoise detection. The report by SMRU is included here as Appendix I.

FORCE commissioned Envirosphere Consultants Ltd. and Dr. Phil Taylor (Acadia University) to synthesize the results of its observational seabird surveys at the FORCE test site, and to evaluate advanced statistical techniques for analysing seabird count data in relation to environmental predictor variables. The data were examined using Generalized Additive Models (GAMs) to characterize seabird abundance and to better understand the potential impacts of tidal turbines on seabirds at the FORCE test site. The results of the analysis revealed that overall model fit is suitable to characterize count data for some species, and that there are clear patterns of effects of time of year, wind speed and direction, tide height and time of day on the number of seabirds observed. This work contributes to the development of appropriate analytical methods for assessing the impacts of tidal power development in the Minas Passage on seabird populations and supports the continued responsible development of tidal energy at FORCE. The report by Envirosphere Consultants Ltd. is included here as Appendix II and includes the code (R script) used in the analysis of the seabird count data.

FORCE is working collaboratively with the OERA to advance 'The Pathway Program' to identify effective and regulator approved monitoring solutions for the tidal energy industry in Nova Scotia. Phase I of the program consists of a 'Global Capability Assessment' that involved comprehensive literature reviews about the use of different classes of environmental monitoring technologies for monitoring tidal energy devices around the world. While this element of Phase I was completed in 2019, ongoing international engagement and knowledge exchange is fostered through a series of workshops. To that end, a workshop focused on data automation and data management was held in Halifax on March 4, 2020, with additional workshops planned for this year. Phase II, 'Advancing Data Processing and Analysis', has commenced and work is underway with DeepSense (Dalhousie University) to automate the post-processing of hydroacoustic fish survey data. Automation of other types of monitoring data such as PAM will commence in the near future. Phase III, 'Technology Validation', has also begun and FORCE is working collaboratively with Sustainable Marine Energy Canada (SME) to assess the capabilities of different classes of environmental monitoring technologies in high flow environments.

This report provides a summary of monitoring activities and data analysis completed at the FORCE site up to the end of the first quarter of 2020. In addition, it also highlights findings from international research efforts, previous data collection periods at the FORCE site, and additional research work that is being conducted by FORCE and its partners. This includes supporting fish tagging efforts with Acadia University and the Ocean Tracking Network, radar research projects, and subsea instrumentation platform deployments through the Fundy Advanced Sensor Technology (FAST) Program. Finally, the report presents details regarding future research and monitoring efforts at the FORCE test site; notably, in response to public health directives related to COVID19, FORCE staff are working from home. Marine activities are temporarily suspended; staff focus has shifted to tackling the high volume of site data that requires processing, integration and analysis as well as ongoing physical and biological research modelling that can be completed via computer. This also shifts planned fish and marine mammal monitoring activities to a later date (TBD).

All reports, including quarterly monitoring summaries, are available online at www.fundyforce.ca/document-collection.

Contents

Acronyms.....	4
Introduction	6
International Experience & Cooperation	9
Mid-Field Monitoring Activities.....	10
Lobster	12
Fish	13
Marine Mammals.....	14
Marine Sound (Acoustics).....	16
Seabirds	16
Near-field Monitoring Activities.....	17
Other FORCE Research Activities	17
Discussion	22
References	22

Appendices

Appendix I	FORCE echolocating marine mammal EEMP 3 rd year monitoring report
Appendix II	Shore-based marine seabird surveys at FORCE: modeling of seabird abundance 2010-2018
Appendix III	Integrating hydroacoustic approaches to predict fish interactions with in-stream tidal turbines

Acronyms

AAM	Active Acoustic Monitoring
ADCP	Acoustic Doppler Current Profiler
AMAR	Autonomous Multichannel Acoustic Recorder
BACI	Before/After, Control/Impact
BC	British Columbia
BoFEP	Bay of Fundy Ecosystem Partnership
CFI	Canadian Foundation for Innovation
CLA	Crown Lease Area
cm	Centimetre(s)
CPUE	Catch Per Unit Effort
CSTV	Cape Sharp Tidal Venture
DFO	Department of Fisheries and Oceans (Canada)
DEM	Department of Energy and Mines (Nova Scotia)
EA	Environmental Assessment
EEMP	Environmental Effects Monitoring Program
EMAC	Environmental Monitoring Advisory Committee
EMP	Environmental Management Plan
FAD	Fish Aggregation Device
FAST	Fundy Advanced Sensor Technology
FAST-EMS	Fundy Advanced Sensor Technology – Environmental Monitoring System
FERN	Fundy Energy Research Network
FORCE	Fundy Ocean Research Center for Energy
GPS	Global Positioning System
hr	Hour(s)
IEA	International Energy Agency
kg	Kilogram(s)
km	Kilometer(s)
kW	Kilowatt(s)
m	Meter(s)
MET	Meteorological
MRE	Marine Renewable Energy
MREA	Marine Renewable-electricity Area
NL	Newfoundland and Labrador
NRCan	Natural Resources Canada
NS	Nova Scotia
NSDEM	Nova Scotia Department of Energy and Mines
NSE	Nova Scotia Department of Environment
NSERC	Natural Sciences and Engineering Research Council
NSPI	Nova Scotia Power Inc.
OERA	Offshore Energy Research Association of Nova Scotia
OES	Ocean Energy Systems
ONC	Ocean Networks Canada
ORJIP	Offshore Renewables Joint Industry Programme
OSC	Ocean Supercluster
OTN	Ocean Tracking Network
PAM	Passive Acoustic Monitoring
Q1/2/3	Quarter (1, 2, 3), based on a quarterly reporting schedule
R&D	Research and Development
TC114	Technical Committee 114

TISEC	Tidal In-Stream Energy Converter
SUBS	Streamlined Underwater Buoyancy System
SME	Sustainable Marine Energy (Canada)
UAV	Unmanned Aerial Vehicle
UK	United Kingdom
VEC(s)	Valuable Ecosystem Component(s)

Introduction

This report outlines monitoring activities occurring at the Fundy Ocean Research Center for Energy test site in the Minas Passage, Bay of Fundy up to the end of the first quarter of 2020. Specifically, this report highlights results of environmental monitoring activities conducted in the mid-field zone and other research and development activities conducted at the FORCE site. This report also provides a summary of international research activities around tidal stream energy devices.

About FORCE

FORCE was created in 2009 to lead research, demonstration, and testing for high flow, industrial-scale tidal stream energy devices. FORCE is a not-for-profit entity that has received funding support from the Government of Canada, the Province of Nova Scotia, Encana Corporation, and participating developers.

FORCE has two central roles in relation to the demonstration of tidal stream energy converters in the Minas Passage:

1. Host: providing the technical infrastructure to allow demonstration devices to connect to the transmission grid; and
2. Steward: research and monitoring to better understand the interaction between devices and the environment.

The FORCE project currently consists of five undersea berths for subsea turbine generators, four subsea power cables to connect the turbines to land-based infrastructure, an onshore substation and power lines connected to the Nova Scotia Power transmission system, and a Visitor Centre that is free and open to the public from May to November annually. These onshore facilities are located approximately 10 km west of Parrsboro, Nova Scotia.

The marine portion of the project is located in a 1.6 km x 1.0 km Crown Lease Area in the Minas Passage. It is also identified as a Marine Renewable-electricity Area under the Province's Marine Renewable-energy Act. This area consists of five subsea berths that are leased to tidal energy companies¹ selected by the Nova Scotia Department of Energy and Mines. Current berth holders at FORCE are:

Berth A: Minas Tidal Limited Partnership
Berth B: Sustainable Marine Energy (Canada)²
Berth C: Rio Fundo Operations Canada Limited³
Berth D: Unassigned (formerly Cape Sharp Tidal Venture)⁴
Berth E: Halagonia Tidal Energy Limited⁵

¹ Further information about each company may be found at: fundyforce.ca/partners

² On May 15, 2019 the Department of Energy and Mines issued an approval for Black Rock Tidal Power to change its name to Sustainable Marine Energy (Canada) Ltd. with the transfer of assets from SCHOTTEL to Sustainable Marine Energy. Learn more: sustainablemarine.com/news/schottel

³ On April 30, 2019 the Department of Energy and Mines approved the transfer of the Project Agreement and FIT approvals from Atlantis Operations (Canada) Ltd. to Rio Fundo Operations Canada Ltd.

⁴ On April 1, 2019 the Department of Energy and Mines revoked Cape Sharp Tidal's Marine Renewable Electricity License thereby triggering a default of the company's berth holder status at FORCE.

⁵ Berth E does not have a subsea electrical cable provided to it.

Research, monitoring, and associated reporting is central to FORCE's steward role, to assess whether tidal stream energy devices can operate in the Minas Passage without causing significant adverse effects on the environment, electricity rates, and other users of the Bay.

As part of this mandate FORCE has a role to play in supporting informed, evidence-based decisions by regulators, industry, the scientific community, and the public. As deployments of different technologies are expected to be phased in over the next several years, FORCE and regulators will have the opportunity to learn and adapt environmental monitoring approaches as lessons are learned.

Background

The FORCE demonstration project received its environmental assessment (EA) approval on September 15, 2009 from the Nova Scotia Minister of Environment. The conditions of its EA approval⁶ provide for comprehensive, ongoing, and adaptive environmental management. The EA approval has been amended since it was issued to accommodate changes in technologies and inclusion of more berths to facilitate provincial demonstration goals.

In accordance with this EA approval, FORCE has been conducting an Environmental Effects Monitoring Program to better understand the natural environment of the Minas Passage and the potential effects of turbines as related to fish, seabirds, marine mammals, lobster, marine sound, benthic habitat, and other environmental variables. All reports on site monitoring are available online at: www.fundyforce.ca/document-collection.

Since 2009, more than 100 related research studies have been completed or are underway with funding from FORCE, the Offshore Energy Research Association (OERA) and others. These studies have considered socioeconomics, biological, and other research areas.⁷

Monitoring at the FORCE site is currently focused on lobster, fish, marine mammals, seabirds, and marine sound and is divided into 'near-field' (≤ 100 m from a turbine) and 'mid-field' or 'site-level' (> 100 m from a turbine) monitoring. As approved by regulators, individual berth holders are responsible for leading near-field monitoring in direct vicinity of their turbine(s), in recognition of the unique design and operational requirements of different turbine technologies. FORCE completes 'mid-field' monitoring activities as well as supporting integration of data analysis between these monitoring zones, where applicable.

All near-field and mid-field monitoring programs are reviewed by FORCE's Environmental Monitoring Advisory Committee (EMAC), which includes representatives from scientific, First Nations, and local fishing communities.⁸ These programs are also reviewed by federal and provincial regulators prior to turbine installation. In addition, FORCE and berth holders also submit an Environmental Management Plan (EMP) to regulators for review prior to turbine installation. EMP's include: environmental management roles and responsibilities and commitments, environmental protection plans, maintenance and inspection requirements, training and education requirements, reporting protocols, and more.

⁶ FORCE's Environmental Assessment Registration Document and conditions of approval are found online at: www.fundyforce.ca/document-collection.

⁷ OERA's Tidal Energy Research Portal (<http://tidalportal.oera.ca/>) includes studies pertaining to infrastructure, marine life, seabed characteristics, socio-economics and traditional use, technology, and site characterization.

⁸ Information about EMAC may be found online at: www.fundyforce.ca/about-us

Turbine Deployments

Since FORCE's establishment in 2009, turbines have been installed at the FORCE site three times: once in 2009/2010, November 2016 – June 2017, and July 2018 – present. Given the limited timescales in which a tidal turbine has been present and operating at the FORCE site, environmental studies to-date have largely focused on the collection of baseline data and developing an understanding of the capabilities of monitoring devices in high flow tidal environments.

On July 22, 2018, CSTV installed a two-megawatt OpenHydro turbine at Berth D of the FORCE site and successfully connected the subsea cable to the turbine. CSTV confirmed establishment of communication with the turbine systems on July 24. On July 26, 2018, Naval Energies unexpectedly filed a petition with the High Court of Ireland for the liquidation of OpenHydro Group Limited and OpenHydro Technologies Limited.⁹ For safety purposes, the turbine was isolated from the power grid that same day. On September 4, 2018, work began to re-energize the turbine, but soon afterwards it was confirmed that the turbine's rotor was not turning. It is believed that an internal component failure in the generator caused sufficient damage to the rotor to prevent its operation. Environmental sensors located on the turbine and subsea base continued to function at that time with the exception of one hydrophone.

As a result of the status of the turbine, the monitoring requirements and reporting timelines set out in CSTV's environmental effects monitoring program were subsequently modified under CSTV's Authorization from Fisheries and Oceans Canada. The modification requires that CSTV provide written confirmation to regulators on a monthly basis that the turbine is not spinning by monitoring its status during the peak tidal flow of each month. This began October 1, 2018 and was expected to continue until the removal of the turbine; however, as a result of the insolvency of OpenHydro Technology Ltd., all near-field reporting activities by CSTV ceased as of March 1, 2019. Since that time, FORCE has provided monthly reports to regulators confirming the continued non-operational status of the CSTV turbine.

Additional turbines are expected to be deployed at the FORCE site in the coming years. In 2018, Sustainable Marine Energy (formerly Black Rock Tidal Power) installed a PLAT-I system in Grand Passage, Nova Scotia under a Demonstration Permit.¹⁰ This permit allows for a demonstration of the 280 kW system to help SME and its partners learn about how the device operates in the marine environment of the Bay of Fundy. Also in 2018, Natural Resources Canada announced a \$29.8 million contribution to Halagonia Tidal Energy's project at the FORCE site through its Emerging Renewable Power Program.¹¹ The project consists of submerged turbines for a total of nine megawatts – enough capacity to provide electricity to an estimated 2,500 homes.

Each berth holder project will be required to develop a turbine-specific monitoring program, which will be reviewed by FORCE's EMAC and federal and provincial regulators including Fisheries and Oceans Canada, the Nova Scotia Department of Environment, and the Nova Scotia Department of Energy and Mines prior to turbine installation.

⁹ See original news report: <https://www.irishexaminer.com/breakingnews/business/renewable-energy-firms-with-more-than-100-employees-to-be-wound-up-857995.html>.

¹⁰ To learn more about this project, see: <https://novascotia.ca/news/release/?id=20180919002>.

¹¹ To learn more about this announcement, see: <https://www.canada.ca/en/natural-resources-canada/news/2018/09/minister-sohi-announces-major-investment-in-renewable-tidal-energy-that-will-power-2500-homes-in-nova-scotia.html>.

Overall, the risks associated with single device or small array projects are anticipated to be low given the relative size/scale of devices (Copping, 2018). For example, at the FORCE site a single two-megawatt OpenHydro turbine occupies $\sim 1/1,000^{\text{th}}$ of the cross-sectional area in the Minas Passage (Figure 1). A full evaluation of the risks of tidal stream energy devices, however, will not be possible until more are tested over a longer-term period with monitoring that documents local impacts, considers far-field and cumulative effects, and adds to the growing global knowledge base.



Figure 1: The scale of a single turbine (based on the dimensions of the OpenHydro turbine deployed by CSTV, indicated by the red dot and above the blue arrow) in relation to the cross-sectional area of the Minas Passage. The Passage reaches a width of ~ 5.4 km and a depth of 130 m.

International Experience & Cooperation

The research and monitoring being conducted at the FORCE test site is part of an international effort to evaluate the risks tidal energy poses to marine life (Copping et al., 2016). Presently, countries such as China, France, Italy, the Netherlands, South Korea, the United Kingdom, and the United States (Marine Renewables Canada, 2018) are exploring tidal energy, supporting environmental monitoring and innovative R&D projects. Tidal energy and other marine renewable energy technologies such as tidal range, tidal current, wave, and ocean thermal energy offer significant opportunities to replace carbon fuel sources in a meaningful and permanent manner. Some estimates place MRE's potential as exceeding current human energy needs (Gattuso et al., 2018; Lewis et al., 2011). Recent research includes assessments of operational sounds on marine fauna (Lossent et al., 2017; Schramm et al. 2017; Polagye et al. 2018; Pine et al. 2019), the utility of PAM sensors for monitoring marine mammal interactions with turbines (Malinka et al., 2018) and collision risk (Joy et al. 2018a), and the influence of tidal turbines on fish behavior (Fraser et al. 2018).

Through connections to groups supporting tidal energy demonstration and R&D, FORCE is working to inform the global body of knowledge pertaining to environmental effects associated with tidal power projects. This includes participation in the Fundy Energy Research Network¹², the Bay of Fundy Ecosystem Partnership¹³, TC114¹⁴, and the Atlantic Canadian-based Ocean Supercluster.¹⁵

¹² FERN is a research network designed to "coordinate and foster research collaborations, capacity building and information exchange" (Source: fern.acadiau.ca/about.html). FORCE participates in the Natural Sciences, Engineering, and Socio-Economic Subcommittees of FERN.

¹³ BoFEP is a 'virtual institute' interested in the well-being of the Bay of Fundy. To learn more, see www.bofep.org.

¹⁴ TC114 is the Canadian Subcommittee created by the International Electrotechnical Commission (IEC) to prepare international standards for marine energy conversion systems. Learn more: tc114.oreg.ca.

¹⁵ The OSC was established with a mandate to "better leverage science and technology in Canada's ocean sectors and to build a digitally-powered, knowledge-based ocean economy." Learn more: www.oceansupercluster.ca.

Another key group is OES Environmental; a forum to explore the present state of environmental effects monitoring around MRE devices.¹⁶ OES Environmental is preparing to release a landmark publication later this year: ‘*The 2020 State of the Science Report: Environmental Effects of Marine Renewable Energy Development Around the World*’; an update from its 2016 State of the Science Report. FORCE played a significant role in the development of this publication; Dr. Daniel Hasselman, FORCE’s science director, lead a team of 13 international researchers to write a chapter entitled “*Environmental Monitoring Technologies and Techniques for Detecting Interactions of Marine Animals with MRE Devices*”. The objective of this chapter is to describe the state of the science in environmental monitoring technologies and techniques for MRE devices, with a focus on i) different instrument classes used for monitoring, ii) challenges of monitoring in highly dynamic marine environments, and iii) integrated monitoring platforms that are currently used for monitoring. To that end, the chapter overviews the state of the science in environmental monitoring and methodologies, provides information about lessons learned from monitoring activities, and conveys recommendations for quality data collection, management and analysis. FORCE will continue to work closely with OES Environmental and its members to document and improve the state of knowledge about the interactions of MRE devices interactions with the marine environment.

FORCE also fostered international engagement by co-sponsoring and participating in multiple workshops held alongside the 1st Pan-American Marine Energy Conference in San Jose, Costa Rica (January 26-28, 2020). FORCE general manager, Mr. Tony Wright, co-hosted a workshop entitled ‘Test and Research Centers – Fostering International Collaboration’ and Dr. Hasselman presented an overview of the FORCE demonstration site. Dr. Hasselman also participated in additional workshops focused on i) environmental effects of MRE devices, and ii) data systems and modelling approaches sponsored by OES Environmental. These workshops included a series of presentations from key groups at various MRE test centres around the world (i.e., FORCE, EMEC, MERIC, IMARES, CEMIE, DMEC, and various test centres in the United States), and those actively engaged environmental monitoring, marine spatial planning and modelling. Break-out groups convened following presentations to discuss the role of test centres in fostering international collaboration, identifying priority areas for research and knowledge sharing, advancing monitoring capabilities and modelling approaches.

Mid-Field Monitoring Activities

FORCE has been leading ‘mid-field area’ or ‘site-level’ monitoring for a number of years, focusing on a variety of environmental variables. FORCE’s present environmental effects monitoring program, introduced in May 2016, was developed in consultation with SLR Consulting (Canada).¹⁷ FORCE’s EEMP was subsequently strengthened by review and contributions by national and international experts and scientists, DFO, NSE, and FORCE’s EMAC, and has been adjusted based on experience and lessons learned. This is consistent with the adaptive management approach inherent to FORCE EEMP – the process of

¹⁶ OES Environmental was established by the International Energy Agency (IEA) Ocean Energy Systems (OES) in January 2010 to examine environmental effects of marine renewable energy development. Member nations include: Australia, China, Canada, Denmark, France, India, Ireland, Japan, Norway, Portugal, South Africa, Spain, Sweden, United Kingdom, and United States. Further information is available at <https://tethys.pnnl.gov>.

¹⁷ This document is available online at: www.fundyforce.ca/document-collection.

monitoring, evaluating and learning, and adapting (AECOM, 2009) that has been used at the FORCE site since its establishment in 2009.¹⁸

FORCE's EEMP currently focuses on the impacts of operational turbines on lobster, fish, marine mammals, and seabirds as well as the impact of turbine-produced sound. Overall, these research and monitoring efforts, detailed below, were designed to test the predictions made in the FORCE EA. As mentioned above in the Executive Summary, since the latest EEMP was initiated in 2016, FORCE has completed approximately:

- 408 hours of hydroacoustic fish surveys;
- more than 4,385 'C-POD' (marine mammal monitoring) days;
- bi-weekly shoreline observations;
- 49 observational seabird surveys;
- four drifting marine sound surveys and additional bottom-mounted instrument sound data collection; and
- 11 days of lobster surveys.

The following pages provide a summary of the mid-field monitoring activities conducted at the FORCE site up to the end of the first quarter of 2020, including data collection, data analyses performed, initial results, and lessons learned; building activities and analyses from previous years. Where applicable this report also presents analyses that have integrated data collected through the near-field and mid-field monitoring programs in an effort to provide a more complete understanding of turbine-marine life interactions.

Monitoring Objectives

The overarching purpose of environmental monitoring is to test the accuracy of the environmental effect predictions made in the original EA. These predictions were generated through an evaluation of existing physical, biological, and socioeconomic conditions of the study area, and an assessment of the risks the tidal energy demonstration project poses to components of the ecosystem.

A comprehensive understanding of turbine-marine life interactions will not be possible until turbine-specific and site-level monitoring efforts are integrated, and additional data is collected in relation to operating turbines. Further, multi-year data collection will be required to consider seasonal variability at the FORCE test site and appropriate statistical analyses of this data will help to obtain a more complete understanding of marine life-turbine interactions.

Table 1 outlines the objectives of the respective mid-field monitoring activities conducted at the FORCE demonstration site. Near-field monitoring summaries will be updated as turbines are scheduled for deployment at FORCE. At this time, and considering the scale of turbine deployments in the near-term at FORCE, it is unlikely that significant effects in the far-field will be measurable (SLR, 2015). Far-field studies such as sediment dynamics will be deferred until such time they are required. As more devices are scheduled for deployment at the FORCE site and as monitoring techniques are improved, monitoring protocols will be revised in keeping with

¹⁸ The adaptive management approach is necessary due to the unknowns and difficulties inherent with gathering data in tidal environments such as the Minas Passage and allows for adjustments and constant improvements to be made as knowledge about the system and environmental interactions become known. This approach has been accepted by scientists and regulators.

the adaptive management approach. These studies will be developed in consultation with FORCE's EMAC, regulators, and key stakeholders.

Table 1: The objectives of each of the 'mid-field' environmental effects monitoring activity, which consider various Valued Ecosystem Components (VECs), led by FORCE.

Mid-Field Environmental Effects Monitoring VEC	Objectives
Lobster	<ul style="list-style-type: none"> to determine if the presence of a tidal stream energy turbine affects commercial lobster catches
Fish	<ul style="list-style-type: none"> to test for indirect effects of tidal stream energy turbines on water column fish density and fish vertical distribution to estimate probability of fish encountering a device based on fish density proportions in the water column relative to turbine depth in the water column
Marine Mammals	<ul style="list-style-type: none"> to determine if there is permanent avoidance of the mid-field study area during turbine operations to determine if there is a change in the distribution of a portion of the population across the mid-field study area
Marine Sound (Acoustics)	<ul style="list-style-type: none"> to conduct ambient sound measurements to characterize the soundscape prior to and following deployment of the in-stream turbines
Seabirds	<ul style="list-style-type: none"> to understand the occurrence and movement of bird species in the vicinity of tidal stream energy turbines to confirm FORCE's Environmental Assessment predictions relating to the avoidance and/or attraction of birds to tidal stream energy turbines

Lobster

FORCE conducted a baseline lobster catchability survey in fall 2017 (NEXUS Coastal Resource Management Ltd., 2017). This catch-and-release survey design was conducted over 11 days and consisted of commercial traps deployed at varying distances around the future location of the CSTV turbine deployment planned for 2018. Captured lobsters were measured (carapace length), had their sex and reproductive stage determined (male, female, and berried female), and shell condition evaluated. This baseline survey captured 351 lobsters and reported a high catchability rate (> 2.7 kg/trap).¹⁹ Preliminary qualitative analyses indicated that catch rates declined during the survey and were associated with increasing tidal velocities; a statistically significant negative relationship was detected between catch rates and maximum tidal range. No significant difference in catch rates was detected across separate locations from the proposed turbine location. Cumulatively, these results suggested that the impact of turbines may be higher on lobster catchability than anticipated in the EA (AECOM, 2009), but a repeat of the study in the presence of an operational turbine is required to verify this prediction.

Indeed, a repeat of this catchability survey was planned for fall 2018 in the presence of an operational turbine to test the EA prediction (with pre-installation and operating turbine collection periods) that tidal stream turbines will have minimal impacts on lobster populations within the FORCE test site (AECOM, 2009). However, given the non-operational status of the CSTV

¹⁹ This is classified as 'high' according to DFO's Catch Per Unit Effort (CPUE) index (Serdynska and Coffen-Smout, 2017).

turbine, the objectives of the 2018 survey effort could not be achieved, and the survey has been postponed until such time that an operational turbine is present at the site.

In 2019, FORCE commissioned TriNav Fisheries Consultants Ltd. to redesign FORCE's lobster monitoring program based on feedback from regulators to include a more statistically robust study design for monitoring lobster at the FORCE test site. TriNav Fisheries Consultants evaluated the efficacy of using a variety of methods including divers and hydroacoustic tags to track lobster movements. However, given the strong tidal flows and brief window available during periods of slack tide, divers are not a viable option due to safety concerns. Ultimately, TriNav Fisheries Consultants identified the combination of a modified catchability survey design and a mark-recapture study using conventional tags as the best approach for monitoring lobster at the FORCE site. This new study design is intended to be implemented in fall 2019, pending any restrictions that the COVID-19 pandemic and associated federal and provincial government health department recommendations places on the ability to conduct the study.

Fish

FORCE has been conducting mobile fish surveys since May 2016 to test the EA prediction that tidal stream turbines are unlikely to cause substantial impacts to fishes at the test site (AECOM, 2009). To that end, the surveys are designed to:

- test for indirect effects of tidal stream energy turbines on water column fish density and fish vertical distribution; and
- estimate the probability of fish encountering a device based on any 'co-occurrence' relative to turbine depth in the water column.

Moreover, these surveys follow a 'BACI' (Before/After, Control/Impact) design to permit a comparison of data collected before a turbine is installed with data collected while a turbine is operational at the FORCE site, and in relation to a reference site along the south side of the Minas Passage. These 24-hour mobile surveys encompass two tidal cycles and day/night periods using a scientific echosounder, the Simrad EK80, mounted on a vessel, the Nova Endeavor (Huntley's Sub-Aqua Construction, Wolfville, NS). This instrument is an active acoustic monitoring device and uses sonar technology to detect fish by recording reflections of a fish's swim bladder.

Analyses of hydroacoustic fish surveys completed during baseline studies in 2011 and 2012 (Melvin and Cochrane, 2014) and surveys during May 2016 – August 2017 (Daroux and Zydlewski, 2017) evaluated changes in fish densities in association with diel stage (day/night), tidal stage (ebb/flood), and turbine presence or absence (an OpenHydro turbine was present November 2016 – June 2017). Results support the EA prediction that tidal stream devices have minimal impact on marine fishes. However, additional surveys in relation to an operating turbine are required to fully test this prediction.

In 2019, the University of Maine conducted a thorough analysis for 15 fish surveys conducted by FORCE from 2011-2017. The hydroacoustic data set included six 'historical' surveys conducted between August 2011 and May 2012, and nine 'contemporary' surveys conducted between May 2016 and August 2017. The analyses included comparisons of fish presence/absence and relative fish density with respect to a series of temporal (historical vs. contemporary, or by survey), spatial (CLA vs. reference study area, or by transect) and environmental (tide phase, diel state, or with/against predicted tidal flow) explanatory variables. The report identified a

statistically significant difference in fish presence/absence and relative fish density between the historical and contemporary data sets that may be attributable to differences in the survey design/execution between the time periods, or could reflect changes in fish usage of the site. As such, remaining analyses were restricted to the contemporary data sets. The results revealed that: i) data collection during the ebb tide and at night are important for understanding fish presence in the CLA, ii) various explanatory variables and their additive effects should be explored further, and iii) increasing the frequency of surveys during migratory periods (consecutive days in spring/fall) may be required to understand to patterns and variability of fish presence and density in Minas Passage. Importantly, the report suggested a statistically significant difference in fish presence/absence and relative density between the CL and reference site, suggesting that the reference site may not be sufficiently representative to serve as a control for the CLA, and for testing the effects of an operational turbine on fish density and distribution in Minas Passage. Additional work is underway using data from eight additional contemporary fish surveys (2017-2018) to determine whether this finding is biologically meaningful, or whether it is simply a statistical artefact of how the data was aggregated in the original analysis.

Marine Mammals

In 2020, FORCE continues to conduct two main activities to test the EA prediction that project activities are not likely to cause significant adverse residual effects on marine mammals within the FORCE test site (AECOM, 2009). These activities have been ongoing on a regular basis since 2016. Specifically, FORCE is continuing to:

- conduct passive acoustic monitoring (PAM) using ‘click recorders’ known as C-PODs; and
- implement an observation program that includes shoreline, stationary, and vessel-based observations.

Passive Acoustic Monitoring

The first component of FORCE’s marine mammal monitoring program involves the use of PAM mammal detectors known as C-PODs, which record the vocalizations of toothed whales, porpoises, and dolphins.²⁰ The program focuses mainly on harbour porpoise – the key marine mammal species in the Minas Passage that is known to have a small population that inhabits the inner Bay of Fundy (Gaskin, 1992). The goal of this program is to understand if there is a change in marine mammal presence in proximity to a deployed tidal stream energy device and builds upon baseline C-POD data collection within the Minas Passage since 2011.

From 2011 to early 2018, more than 4,695 ‘C-POD days’²¹ of data were collected in the Minas Passage. Over the study period, it was found that harbour porpoise use and movement varies over long (i.e., seasonal peaks and lunar cycles) and short (i.e., nocturnal preference and tide stage) timescales. This analysis, completed by Sea Mammal Research Unit (Canada) (Vancouver, BC), showed some evidence to suggest marine mammal exclusion within the near-field of CSTV turbine when it was operational (November 2016 – June 2017) (Joy et al., 2018b).

²⁰ The C-PODs, purchased from Chelonia Limited, are designed to passively detect marine mammal ‘clicks’ from toothed whales, dolphins, and porpoises.

²¹ A ‘C-POD day’ refers to the number of total days each C-POD was deployed times the number of C-PODs deployed.

This analysis revealed that the C-PODs in closest proximity to the turbine (230 m and 210 m distance) had reduced frequency of detections, but no evidence of mid-field avoidance with a turbine present and operating. The latest findings also revealed a decrease in detections during turbine installation activities; consistent with previous findings (Joy et al., 2017), but requiring additional data during an operational turbine to permit a full assessment of the EA predictions.

SMRU provided their 3rd year report of harbour porpoise monitoring using C-PODs at the FORCE test site (see Appendix I). The report describes the results of C-POD deployments #7-10 (i.e., 416 days from May 5, 2018 – August 14, 2019), and places the results in the broader context of the overall marine mammal monitoring program at FORCE. This ongoing monitoring program continues to show the prevalence of harbour porpoise at FORCE, with the species being detected on 98.8% of the 1,626 calendar days since monitoring with C-PODs commenced in 2011. Harbour porpoise detections at FORCE varies seasonally, with peak activity occurring during May – August, and lowest detections during December – March. Harbour porpoise detections also vary spatially, with C-PODs deployed at locations W2 and S2 recording the greatest detection rates, and D1 values typically low. Mean lost time across C-PODs, due to ambient flow noise saturating the detection buffer on the C-POD, averaged 22.6%. Interestingly, an analysis against past datasets that controlled for time of year, indicated that the effects of the non-operational CSTV turbine structure had no detectable effect on the rate of harbour porpoise detection.

C-PODs were not deployed during the first quarter of 2020 due to a combination of weather-related delays and the availability of vessels suitable for deployment during January and February, and the spread the COVID-19 virus in March and federal and provincial government requirements to maintain social distancing. This coincides with the period of reduced harbour porpoise activity at the FORCE site. C-PODs will undergo regular annual maintenance once these regulations are lifted and will include replacement of CPOD batteries, replacement of acoustic release batteries, refurbishment of SUBS packages as required, and the fabrication and installment of mounts for the MetOcean Telematics (Dartmouth, NS) beacons as needed. Following this regular maintenance, the C-PODs will be deployed at FORCE to resume monitoring.

Harbor porpoise (Phocoena phocoena) monitoring at the FORCE Test Site, Canada featured on Tethys (by FORCE and SMRU): <https://tethys.pnnl.gov/tethys-stories/harbor-porpoise-phocoena-phocoena-monitoring-force-test-site-canada>

Observation Program

FORCE's marine mammal observation program in 2020 includes observations made during bi-weekly shoreline surveys, stationary observations at the FORCE Visitor Centre, and marine-based observations during marine operations. All observations and sightings are recorded, along with weather data, tide state, and other environmental data. Any marine mammal observations are shared with SMRU Consulting to support validation efforts of PAM activities.

FORCE is preparing to use an Unmanned Aerial Vehicle (UAV) for collecting observational data along the shoreline and over the FORCE site using transects by programming GPS waypoints in the UAV to standardize flight paths. Several FORCE staff including *Science Director* Dr. Dan Hasselman, *Facility Manager* Sandra Currie, and Ocean Technologists Tyler Boucher, and Jessica Douglas received training to operate FORCE's UAV, and have acquired UAV pilot certification by successfully passing the 2019 Canadian Drone Pilot Basic Operations Examination, administered by Transport Canada. These staff are now licensed to safely operate the UAV at the FORCE site. FORCE also hosts a public reporting tool that allows members of the public to report observations of marine life: mmo.fundyforce.ca

Marine Sound (Acoustics)

Marine sound – often referred to as ‘acoustics’ or ‘noise’ – monitoring efforts are designed to characterize the soundscape of the FORCE test site. Data collected from these monitoring efforts will be used to test the EA predictions that operational sounds produced from functioning tidal stream turbines are unlikely to cause mortality, physical injury or hearing impairment to marine animals (AECOM, 2009).

Results from previous acoustic analyses completed at the FORCE site indicate that the CSTV turbine was audible to marine life at varying distances from the turbine, but only exceeded the threshold for behavioural disturbance at very short ranges and during particular tide conditions (Martin et al., 2018). This is consistent with findings at the Paimpol-Bréhat site in France where an OpenHydro turbine was also deployed – data suggests that physiological trauma associated with a tidal turbine is improbable, but that behavioural disturbance may occur within 400 m of a turbine for marine mammals and at closer distances for some fish species (Lossent et al., 2017).

In previous years, regulators have encouraged FORCE to pursue integration of results from multiple PAM instruments deployed in and around the FORCE test site. To that end, FORCE and its partner JASCO Applied Sciences (Canada) Ltd. pursued a comparative integrated analysis of sound data collected by various hydrophones (i.e., underwater sound recorders) deployed autonomously and mounted on the CSTV turbine. That work revealed that flow noise increased with the height of the hydrophone off the seabed but had little effect on hydrophones deployed closer to the sea floor. The comparative integrated analysis provided valuable information about future marine sound monitoring technologies and protocols while building on previous acoustics analyses at the FORCE site. Plans are currently being developed to test the capabilities of recent technological advancements (‘NoiseSpotter’; Raghukumar et al. 2019) for characterizing the soundscape of the FORCE test site and for assessing turbine generated sound in high-flow environments like the Minas Passage.

Seabirds

FORCE’s seabird monitoring program is designed to test the EA prediction that project activities are not likely to cause adverse residual effects on marine birds within the FORCE test area (AECOM, 2009). However, there has been limited opportunity to determine potential effects of an operational turbine on seabirds at the FORCE test site and to test the EA predictions.

Since 2011, FORCE and EnviroSphere Consultants Ltd. (Windsor, NS) have collected observational data from the deck of the FORCE Visitor Centre, documenting seabird species presence, distribution, behaviour, and seasonality throughout the FORCE site (EnviroSphere Consultants, 2009, 2017; Stewart and Lavender, 2010; Stewart et al., 2011, 2012, 2013; Stewart et al., 2018). FORCE recently commissioned EnviroSphere Consultants Ltd. and Dr. Phil Taylor (Acadia University) to synthesize the results of its observational seabird surveys (2011-2018) at the FORCE test site, and to evaluate advanced statistical techniques for analysing seabird count data in relation to environmental predictor variables (see Appendix II). The seabird count data were examined using Generalized Additive Models (GAMs) to characterize seabird abundance and to better understand the potential impacts of tidal turbines on seabirds at the FORCE test site. The results of the analyses revealed that overall model fit is suitable to characterize count data for some species, and that there are clear patterns of effects

of time of year, wind speed and direction, tide height and time of day on the number of seabirds observed. However, the analyses also revealed that not all species reported at FORCE have been observed frequently enough to be modelled effectively using the GAM approach. This is due in part to the variability in count data that is particularly relevant for modelling abundance of migratory species that are only present at the FORCE site for brief periods during annual migrations. This is consistent with observational data collected over the course of these surveys that have demonstrated that the FORCE site has a lower abundance of seabirds in relation to other areas of the Bay of Fundy, and even other regions of Atlantic Canada. Given these results, the report recommends that future monitoring and analyses focus on locally resident species (i.e., great black-backed gull, herring gull, black guillemot and common eider) so that the EA predictions can be tested most effectively. This work contributes to the development of appropriate analytical methods for assessing the impacts of tidal power development in the Minas Passage on relevant seabird populations and supports the continued responsible development of tidal energy at FORCE.

Near-field Monitoring Activities

While FORCE completes site-level or ‘mid-field’ monitoring activities at the FORCE site, near-field monitoring is led by individual berth holders. Like the mid-field monitoring programs, the near-field monitoring plans and reports undergo review by FORCE’s EMAC and regulators. In anticipation of a planned deployment at FORCE in late 2020, Sustainable Marine Energy Canada (SMEC) recently submitted a near-field EEMP plan that is undergoing internal review by FORCE staff before review by EMAC and submission to regulators for approval.

In September 2018, it was confirmed that that CSTV turbine rotor was not spinning. Since that time, CSTV had been providing written confirmation to regulators on a monthly basis that the turbine is not operational by monitoring its status during the peak tidal flow of each month. However, as a result of the insolvency of OpenHydro Technology Ltd., all reporting activities by CSTV ceased as of March 1, 2019. Data collection from the turbine-mounted ADCPs to confirm the turbine is no longer spinning is being managed and reported by FORCE to regulators on a monthly basis. Data is also still being collected from two of the four hydrophones on the CSTV turbine.

As additional near-field, device-specific environmental effects monitoring programs are required and implemented for deployed tidal stream devices, berth holder updates will be included as appendices to this report.

Other FORCE Research Activities

The Pathway Program

The Pathway Program is a collaborative effort between FORCE and OERA to identify an effective and regulator approved monitoring solution for the tidal energy industry in Nova Scotia. The Pathway Program involves several phases, including i) Global capability Assessment, ii) Advancing Data Processing and Analytics, and iii) Technology Validation. The first phase of this program, a Global Capability Assessment, involved a comprehensive literature review about the use of different classes of environmental monitoring technologies (i.e., PAM, imaging sonars, echosounders) for monitoring tidal energy devices around the world. Subject matter experts

were commissioned to provide reports on these instrument classes, and these reports are publicly available.²²

FORCE is collaborating with SMEC and using the floating tidal energy platform (PLAT-I) deployed in Grand Passage, NS, to conduct four projects outlined in Phase III (Technology validation) of the Pathway Program (Figure 1). Three of these projects focus on evaluating the utility of echosounders for quantifying biological targets in high flow environments. These projects evaluate the performance of echosounders in bottom and surface deployments and using a suite of complementary technologies (optical cameras and imaging sonars) to investigate target detections. The fourth project involves an assessment of the relative performance of PAM instruments for detecting synthetic harbour porpoise clicks in high flow environments using similar bottom and surface deployments (Figure 2).

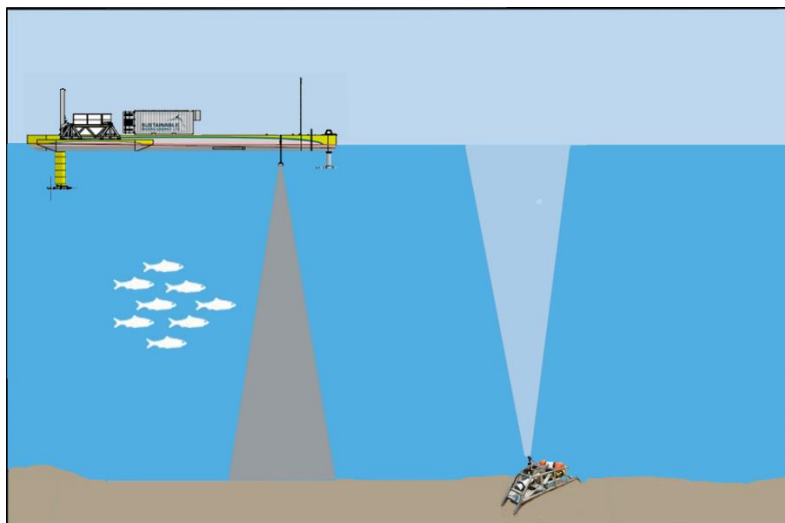


Figure 1: Schematic of the conceptual study design for an assessment of the relative performance of echosounders in bottom-deployments (FAST platform) surface deployments (PLAT-I). Shaded areas are intended for visualization purposes only, and do not accurately represent sample volumes.

²² These are available online at: <https://oera.ca/research/pathway-program-towards-regulatory-certainty-instream-tidal-energy-projects>



Figure 2: Deployment of the FAST platform in Grand Passage for an assessment of PAM instrument performance.

Fundy Advanced Sensor Technology (FAST) Activities

FORCE's Fundy Advanced Sensor Technology Program is designed to advance capabilities to monitor and characterize the FORCE site. Specifically, the FAST Program was designed to achieve the following objectives:

- 1) To advance capabilities of site characterization;
- 2) To develop and refine environmental monitoring standards and technologies; and
- 3) To enhance marine operating methodologies.

FAST combines both onshore and offshore monitoring assets. Onshore assets include a meteorological station, video cameras, an X-band radar system, and tide gauge. Offshore assets include modular subsea platforms for both autonomous and cabled data collection and a suite of instrumentation for a variety of research purposes. Real-time data collected through FAST assets is broadcasted live on the Ocean Networks Canada's (ONC; Victoria, BC) website.²³

Platform Projects

The first and largest of the FAST platforms houses an instrument called the Vectron. Developed in partnership with Nortek Scientific (Halifax, NS), Memorial University (St. John's, NL), and Dalhousie University (Halifax, NS), the Vectron is the world's first stand-alone instrument to remotely measure, in high resolution, turbulence in the mid-water column. Measurements and

²³ This is available online at: www.oceannetworks.ca/observatories/atlantic/bay-fundy

analysis from the Vectron will help tidal energy companies to better design devices, plan marine operations, and characterize the tidal energy resource.

A smaller platform called FAST-3 was equipped with an upward looking echosounder and deployed during 2017-2018 to monitor fish densities at the FORCE site. FORCE and its partners, including Echoview Software completed data processing and analysis in 2019. This data was integrated with the mobile hydroacoustic surveys that FORCE conducts as part of its EEMP to evaluate the temporal and spatial representativeness of each method and to determine the degree to which results were corroborative (Figure 3). Although the spatial representative range of the stationary results could not be determined from the mobile data, it did reveal strong tidal and diel periods in fish density estimates at the site, with greater variation over shorter time frames than over the course of a year. These findings reinforce the importance of 24-hr data collection periods in ongoing monitoring efforts. The report reveals that collecting 24 hours of data allows the tidal and diel variability to be quantified and isolated from the longer-term trends in fish density and distribution that need to be monitored for testing the EA predictions. This project was funded by Natural Resources Canada (NRCan), the NSDEM, and the OERA, and the report is provided here as Appendix III.

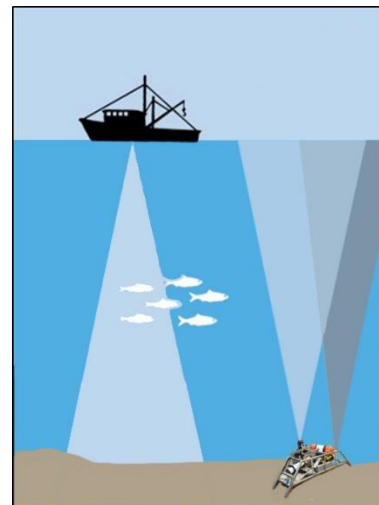


Figure 3: A representation of the data collection methods of the FORCE mid-field fish EEMP and the FAST-3 platform.

Fish Tracking

To enhance fish monitoring and to expand its data collection capacity, FORCE partnered with the Ocean Tracking Network (OTN)²⁴ and attached one VEMCO²⁵ fish tag receiver (a VR2 receiver) to each C-POD mooring/SUBS (Streamlined Underwater Buoyancy System) package (see above). These receivers are used to supplement OTN's ongoing data collection program within the Minas Passage and are referred to as 'Buoys of Opportunity.' Upon retrieval of the C-PODs and receivers, instruments are shared with OTN where data is offloaded prior to redeployment. This effort will support increased knowledge of fish movement within the Minas Passage, which has applicability beyond tidal energy demonstration, as well as complement FORCE's hydroacoustic data collection efforts that do not allow for species identification.

OTN data managers are in the process of acquiring information, including species identification, and sharing this with FORCE. Initial results show that the OTN receivers deployed by FORCE have detected tags from the following projects:

- Maritimes Region Atlantic salmon marine survival and migration (Hardie, D.C., 2017);
- Quebec MDDEFP Atlantic Sturgeon Tagging (Verreault, G., Dussureault, J., 2013);
- Gulf of Maine Sturgeon (Zydlewski, G., Wippelhauser, G. Sulikowski, J., Kieffer, M., Kinnison, M., 2006);

²⁴ Ocean Tracking Network's website: www.oceantrackingnetwork.org.

²⁵ VEMCO is "the world leader in the design and manufacture of acoustic telemetry equipment used by researchers worldwide to study behaviour and migration patterns of a wide variety of aquatic animals." Learn more: www.vemco.com.

- OTN Canada Atlantic Sturgeon Tracking (Dadswell, M., Litvak, M., Stokesbury, M., Bradford, R., Karsten, R., Redden, A., Sheng, J., Smith, P.C., 2010);
- Darren Porter Bay of Fundy Weir Fishing (Porter, D., Whoriskey, F., 2017);
- Movement patterns of American lobsters in the Minas Basin, Minas Passage, and Bay of Fundy Canada (2017);
- Shubenacadie River Monitoring Project: Tomcod (Marshall, J., Fleming, C., Hunt, A., and Beland, J., 2017);
- MA Marine Fisheries Shark Research Program (Skomal, G.B., Chisholm, J., 2009);
- UNB Atlantic Sturgeon and Striped Bass tracking (Curry, A., Linnansaari, T., Gautreau, M., 2010); and
- Inner Bay of Fundy Striped Bass (Bradford, R., LeBlanc, P., 2012).
- Minas Basin Salmon Kelt (McLean, M., Hardie, D., Reader, J., Stokesbury, M.J.W., 2019)

Further information about these Buoys of Opportunity, and the projects listed above, can be found on OTN's website: <https://members.oceantrack.org/project?ccode=BOOFORCE>

Starting in 2018, FORCE has worked in collaboration with Dr. Mike Stokesbury at Acadia University to install additional VEMCO receivers of a new design on FORCE's C-POD moorings/SUBS packages. These new receivers are expected to be even more effective in picking up acoustic detections in high flow environments, where tag signals can be obscured by noise. This partnership will contribute additional information regarding movement patterns of Atlantic salmon, sturgeon, striped bass, and alewife in Minas Passage and Basin. This work is sponsored by the OERA, NRCan, NSDEM, the Natural Sciences and Engineering Research Council of Canada (NSERC), and the Canadian Foundation for Innovation (CFI).²⁶

²⁶ Information about this project, and others funded through this program, is available online at: www.oera.ca/press-release-research-investments-in-nova-scotia-in-stream-tidal-technology-research/

Discussion

The year 2020 represents a strategic opportunity for FORCE and its partners to learn from previous experiences, incorporate regulatory advice, and to re-evaluate approaches to research and monitoring in the high flows of the Minas Passage.

In response to the COVID19 pandemic, the Nova Scotia provincial government has directed non-essential workers to remain home and practice social distancing. For FORCE, this means staff work from home; regular office, engagement, and marine activities have shifted to a focus on tackling a high volume of site data that requires processing, integration and analysis. With three ocean techs now employed full-time in-house, FORCE has a unique capacity to process biological data with both Echoview (hydroacoustics) and Seatec (multibeam imaging sonar) software. In the longer term, the COVID19 outbreak will impact our ability to gather data at our site and conduct marine operations – all of which require multiple people working in close proximity.

Once operations can resume safely, FORCE and its partners will continue to conduct monitoring, engage in meaningful assessments of monitoring technology capabilities, and to provide data analyses and interpretation that advance our ability to effectively monitor the effects of tidal turbines in high flow environments, and specifically at the FORCE test site. Reports from FORCE's partners and updates routinely underwent review by FORCE's EMAC and regulators, along with continued results from FORCE's ongoing monitoring efforts.

FORCE continues to implement lessons learned from the experiences of local and international partners, build local capacity and enhance skills development, test new sensor capabilities, and integrate results from various instruments. Cumulatively, these efforts provide an opportunity for adaptive management and the advancement and refinement of scientific approaches, tools, and techniques required for effectively monitoring the near- and mid-field areas of tidal stream energy devices in dynamic, high-flow marine environments.

Ongoing monitoring efforts will continue to build on the present body of knowledge of marine life-turbine interactions. While it is still early to draw conclusions, initial findings internationally and at the FORCE test site have documented some disturbance of marine mammals primarily during marine operations associated with turbine installation/removal activities, but otherwise have not observed significant effects.

FORCE will continue to conduct environmental research and monitoring to increase our understanding of the natural conditions within the Minas Passage and, when the next turbine(s) are deployed and operating, test the EA prediction that tidal energy is unlikely to cause significant harm to marine life. In the longer-term, monitoring will need to be conducted over the full seasonal cycle and in association with multiple different turbine technologies in order to understand if tidal energy can be a safe and responsibly produced energy source. FORCE will continue to report on progress and release results and lessons learned in keeping with its mandate to inform decisions regarding future tidal energy projects.

References

- AECOM. (2009). *Environmental Assessment Registration Document – Fundy Tidal Energy Demonstration Project Volume I: Environmental Assessment*. Available at www.fundyforce.ca.
- Copping, A. (2018). *The State of Knowledge for Environmental Effects: Driving Consenting/Permitting for the Marine Renewable Energy Industry*. Available at: tethys.pnnl.gov.
- Daroux, A. and Zydlewski, G. (2017). *Marine Fish Monitoring Program Tidal Energy Demonstration Site – Minas Passage*. Prepared for Fundy Ocean Research Center for Energy.
- Envirosphere Consultants Limited. (2017). *Marine Seabirds Monitoring Program – Tidal Energy Demonstration Site – Minas Passage, 2016 – 2017*. Prepared for Fundy Ocean Research Center for Energy.
- Envirosphere Consultants Limited. (2009). *Marine Bird and Mammal Observations—Minas Passage Study Site*. Prepared for Minas Basin Pulp and Power Co. Ltd.
- Fraser, S., Williamson, B., Nikora, V., Scott, B. (2018). *Fish Distributions in a Tidal Channel Indicate the Behavioural Impact of a Marine Renewable Energy Installation*. Energy Reports, 4, 65-69.
- Gaskin, D.E. (1992). *Status of the harbour porpoise, Phocoena phocoena, in Canada*. Canadian Field-Naturalist 196: 36 – 54.
- Gattuso J.-P., Magnan A.K., Bopp L., Cheung W.W.L., Duarte C.M., Hinkel J., Mcleod E., Micheli F., Oschlies A., Williamson P., Billé R., Chalastani V.I., Gates R.D., Irsson J.-O., Middelburg J.J., Pörtner H.-O. and Rau G.H. (2018). *Ocean Solutions to Address Climate Change and Its Effects on Marine Ecosystems*. Frontiers in Marine Science. 5:337.
- Joy, R., Wood, J., Robertson, F., and Tollit, D. (2017). *FORCE Marine Mammal Environmental Effects Monitoring Program – 1st Year (2017) Monitoring Report*. Prepared by SMRU Consulting (Canada) on behalf of FORCE.
- Joy, R., Wood, J., Sparling, C., Tollit, D., Copping, A., McConnell, B. (2018a). *Empirical measures of harbor seal behavior and avoidance of an operational tidal turbine*. Marine Pollution Bulletin, 136, 92-106.
- Joy, R., Wood, J., and Tollit D. (2018b). *FORCE Echolocating Marine Mammal Environmental Effects Monitoring Program – 2nd Year (2018) Monitoring Report*. Prepared by SMRU Consulting (Canada) on behalf of FORCE, December 8, 2018.
- Lewis, A., Estefen, S., Huckerby, J., Musial, W., Pontes, T., Torres-Martinez, J., et al. (2011). *“Ocean energy,” in Renewable Energy Sources and Climate Change Mitigation. Special Report of the Intergovernmental Panel on Climate Change*, eds O. Edenhofer, R. Pichs-Madruga, Y. Sokona, K. Seyboth, P. Matschoss, S. Kadner, et al. (Cambridge: Cambridge University Press), 497–534.
- Lossent, J., Gervaise, C., Iorio, L., Folegot, T., Clorennec, D., Lejart, M. (2017). *Underwater operational noise level emitted by a tidal current turbine and its potential impact on marine fauna*. The Journal of the Acoustical Society of America, 141(5).
- Malinka, C., Gillespie, D., Macaulay, J., Joy, R., Sparling, C. (2018). *First in situ Passive Acoustic Monitoring for Marine Mammals during Operation of a Tidal Turbine in Ramsey Sound, Wales*. Marine Ecology Progress Series, 590, 247-266.

Marine Renewables Canada. (2018). *State of the Sector Report: Marine Renewable Energy in Canada*.

Martin, B., Whitt, C., and Horwich, L. (2018). *Acoustic Data Analysis of the OpenHydro Open-Centre Turbine at FORCE: Final Report*. Document 01588, Version 3.0b. Technical report by JASCO Applied Sciences for Cape Sharp Tidal and FORCE.

Melvin, G.D., and Cochrane, N.A. (2014). *Investigation of the vertical distribution, movement, and abundance of fish in the vicinity of proposed tidal power energy conversion devices*. Final Report for Offshore Energy Research Association. Research Project 300-170-09-12.

NEXUS Coastal Resource Management Ltd. (2017). *Lobster Catchability Study Report*.

Pine, M., Schmitt, P., Culloch, R., Lieber, L., Kregting, L. (2019). Providing ecological context to anthropogenic subsea noise: Assessing listening space reductions of marine mammals from tidal energy devices. *Renewable and Sustainable Energy Reviews*, 103, 49-57.

Polagye, B., Wood, J., Robertson, F., Joslin, J., Joy, R. (2018). *Marine Mammal Behavioral Response to Tidal Turbine Sound*. Report by Sea Mammal Research Unit (SMRU) and University of Washington. pp 65.

Raghukumar, K., Chang, G. Spada, F.W., and Jones, C.A. 2019. Performance characteristics of the NoiseSpotter: an acoustic monitoring and localization system. *Offshore Technology Conference*, Houston, USA May 6-9, 2019.

Schramm, M., Bevelhimer, M., Scherelis, C. (2017). Effects of hydrokinetic turbine sound on the behavior of four species of fish within an experimental mesocosm. *Fisheries Research*, 190, 1-14.

SLR Consulting. (2015). *Proposed Environmental Effects Monitoring Programs 2015-2020 for Fundy Ocean Research Center for Energy (FORCE)*.

Stewart, P.L., Kendall, V.J., and Lavender, F.L. (2018). *Marine Seabirds Monitoring Program Tidal Energy Demonstration Site – Minas Passage, Year-2: 2017 – 2018*. Prepared for Fundy Ocean Research Center for Energy.

Stewart, P.L., and Lavender, F.L. (2010). *Marine Mammal and Seabird Surveys Tidal Energy Demonstration Site — Minas Passage, 2009*. Prepared for Fundy Ocean Research Center for Energy.

Stewart, P.L., Lavender, F.L., and Levy, H. A. (2013). *Marine Mammal and Seabird Surveys Tidal Energy Demonstration Site — Minas Passage, 2012*. Prepared for Fundy Ocean Research Center for Energy.

Stewart, P.L., Lavender, F.L., and Levy, H. A. (2012). *Marine Mammal and Seabird Surveys Tidal Energy Demonstration Site — Minas Passage, 2011*. Prepared for Fundy Ocean Research Center for Energy.

Stewart, P.L., Lavender, F.L., and Levy, H. A. (2011). *Marine Mammal and Seabird Surveys Tidal Energy Demonstration Site — Minas Passage, 2010*. Prepared for Fundy Ocean Research Center for Energy.



FORCE Echolocating Marine Mammal EEMP 3rd Year Monitoring Report

Prepared for FORCE

[Jan 2020]

PO Box 764
Friday Harbor, WA 98250
USA

SMRU Consulting North America

55 Water Street, Suite 604
Vancouver, BC V6B 1A1
Canada

**FORCE Echolocating Marine Mammal EEMP
3rd Year (2019) Monitoring Report**

14 January 2020

Prepared by SMRU Consulting

Canada Office
55 Water Street, Suite 604
Vancouver, BC
V6B 1A1

Authors:

Dominic Tollit, PhD
Senior Research Scientist, SMRU Consulting

Ruth Joy, PhD
Senior Research Scientist, SMRU Consulting

Jason Wood, PhD
Senior Research Scientist, SMRU Consulting

Suggested citation: Tollit, D., Joy, R. and Wood, J. (2020). FORCE Echolocating Marine Mammal Environmental Effects Monitoring Program – 3rd Year (2019) Monitoring Report. Prepared by SMRU Consulting (Canada) on behalf of FORCE, January 2020.

For its part, the Buyer acknowledges that Reports supplied by the Seller as part of the Services may be misleading if not read in their entirety, and can misrepresent the position if presented in selectively edited form. Accordingly, the Buyer undertakes that it will make use of Reports only in unedited form, and will use reasonable endeavours to procure that its client under the Main Contract does likewise. As a minimum, a full copy of our Report must be appended to the broader Report to the client.

Executive Summary

Tidal inlets are dynamic regions that provide important habitat for harbour porpoise (*Phocoena phocoena*). Harbour porpoise use echolocation to hunt and communicate (Kastelein et al. 2002), and they are known to be susceptible to noise disturbance (Tougaard et al. 2009). Few studies to date have focused on exposure to continuous low frequency noise such as that emitted by tidal turbines. C-PODs can detect echolocating cetacean species including dolphins, but not whales. C-POD monitoring of the FORCE demonstration site began on 5 May 2011, with a total of 929,846 10-minute periods currently collected across 1,626 calendar days. Porpoise clicks were detected on 98.8% of days, with an overall median of 8 minutes per day. The minimum estimate of the probability of porpoise presence detection was 7.0% of all 10-minute periods. No confirmed dolphin detections have been made.

This year 3 report describes the results of deployments 7 through 10 of the overall Marine Mammal C-POD Monitoring Program, put in place as part of FORCE's multi-year Environmental Effects Monitoring Program (EEMP) at its marine demonstration and testing facility in Minas Passage. This report provides summary data for 416 days across the period between 5 May 2018 to 14 August 2019 in the four deployments of 5 C-PODs. A second 2 MW OpenHydro tidal turbine was deployed by Cape Sharp Tidal Venture on 22 July 2018 and grid connected on 24 July 2018. The turbine is believed to have worked briefly (and then possible to have been free-spinning) until 9 August 2018 (i.e., within deployment 7). The non-operational nor free-spinning turbine was present for the rest of the year 3 EEMP (deployments 8-10). A period of less than 18 days of operational or free-spinning turbine was not considered sufficient for a robust GAM-GEE turbine effects analysis as undertaken in 2018 following the deployment of the first OpenHydro turbine (See Joy et al. 2018, Tollit et al. 2019). Following discussions with FORCE, this report summarizes overall porpoise detection rates since 2011, documents and compares C-POD detection data across each of the four year 3 EEMP deployment periods and additionally compares year 3 EEMP datasets with previous periods (including both baseline and previous turbine deployment periods).

Porpoises were detected between 95-100% of days across all C-PODs combined for the year 3 EEMP deployments, with medians of 5-15 minutes per day across the four separate deployments. Values for deployments 7 and 10 are equal or higher than values collected during 2011-2014 baseline, noting both these deployments cover a period of May-August, a peak period of porpoise activity. Deployment 9, covering a period of December-March saw the lowest detection rates, noting these remained higher than when the turbine was operational in 2016-2017. Mean time lost averaged 22.6%, with a median of 0% and interquartile range of 0-0%. Porpoise detections rates also varied by location, with D1 values typically low (deployment average 3.2%) and S2 and W2 typically high (deployment averages of 6.6% and 6.4% respectively). E1 averaged 4.3% across all four deployments, while W1 averaged 4.8%. A peak rate of 8.8% was observed at E1 and W2 during deployment 10, while the lowest rate of 1.4% was observed at D1 during deployment 8. With the exception of the site located in deeper water (S2), detection rates are consistently higher in summer deployments (7 and 10) compared to the fall through spring deployments 8 and 9. An analysis against past datasets (that controlled for time of year) clearly suggest that the effect of a turbine structure (i.e., non-operational) had no detectable effect on porpoise local detection rates.

Table of Contents

Executive Summary	i
1. Introduction and EEMP Objectives	1
2. Methods and Results	3
2.1. C-POD deployment and recovery information (conducted by FORCE Field Scientists)	3
2.2. C-POD Data QA	5
2.3. Porpoise click detection rates.....	8
2.3.1. Overall summary of detection rates.....	9
2.3.2. C-POD detection rates for year 3 EEMP deployments 7-10	13
2.3.3 Comparison of year 3 EEMP porpoise detection rates with previous C-POD deployments.....	16
3. Discussion.....	18
4. Acknowledgements.....	19
5. References	19

List of Figures

Figure 1 Regional location of FORCE test site. Figure 2 Detailed location in Minas Passage.....	1
Figure 3 Locations of five monitoring C-PODs and CSTV turbine installed at Berth D. The hatched box denotes the FORCE demonstration area. Shallow water is depicted by warmer colours. C-POD locations are marked and labelled as E1 = East1, D1 = Berth D, W1 = West1, W2 = West2 and S2 = South2. Locations of three previously used C-POD locations (N1, E2, S1; black circles) are provided.....	3
Figure 4 Diagram of FORCE C-POD mooring.....	4
Figure 5 Distribution of Percent Time Lost across all 5 C-POD monitoring locations for the four year 3 EEMP deployment periods (Top left=D7, top right=D8, bottom left=D9, bottom right=D10).....	8
Figure 6. Entire FORCE C-POD deployment history at eight monitoring locations between 5 May 2011 and 14 August 2019. FORCE's EEMP (2016-2019) currently involves ten deployment periods denoted by the labels on the bottom x-axis and five C-POD monitoring locations. Two turbine deployments are highlighted (turbine 1 in November 2016 and turbine 2 in July 2018). The pink cross-hatch represent the presence of an operating turbine (termed 'turbine on'), while the pink tight square hatch represents turbine presence in free-spinning mode, and the pink wide square hatch represents turbine presence but not in free-spinning mode (only deployments 7-10). The grey shading denotes when at least one C-POD was operating.....	9
Figure 7 Summary of percent of days porpoise present across C-PODs by deployment scenario periods (data summarized from Table 4).....	13
Figure 8 Percent probability of detecting a porpoise in a 10-minute Interval ($P(\text{BinDPM}=1)$) at each C-POD monitoring location for the four year 3 EEMP deployment periods. Turbine 2 was briefly operational or free-spinning in July-August 2018 and present following this period (data summarized from Table 5).	15
Figure 9 Sum of DPM per day for each C-POD monitoring location for the four year 3 EEMP deployment periods (Top left=D7, top right=D8, bottom left=D9, bottom right=D10).	15
Figure 10 Percent probability of detecting a porpoise in a 10-minute Interval ($P(\text{BinDPM}=1)$) at each C-POD monitoring location for key deployment periods. The overall number of days associated with each dataset is provided in red at the bottom of the graph.....	16
Figure 11 Probability of detecting a porpoise per day at each of 5 C-POD monitoring locations with time of year controlled for. Orange bars correspond to dates turbine 1 was operational (Nov 7, 2016 – Apr 21, 2017). Blue bars represent the same days of the year, but for 'baseline' years (Pre turbine or no turbine 1; 318 days matched between Nov 7 and Apr 21), while black bars correspond to the same year 3 EEMP period (Nov 7, 2018 – Apr 21, 2019), when turbine 2 was present but non-operational.....	17

List of Tables

Table 1 Deployment location details of 5 C-PODs in Minas Passage	5
Table 2 C-POD deployment and retrieval information	6
Table 3 Definitions of deployment scenarios and associated summary of C-POD monitoring effort, turbine status, and EEMP details. The turbine operational period is highlighted in bold (*), the Year 2 EEMP deployments highlighted in italics (+), and the Year 3 EEMP deployments highlighted in blue (#).	10
Table 4 FORCE site monitoring summary: Percent of monitoring days with and without porpoise (all pods combined), and percent across each C-POD location during each deployment scenario. Number of days in region without porpoise (all pods combined), and median number of minutes when present (Interquartile Range) for each deployment scenario. The turbine operational period is highlighted in bold (*), the Year 2 EEMP deployments highlighted in italics (+), and the Year 3 EEMP deployments highlighted in blue (#).	11
Table 5 Descriptive statistics for the 5 C-POD locations for each deployment period. Percent probability (95% CI) of detecting a porpoise in a 10-minute Interval ($P(\text{BinDPM}=1)$).	14

List of Acronyms

BinDPM=1: At least one porpoise detected within a consecutive 10-minute period
$P(\text{BinDPM}=1)$: Probability of there being at least 1 detection positive minute of 10-minute period.
CI: Confidence interval
CSTV: Cape Sharp Tidal Venture
DPM: Detection Positive Minutes (a count of the number of minutes a porpoise is detected
E1: C-POD location East 1
D1: C-POD location specific to berth D.
EEMP: Environmental Effects Monitoring Program
FORCE: Fundy Ocean Research Center for Energy
GAM: Generalized Additive Model
GEE: Generalized Estimating Equation with a General Linear Model
IQR: Interquartile Range
OERA: Offshore Energy Research Association
S2: C-POD location South 2
W1: C-POD location West 1
W2: C-POD location West 2

1. Introduction and EEMP Objectives

Tidal energy is an excellent potential renewable energy source. Worldwide, only a small number of in-stream tidal turbines have been deployed to date. The Fundy Ocean Research Center for Energy (FORCE) is a Canadian non-profit institute that owns and operates a facility in the Bay of Fundy, Nova Scotia (Figure 1), where grid connected tidal energy turbines can be tested and demonstrated. It enables developers, regulators and scientists to study the performance and interaction of tidal energy turbines with the environment. The offshore test site is in the Minas Passage area of the Bay of Fundy west Cape Sharp, close to and west of Black Rock (Figure 2).



Figure 1 Regional location of FORCE test site. Figure 2 Detailed location in Minas Passage.

Harbor porpoise (*Phocoena phocoena*), the key marine mammal species in Minas Passage (Tollit et al. 2011; 2019, Wood et al. 2013 and Porskamp et al. 2015), use high frequency echolocation clicks to hunt and communicate and are known to be very susceptible to pulsed noise disturbance (Tougaard et al. 2009), but few studies have focused on exposure to continuous low frequency noise sources, such as those emitted by tidal turbines.

This year 3 final report describes the results of deployments 7 through 10 of the Marine Mammal C-POD Monitoring Program, put in place as part of FORCE's multi-year Environmental Effects Monitoring Program (EEMP) at its marine demonstration and testing facility in Minas Passage. The main objectives of the marine mammal EEMP are to assess long-term effects of direct and indirect stressors on harbor porpoise by monitoring porpoise activity and site use, with the primary objectives to assess: 1) Permanent avoidance of the mid field study area during turbine installation and operation. 2) Large magnitude (~50%) change in the distribution (echolocation activity levels) of a portion of the population in the study mid-field area (see SLR Consulting Ltd. 2015). C-PODs (Chelonia Ltd) incorporate a hydrophone, battery pack, memory, and a data-logger that detects and logs cetacean echolocation clicks 24 hours per day over extended periods. They store compressed data on each detected click and monitor 20-160 kHz continuously. C-PODs are typically deployed on bottom moorings for periods of three to four months, after which they need to be recovered and the data downloaded, before redeployments with new batteries. C-POD hydrophones are focused on detecting click trains of porpoises as well as other species of echolocating delphinids and do not detect non-echolocating whales (e.g., Right whales or minke

whales). C-POD monitoring has been ongoing since 2011 (see references above) and results from year 1 and 2 EEMP results are documented in Joy et al. (2017, 2018) and have been recently published in Tollit et al. (2019). These showed the installation and operation of a 2 MW OpenHydro turbine did not exclude porpoises over the mid-field study area, but GAM-GEE modelling identified a significant decrease in porpoise vocal activity when the turbine was operational but only at the closest two C-POD locations (200-230 m away). These studies also highlight a longer time series is believed required before robust conclusions can be drawn on turbine effects.

This report provides summary data for 416 days across the period between 5 May 2018 to 14 August 2019 in four separate deployments of 5 C-PODs. A second 2 MW OpenHydro tidal turbine was deployed by Cape Sharp Tidal Venture on 22 July 2018 and grid connected on 24 July 2018. The turbine is believed to have worked briefly (and then possible to have been free-spinning) until 9 August 2018 (i.e., within deployment 7). The non-operational nor free-spinning turbine was present for the rest of the year 3 EEMP (deployments 8-10). A period of less than 18 days of operational or free-spinning turbine was not considered sufficient for a robust GAM-GEE turbine effects analysis as undertaken in 2018, following the deployment of the first OpenHydro turbine (See Joy et al. 2018, Tollit et al. 2019). Following discussions with FORCE, this report summarizes overall porpoise detection rates since 2011, documents and compares C-POD detection data across each of the four year 3 EEMP deployment periods and additionally compares year 3 EEMP datasets with previous periods (including both baseline and previous turbine deployment periods).

The locations of the five long-term EEMP C-POD monitoring sites relative to the OpenHydro turbine deployment site are found in Figure 3. The locations of older C-POD monitoring sites are also provided as well as local bathymetric information and the location of FORCE demonstration area.

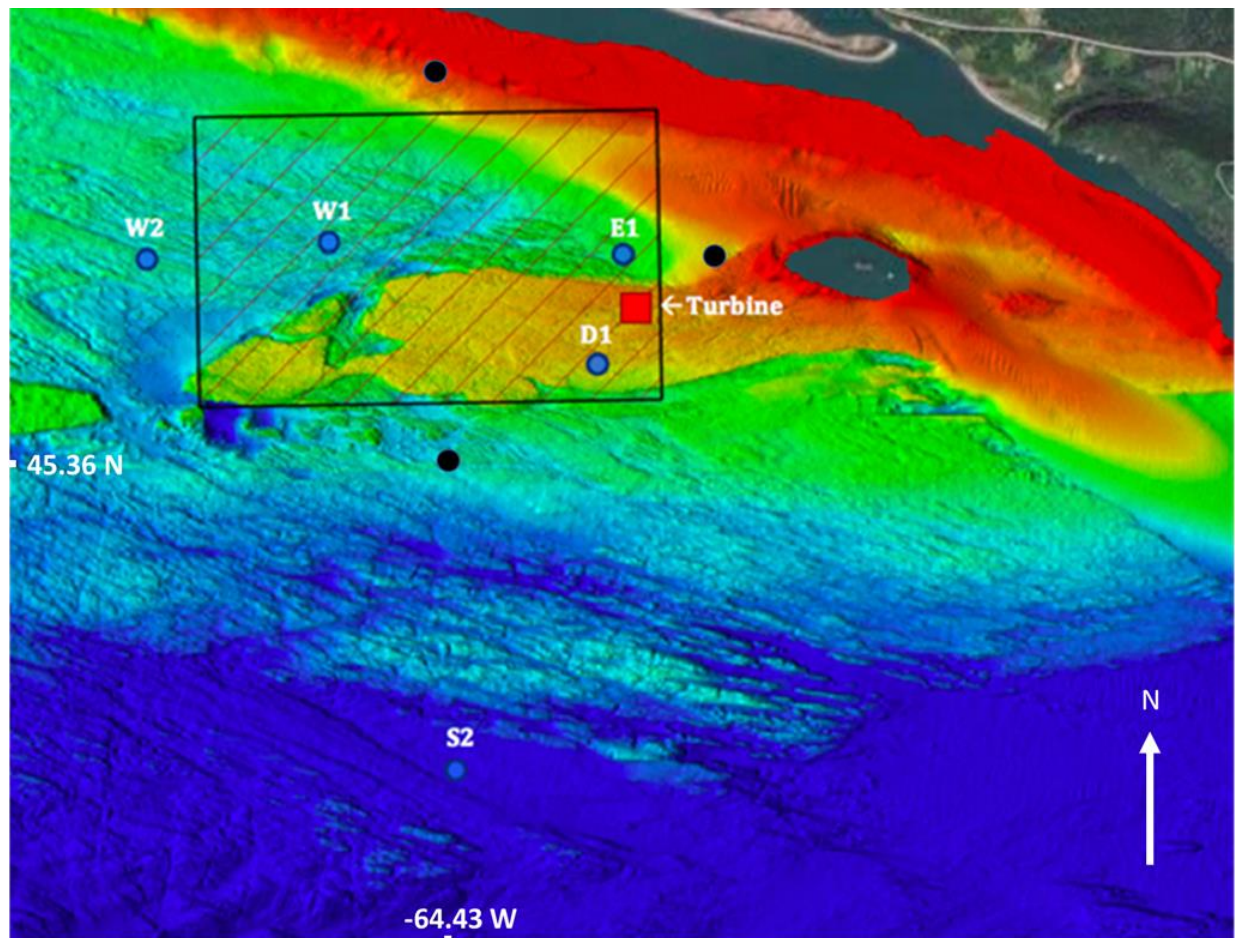


Figure 3 Locations of five monitoring C-PODs and CSTV turbine installed at Berth D. The hatched box denotes the FORCE demonstration area. Shallow water is depicted by warmer colours. C-POD locations are marked and labelled as E1 = East1, D1 = Berth D, W1 = West1, W2 = West2 and S2 = South2. Locations of three previously used C-POD locations (N1, E2, S1; black circles) are provided.

2. Methods and Results

2.1. C-POD deployment and recovery information (conducted by FORCE Field Scientists)

All C-PODs and associated moorings and buoys were loaded onto the modified lobster fishing boat in Parrsboro, Nova Scotia and deployed in a single tide. Each torpedo shaped C-POD is approximately 1.21 m (4 ft.) long and approximately 40 cm (16") in diameter. The C-PODs are assembled into a "subs package" containing the acoustic release mechanism and recovery buoy. This is connected by a 2.5 m long chain to an anchor made of several lengths of chain (Figure 4).

Deployment (lowering overboard) of the C-PODs was achieved by assembling each individual mooring on board. The mooring was placed in the water over the stern, the anchor then raised with the capstan via the a-frame mounted on the stern, lifted clear of the deck, and pushed forward away from the vessel and deployed using a quick release when safe to do so, allowing the C-POD and mooring to free fall to the sea bottom. Location, water depth and time of deployment were recorded after each release.

FORCE EEMP C-POD MOORING

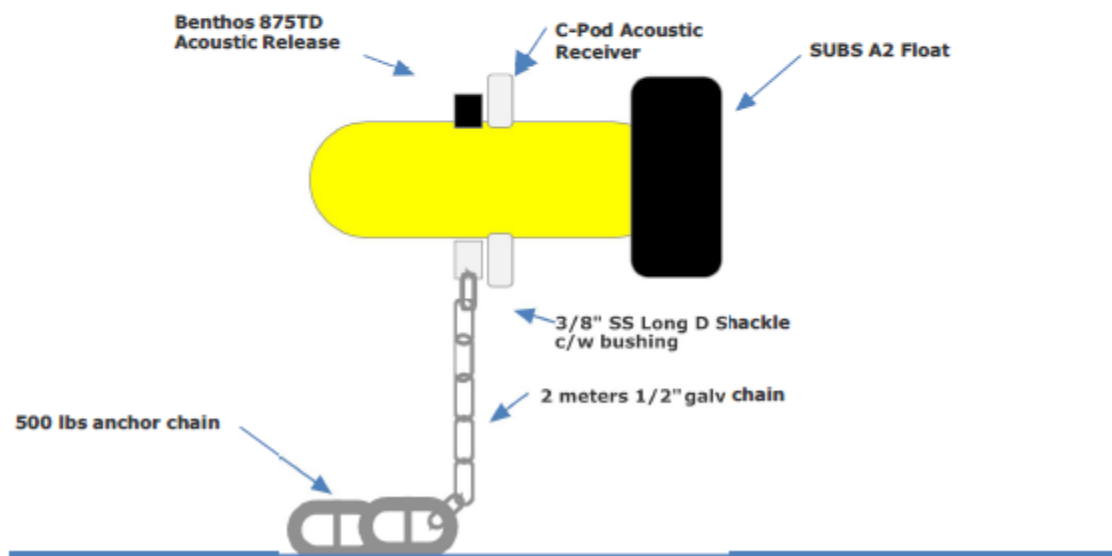


Figure 4 Diagram of FORCE C-POD mooring

Fine-scale details of the five EEMP deployment locations depicted in Figure 3 are provided in Table 1. Water depths measured during deployment ranged from 32-81 m. Locations were kept as similar as possible to those deployed in 2017 (EEMP deployment 1).

Table 1 Deployment location details of 5 C-PODs in Minas Passage

Deployment number	Location number	Deployment date	Latitude	Longitude	Depth (m)
7	W2	5/4/2018	45.36595	-64.4433	47
7	W1	5/4/2018	45.36555	-64.4352	48
7	S2	5/4/2018	45.3505	-64.4299	72
7	D1	5/4/2018	45.3628	-64.4234	33
7	E1	5/4/2018	45.3662	-64.4223	43
8	W2	9/6/2018	45.36592	-64.4435	46
8	W1	9/6/2018	45.36595	-64.4341	47
8	S2	9/6/2018	45.35028	-64.4297	69
8	S2 (re-deploy)	10/10/2018	45.3502	-64.4297	66
8	D1	9/6/2018	45.3627	-64.424	32
8	E1	9/6/2018	45.3662	-64.4262	40
8	E1 (re-deploy)	10/10/2018	45.36622	-64.4264	34
9	W2	12/6/2018	45.36605	-64.4433	58
9	W1	12/6/2018	45.36622	-64.4346	57
9	S2	12/6/2018	45.35017	-64.4295	81
9	D1	12/6/2018	45.36278	-64.4237	44
9	E1	12/6/2018	45.36625	-64.4264	50
10	W2	5/3/2019	45.3660	-64.4435	56
10	W1	5/3/2019	45.36621	-64.4344	59
10	S2	5/3/2019	45.35017	-64.4296	78
10	D1	5/3/2019	45.36285	-64.4238	41
10	E1	5/3/2019	45.36623	-64.4263	78

2.2. C-POD Data Quality Assurance

C-POD.exe V2.044 was used to process the data and custom Matlab R2016a code used to calculate statistical outputs and create data plots using detection positive minutes (DPM) per day and DPM per 10-minute period (DPMp10M) as the key metrics for comparison. The quality assurance assessment specifically targets if non-biological interference has occurred, confirms that the porpoise click detector is operational and assess the scale of % time lost due to click maximum buffer exceedance (due to internal memory restrictions, non-target noise from sediment movement and moorings result in periods of lost recording time in each minute). C-PODs were deployed and retrieved as shown in Table 2 below. All times in this report are given in Universal Time Coordinated (UTC).

In summary, 5 C-PODs were deployed on 4 May 2018 (Table 2). Data were collected for this 7th deployment throughout the entire 111-day monitoring period on four C-PODs, with the battery expiring on 10 August on the C-POD at E1 (for a total of 98 monitoring days or 13 days loss of data). 5 C-PODs were next deployed on 6 September 2018. Data were collected for this 8th deployment

throughout the entire 86-day monitoring period, however C-PODs at E1 and S2 were released early (found 18 September) and redeployed on 10 October, with a loss of 21 days of data within this period. 5 C-PODs were then deployed on 6 December 2018. Data were collected for this 9th deployment throughout the entire 117-day monitoring period, however C-POD at W1 released early (20 February) with a loss of 37 days of data within this period, while an unknown failure of the C-POD at W2 resulted in a 25 day loss of data within this period. Finally, 5 C-PODs were deployed on 3 May 2019. Data were collected for this 10th deployment throughout the entire 103-day monitoring period, however C-PODs at E1 ran out of power 9 days early. There was no evidence of data corruption or obvious clock drift across these four deployments.

Table 2 C-POD deployment and retrieval information

Deployment number	Location number	C-POD number	Deployment date and time	Retrieval date and time
7	W2	2792	5/4/2018 T12:35:00	8/23/2018 T19:59:00
7	W1	2793	5/4/2018 T12:42:00	8/23/2018 T20:09:00
7	S2	2931	5/4/2018 T12:55:00	8/23/2018 T19:45:00
7	D1	2790	5/4/2018 T14:10:00	8/23/2018 T20:33:00
7	E1	2765	5/4/2018 T14:15:00	8/23/2018 T20:23:00
8	W2	2792	9/6/2018 T18:39:57	11/30/2018 T15:15:55
8	W1	2793	9/6/2018 T18:47:40	11/30/2018 T15:28:15
8	S2	2931	9/6/2018 T18:29:45	9/18/2018 T=unknown
8	S2 re-deploy	2931	10/10/2018 T10:29:10	11/30/2018 T16:00:05
8	D1	2790	9/6/2018 T18:58:59	11/30/2018 T15:46:05
8	E1	2765	9/6/2018 T18:54:36	9/18/2018 T=unknown
8	E1 re-deploy	2765	10/10/2018 T10:41:50	11/30/2018 T15:38:08

9	W2	2792	12/6/2018 T16:22:45	3/29/2019 T17:05:40
9	W1	2793	12/6/2018 T16:17:29	2/20/2019 (Released Early)
9	S2	2931	12/6/2018 T16:34:41	3/29/2019 T16:51:35
9	D1	2790	12/6/2018 T16:07:30	3/29/2019 T17:20:22
9	E1	2765	12/6/2018 T16:11:55	3/29/2019 T17:29:15
10	W2	2792	5/3/2019 T15:48:07	8/14/2019 T16:53:32
10	W1	2793	5/3/2019 T15:54:20	8/14/2019 T16:46:06
10	S2	2931	5/3/2019 T15:25:14	8/14/2019 T17:19:07
10	D1	2790	5/3/2019 T16:03:10	8/14/2019 T16:23:18
10	E1	2765	5/3/2019 T16:09:18	8/14/2019 T16:38:50

C-PODs monitor underwater noise each minute, however, in each minute, the units will only 'listen' until a maximum memory buffer is reached (called the ClickMax buffer). If this buffer is reached then the remainder of the minute monitoring is lost (termed Percent Time Lost). This occurs largely when non-biological clicks associated with sediment transfer are high, most often during periods of relatively high current velocity (Joy et al. 2018). Percent Time Lost has little effect on data quality between an ebb current speed of <2.4 m/s (95% of 10-minute periods) and a flood current speed of <2 m/s (71% of 10-minute periods) and has notable effects at ebb current speeds beyond 2.9 m/s (estimated 1% of 10-minute periods) and flood current speeds beyond 3.5 m/s (estimated 4.5% of 10-minute periods). At these current speeds C-POD monitoring is clearly less reliable, noting that these speeds only occur a very small fraction of the tidal cycle. Time lost calculated across all five C-PODs for each of year 3 EEMP deployment is presented in Figure 5. For all deployments Percent Time Lost was similar with a median of 0% and interquartile range of 0-0% and distributions similar to previous years. In other words, there was no Time Lost in >75% of all minutes collected on all C-PODs.

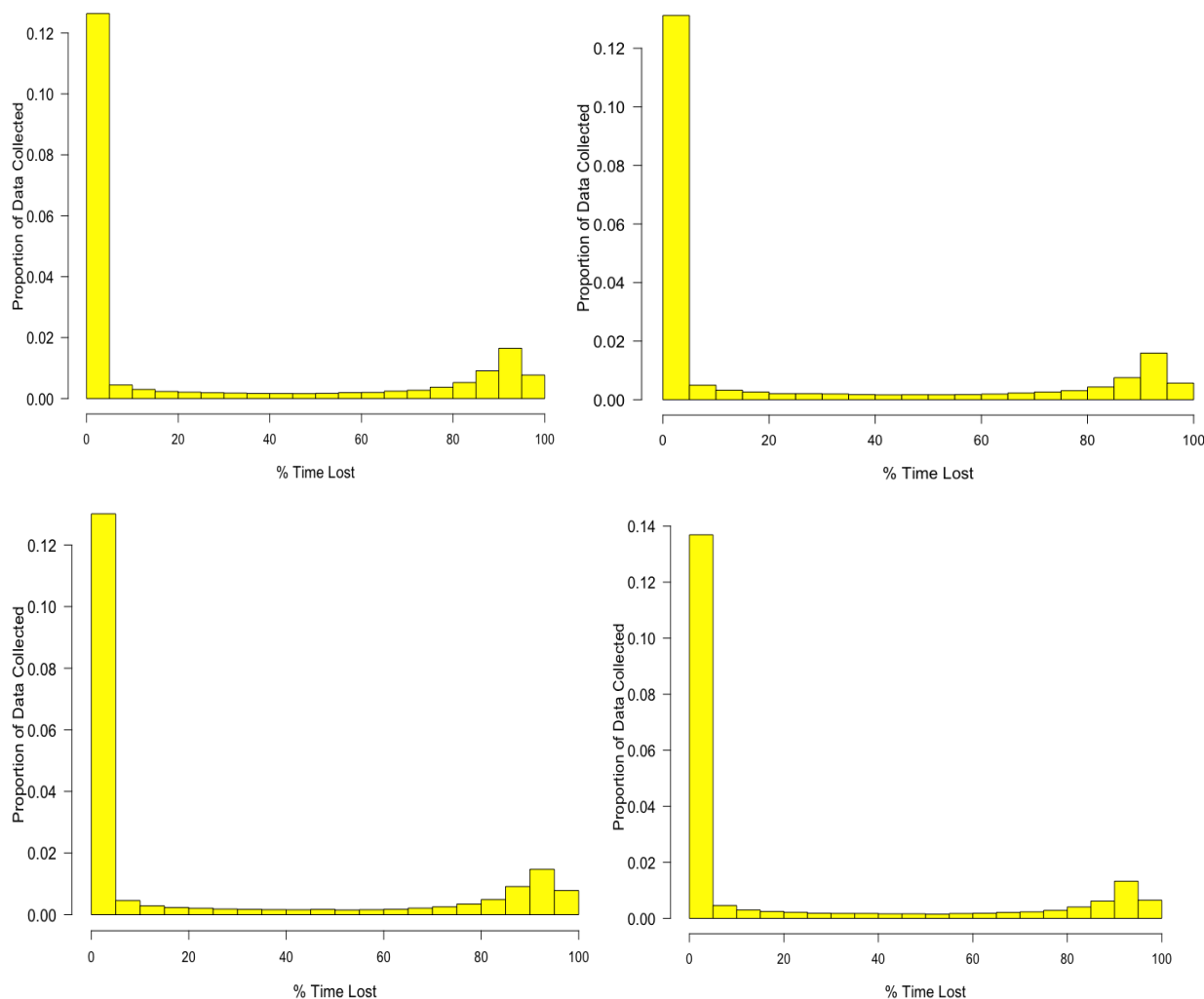


Figure 5 Distribution of Percent Time Lost across all 5 C-POD monitoring locations for the four year 3 EEMP deployment periods (Top left=D7, top right=D8, bottom left=D9, bottom right=D10).

2.3. Porpoise click detection rates

Across all years of the Minas Passage C-POD monitoring study, there have been a total of 6,519 C-POD days across 1,626 calendar days, with a total of 929,846 10-minute monitoring periods (Table 3, Figure 6). Year 3 EEMP deployments covered 416 calendar day, 1868 C-POD days with a total of 265,646 10-minute monitoring periods (Table 3).

Figure 6 provides an overview of the temporal and spatial coverage across all C-POD deployments since 2011 and includes periods of turbine operation and free-spinning presence (denoted by pink cross and tight square hatch respectively). Less than 18 days of turbine operation (and/or free-spinning activity) was believed to have occurred in year 3 EEMP deployment 7. This same turbine was present but non-operational (nor free-spinning) throughout the last three deployments (8-10) in this year 3 EEMP period, denoted by the wide pink square hatch (Figure 6). This period represents 305 monitoring days.

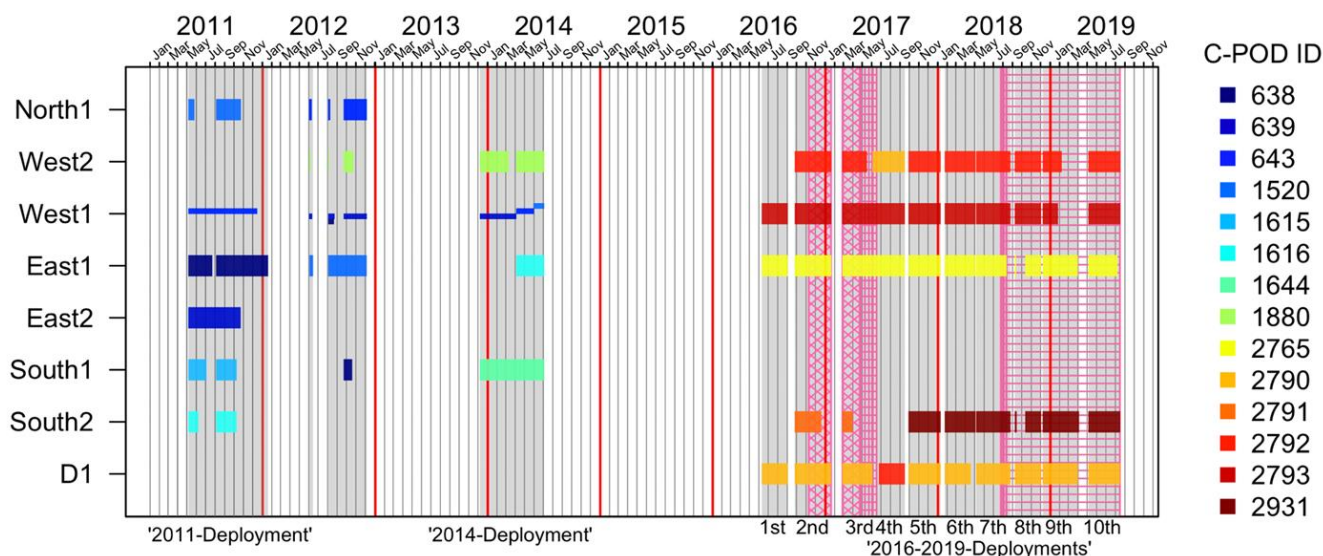


Figure 6. Entire FORCE C-POD deployment history at eight monitoring locations between 5 May 2011 and 14 August 2019. FORCE's EEMP (2016-2019) currently involves ten deployment periods denoted by the labels on the bottom x-axis and five C-POD monitoring locations. Two turbine deployments are highlighted (turbine 1 in November 2016 and turbine 2 in July 2018). The pink cross-hatch represent the presence of an operating turbine (termed 'turbine on'), while the pink tight square hatch represents turbine presence in free-spinning mode, and the pink wide square hatch represents turbine presence but not in free-spinning mode (only deployments 7-10). The grey shading denotes when at least one C-POD was operating.

2.3.1. Overall summary of detection rates

Porpoises were detected on 98.8% of days across all C-PODs combined (in other words on any one or more C-POD), with an overall median of 8 minutes per day, and with the probability of porpoise presence detected in 7.0% of all 10-minute periods across this overall monitoring period. This latter statistic (termed 'PBinDPM=1' within Joy et al. 2018) is considered the optimal comparative metric to assess trends and effects, as mean DPM values are skewed by the number of periods without detection. Across individual C-PODs, detection rates averaged 88.5% of days with a C-POD median detection positive minutes (DPM) per day of 8 minutes (IQR = 3-17) (Table 4).

Porpoises were detected between 95-100% of days across all C-PODs combined for the year 3 EEMP deployments, with median DPMs of 5-15 minutes per day across the four separate deployments. Values for deployments 7 and 10 are equal or higher than values collected during 2011-2014 baseline, noting both these deployments cover a period of May through August, a peak period of past porpoise activity. Deployment 9, covering a period of December through March saw the lowest detection rates, noting these remained higher than when the turbine was operational in 2016-2017. No dolphin clicks were detected in Minas Passage during this study's C-POD deployments, as also found during previous deployments (Wood et al. 2013; Joy et al. 2017; 2018). Mean time lost averaged 22.6%, with a median of 0% and interquartile range of 0-0%. Figure 7 presents an overall summary of percent of days porpoise present across C-PODs by deployment scenario periods detailed in Table 4. Porpoise presence varies between 74% and 100%, with the lowest value observed during the first period of turbine operations in 2016 and the highest value observed when turbine 1 was present but only free-spinning.

Table 3 Definitions of deployment scenarios and associated summary of C-POD monitoring effort, turbine status, and EEMP details. The turbine operational period is highlighted in bold (*), the Year 2 EEMP deployments highlighted in italics (+), and the Year 3 EEMP deployments highlighted in blue (#).

Deployment Scenario and Turbine Status	Deployment Dates	# of Days Monitored	# of Pod-Days	# 10-Min Intervals
2011 Deployment: Absent	2011-05-05 - 2012-01-17	258	958	136,446
2012 Deployment: Absent	2012-05-31 - 2012-12-03	137	391	56,795
2014 Deployment: Absent	2013-12-06 - 2014-07-01	208	689	99,108
2016 Deployment 1: Absent	2016-06-08 - 2016-08-30	84	252	35,775
2016 Deployment 2: Absent	2016-09-23 - 2016-11-06	45	225	32,065
*2016 Deployment 2: Turbine 1 Operational	2016-11-07 - 2017-01-18	73	332	47,403
+*2017 Deployment 3: Turbine 1 Operational	2017-02-24 - 2017-04-21	57	262	37,229
<i>+2017 Deployment 3: Turbine 1 Free-spinning</i>	<i>2017-04-22 - 2017-06-01</i>	41	146	20,756
<i>+2017 Deployment 4: Turbine 1 Free-spinning</i>	<i>2017-06-03 - 2017-06-15</i>	13	39	5,382
<i>+2017 Deployment 4: Turbine 1 Absent</i>	<i>2017-06-16 - 2017-09-14</i>	91	357	51,009
<i>+2017 Deployment 5: Turbine 1 Absent</i>	<i>2017-09-27 - 2018-01-08</i>	104	520	74,135
<i>+2018 Deployment 6: Turbine 1 Absent</i>	<i>2018-01-23 - 2018-05-18</i>	99	480	68,094
#*2018 Deployment 7: Turbine 2 operational or free-spinning 07-22 to 08-09, then present (non-operational/non-free-spinning)	2018-05-05 - 2018-08-23	111	542	77,419
#2018 Deployment 8: Turbine 2 Present, non-operational/non-free-spinning	2018-09-07 - 2018-11-30	85	367	51,722
#2018 Deployment 9: Turbine 2 Present, non-operational/non-free-spinning	2018-12-07 - 2019-04-02	117	453	64,418
#2019 Deployment 10: Turbine 2 Present, non-operational/non-free-spinning	2019-05-04 - 2019-08-14	103	506	72,090
All Deployment data		1,626	6,519	929,846

Table 4 FORCE site monitoring summary: Percent of monitoring days with and without porpoise (all pods combined), and percent across each C-POD location during each deployment scenario. Number of days in region without porpoise (all pods combined), and median number of minutes when present (Interquartile Range) for each deployment scenario. The turbine operational period is highlighted in bold (*), the Year 2 EEMP deployments highlighted in italics (+), and the Year 3 EEMP deployments highlighted in blue (#).

Deployment Scenario and Turbine Status	Overall % Days Porpoise Present	% Days Across C-PODs Porpoise present	Days Without Porpoise (Days Monitored)	Median (IQR) of Minutes of Detection if Present
2011 Deployment: Absent	99.2	83.2	2 (258)	7 (2, 17)
2012 Deployment: Absent	95.6	82.9	6 (137)	5 (1, 13)
2014 Deployment: Absent	99.0	87.5	2 (208)	9 (3, 16)
2016 Deployment 1: Absent	98.8	92.5	1 (84)	7 (3.8, 14)
2016 Deployment 2: Absent	100.0	76.4	0 (45)	4 (1, 10)
*2016 Deployment 2: Turbine 1 Operational	97.3	73.8	2 (73)	3 (0, 7)
+*2017 Deployment 3: Turbine 1 Operational	100.0	92.4	0 (57)	7 (3, 14.8)
<i>+2017 Deployment 3: Turbine 1 Free-spinning</i>	<i>100.0</i>	<i>95.2</i>	<i>0 (41)</i>	<i>7 (4, 12)</i>
<i>+2017 Deployment 4: Turbine 1 Free-spinning</i>	<i>100.0</i>	<i>100</i>	<i>0 (13)</i>	<i>12 (7, 18.5)</i>
<i>+2017 Deployment 4: Turbine 1 Absent</i>	<i>100.0</i>	<i>96.9</i>	<i>0 (91)</i>	<i>12 (6, 21)</i>
<i>+2017 Deployment 5: Turbine 1 Absent</i>	<i>100.0</i>	<i>88.3</i>	<i>0 (104)</i>	<i>8 (2.8, 20)</i>
<i>+2018 Deployment 6: Turbine 1 Absent</i>	<i>100.0</i>	<i>88.3</i>	<i>0 (99)</i>	<i>7 (2, 16)</i>
#*2018 Deployment 7: Turbine 2 operational or free-spinning 07-22 to 08-09, then present (non-operational/non-free-spinning)	100.0	98	0(111)	12 (6, 20)
#2018 Deployment 8: Turbine 2 Present, non-operational/non-free-spinning	98.8	84.7	1(85)	5 (1.5, 11)

#2018 Deployment 9: Turbine 2 Present, non-operational/non-free-spinning	94.9	88.1	6(117)	7 (3, 19)
#2019 Deployment 10: Turbine 2 Present, non-operational/non-free-spinning	100.0	99.8	0(103)	15 (8, 24)
All Deployment data	98.8	88.5	20(1626)	8 (3, 17)

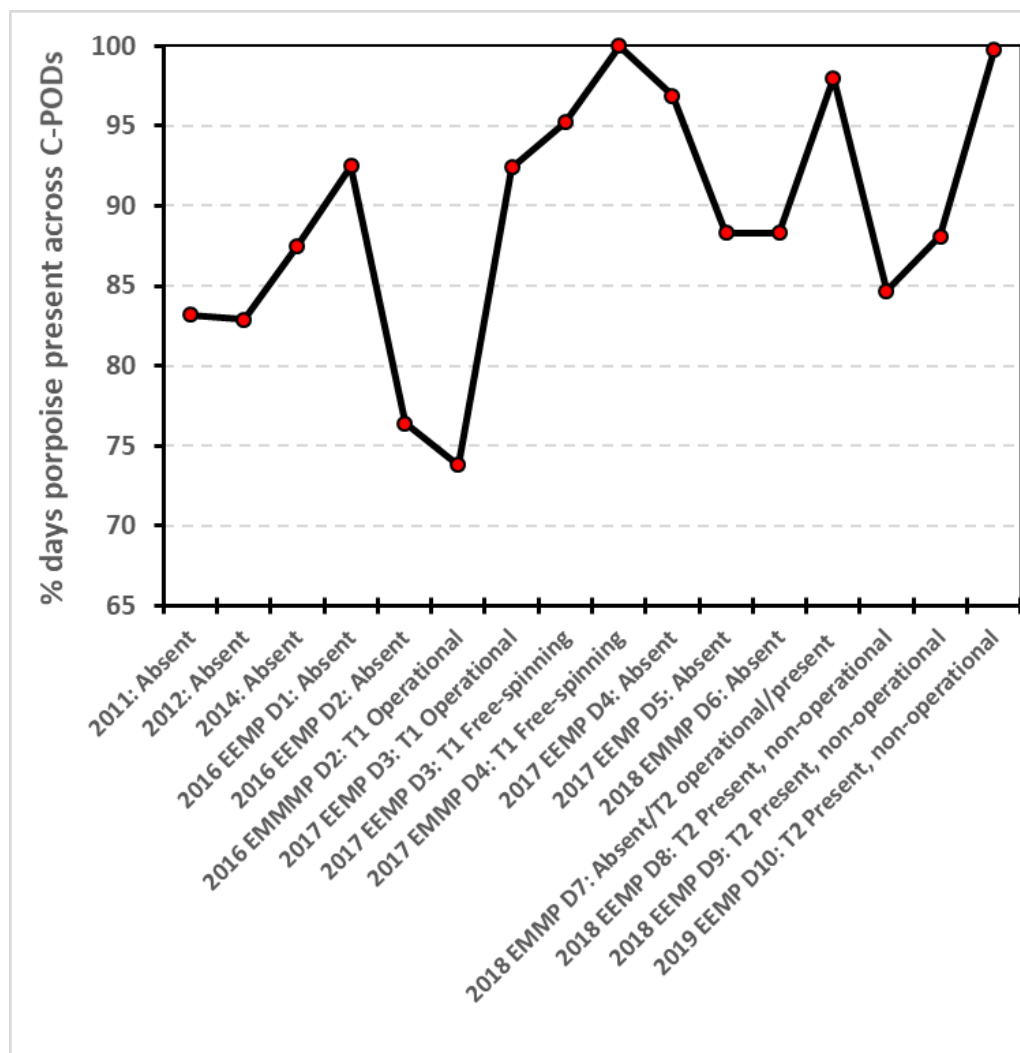


Figure 7 Summary of percent of days porpoise present across C-PODs by deployment scenario periods (data summarized from Table 4).

2.3.2. C-POD detection rates for year 3 EEMP deployments 7-10

Table 5 provides summary of percent probability of detecting a porpoise in a 10-minute interval ($P(\text{BinDPM}=1)$), together with 95th percentile confidence intervals. Porpoise detection rates clearly vary across both locations and deployments, with D1 values typically low (deployment average 3.2%) and S2 and W2 typically high (deployment averages of 6.6% and 6.4% respectively). E1 averaged 4.3% across all four deployments, while W1 averaged 4.8%. A peak rate of 8.8% was observed at E1 and W2 during deployment 10, while the lowest rate of 1.4% was observed at D1 during deployment 8. With the exception of the site located in deeper water (S2), detection rates are consistently higher in summer deployments (7 and 10) compared to the fall through spring deployments 8 and 9 (see Figure 8).

A similar pattern is observed when summing all detection positive minutes per day (Figure 9). Median rates overall are higher (12-15 minutes/day) in summer deployments 7 and 10 (especially W2), compared to 5-7 minutes during deployments 8 and 9. Low rates at D1 (as little as 1

minute/day) and E1 and conversely high rates (peak of 24 minutes/day) in the deeper water S2 site were notable for deployments 8 and 9.

Table 5 Descriptive statistics for the 5 C-POD locations for each deployment period. Percent probability (95% CI) of detecting a porpoise in a 10-minute Interval ($P(\text{BinDPM}=1)$).

Deployment number	Location number	Mean percent ($P(\text{BinDPM}=1)$ (95%ile C.I.)	# of 10-minute Intervals
7	W2	8.03 (7.61, 8.47)	15865
7	W1	6.55 (6.18, 6.95)	15867
7	E1	3.5 (3.21, 3.83)	13953
7	S2	5.97 (5.61, 6.35)	15867
7	D1	4.82 (4.5, 5.17)	15867
8	W2	3.92 (3.58, 4.28)	12075
8	W1	2.67 (2.39, 2.97)	12075
8	E1	2.11 (1.8, 2.46)	7638
8	S2	6.95 (6.4, 7.54)	7859
8	D1	1.37 (1.18, 1.6)	12075
9	W2	4.93 (4.48, 5.41)	8626
9	W1	3.57 (3.15, 4.04)	6841
9	E1	2.58 (2.34, 2.84)	16128
9	S2	7.14 (6.76, 7.54)	16695
9	D1	1.89 (1.69, 2.12)	16128
10	W2	8.79 (8.34, 9.27)	14682
10	W1	6.27 (5.88, 6.67)	14682
10	E1	8.82 (8.34, 9.31)	13362
10	S2	6.27 (5.88, 6.67)	14682
10	D1	4.85 (4.51, 5.21)	14682

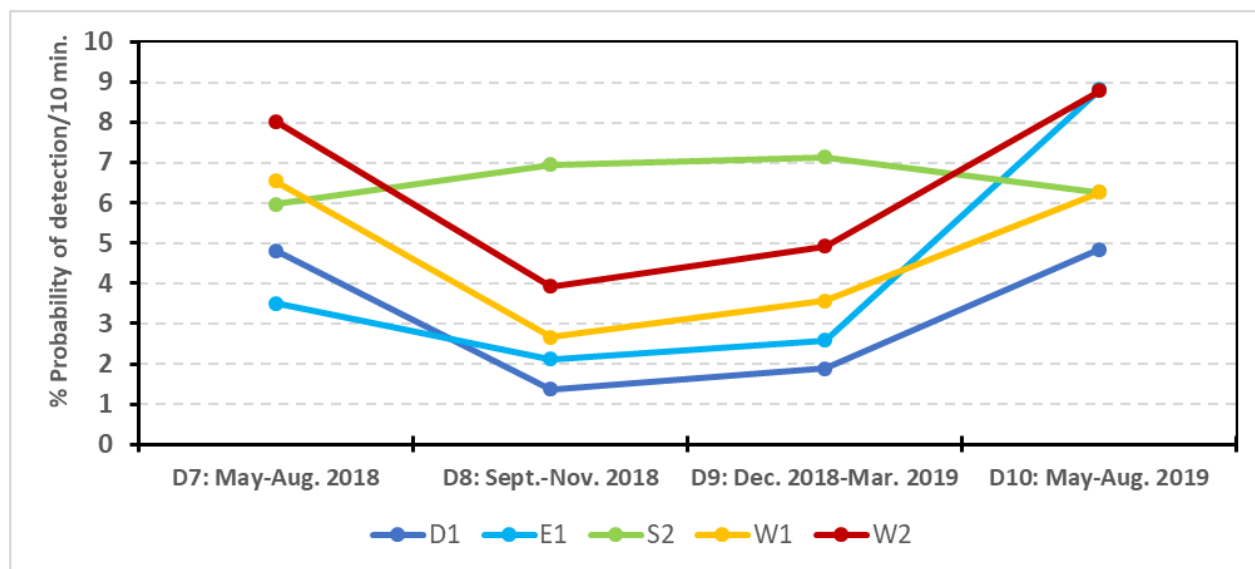


Figure 8 Percent probability of detecting a porpoise in a 10-minute Interval ($P(\text{BinDPM}=1)$) at each C-POD monitoring location for the four year 3 EEMP deployment periods. Turbine 2 was briefly operational or free-spinning in July-August 2018 and present following this period (data summarized from Table 5).

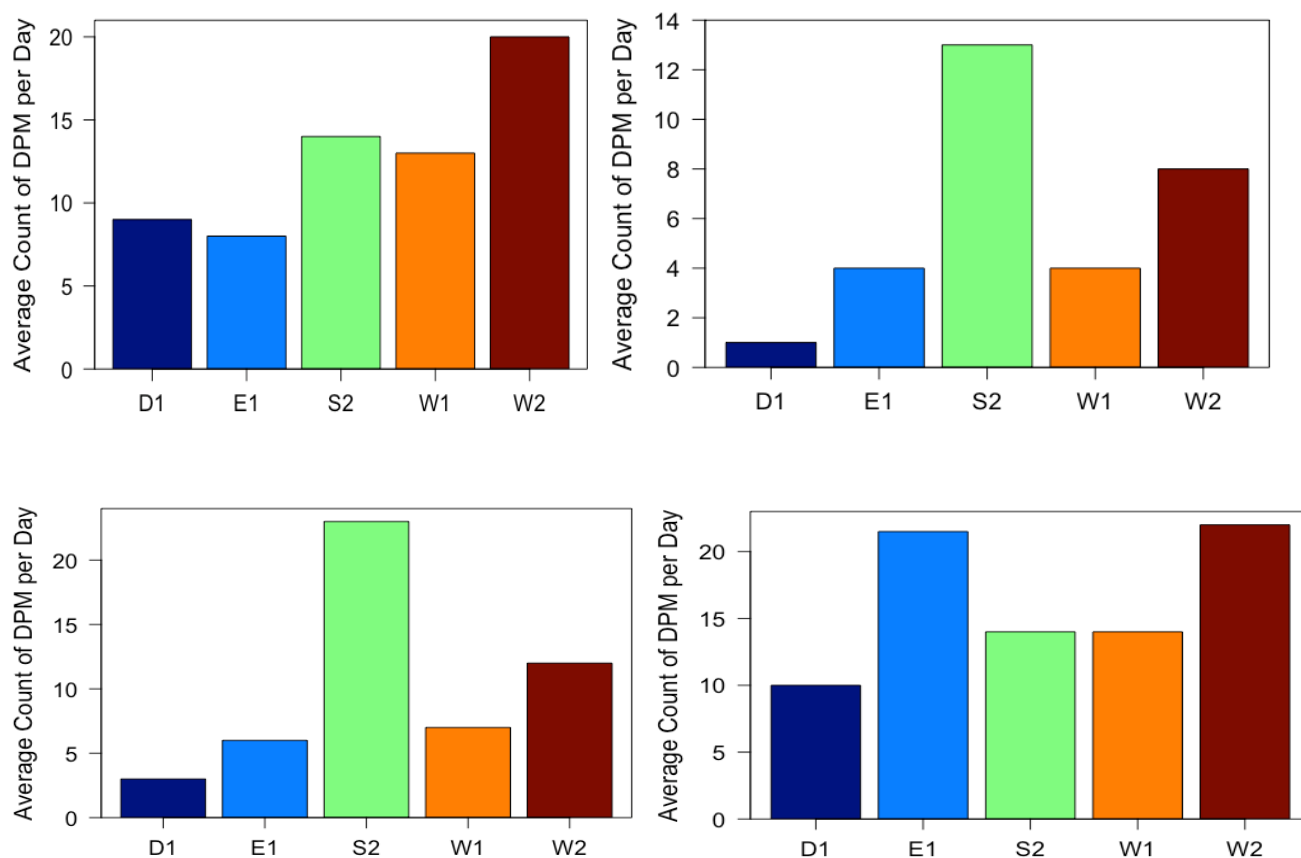


Figure 9 Sum of DPM per day for each C-POD monitoring location for the four year 3 EEMP deployment periods (Top left=D7, top right=D8, bottom left=D9, bottom right=D10).

2.3.3 Comparison of year 3 EEMP porpoise detection rates with previous C-POD deployments

C-POD deployment scenarios were combined into logical time periods before and after each turbine deployment and percent probability of detecting a porpoise in a 10-minute interval ($P(\text{BinDPM}=1)$) at each C-POD deployment location calculated for each period (Figure 10). These periods include all monitoring periods up to the deployment of turbine 1 in 2016 (a total of monitoring 648 days, termed Pre Turbine 1), the 130 day period C-PODs were present when turbine 1 was operational (Turbine 1 on) and the 54 day period it was considered to be free-spinning. There was a 371-day monitoring period between turbine 1 removal and the deployment of turbine 2 (termed Post Turbine 1). There was then a short 18-day period of turbine 2 operations and finally after turbine 2 became non-operational, there was a 305-day monitoring period of turbine 2 presence. No data was available for S2 during the Turbine 1 free-spin period. This summary synthesis analysis reiterates a number of previously observed patterns, for example the lower rates typically observed at D1 and E1 and higher rates typically observed at W2 and S2, as well as reductions observed during the Turbine 1 on period, followed by detection rates returning to Pre turbine 1 (baseline) levels. The period of turbine 2 operations is short, relatively small declines are seen at D1, E1 and S2 and increases observed at W1 and W2, but any interpretation is cautioned. Detection rates with turbine 2 present but non-operational are observed to be higher or similar to baseline (no turbine present) rates observed.

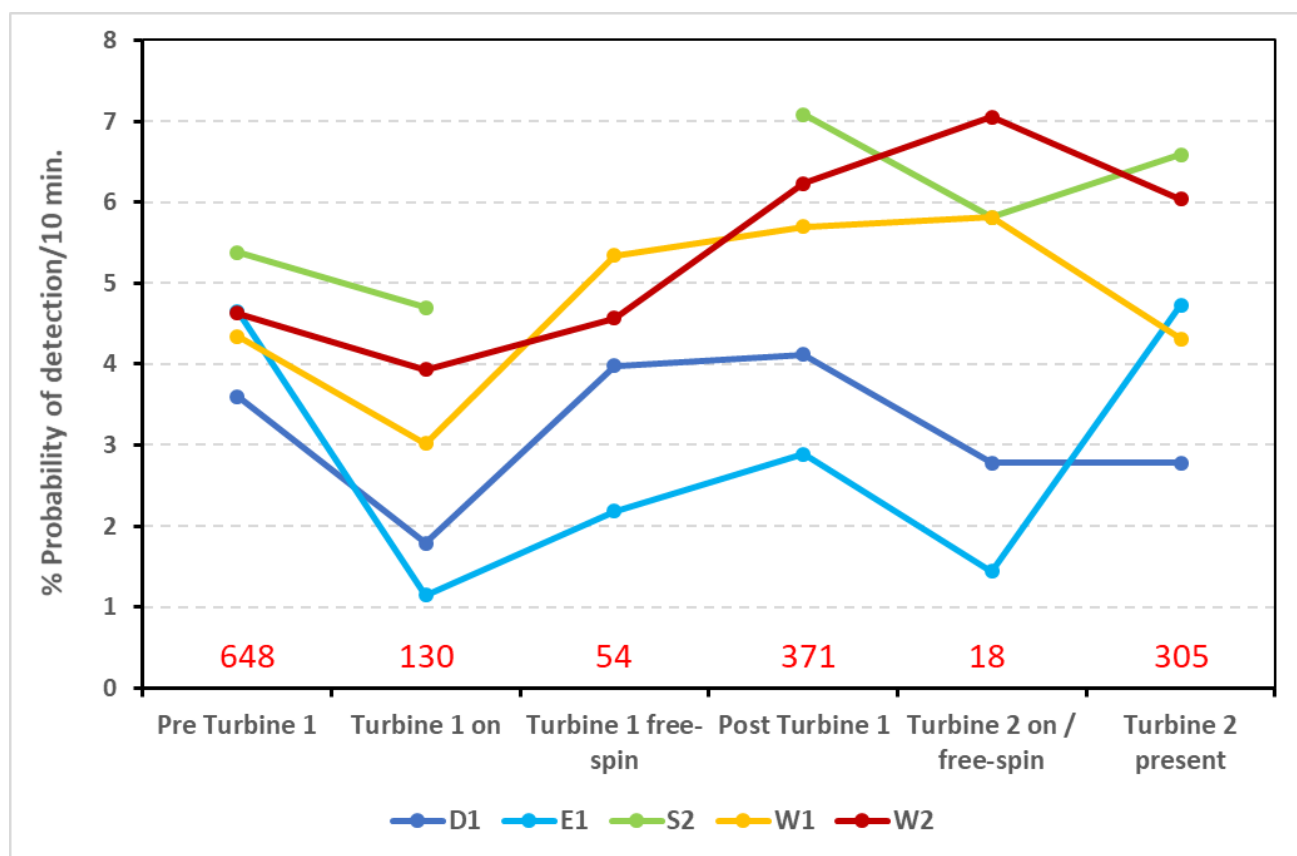


Figure 10 Percent probability of detecting a porpoise in a 10-minute Interval ($P(\text{BinDPM}=1)$) at each C-POD monitoring location for key deployment periods. The overall number of days associated with each dataset is provided in red at the bottom of the graph.

The interpretation that the presence of a non-operational turbine (turbine 2 present) has no marked effect on porpoise activity was explored further by taking into account temporal variability. Joy et al. (2018) compared the probability of detecting a harbour porpoise during the 166-day turbine operation period of 2016-2017 with the same Julian Days for two baseline years when the turbine was absent. This approach takes into account the primary variable affecting porpoise detection in the regional C-POD dataset (Joy et al. 2018), that of time of year. This analysis showed D1 and E1 having the biggest decline in detectability with turbine 1 present (particularly seen at E1). The same Julian Days period was selected for data collected during EEMP year 3, during which a non-operating turbine was present (Figure 11). This direct comparison indicated that porpoise detections in 2018-2019 were well above or similar to previously collected baseline values, with all values exceeding 90%. It is reasonable to conclude that the effect of a turbine structure had no detectable effect on porpoise detection rates in the mid-field study area.

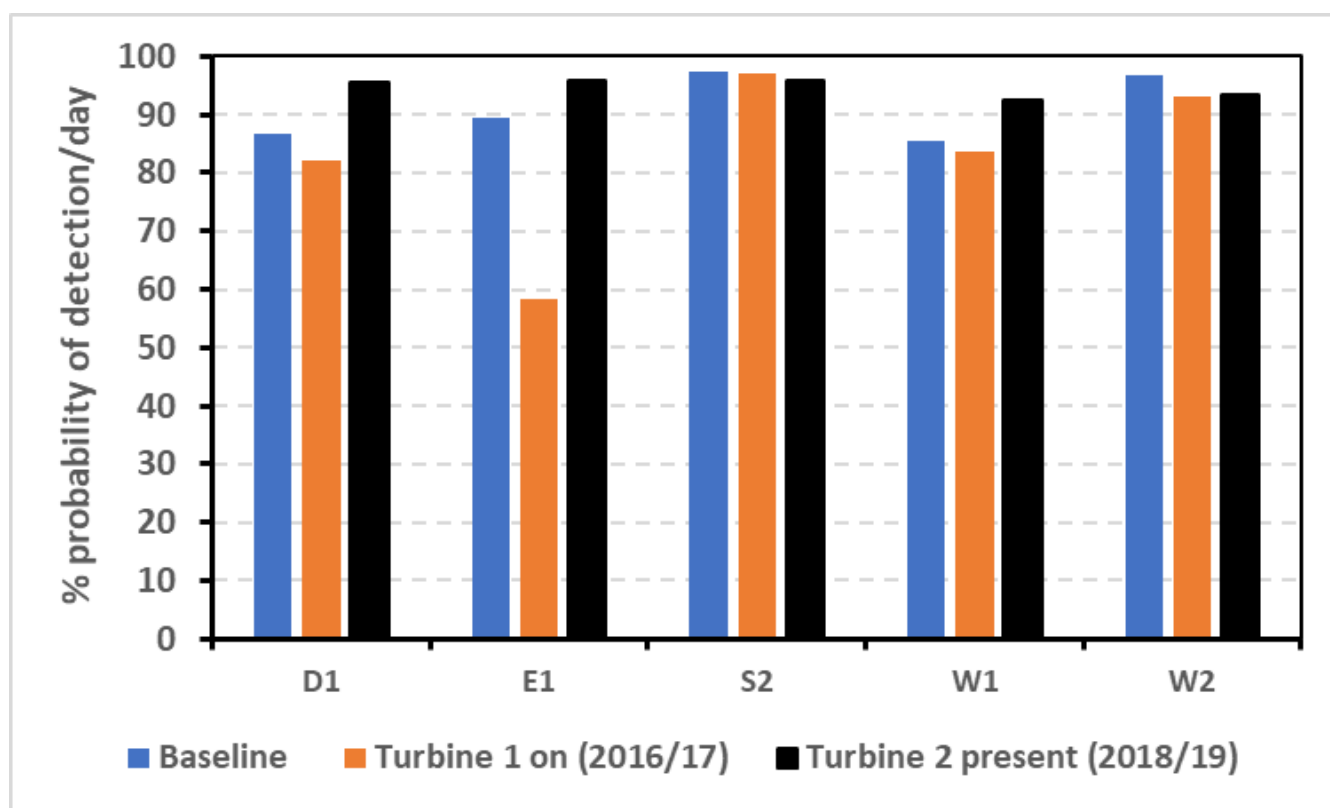


Figure 11 Probability of detecting a porpoise per day at each of 5 C-POD monitoring locations with time of year controlled for. Orange bars correspond to dates turbine 1 was operational (Nov 7, 2016 – Apr 21, 2017). Blue bars represent the same days of the year, but for ‘baseline’ years (Pre turbine or no turbine 1; 318 days matched between Nov 7 and Apr 21), while black bars correspond to the same year 3 EEMP period (Nov 7, 2018 – Apr 21, 2019), when turbine 2 was present but non-operational.

3. Discussion

Harbour porpoise use echolocation to hunt and communicate (Kastelein et al. 2002), and they are known to be susceptible to noise disturbance (Tougaard et al. 2009). Tidal turbines have the potential to cause acoustic effects on porpoise from continuous low-frequency noise, noting that emitted noise levels and range of effects will likely vary with current speed (Ellison et al. 2012, Polagye et al. 2011). The main objectives of FORCE's marine mammal EEMP in Minas Passage are to assess long-term effects of direct and indirect stressors on harbour porpoise by monitoring their activity and spatial use around Berth D and other tidal turbine berth deployments. C-POD hydrophones can detect echolocating cetacean species including dolphins, but not whales.

This echolocating Marine Mammal EEMP Report describes the results of the third year of the C-POD monitoring program as part of FORCE's multi-year (2016-2021) EEMP at its marine demonstration and testing facility in Minas Passage. Five C-PODs were successfully deployed through four deployments (5 May 2018 to 14 August 2019, termed deployments 7 through 10) and collected porpoise detection data across 416 calendar days, 1868 C-POD days with a total of 265,646 10-minute data periods. Across all years of the Minas Passage C-POD monitoring study, there have been a total of 6,519 C-POD days across 1,626 calendar days, with a total of 929,846 10-minute periods. To date, porpoises have been detected on 98.8% of days, with an overall average median of 8 detection minutes per day and with the minimum estimate of the probability of porpoise presence detection in 7.0% of all 10-minute periods. Across individual C-PODs, overall detection rates averaged 88.5% of days and an IQR of 3-17 detection minutes per day. Average percent time lost due to sediment interference was 22.6%, with a median 0%, similar to previous studies at these locations. No dolphin clicks were detected in Minas Passage during this study's C-POD deployments, as also found during previous deployments (Wood et al. 2013; Joy et al. 2018).

A second 2 MW OpenHydro tidal turbine was deployed by Cape Sharp Tidal Venture on 22 July 2018 and grid connected on 24 July 2018. The turbine is believed to have worked briefly (and then possible to have been free-spinning) until 9 August 2018 (i.e., within deployment 7). The non-operational nor free-spinning turbine was present for the remaining year 3 EEMP (i.e., deployments 8-10). A period of less than 18 days of operational or free-spinning turbine was not considered sufficient for a robust GAM-GEE turbine effects analysis as undertaken in 2018 following the deployment of the first OpenHydro turbine (See Joy et al. 2018, Tollit et al. 2019). Following discussions with FORCE, this report summarizes overall porpoise detection rates since 2011, documents and compares C-POD detection data across each of the four year 3 EEMP deployment periods and additionally compares year 3 EEMP datasets with previous periods (including both baseline and previous turbine deployment periods).

Porpoises were detected between 95-100% of days across all C-PODs combined for the year 3 EEMP deployments, with medians of 5-15 detection minutes per day across the four separate deployments (IQR 1.5-24). Values for deployments 7 and 10 are equal or higher than values collected during 2011-2014 baseline studies, noting both these deployments cover a period of May through August, a peak period of past porpoise activity (Tollit et al. 2019). Deployment 9, covering a period of December through March saw the lowest detection rates, noting values remained higher than when the turbine was operational in 2016-2017. Mean time lost averaged 22.6%, with a median of 0% and interquartile range of 0-0% (i.e., more than 75% of minutes has no time lost).

Porpoise detection rates also varied by location, with D1 values typically low (deployment average 3.2%) and S2 and W2 typically high (deployment averages of 6.6% and 6.4% respectively). E1 averaged 4.3% across all four deployments, while W1 averaged 4.8%. A peak rate of 8.8% was observed at E1 and W2 during deployment 10, while the lowest rate of 1.4% was observed at D1 during deployment 8. With the exception of the site located in deeper water (S2), detection rates are consistently higher in summer deployments (7 and 10) compared to the fall through spring deployments 8 and 9. The period of turbine 2 operations was short, relatively small declines were seen at D1, E1 and S2 and increases observed at W1 and W2, but any interpretation is cautioned. An analysis against past datasets (that controlled for time of year) clearly suggest that the effect of a turbine structure had no detectable effect on porpoise local detection rates.

It is important to note that C-PODs only record porpoises that are actively echolocating and detection range is likely to vary depending on direction of travel and orientation of the porpoise, as well as both natural and anthropogenic ambient noise levels. In extremely noisy environments, detectors may not be as efficient (higher false negative rates), and animals may change their vocalization patterns and affect successful classification. Artificial noise contamination from “flow noise” past the hydrophone and excessive non-biological clicks from sediment transfer are both factors that increase with current speed and therefore detection rates should be considered minimum estimates. While not as sensitive as high quality hydrophone systems and bespoke (human-verified) signal recognition software (Adams et al. 2019), C-PODs have still proved useful in monitoring for impacts from offshore wind farms (Tougaard et al. 2009, Dähne et al. 2013) as well as tidal turbines (Booth et al. 2011).

C-PODs have been redeployed at locations D1, E1, W1, W2 and S2 to continue EEMP monitoring. We recommend that this monitoring continue with the same deployment methodology. We also recommend that studies using hydrophones that monitor sound continuously are used to compare detection rates using C-PODs.

4. Acknowledgements

We acknowledge the financial support of FORCE and previous funding from OERA and FORCE. We would like to thank Tyler Boucher (FORCE Ocean Technologist) for field support and Dan Hasselman (FORCE) as well as Brian Sanderson (Acadia University) in providing technical support. We also acknowledge collaborators on past studies in particular Anna Redden (Acadia University) and Cormac Booth (SMRU Consulting UK). We thank EMAC reviewers for their constructive comments.

5. References

Adams, M, Sanderson, B., and A.M. Redden (2019). Comparison of co-deployed drifting passive acoustic monitoring tools at a high flow site: C-PODs and icListenHF hydrophones. *Journal of Ocean Technology*, Vol. 14, Special Issue, 61-83.

Dähne, M., Gilles, A., Lucke, K., Peschko, V., Adler, S., Krügel, K., Sundermeyer, J., and U. Siebert (2013). Effects of pile-driving on harbor porpoises (*Phocoena phocoena*) at the first offshore wind farm in Germany. *Environmental Research Letters*, Vol. 8, No. 2.

Ellison, W.T., B.L. Southall, C.W. Clark, and A.S. Frankel (2012). A new context-based approach to assess marine mammal behavioral responses to anthropogenic sounds. *Conservation Biology*, 26(1):21-28.

Joy, R., Wood, J., Robertson, F. and D.J. Tollit (2017). Force Marine Mammal Environmental Effects Monitoring Program – 1st Year (2017) Monitoring Report. Prepared by SMRU Consulting (Canada) on behalf of FORCE, May 1, 2017.

Joy, R., Wood, J., and D.J. Tollit (2018). FORCE Echolocating Marine Mammal Environmental Effects Monitoring Program – 2nd Year (2018) Monitoring Report. Prepared by SMRU Consulting (Canada) on behalf of FORCE, December 9, 2018.

Kastelein, R.A., W.W. Au, and D. de Haan (2002). Audiogram of a harbour porpoises (*Phocoena phocoena*) measured with narrow-band frequency-modulated signals. *The Journal of the Acoustical Society of America*, 112:334-344.

Polagye, B., J. Wood, C. Bassett, D. Tollit, and J. Thomson (2011). Behavioral response of harbour porpoises to vessel noise in a tidal strait, Meeting of the Acoustical Society of America 2011. See <https://tethys.pnnl.gov/sites/default/files/2011-12-14-4-Brian-Polagye.pdf>

Porskamp, P., A. Redden, J. Broome, B. Sanderson and J. Wood (2015). Assessing marine mammal presence in and near the FORCE Lease Area during winter and early spring – addressing baseline data gaps and sensor performance. Final Report to the Offshore Energy Research Association and Fundy Ocean Research Center for Energy.

R Core Team. (2016). R: A language and environment for statistical computing. R Foundation for Statistical Computing, Vienna, Austria. URL <https://www.R-project.org/>

SLR consulting Ltd (2015). Proposed Environmental Effects Monitoring Programs 2015-2020 Fundy Ocean Research Center for Energy (FORCE).

Tollit, D., J. Wood, J. Broome and A. Redden (2011). Detection of Marine Mammals and Effects Monitoring at the NSPI (OpenHydro) Turbine Site in the Minas Passage during 2010. Publication No. 101 of the Acadia Centre for Estuarine Research (ACER) Acadia University, Wolfville, NS, Canada prepared for Fundy Ocean Research Centre for Energy (FORCE). FORCE: Fundy Ocean Research Center for Energy. 2011. Environmental Effects Monitoring Report, September 2009 to January 2011. Appendix D.

Tollit, D., R. Joy, J. Wood, A.M. Redden, C. Booth, T. Boucher, P. Porskamp and M. Oldreive (2019) Baseline presence and operations on harbor porpoise in Minas Passage, Bay of Fundy, Canada. *Journal of Ocean Technology*, Vol. 14, Special Issue, 24-48.

Tougaard, J., J. Carstensen, J. Teilmann, H. Skov, and P. Rasmussen (2009). Pile driving zone of responsiveness extends beyond 20 km for harbour porpoises (*Phocoena phocoena* (L.)). The Journal of the Acoustical Society of America, 126(1), 11–14. doi:10.1121/1.3132523.

Wood, J., D. Tollit, A. Redden, P. Porskamp, J. Broome, L. Fogarty, C. Booth and R. Karsten (2013). Passive Acoustic Monitoring of Cetacean Activity Patterns and Movements in Minas Passage: Pre-Turbine Baseline Conditions (2011-2012). SMRU Consulting and ACER collaborative report prepared for Fundy Ocean Research Center for Energy (FORCE) and the Offshore Energy Research Association of Nova Scotia (OERANS). FORCE; Fundy Ocean Research Center for Energy. 2015. Environmental Effects Monitoring Report, 2011 to 2013. Appendices C.



Shore-based Marine Seabird Surveys Fundy Ocean Research Center for Energy: Modeling of Seabird Abundance 2010-2018

Prepared for:

Fundy Ocean Research Center for Energy
1690 Hollis Street, Unit 1001
Halifax, Nova Scotia B3J 1V7

Prepared by:

Envirosphere Consultants Limited
120 Morison Drive, Windsor Nova Scotia Unit 5 B0N 2T0
902 798 4022 | enviroco@ns.sympatico.ca | www.envirosphere.ca

In collaboration with: Dr. Phil Taylor, Acadia University, Wolfville, Nova Scotia

Table of Contents

Executive Summary.....	ii
Introduction and Background	1
Methodology.....	2
Generalized Additive Modeling (GAM)	3
Models - General Considerations.....	3
Preliminary Data Treatment and Analysis	3
Conducting Analyses	4
Example Analysis – Great Black-backed Gull	9
Example Analysis - Red-throated Loon	15
Correlation with Regional Seabird Datasets	17
Conclusions and Recommendations for GAM Analysis of Test / Sample Dataset.....	17
Reference Material on GAM Analysis	18
Polynomial Regression	19
Overview	19
Application	19
Conclusions and Recommendations – Polynomial Regression Analysis.....	27
References	28
Appendix A – R Code for Generalized Additive Modeling (GAM) Analysis.....	A-1
Appendix B – FORCE Seabird Database Data Structure.....	B-1
Appendix C1 – Polynomial Regression Equations (Abundance versus Julian Day) for Dominant Seabirds or Seabird Groups, 2010-2018.	C1-1
Appendix C2 – Polynomial Regression Relationships of Dominant Waterbirds Species and Groups, 2010-2019	C2-1

Executive Summary

Seabirds and other water-associated birds are found in coastal environments in all areas of marine renewable energy (wind, tidal, and wave) development, and have the potential to interact with and be impacted by such projects. This report focuses on evaluating techniques for analysis of observational data on seabird abundance, micro-distribution, and behaviour relevant to assessing impacts of tidal energy development in the Minas Passage area of the Bay of Fundy. The project uses a dataset on seabird abundance developed from observations undertaken by the Fundy Ocean Research Center for Energy (FORCE) at its tidal energy demonstration site. Scripts in the R statistical programming language, were developed and applied using Generalized Additive Modeling (GAM). The data were examined to determine more effective approaches to surveys and species studied to better determine impacts of tidal energy devices. A statistical hypothesis-testing approach based on polynomial regression was developed to compare seasonal abundance patterns for critical periods in the annual cycle of seabirds at the site in present and subsequent years, to standardize the abundance curves based on fixed dates. The approach promises to help identify year-to-year changes against which changes observed during periods of tidal device installation may be compared. The preliminary assessment conducted contributes to data acquisition and the development of analysis methods for seabirds which will allow improved precision and certainty in detecting impacts of tidal energy on seabird populations and tools to support the continued responsible development of the marine renewable energy sector in Nova Scotia.

Introduction and Background

Seabird monitoring at the FORCE tidal energy demonstration site at Black Rock, Minas Passage, Nova Scotia, has generated multiple years of data (2010-2012; 2016-2018) on seabird occurrence, abundance, and seasonal patterns, summarized in a series of monitoring and baseline reports (www.fundyforce.ca). An underlying goal of recent environmental monitoring surveys carried out under the FORCE Environmental Effects Monitoring Program (EEMP) begun in 2016, is to generate data to determine whether impacts of tidal energy devices on seabirds occur. Limited evaluation of the seabird data was conducted for periods before and after deployments of the Cape Sharp Tidal Energy Development *OpenHydro* turbine, using simple non-parametric statistics in monitoring reports for the EEMP (Envirosphere Consultants Limited 2017 and 2018). The current project was initiated to determine if the more-powerful analysis techniques for biological abundance data (Generalized Additive Modeling (GAM)) and Bayesian Probability Analysis (BPA) could improve hypothesis testing of impacts of tidal energy devices on seabirds at the FORCE site. Integration of improved techniques and protocols is central to the adaptive management framework that FORCE has adopted in its EEMP.

Seabird populations show high temporal and spatial variability in abundance, and substantial observational effort is required to collect enough data so that scientifically defensible conclusions can be reached about the impacts of marine renewable energy (MRE) devices on underlying populations or behaviours. Furthermore, observation-based surveys of seabirds are subject to various environmental factors (e.g., distance, glare, wave action, time of day, varying daylight conditions, etc.) that also contribute to variability in the observational data and obscure the ability to make meaningful inferences. The modeling approaches proposed (GAM and BPA) provide an opportunity to control for these effects to highlight changes which may be due to impacts of tidal energy devices. These semiparametric regression modeling approaches (GAM, Hastie and Tibshirani 1990; BPA, Fahrmeir and Kneib 2011) relax some of the assumptions of linear models typically used in analysis of environmental data. Recent applications to modeling bird abundance data (e.g. Pederson et al 2019; Wu et al 2015; Thogmarten et al 2004; Martin et al 2005 and others) provide examples of approaches which may be useful for modeling the FORCE seabird data.

The current project focused on the use of GAM for analysis of the seabird abundance data available from the FORCE site. The goal of the analysis was to allow fitting generalized additive models relating the counts to time of year, time of day, tidal heights and weather (wind direction and speed, cloud cover, precipitation etc.), which is the preliminary framework for an ultimate analysis that may test for differences in observations pre- and post- placement of tidal energy devices. A framework was set up using the FORCE data and a preliminary analysis conducted using the approach. The same framework can be used for conducting BPA; time constraints, however, did not allow this analysis to be carried out. We also looked at the data with a view to determining more efficient study design for determining impacts using available data. Polynomial regression was also used to summarize abundance and abundance patterns in the data set for key species and species groups, as a simpler—although not as powerful—approach to assessing change related to tidal energy device installations in seabird communities at the site.

Methodology

The FORCE Tidal Energy Demonstration Site is located west of Cape Sharp on Minas Passage, near Parrsboro, Nova Scotia (Figure 1). Observational data for birds which was analyzed in this study were collected for sub-areas of the study site referred to in the text are shown in Figure 2.

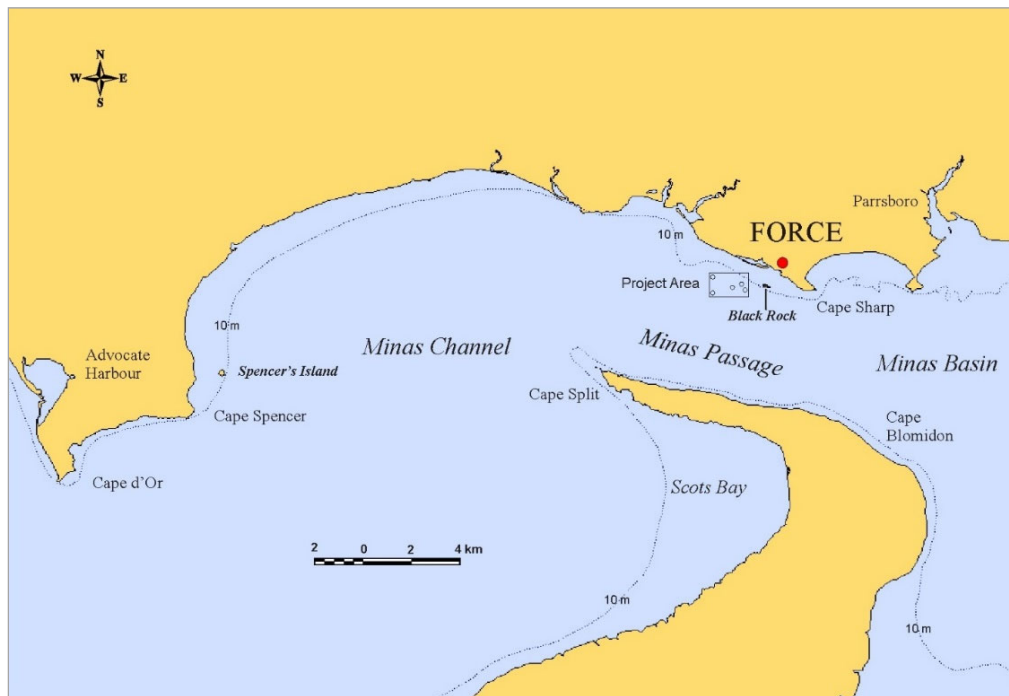


Figure 1. Study area showing project location and major geographic features.

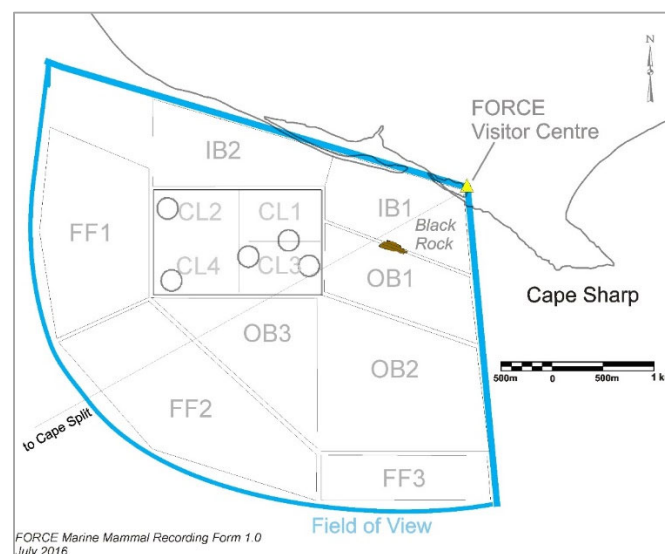


Figure 2. Study area field of view with grid showing open water subdivisions to document seabird occurrences. (CL1-4 = turbine field/crown lease area; IB1-2 = Nearshore area/Inside Black Rock; OB1-3 Buffer area/outside Black Rock; FF1-3 Far-field).

Generalized Additive Modeling (GAM)

Data analysis using GAM was conducted through a sub-contract to Dr. Phil Taylor, Department of Biology, Acadia University. Generalized additive models are an extension of the generalized linear model that allow for a non-linear relationship between the response and the predictor. These non-linear relationships are termed ‘smoothing’ functions or ‘smooths’ and can take multiple forms. For example, smooths can be cyclical, allowing one to fit a linear-circular relationship – as with counts of birds and time of year. Because they are an extension of the generalized linear model, they allow for fitting models with proper relationships between responses and predictors, and with appropriate distributional assumptions. For example many types of count data follow a Poisson distribution, and so both generalized linear and generalized additive models allow one to fit a model whereby the expected relationship between the response (a count) and the predictor is on the log scale, and the errors are assumed to be drawn from a Poisson distribution. A good overview of generalized additive models can be found in Wood (2017).

Models - General Considerations

The goal of the analysis is to allow fitting generalized additive models relating the counts to time of year, time of day, tidal heights and weather, which is the preliminary framework for an ultimate analysis that may test for differences in observations pre- and post- placement of tidal energy devices. The analysis approach must consider that periods pre- and post-placement and year are confounded in an overall analysis. The models fitted in the analysis relate the observed counts of each species (or species group) at the site (or within sub-sites) within each 30-minute survey period. Two species that show contrasting seasonal patterns, and distributions of counts – Great Black Backed Gull and Red-throated Loon—are representative of a range of the species occurring in the area, and were used to illustrate the modeling approach.

Since much of the data is cyclic, a cyclic smoothing spline was selected (to link the last observation in the cycle (e.g. December) with the first (January)). Some examples are presented at: <https://www.r-bloggers.com/modelling-seasonal-data-with-gams/>. Autocorrelation can also occur in data sets, and packages in R are available (e.g. ‘*itsadug*’), although autocorrelation was not dealt with in this preliminary analysis. A discussion of the issues of temporal autocorrelation, and intermittency of the time series is presented in Simpson (2018).

Preliminary Data Treatment and Analysis

The R code and approach to the analyses is presented in Appendix A. The general features and structure of the FORCE database is presented in Appendix B. It consists of two tables of data records of individual sightings of birds and counts, organized by survey and half-hour survey period (with typically from nine to thirteen half-hour periods by survey on a given day). Data were provided as “.xls” files and then saved as “.csv” files with no additional changes. Three files were provided – one containing ‘environmental’ and survey data, and two containing observations (one from the period 2010-2012, the other from the period 2016-2019). Methodology for the surveys is summarized in monitoring reports (Envirosphere

Consultants 2011-2013 and 2017-2018). Environmental data was supplemented with Environment Canada weather data for Parrsboro¹.

Environmental and survey data were processed to a form that could be used for analysis (see Appendix A²). Two main tasks were undertaken. First, the FORCE database only contains records for periods in which birds were seen; consequently the observations table needed to be expanded to ensure that periods with zero counts were included. A number of adjustments and corrections needed to be made to the environmental and survey data. For example, observation times were adjusted to times relative to high tide and sunrise (i.e. 'Local Time') (they had been recorded in ADT and AST depending on season) to allow the data to be linked properly to the environmental data. In particular the data obtained from the Environment Canada weather station in Parrsboro uses local time. The environmental data table was further also adjusted to deal with non-standard codes for some of the variables. The majority of the relevant variables for the analysis were found in the Environment Canada data set, and as they are more complete (collection of weather data was not an objective of the 2010-2012 surveys and consequently the weather data for those years is incomplete), they were used in the trial analysis. The FORCE data could be used, however, in future for example to more formally compare the Environment Canada weather data with the on-site observations.

Environmental and observational data were then linked based on the combination of the common variables 'survey' and 'period' to create a working data matrix ("data frame") in the R environment. The final data frame also allows for easy summaries of individual species or groups of species, which could be used to produce summary statistics useful for assessing patterns of abundance and change. The "data frame" in R (sum.df) which was developed, or derivations of it or other data frames can also be used in other analyses.

Conducting Analyses

Abundance summaries both as tables and in graphical form can be produced (Figures 3-6, Tables 1 & 2) using the code in Appendix A and the data matrix produced by the analysis. Figure 3 shows annual occurrence statistics of a large cross-section of species which have occurred at the site. The presentation in Figure 4 shows a reduced list, and Figure 5 demonstrates a comparison of areas within the FORCE site. Figure 6 is a presentation of the abundance of several of the numerically abundant species and their presence on and off Black Rock, but assembled on a weekly basis.

¹ Data from the Environment Canada site was 'harvested' using the functions provided in the blog post: <https://www.fromthebottomoftheheap.net/2015/01/14/harvesting-canadian-climate-data/>. The relevant functions are found in a separate file (*weather.fun.2.R* and *functions.R*). The form of the data available from Environment Canada is subject to periodic changes which can affect routine use of the functions without adjustment.

² A version of the code in Appendix A, in its logical order is available to provide sequential instructions for conducting the analysis.

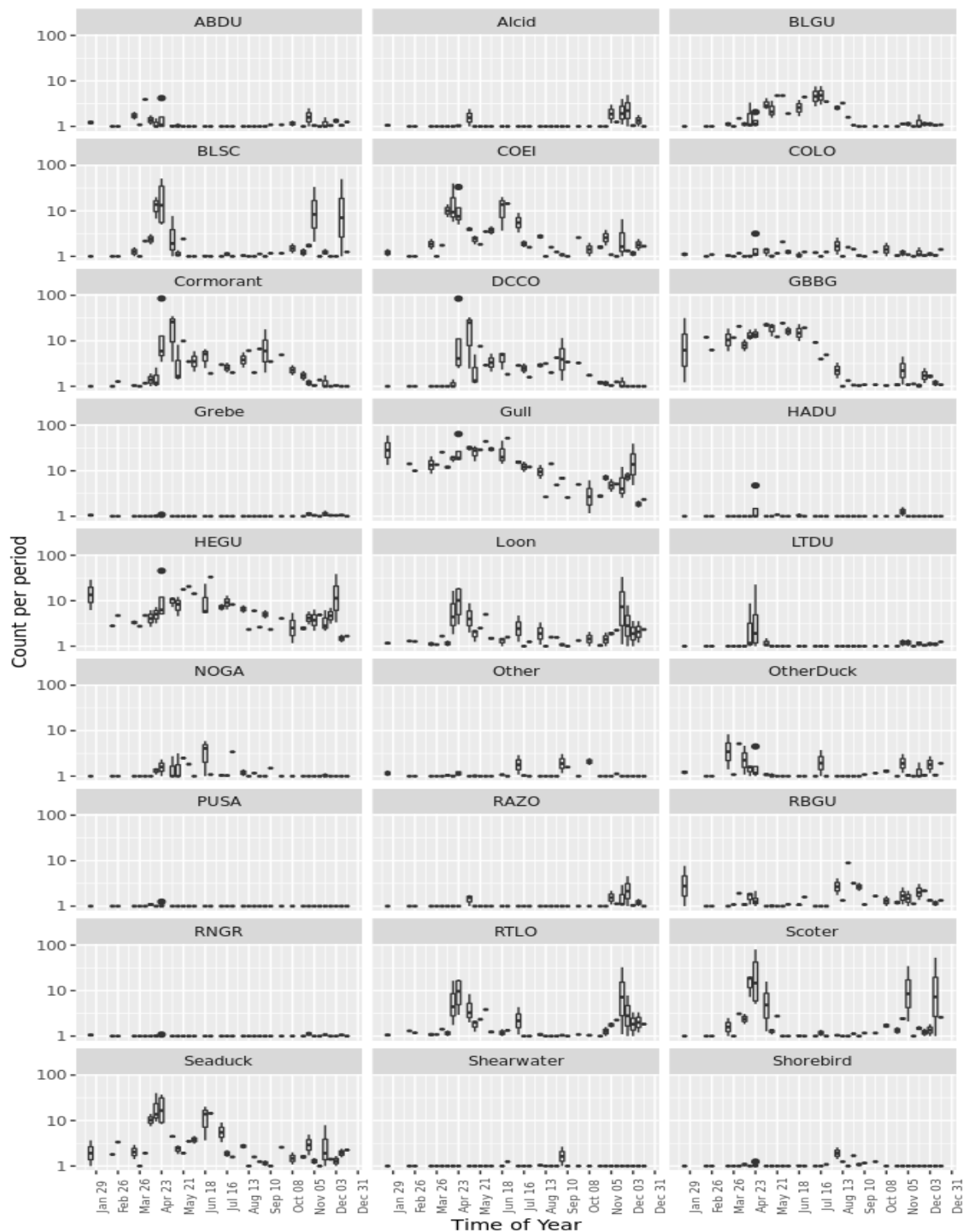


Figure 3. Abundance (counts per 30-minute period) and ranges (box and whisker plots) of abundance of seabirds and seabird groups, 2010-2019, versus date.

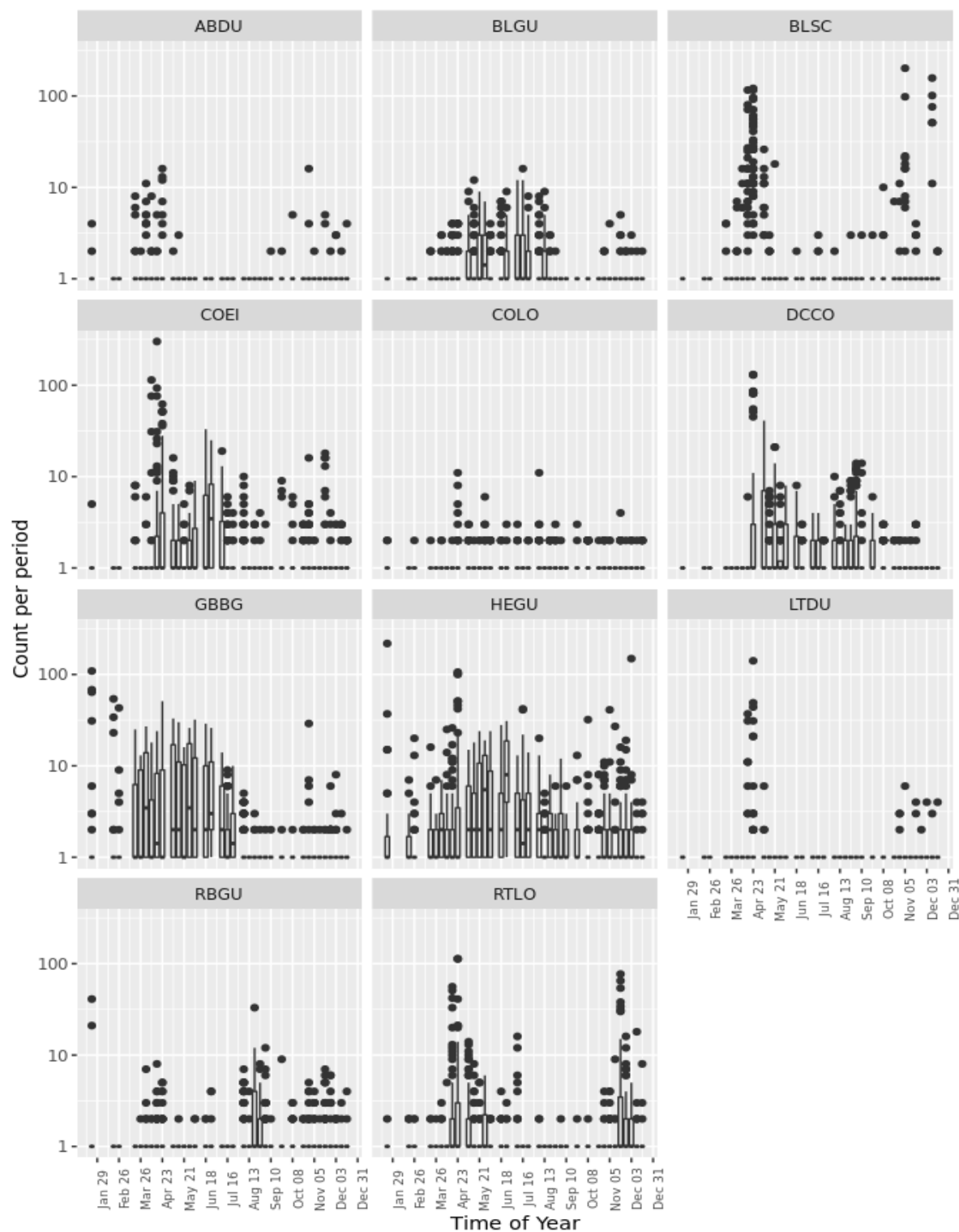


Figure 4. Abundance (counts per 30-minute period) and ranges (box and whisker plots) of abundance of seabirds and seabird groups, 2010-2019, versus date. Smaller list of species represented than in Figure 1.

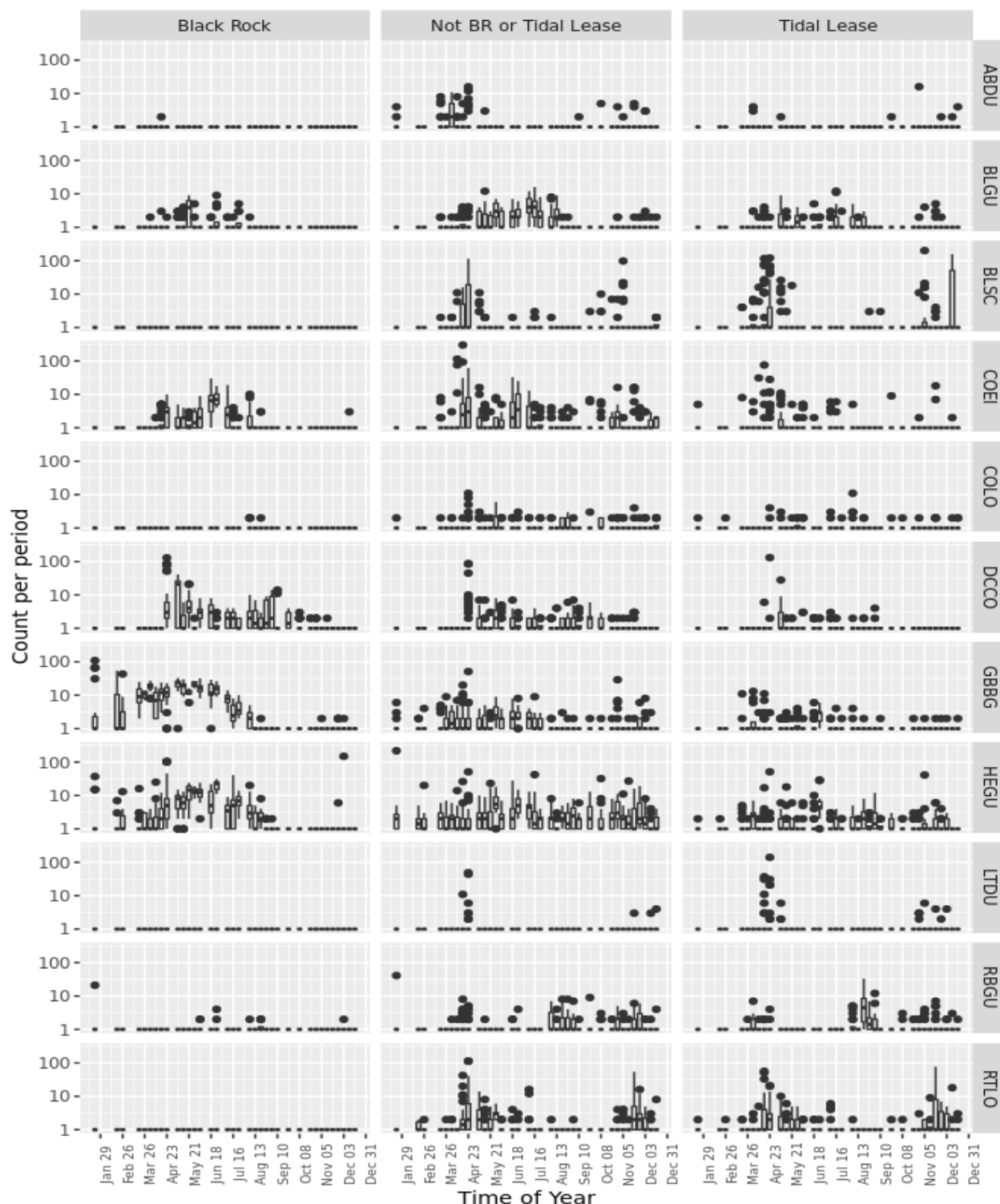


Figure 5. Abundance (counts per 30-minute period) and ranges (box and whisker plots) of abundance of seabirds versus geographic sub-areas of the FORCE tidal energy site, 2010-2019, versus date.

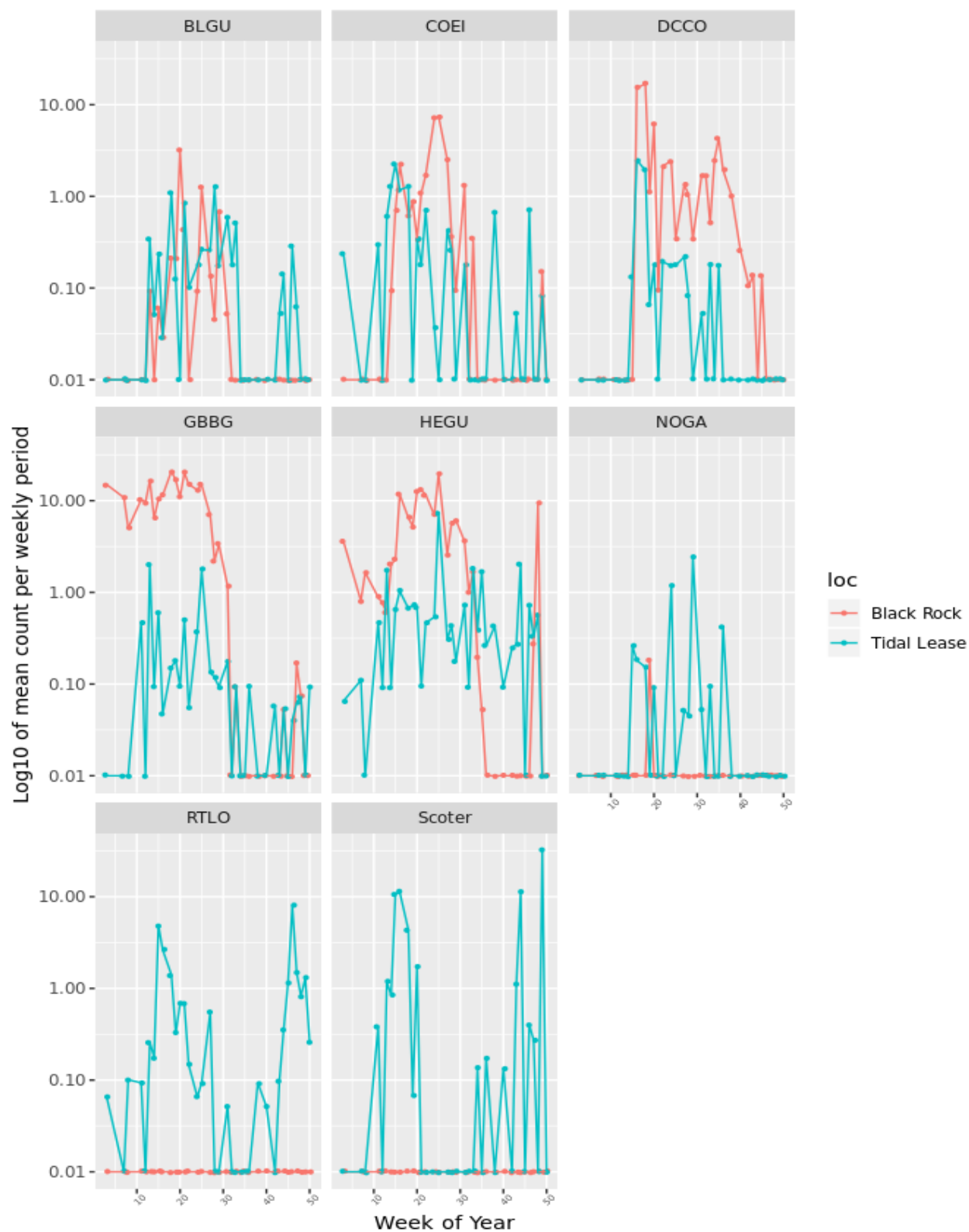


Figure 6. Abundance (counts per 30-minute period) of seabirds, FORCE tidal energy site, 2010-2019, presented by week.

Table 1. Tabular output generated by the R code, showing the number of sampling periods in which dominant species were present, for Black Rock, The Tidal Lease, or neither.

##	loc		
##	sp.grp	Black Rock	Not BR or Tidal Lease
##	ABDU	0	4
##	BLGU	4	25
##	BLSC	0	9
##	COEI	23	26
##	COLO	0	10
##	DCCO	31	18
##	GBBG	55	27
##	HEGU	46	55
##	LTDU	0	1
##	RBGU	1	13
##	RTLO	0	22

Table 2. Tabular output giving a summary of number of 30-minute observation periods by month.

##	month												
##	year	1	2	3	4	5	6	7	8	9	10	11	12
##	2010	0	0	0	0	35	12	0	0	0	12	23	0
##	2011	0	0	24	24	0	0	0	0	0	0	0	24
##	2012	0	0	0	0	0	12	24	36	0	0	0	0
##	2016	0	0	0	0	11	12	12	12	12	24	23	4
##	2017	9	11	12	25	24	12	16	16	12	9	21	9
##	2018	9	10	12	24	22	12	12	12	12	23	16	5
##	2019	0	0	0	56	0	0	0	0	0	0	0	0

One approach considered for the modeling is to:

- 1) Model all counts by environmental and temporal variables, to provide a description of the patterns observed, and how they relate to those environmental and temporal variables.
- 2) Model counts with environment and temporal variables (as above) but compare counts on Black Rock with all other counts.
- 3) Model counts as in 2, but compare counts on Tidal Lease to Not on Black Rock or in Tidal lease. That is, after accounting for temporal and environmental variables, are there differences between the 'at sea' counts and the two areas.

Such models cannot be used for all species (or groups) because there aren't enough data for many of them. Tests of the models using Great Black-backed Gull and Red-throated Loon were run and illustrate some of the issues with properly describing the patterns observed.

Example Analysis – Great Black-backed Gull

The approach was used to examine the properties of the dataset for Great Black-backed Gull. Steps in the analysis (see Appendix A) determined that the properties conformed better to a negative-binomial

distribution which was used in transforming the abundance data prior to analysis. The properties of the data used in the GAM analysis using the assumption of a negative binomial distribution are shown in Figure 7. The analysis shows a moderate suitability of the model. However there are some high counts that aren't estimated well, due to the paucity of data in periods when they occur. These can be considered and adjusted for in more in-depth analysis in future.

Outputs of the analysis and relationship to environmental variables for Great Black-backed Gull are presented in Figure 8, showing an overall pattern for the year, with most GBBG found during the first half. There are only moderate effects of most of the other variables, with the exception of time relative to high tide, where there is clearly a positive effect at high tide and at low tide.

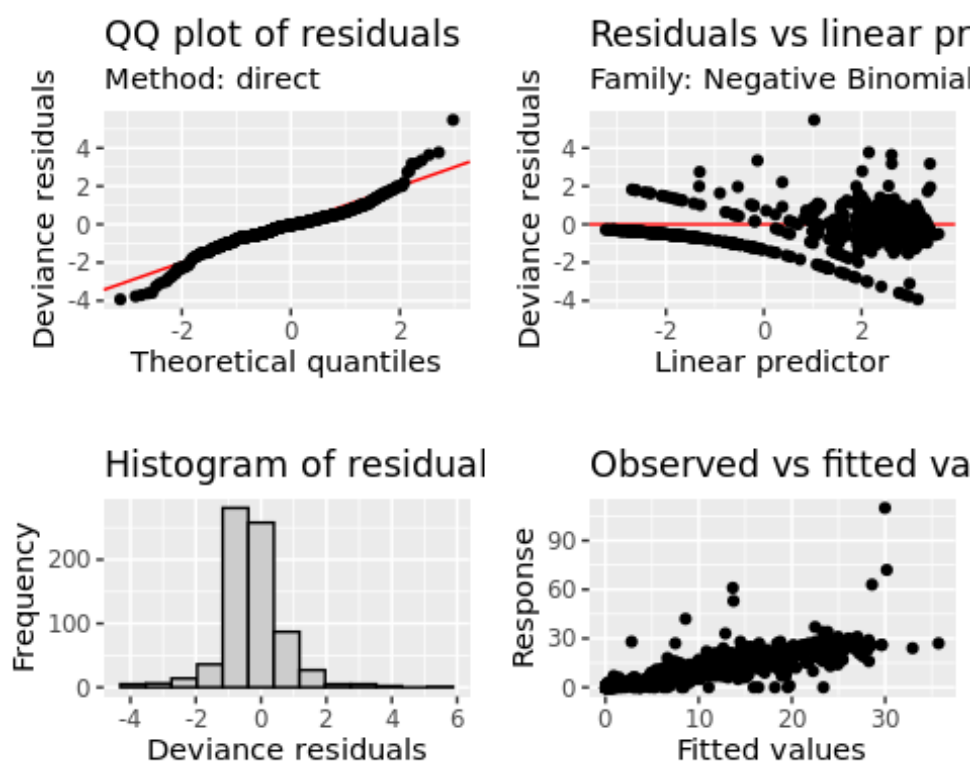


Figure 7. Properties of negative-binomial model distribution of Great Black-backed Gull.

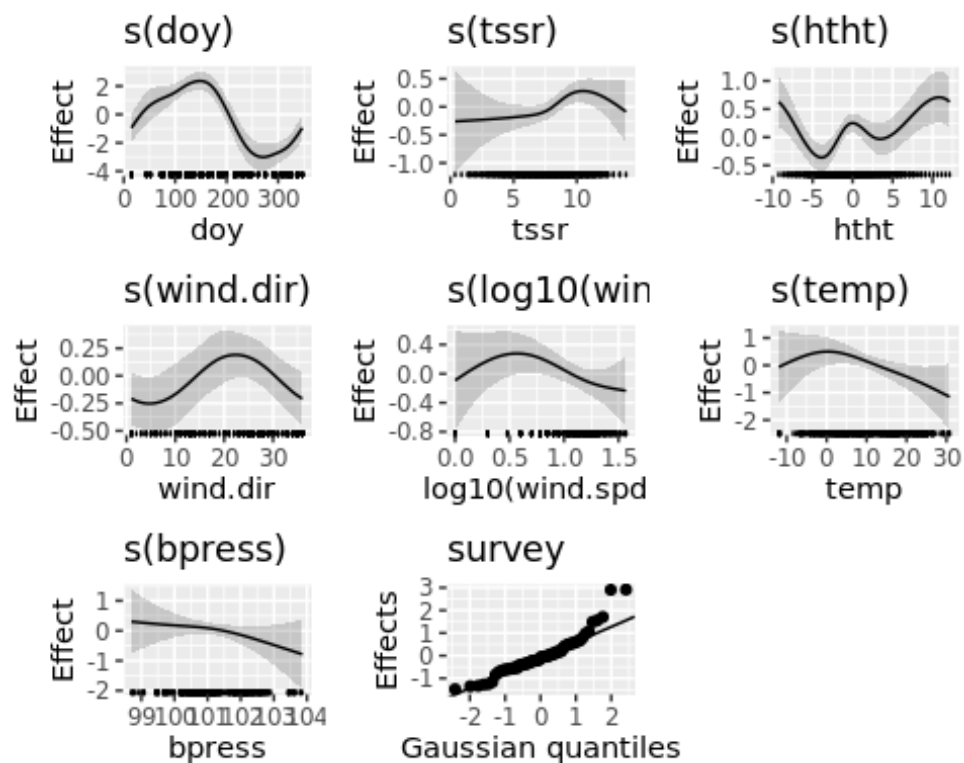


Figure 8. Summary statistics produced for the Great Black-backed Gull dataset.

Significance statistics produced for the environmental variables in relation to Great Black-backed Gull annual abundance are shown in the text box below.

```
##
## Family: Negative Binomial(4.031)
## Link function: log
##
## Formula:
## count ~ s(doy, bs = "cc", k = 25) + s(tssr, bs = "cr", k = 5) +
##       s(htht, bs = "cc", k = 5) + s(wind.dir, bs = "cc", k = 5) +
##       s(log10(wind.spd), k = 5) + s(temp, k = 5) + s(bpress, k = 5) +
##       s(survey, bs = "re")
##
## Parametric coefficients:
##               Estimate Std. Error z value Pr(>|z|)
## (Intercept)   0.6230      0.1488   4.187 2.83e-05 ***
## ---
## Signif. codes:  0 '***' 0.001 '**' 0.01 '*' 0.05 '.' 0.1 ' ' 1
##
## Approximate significance of smooth terms:
##               edf Ref.df   Chi.sq p-value
## s(doy)         5.170 23.000 17156.682 < 2e-16 ***
## s(tssr)         3.374  3.771   11.976 0.00820 **
## s(htht)         2.886  3.000   141.481 0.10360
## s(wind.dir)     1.723  3.000   176.614 0.00744 **
## s(log10(wind.spd)) 2.543  3.088    6.950 0.09557 .
## s(temp)         2.535  2.950    5.985 0.09515 .
## s(bpress)       1.505  1.701    1.436 0.30989
## s(survey)      45.191 63.000   387.500 < 2e-16 ***
## ---
## Signif. codes:  0 '***' 0.001 '**' 0.01 '*' 0.05 '.' 0.1 ' ' 1
##
## R-sq.(adj) =  0.646   Deviance explained = 83.3%
## -REML = 1623.3   Scale est. = 1           n = 727
```

The Tidal Lease (CL) would be a suitable area for assessing the abundance pattern; however there are few observations of Great Black-backed Gull in the Tidal Lease (Table 1). Consequently a local comparison was conducted of abundance of birds on Black Rock versus those Not Black Rock or to those observed in the Tidal Lease (Figures 9 and 10). The significant parameters are day of year, sunrise time, wind-direction and survey. Based on this analysis, the model was simplified to look for effects of location (see code in Appendix A, Section A.17).

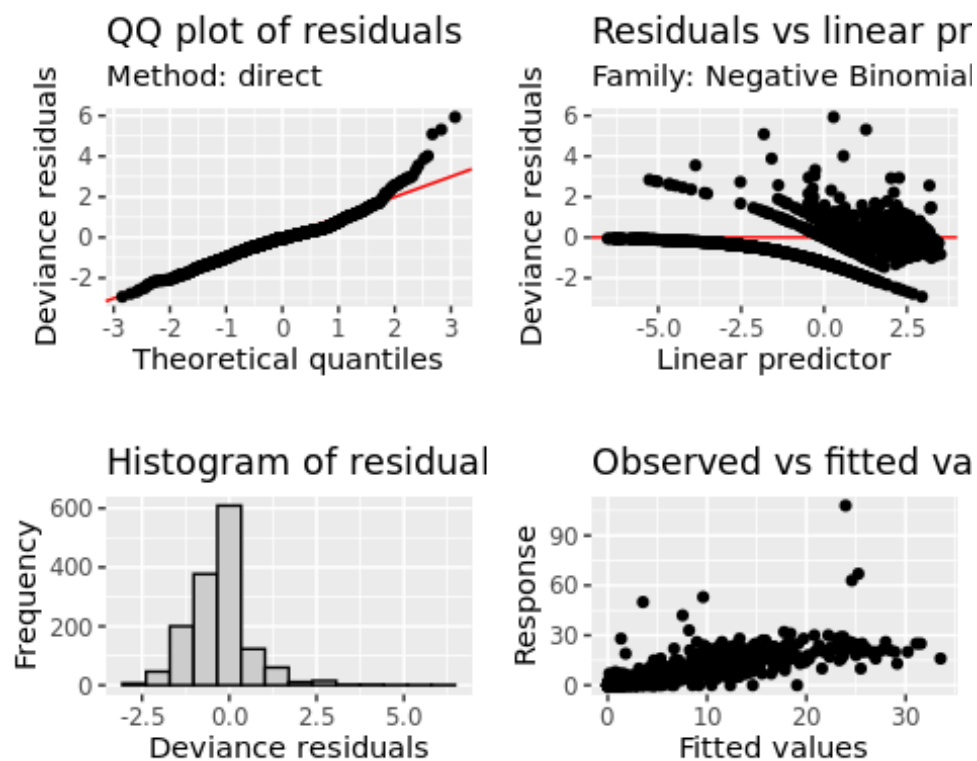


Figure 9. Fitting parameters for negative binomial model of abundance of Great Black-backed Gull on selected locations (Black Rock, Not Black Rock and Tidal Lease).

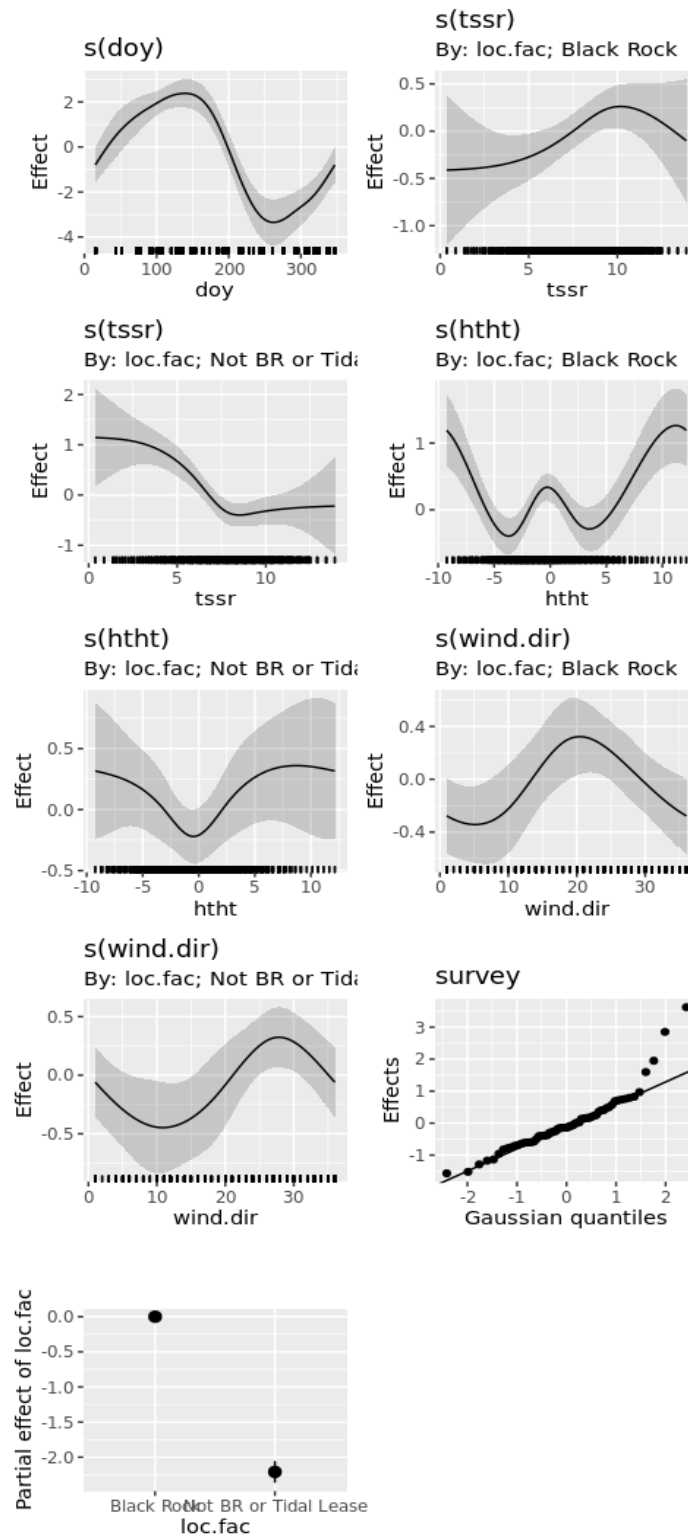


Figure 10. Environmental effects for negative binomial model of abundance of Great Black-backed Gull on selected locations (Black Rock, Not Black Rock and Tidal Lease).

This analysis suggests that tide height and time of day influence the counts differently at the two locations³ but that wind direction doesn't seem to. The models were simplified by removing tide and sunrise time (See Appendix A, Section A.17), and examined using the Akaike Information Criterion (AIC), which tests how well the model predicts the values. The AIC value is not much changed after removal of tide height or time of day from the analysis, indicating that these factors likely don't have a big effect on the differences in counts differ between these locations. There may well be effects, but the data may be insufficient to detect them (which is another way of saying there is so much variability in the system to begin with, these environmental effects are difficult to detect).

Example Analysis - Red-throated Loon

Abundance data for Red-throated Loon was analyzed using a similar approach to that of Great Black-backed Gull, except that a negative-binomial distribution was assumed to be the appropriate transformation for the data. In addition, the species is not associated with Black Rock and the relevant assessment was done for all openwater sub-areas in the study area. The initial diagnostic parameters are shown in Figure 9.

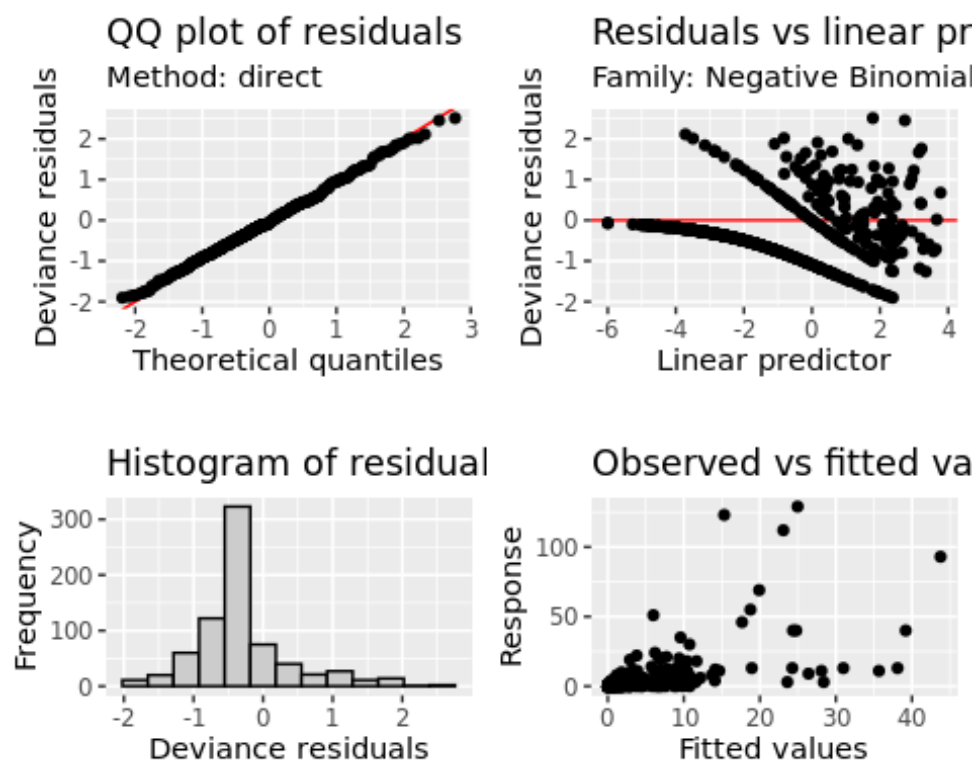


Figure 11. Fitting parameters for negative binomial model of abundance of Red-throated Loon.

³ The differences can be tested but this was not done in the example analysis.

For the Red-throated Loon data, the negative binomial distribution partially deals with the extreme counts, but not as well as in the Great Black-backed Gull model. There are some high counts during the summer (4 July 2012 survey) which should be examined that might be causing this model behaviour. A more detailed analysis, looking at other information, and perhaps fitting these models in a different framework, may be needed to account for the extreme points. The model significance analysis table (see text box below) shows that a similar list of environmental parameters as for the Great Black-backed Gull data are important in influencing the outcome, namely: day of year, sunrise time, wind-direction and survey, but also including wind speed. The analysis outputs of the GAM model for Red-throated Loon show the seasonal pattern of abundance of the species (two annual migration peaks—spring and fall) and importance of the influencing variables at different times of year (Figure 10).

```
##
## Family: Negative Binomial(0.624)
## Link function: log
##
## Formula:
## count ~ s(doy, bs = "cc", k = 25) + s(tssr, bs = "cr", k = 5) +
##       s(htht, bs = "cc", k = 5) + s(wind.dir, bs = "cc", k = 5) +
##       s(log10(wind.spd), k = 5) + s(temp, k = 5) + s(bpress, k = 5) +
##       s(survey, bs = "re")
##
## Parametric coefficients:
##               Estimate Std. Error z value Pr(>|z|)
## (Intercept)   -1.276      0.193   -6.609 3.86e-11 ***
## ---
## Signif. codes:  0 '***' 0.001 '**' 0.01 '*' 0.05 '.' 0.1 ' ' 1
##
## Approximate significance of smooth terms:
##               edf Ref.df Chi.sq p-value
## s(doy)         7.188e+00 23.000 543.309 4.81e-06 ***
## s(tssr)         3.734e+00  3.944  15.012 0.002506 **
## s(htht)         6.268e-05  3.000   0.000 0.829663
## s(wind.dir)     2.463e+00  3.000  93.305 6.98e-05 ***
## s(log10(wind.spd)) 3.505e+00  3.829  23.053 0.000116 ***
## s(temp)         2.420e+00  2.802   5.705 0.079309 .
## s(bpress)       1.550e+00  1.731   4.939 0.054262 .
## s(survey)       3.185e+01 63.000 114.823 < 2e-16 ***
## ---
## Signif. codes:  0 '***' 0.001 '**' 0.01 '*' 0.05 '.' 0.1 ' ' 1
##
## R-sq.(adj) = 0.314   Deviance explained = 73.5%
## -REML = 842.89   Scale est. = 1           n = 727
```

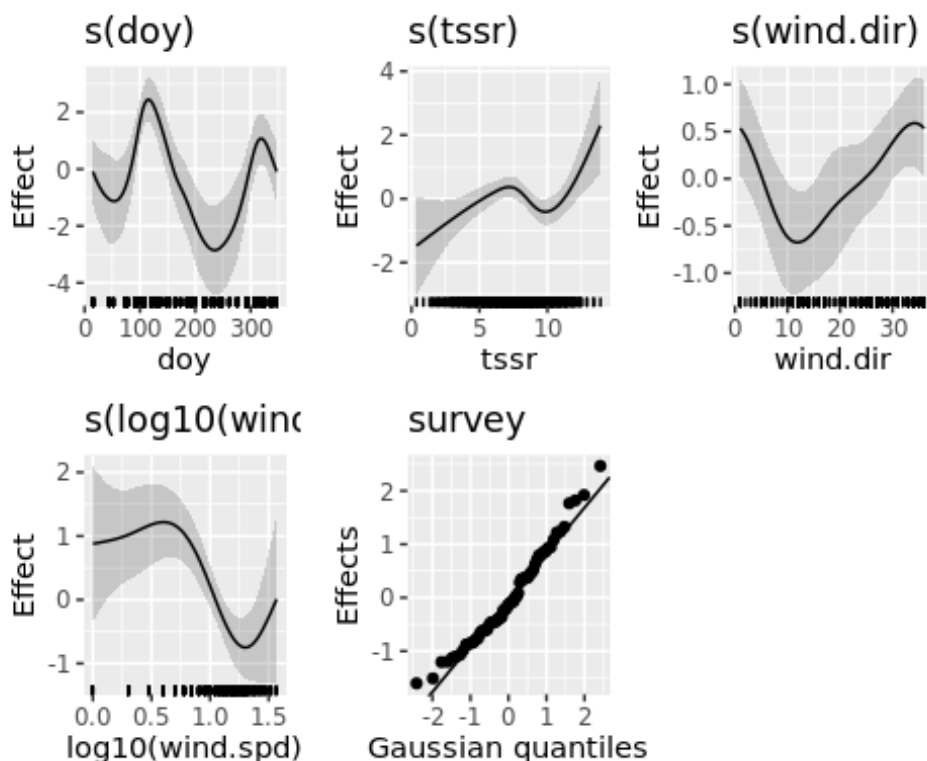


Figure 12. Environmental effects for negative binomial model of abundance of Great Black-backed Gull on selected locations (Black Rock, Not Black Rock and Tidal Lease).

The GAM models used for both Great Black-backed Gull and Red-throated Loon show that: 1) the overall fit is not bad, although the models sometimes don't predict the higher values well; and 2) that there are clear patterns of effect of time of year, wind speed and direction, tide height, and time of day on the numbers observed.

Correlation with Regional Seabird Datasets

The project also sought other regional datasets for future inclusion in the analysis. While the majority were not acquired prior to the completion of this study, and could not be included in the trial analyses, they will be available for future application by FORCE in interpreting the dataset. These included:

- 1) eBird; 2) Point Lepreau seabird counts ; 3) Point Lepreau radar counts (one year) ; 4) Tantramar radar counts (one year) ; 5) Tantramar acoustic counts (one year); 6) tracking databases for Common Eider and Scoters; and 7) Radar data at the FORCE site.

Conclusions and Recommendations for GAM Analysis of Test / Sample Dataset

The GAM models provide useful information regarding the effects of the various temporal and environmental data and the counts. As expected, the count data are highly variable, and analysis of the fits of these preliminary models suggest that additional work needs to be done. Primarily, there are

numerous instances of extreme counts (for a given time of year or situation) that are not well captured by the existing approach.

There are several possible next steps. One is to explore additional possible explanatory factors that may aid in explaining this variability, including possible additional environmental variables, or possibly interactions between variables. In particular, determining more precisely the interaction between wind speed and direction, season, and species would be useful for future analyses. A second possibility is to explore alternate distributional assumptions about statistical distributions of the counts data that might provide better fits. Finally, it is possible that using Bayesian generalized additive models (as implemented in the *brms* package in R) could provide additional tools (e.g. robust regression) that would aid in improving the fits. Such models would allow us to add informed “priors”⁴ (e.g. time of year) from alternative data sets. There may be some other advantages to using this type of model (including allowing for more species to be modelled together, where appropriate) or including data from other sources. Other approaches that may be used included boosted regression trees, but there is an intuitive appeal to using the GAMs due to the varying and sometimes cyclic nature of the data.

Reference Material on GAM Analysis

Numerous issues need to be explored within this set of models. Apart from the advice in Simon Wood’s book on GAMs (and the package *mgcv*) (Wood 2017) there are some good examples on the website *stackexchange.com* (e.g. <https://stats.stackexchange.com/questions/32730/how-to-include-an-interaction-term-in-gam>).

Also see: <https://stats.stackexchange.com/questions/403772/different-ways-of-modelling-interactions-between-continuous-and-categorical-pred>.

More tutorials about gams: <https://petolau.github.io/Analyzing-double-seasonal-time-series-with-GAM-in-R/> <https://jacolienvanrij.com/Tutorials/GAMM.html>

⁴ Priors are assessments of the state of the system known at the beginning of the analysis.

Polynomial Regression

Overview

In this component, we developed a simple approach to assessing change in seabird abundance and seasonal patterns at the FORCE site based on polynomial regression. Polynomial regression had earlier been used to help visualize seasonal patterns in abundance at the site (Figure 13). Seasonal abundance patterns for species and species groups (e.g. scoters) in the dataset were screened initially for potentially useful species and seasonal abundance patterns by applying polynomial regression to their seasonal abundances (Appendix C). Many of the regression relationships showed a good fit to the data, explaining a high proportion in the variance. In particular, overall abundance as well as abundance of the common resident species including Great Black-backed Gull, Herring Gull, Black Guillemot and Common Eider had good polynomial regression relationships (i.e. explained a large proportion of the variation in the data) and may be suitable for use in comparing years, and periods of tidal device impacts, at the FORCE site.

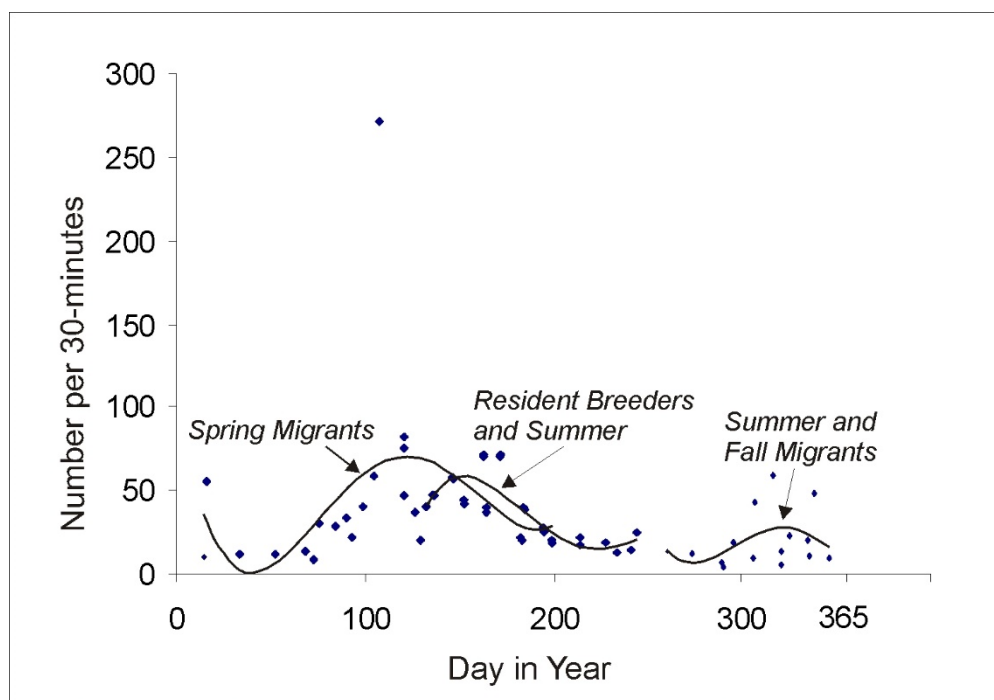


Figure 13. 4th order polynomial regression curves for seabird data at the FORCE site (2010-2012 and 2016-2018). Spring Migrants (January 1 – July 31); Resident Breeders and Summer Migrants (May 13 – August 31); and late summer, fall and early winter residents and migrants (mid-September to mid-December). The best fit was for resident breeders and summer occurrences which explained 72% of the variance; the other two curves explained less of the variance (17% and 15% for spring and fall, respectively) (Source: EnviroSphere Consultants Limited 2018).

Application

The goal of this project component was to suggest a way to use polynomial regression to test for impacts of tidal energy devices on seabird abundance and seasonal abundance patterns at the Minas Passage site. Polynomial or curvilinear regression is primarily a curve-fitting procedure (Snedecor and Cochran 1967; Sokal and Rohlf 1981; Brandt 1999), which is comparatively simple, easily understood and implemented. It is useful when there is reason to believe that the relationship between two

variables is curvilinear (Ostertagova 2012) such as in modeling patterns of abundance typically encountered in the natural environment, which are not typically linear (Sokal and Rohlf 1981). Tremblay et al (1998) used polynomial regression to model mercury in fish tissue in reservoirs which followed a curvilinear relationship with size. Fitted least-squares polynomials are also objective (unbiased) representations of the data, and have the additional asset that they reduce to a familiar linear regression form if the relationship to be modeled or tested is linear. An additional asset is that all necessary components to carry out polynomial regressions and associated statistical tests are found in *MS Excel*, a widely-used spreadsheet program. Polynomial regression curves can be compared statistically, and confidence limits on the curves can be estimated.

We first reviewed literature to look for examples of the use of polynomial regression in similar contexts, but were unable to find any which were relevant. Various modeling techniques are more commonly used (e.g. General Additive Modeling, Bayesian Probability Analysis) and others (see Gitzen et al 2012) but are typically used with larger datasets.

For the test case, polynomial regression equations of $\log(x+1)$ transformed species abundance versus time of year were generated for each year of the monitoring program to date (i.e. 2016, 2017 and 2018) (Figures 14 to 16 respectively), and for the combined data for the three years (Figure 17)^{5,6} Each data point represents the mean of from 9 to 12, 30-minute survey periods per day. Regression equations were estimated and plots generated using Excel⁷. The regressions were intentionally made to be 4th order, but only 3rd order were possible for two of the curves, a limitation imposed by the number of data points available (5 to 7 in each year). Practical application of the approach would require increasing the sampling frequency and number of datapoints in the period in question.

Using the regression equations, abundance was estimated for a series of fixed dates during the time period and year selected (e.g. spring migration, late-spring to summer breeding season)⁸. The selection of the periods was based largely on the patterns demonstrated in the polynomial regressions of the data overall (Figure 3). Model curves and the abundances estimated on each date for each of the three years

⁵ With time-series data of this kind, determining year to year variability is a problem due to sampling dates which almost always differ from year to year. A single polynomial regression curve which combines several years' data masks this year-to-year variability.

⁶ Since data were not available from the mid-March to May period for 2016 (before the present monitoring program was begun), data from the 2011 survey which covered the March-May period was substituted.

⁷ MicroSoft Excel allows trend lines and supporting polynomial equations to be generated in scatterplot charts. In addition, an add-on, Excel Analysis ToolPak (which is intrinsic in the software) provides analysis of variance and assessment of significance of regressions and regression parameters. Some of the polynomial regression analyses were conducted in parallel as multiple regressions in Systat statistical analysis software to check results.

⁸ Spring migration from March 11 to May 10 (day 70 to 130) and summer breeding season from May 10 to July 9 (day 130 to 190).

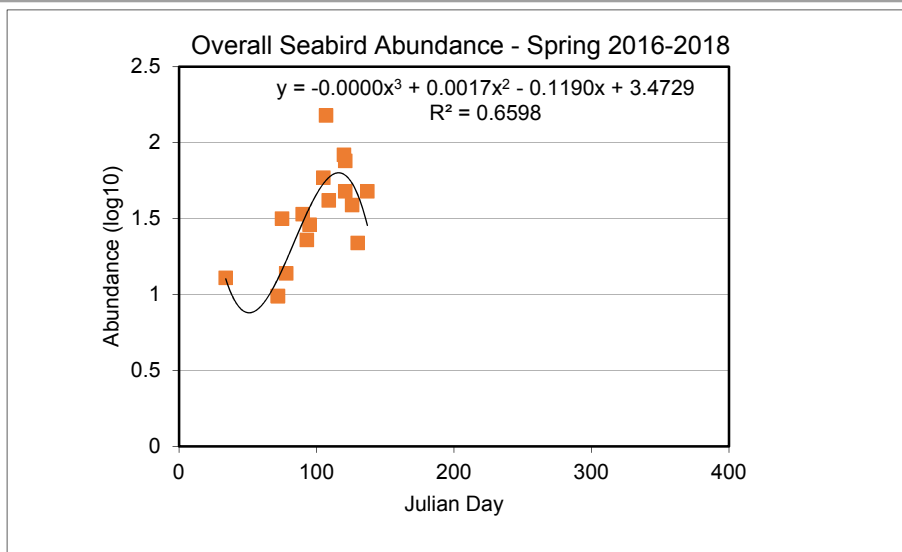


Figure 14. Polynomial regression equation and trend line for log-transformed ($\log(x+1)$) abundance (counts per 30/minute period), during spring migration, 2016-2018.

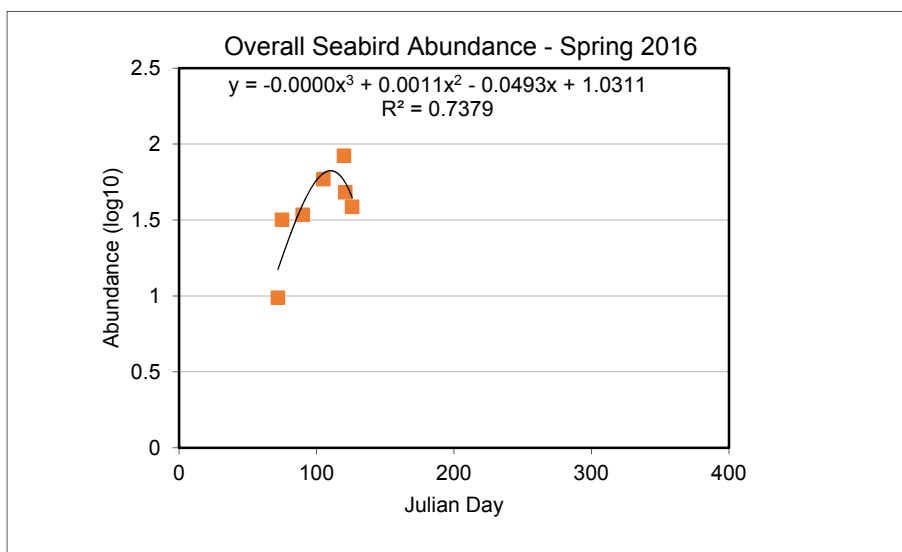


Figure 15. Polynomial regression equation and trend line for log-transformed ($\log(x+1)$) abundance (counts per 30/minute period), during spring migration, 2016.

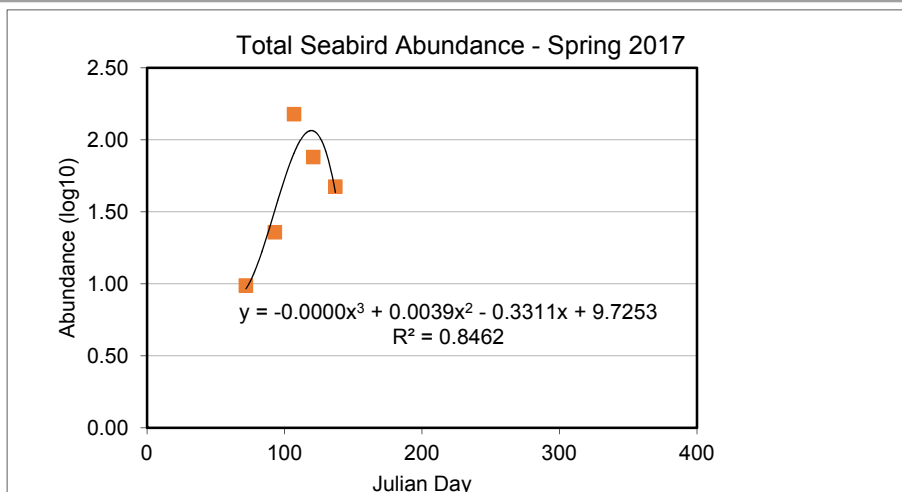


Figure 16. Polynomial regression equation and trend line for log-transformed ($\log (x+1)$) abundance (counts per 30/minute period), during spring migration, 2017.

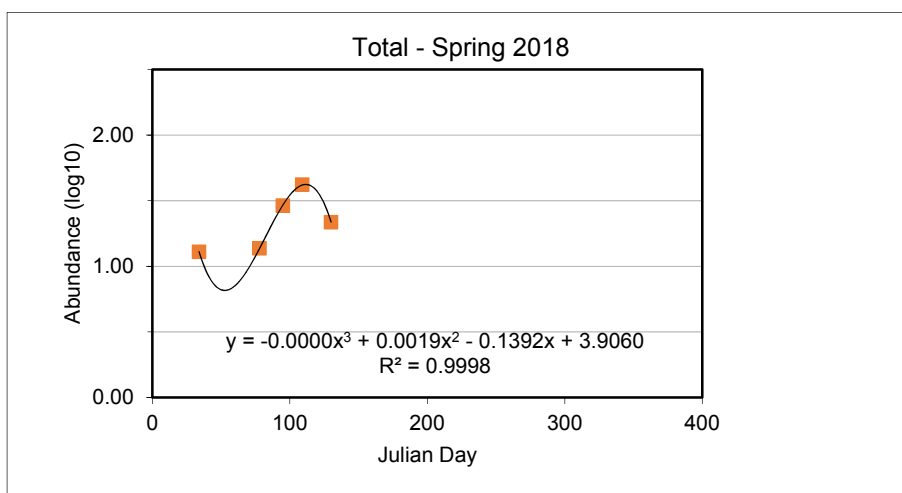


Figure 17. Polynomial regression equation and trend line for log-transformed ($\log (x+1)$) abundance (counts per 30/minute period), during spring migration, 2018.

could then be averaged and resulting statistics (e.g. standard deviation, mean and 95% confidence intervals (which are approximately ± 2 SD of the mean) calculated and plotted (Figures 18 and 19). The approach thus gives an estimate of the range and confidence limits, based on the current monitoring data. Polynomial regressions of future annual monitoring could then be compared to these to determine if patterns observed were out of line with ongoing observations. A rule of thumb is that a significant change is indicated if the curve falls outside (either above or below) the 95% confidence range for normal year-to-year variability. A change does not necessarily indicate an impact but serves as a point of departure in the assessment of possible causes.

Even with the low number of observations available from the target periods in the current monitoring, polynomial regression equations were statistically significant (reflecting a good fit to the data) both for

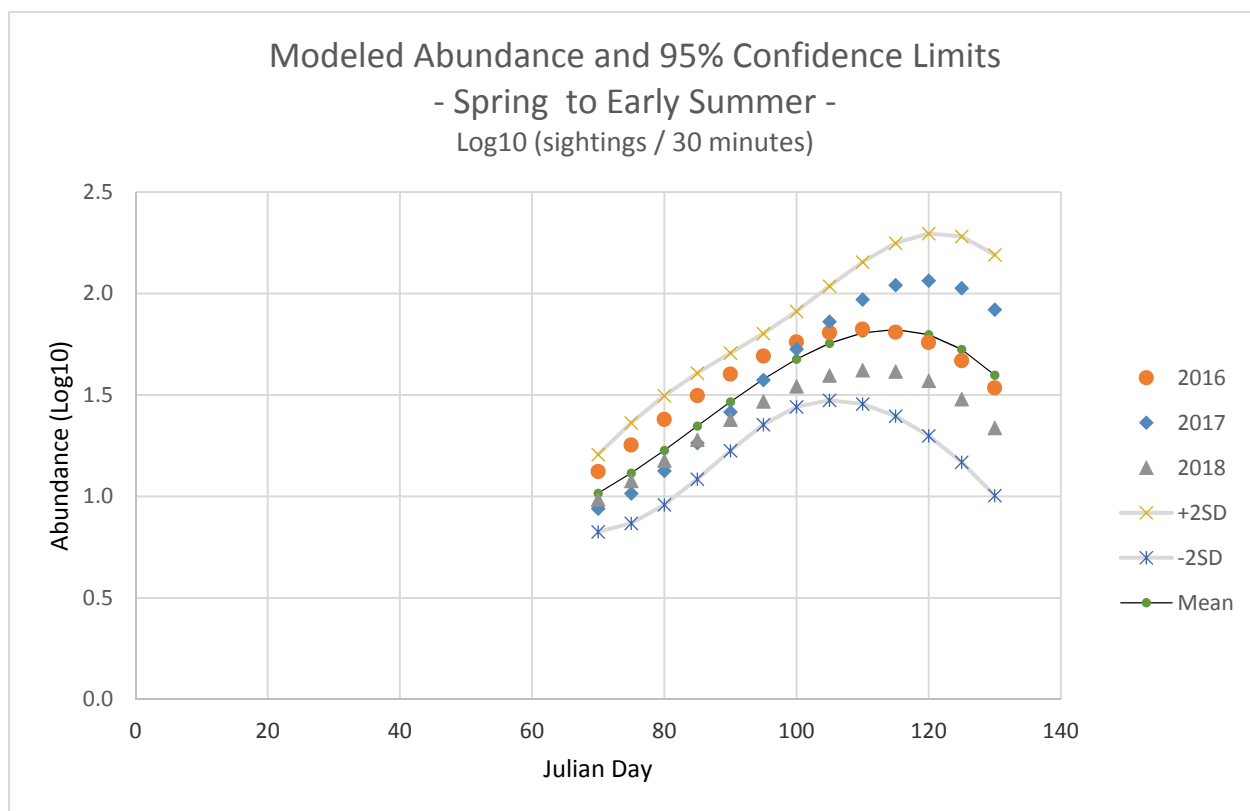


Figure 18. Modeled seabird abundance ($\log(x+1)$) counts/30 minutes) in the spring migration based on polynomial regression equations plotted in Figures 15 to 17, based on standard Julian date.

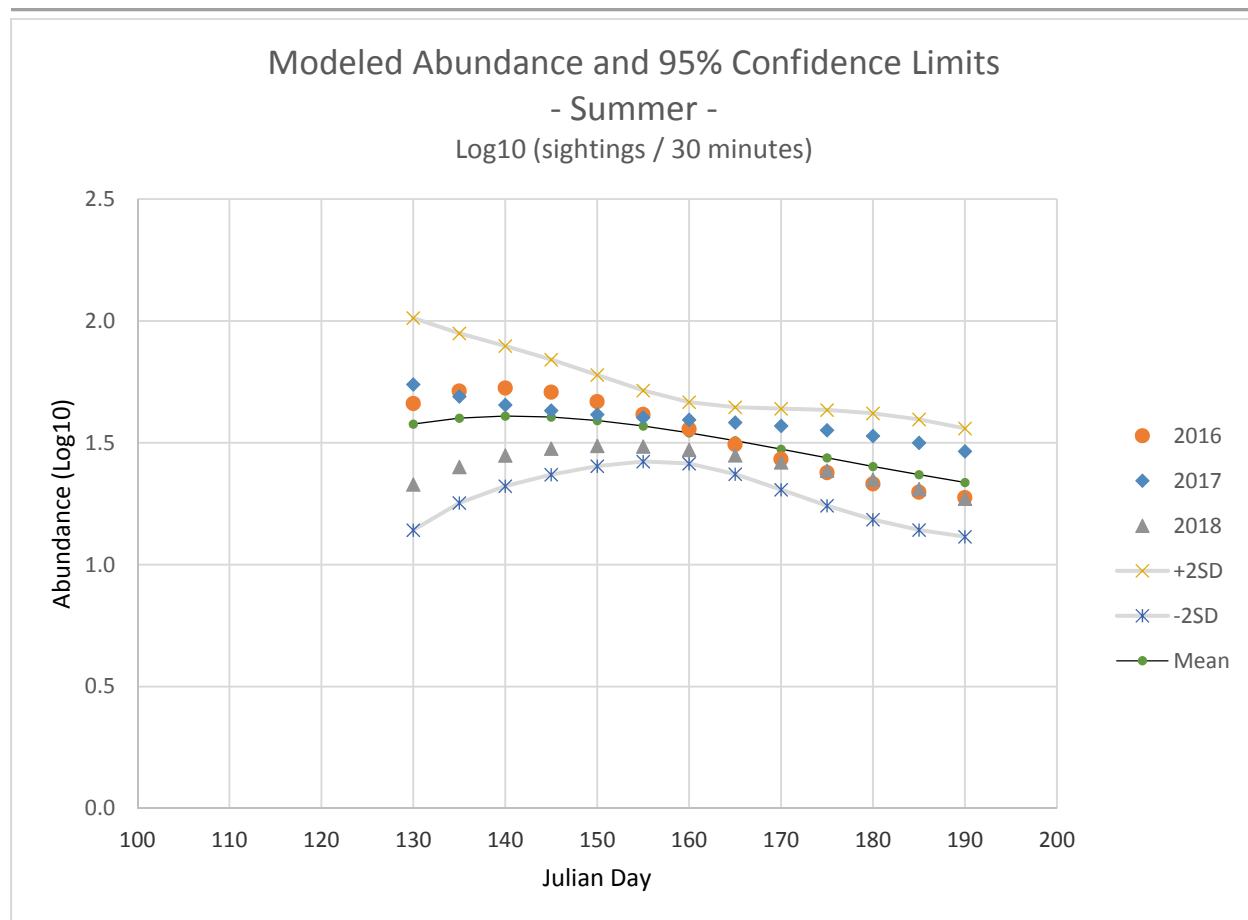


Figure 19. Modeled seabird abundance ($\log(x+1)$) counts/30 minutes in late spring to summer breeding season, based on polynomial regression equations plotted in Figures 15 to 17, based on standard Julian date.

the data overall (i.e. 2016-2018) and for spring 2018 (ANOVA $p < 0.01$ and $p < 0.05$ respectively), while neither the regressions for spring 2016 or 2017 were significant, not unexpectedly due to the low number of observations⁹. The resulting confidence limits on the mean, seem reasonable (i.e. they are in line with the year-to-year variability shown by individual data points (for example the maximum for the study as a whole observed in April 2017 of approximately 270 counts/30 minutes). The resulting confidence limits are higher than, though of the same order, when the data is assessed as a single combined data set for spring migration (Figures 20 and 21) and late-spring to early-summer nesting and breeding season for local resident species (Figures 22 and 23). The pairs of graphs show respectively all available data from the baseline and EEMP monitoring at the FORCE site (Figures 20 and 22) and data available in the 2016 to 2018 EEMP (Figures 21 and 23). In either case, there is an obvious overall scarcity of data points for these key periods. For the approach to implemented, we expect the number of surveys in the target periods for the EEMP would need to be increased to allow a more in-depth analysis to be conducted.

⁹ Only 5 to 7 data points were available for the comparison in target period in each year, representing approximately bi-weekly surveys in those periods.

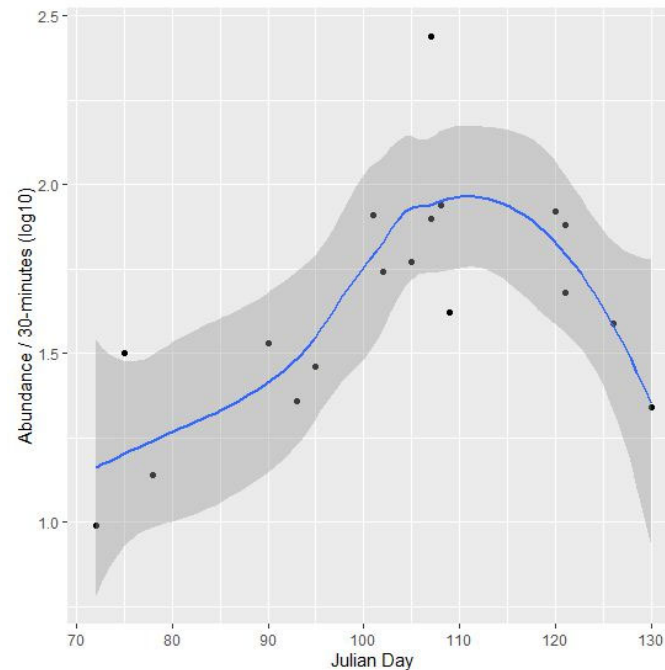


Figure 20. Polynomial regression relationship shown in Figure 4 and 95% confidence limits for seabird abundance at FORCE Minas Passage site in spring (mid-March to late-April). Confidence limits were plotted using the ggplot2 package in the statistical program R (R Development Core Team 2018).

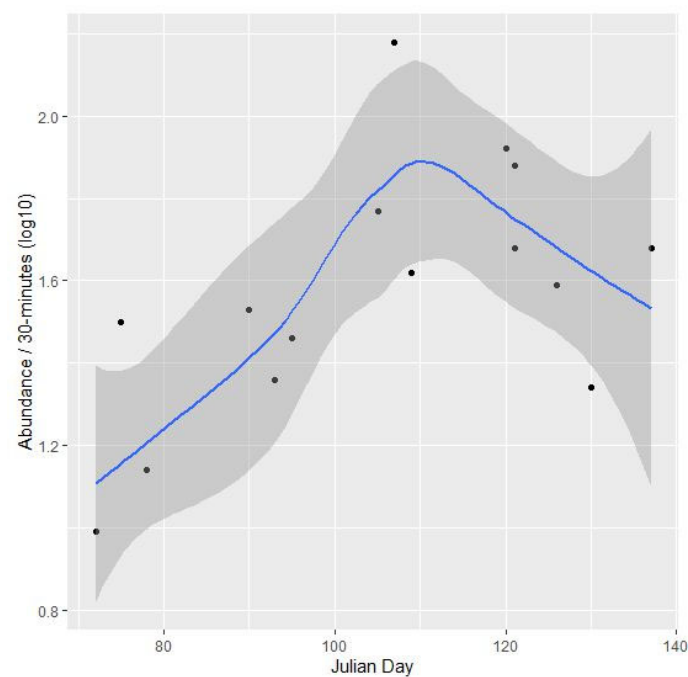


Figure 21. Polynomial regression relationship and 95% confidence limits for seabird abundance at FORCE Minas Passage site for spring (May to early-September) using data from 2016 to 2018 only. Confidence limits were plotted using the ggplot2 package in the statistical program R (R Development Core Team 2018).

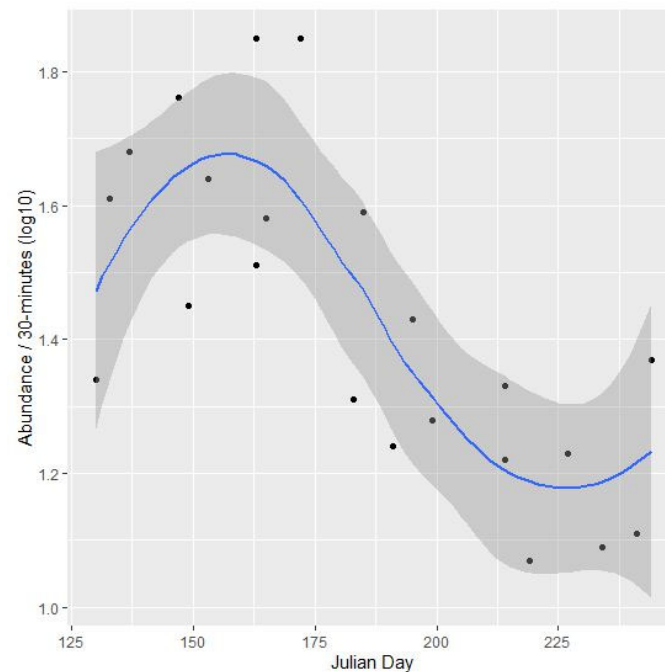


Figure 22. Polynomial relationship and 95% confidence limits for seabird abundance at FORCE Minas Passage site for summer (May to early-September) using data from all years (2010-2012 and 2016-2018). Confidence limits were plotted using the ggplot2 package in the statistical program R (R Development Core Team 2018).

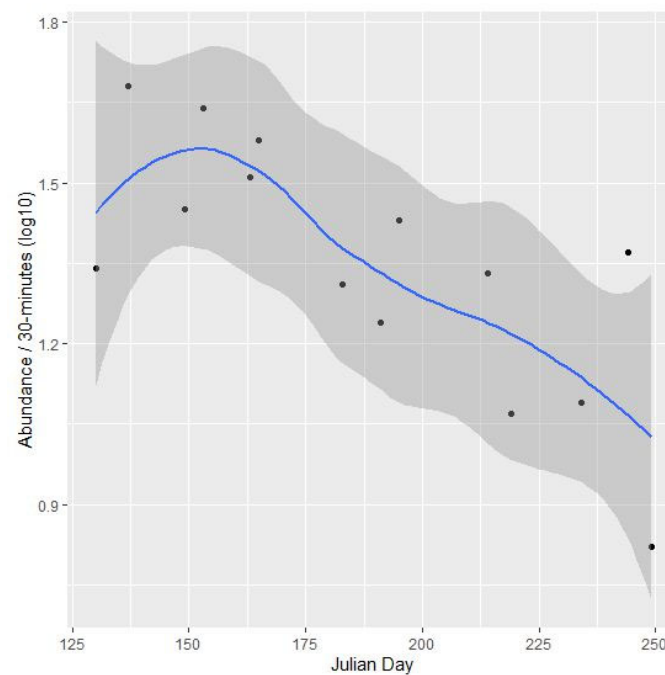


Figure 23. Polynomial relationship and 95% confidence limits for seabird abundance at FORCE Minas Passage site for summer (May to early-September) using data from 2016 to 2018 only. Confidence limits were plotted using the ggplot2 package in the statistical program R (R Development Core Team 2018).

Polynomial regressions for the composite abundance (i.e. abundance of all birds present in a given survey) as well as for individual species and species groups (e.g. scoters) for all surveys (2010 to 2019) are presented in Appendix C. Regressions reflect the various species-specific patterns of abundance at the site; for example the locally-breeding Great Black-backed Gull and Herring Gull show peaks in abundance during breeding, reflecting an aggregation in the mid-spring curves, a secondary abundance peak likely representing the newly fledged generation, and disappearance from the area in summer and fall (Appendix C). Such relationships can be used as a starting point for planning further monitoring and data analysis.

Conclusions and Recommendations – Polynomial Regression Analysis

Polynomial regression may be used as a simple analytical tool to assess changes in abundance of seabirds at the FORCE site; however the approach outlined here requires more frequent observations for the selected periods to adequately capture the inherent variability in seabird numbers than are available in the present monitoring program.

It is expected that ongoing analysis of seabird abundance data at the FORCE site will focus on locally-occurring and breeding species. Migrants, due to the typically short stay in the area and the nature of their movements, are unlikely to interact with tidal devices. In addition, overall abundance and seasonal timing of migrants is affected by factors which sometimes are global in scale. The migrants which pass through quickly and would not likely have an opportunity to interact with tidal energy devices; and their overall abundance is highly variable and depends on factors through their breeding, migration, and overwintering ranges, and therefore would be difficult to attribute to impacts of the tidal energy demonstration site. Local birds demonstrate seasonal cycles including migration, pre-breeding aggregation, breeding abundance, and post-breeding aggregation and movements, which can be modeled by polynomial regression; and because of the longer duration of stay in the area are more likely to interact with tidal devices and experience indirect effects.

Of the large list of species which occur at the site, only locally resident ones, in particular Great Black-backed Gull, Herring Gull, Black Guillemot, and Common Eider, are considered to most relevant. These species aggregate at the site in spring and then establish themselves in the area, experience abundance peaks corresponding to the initial aggregation and presumably the production of the new generation, and whose abundance then drops in the summer. These species make up a relatively small proportion of birds in the peak spring migration period which is dominated by northern migrants such as scoters, cormorants, and Red-throated Loon but their numbers are more stable as the season progresses.

The analysis highlights the fact that there were too few data points to meaningfully document abundance cycles during the critical periods, in particular the spring migration and the breeding season for resident birds. The spring migration is important in assessing the overall importance of Minas Passage as a migratory pathway, although not as likely to be useful for assessing impacts of tidal energy devices at the FORCE site. It would be important to continue to include this period in developing this approach, and in considering designs for further monitoring at the FORCE site, to focus on these two periods and analyze them in relation to local resident species.

The FORCE EEMP has focused observations on a specific time of day and tidal cycle. The other analyses developed (GAM and Bayesian Probability Analysis) may show a better combination of time and tidal

cycle for capturing patterns of abundance. There are a limited number of opportunities, however, to sample mid-day on a high or low tide; consequently to increase the sampling intensity/frequency this objective will have to be sacrificed. We would recommend continuing sampling to coincide with mid-day which provides consistency for that variable, as well as being practical for logistic considerations. In particular the present design allows surveys to be conducted in a single day travelling from the Halifax area and resulting in no overnight costs.

References

- Brandt, S. 1999. *Data Analysis*. Statistical and Computational Methods for Scientists and Engineers.
- Envirosphere Consultants Limited. 2017. Marine Seabirds Monitoring Program. Tidal Energy Demonstration Site—Minas Passage, Year-1: 2016-2017. Report to Fundy Ocean Center for Energy (FORCE).
- Envirosphere Consultants Limited. 2018. Marine Seabirds Monitoring Program. Tidal Energy Demonstration Site—Minas Passage, Year-2: 2017-2018. Report to Fundy Ocean Center for Energy (FORCE).
- Fahrmeir, L. and T. Kneib. 2011. Bayesian Smoothing and Regression for Longitudinal, Spatial and Event History Data. Oxford University Press, New York, 521 p.
- Gitzen, R.A., J.J. Millspaugh, A.B. Cooper and D.S. Licht, eds. 2012. Design and Analysis of Long-term Ecological Monitoring Studies. Cambridge University Press, Cambridge, NY.
- Hastie, J.J. and R.J. Tibshirani. 1990. Generalized Additive Models. Chapman and Hall/ CRC Press.
- in ecology: an Introduction with *mgcv*. PeerJ. DOI 10.7717/peerj.6876.
- Martin, T.G., P.M. Kuhnert, K. Mengersen and H.P. Possingham. 2005. The power of expert opinion in ecological models using Bayesian methods: impact of grazing on birds. *Ecological Applications* 15: 266-280.
- Ostertagova, E. 2012. Modeling using polynomial regression. *Procedia Engineering* 48: 500-506.
- Pederson, E.J., D.L. Miller, G.L. Simpson and N. Ross 2019. Hierarchical generalized additive models in ecology: an Introduction with *mgcv*. PeerJ. DOI 10.7717/peerj.6876.
- R Development Core Team. 2018. R: a language and environment for statistical computing. Vienna: The R Foundation for Statistical Computing. Available at <http://www.R-project.org/>.
- Simpson, G.L. 2018. Modeling Palaeoecological Time Series using Generalized Additive Models. *Front. Ecol. Evol.* <https://doi.org/10.3389/fevo.2018.00149>
- Snedecor, G.W. and W.G. Cochran. 1967. Statistical Methods. Sixth Edition. Iowa State University Press, Ames, Iowa 593 p.
- Sokal, R.R. and F.J. Rohlf. 1981. Biometry. Second Edition. W.H. Freeman and Company, New York, 859 p. Springer Verlag, New York.
- Thogmartin, W.E., J.R. Sauer, and M.G. Knutson. 2004. A hierarchical spatial model of avian abundance with application to Cerulean warblers. *Ecological Applications*, 14: 1766-1779.

Tremblay, G., P. Legendre, J-F. Doyon, R. Verdon and R. Schetagne. 1998. The use of polynomial regression analysis with indicator variables for interpretation of mercury in fish data. *Biogeochemistry* 40, 189–201. doi:10.1023/A:1005997430906

Walker, J. and P.D. Taylor. 2018. Using radar data to evaluate seabird abundance and habitat use at the Fundy Ocean Research Centre for Energy site near Parrsboro, NS. Offshore Energy Research Association (OERA) Project # 300-223. Final Report September 28, 2018. 17 p.

Wood, S.N. 2017. *Generalized Additive Models. An Introduction with R*. Second Edition. CRC Press, Taylor and Francis Group, Boca Raton, FL, USA.

Wu, G., S.H. Holan, C.H. Nilon and C.K. Wikle. 2015. Bayesian binomial mixture models for estimating abundance in ecological monitoring studies. *Annals of Applied Statistics* 9: 1-26.

Appendix A – R Code for Generalized Additive Modeling (GAM) Analysis

A.1 R SCRIPTS FOR READING IN DATA AND ADJUSTING SEABIRD ABUNDANCE DATA TABLE

read in data

Data were provided as “.xls” files and then saved as ‘.csv’ files with no changes. Three files were provided – one containing ‘environmental’ and survey data, and two containing observations. The key that links the two files is the variable ‘survey’ and ‘period’.

Some variables are named differently (case), some missing values are coded as ‘NR’ and some variables are redundant or unnecessary.

The data structure in the FORCE database is presented in Appendix B

```
## include=FALSE suppresses the messages back from read_csv
```

```
knitr::opts_chunk$set(echo = TRUE)
```

```
## read in data
```

```
## environmental data (including all surveys)
```

```
ed.df <- read_csv("Environmental_Data_2010_2019.csv", na = c("NR", "N/R", "/"  
) ) %>%
```

```
  select(-ID, -DATE_DMY)
```

```
names(ed.df) <- tolower(names(ed.df))
```

```
## detection data (two sets)
```

```
fd.1.df <- read_csv("Fundy Data 2010-2012.csv")
```

```
names(fd.1.df) <- tolower(names(fd.1.df))
```

```
fd.2.df <- read_csv("Fundy_Tidal_Seabirds_Main_Table.csv")
```

```
names(fd.2.df) <- tolower(names(fd.2.df))
```

```
## make a data frame with the complete detection data
```

```
## we don't need redundant date_txt field, or the id field (since survey, per  
iod)
```

```
## is the key field
```

```
## but note that 'subperiod' is used differently, and contains some redundant  
data
```

```
## (see database notes and email from patrick in October 2019)
```

```
## so we eliminate subperiod 3 from fd.2.df (9 too I think?).
```

```
## This leaves only sub-periods 1, 2, and 4.
```

```
fd.2.df <- fd.2.df %>% filter(subperiod %in% c(1, 2, 4))

fd.df <- bind_rows(fd.1.df, fd.2.df) %>%
  mutate(date = mdy(date_txt)) %>%
  select(-id, -date_dmy, -date_txt)

## species information
spcd.df <- read_csv("Species_Codes.csv") %>%
  select(-ID)
names(spcd.df) <- tolower(names(spcd.df))

## the following (jd.df) doesn't add any info (julian day, which can be
calculated)
## so don't bother ...
# jd.df <- read_csv("Julian Date.csv")
```

A.2 R SCRIPTS FOR ADJUSTING ENVIRONMENTAL DATA TABLE

The environmental data is adjusted, mostly by calculating times and times to/from high tide.

The main issue with times is that they are recorded in ADT and AST. So, to link properly with the environmental data, all times must be converted to AST ('Local Time') for EC data from the site.

The R package *Lubridate* is used to manage dates. To properly parse the times in *Lubridate*, a leading zero must first be added to the time string.

```
## coordinates of Black Rock (for sunrise times in maptools 'sunriseset' function)
BR.loc <- matrix(c(-64.24, 45.22), nrow=1) ## Black Rock, NS

ed.df <- ed.df %>%
  mutate(start_time = case_when(str_length(start_time) == 3 ~
    paste0("0", start_time),
    TRUE ~ start_time),
    end_time = case_when(str_length(end_time) == 3 ~
    paste0("0", end_time),
    TRUE ~ end_time),
    high_tide = case_when(str_length(high_tide) == 3 ~
    paste0("0", high_tide),
    TRUE ~ high_tide),
    start = mdy_hm(paste(date_txt, start_time),
    tz = "SystemV/AST4"),
```

```

## "SystemV/AST4" is the UNIX designation for Atlantic Standard Time
start = case_when(time_zone == "ADT" ~ start - 3600, ## -1h for DST
  TRUE ~ start),
end = mdy_hm(paste(date_txt, end_time),
  tz = "SystemV/AST4"),
end = case_when(time_zone == "ADT" ~ end - 3600,
  TRUE ~ end),
high.tide = mdy_hm(paste(date_txt, high_tide),
  tz = "SystemV/AST4"),
high.tide = case_when(time_zone == "ADT" ~ high.tide - 3600,
  TRUE ~ high.tide),
date = as.Date(start),
year = year(start),
doy = yday(start),
hour = hour(start),
htht = (as.numeric(high.tide) - as.numeric(start))/3600, # hours
srise = sunriseset(crd = BR.loc, start,
  direction = "sunrise", POSIXct.out = TRUE)[2]$time,
tssr = (as.numeric(start) - as.numeric(srise))/3600, # in hours
sset = sunriseset(crd = BR.loc, start,
  direction = "sunset", POSIXct.out = TRUE)[2]$time,
ttss = (as.numeric(sset) - as.numeric(start))/3600, # in hours
spos = solarpos(crd = BR.loc, start)[2],
cloud_pct = case_when(cloud_pct == "<10" ~ "5",
  cloud_pct == "<100" ~ "90",
  cloud_pct == "<5" ~ "3",
  cloud_pct == "40-50" ~ "45",
  cloud_pct == "OVERCAST" ~ "100",
  TRUE ~ cloud_pct),
cloud_pct = as.numeric(cloud_pct),
dir_nom = factor(dir_nom),
dir_deg = as.numeric(dir_deg),
beaufort = case_when(beaufort == "1-2" ~ "1",
  beaufort == "2-3" ~ "2",
  beaufort == "3-4" ~ "3",
  beaufort == "4-5" ~ "4",
  beaufort == "5-6" ~ "5",
  beaufort == "6-7" ~ "6",
  TRUE ~ beaufort),
beaufort = as.numeric(beaufort),
visibility = case_when(
  visibility_km %in% c(">10", ">5", "5", "7.5", "~5", "3-4") ~ "High
",
  is.na(visibility_km) ~ "Unk",
  TRUE ~ "Low"),
t_deg_c = case_when(t_deg_c == "sunny" ~ NA_character_,
  t_deg_c == "9-16.3" ~ NA_character_,
  t_deg_c == "10-15.6" ~ NA_character_,

```

```
TRUE ~ t_deg_c),  
t_deg_c = as.numeric(t_deg_c))
```

A.3 R SCRIPTS FOR LINKING THE ENVIRONMENTAL DATA WITH THE ABUNDANCE DATA

Missing weather data in the environmental data set was fixed by obtaining consistent data from the Environment Canada weather record for Parrsboro. This data was harvested from the EC site using the functions provided in this blog post:

<https://www.fromthebottomoftheheap.net/2015/01/14/harvesting-canadian-climate-data/>

The format of the EC data was noted to be inconsistent temporally, and consequently for future use, ongoing adjustment and checks may be required when the data is accessed. The EC data was placed in a separate file.

The Environment Canada data are provided in 'Local Standard Time' (that is, no Daylight Saving Time), and times were adjusted in the FORCE data set prior to analysis.

The files are linked to the existing environment data file (ed.df).

```
ed.df <- left_join(ed.df, all.weather, by = c("date", "year", "hour"))  
  
## here I check that there are no missing data in the environmental file.  
## Some earlier issues meant that there were. Should show zero rows.  
ed.df %>% filter(is.na(start_time)) %>% ## just a check  
  select(survey, period, date) %>%  
  distinct() %>% arrange(date)  
  
## # A tibble: 0 x 3  
## # ... with 3 variables: survey <chr>, period <chr>, date <date>
```

A.4 CODE TO CHECK FOR CONSISTENCY OF KEY VARIABLES AND ERRORS ACROSS DATABASE TABLES

This code checks for inconsistencies in matching survey, period and date (between ed and fd). Mismatches between date_txt and date_dmy can be fixed prior to analysis in working copies of the csv files. These issues have been corrected in the main data tables for the FORCE database.

```
ed.surveys <- ed.df %>%  
  select(survey, period, date=date_txt) %>%  
  distinct() %>%  
  mutate(date = mdy(date))  
fd.surveys <- fd.df %>% select(survey, period, date) %>% distinct()
```



```
## all survey dates should match across these two files, so should result in
## zero rows
left_join(ed.surveys, fd.surveys, by = c("survey", "period")) %>%
  filter(!(date.x == date.y))

## # A tibble: 0 x 4
## # ... with 4 variables: survey <chr>, period <chr>, date.x <date>,
## #   date.y <date>
```

A.5 CODE FOR EXTRACTING AND AGGREGATING COUNTS FOR PERIODS BY AREAS AND SPECIES

Inconsistencies in the data must be corrected in the working csv and master database files.

The environmental and observational data are combined, variables needed are selected, and others are dumped in the observation data.

For a preliminary assessment, the total count is used. Extraction is a complex operation, and described in the code below. Apparent duplicates are situations where male and female (M/F) of a species are recorded on separate lines, and are dealt with in the code. In addition, the data are 'partially long and partially wide' – a situation which is fixed below so that there is an observation (zero or otherwise) for every combination of species and observation period.

The data is aggregated across the spatial areas in the following way:

O is the code used for 2010-2012 analyses to signify "outside the lease area" is considered to be the same as sums of OB1-3, FF1-3, IB1-3 in 2016-2018 period. BR is the code considered the same in both periods, referring to birds sitting on Black Rock. CL and CLT were different codes but referring to the Tidal ("Crown") Lease area in both periods.

```
fd.df <- fd.df %>%
  mutate(
    spcd = str_trim(species), ## some extra blank spaces somewhere
    spcd = ifelse(spcd == "Alcid.Sp.", "ALCID", spcd), ## fix to make the same
    spcd = ifelse(spcd == "SCSp.", "SCOTER", spcd)) %>% ## ditto
  left_join(spcd.df, by = c("species")) %>% ## join in species names
  select(survey, period, date, area,
    spcd, species = common_name, b:f1) %>%
  filter(!spcd %in% c("HAPO", "HASE", "HRSE", "GRSE"),
    !is.na(species)) %>% ## get rid of seals and the 'Alcid' with no species name
  group_by(survey, period, date, spcd, species, area) %>% ## this sums over subperiods
  summarize(total = sum(b, u, nb, `1c`, `2c`, `3c`, `4c`)) %>%
  ## OW and FL are not used consistently across surveys,
  ## My understanding is that the total number of birds is the
  ## sum of those categories .... #### CHECK THIS ####
```

```

ungroup() %>%
  ## get counts across all 'areas' and sum accordingly
  pivot_wider(names_from = area,
               values_from = total,
               values_fill = list(total = 0)) %>%
  mutate(total.br = BR, # On Black Rock -- same in two pe
riods
         total.tl = CLT + CL, # Turbine Lease -- CLT in 2010-20
12;
                                # CL in 2016-2019
         total.far = FF1 + FF2 + FF3, # Far afield -- only in 2016-2019
         total.obr = OB1 + OB2 + OB3, # Outside Black Rock --- 2016-201
9
         total.ibr = IB1 + IB2, # Inside Black Rock -- 2016-2019
         total.a = 0 + total.tl + total.far + total.obr + total.ibr, ## total
not Black Rock
         total.b = total.a + total.br, ## everything
         total.c = total.a - total.tl) ## total not Black Rock or Tidal Lease

```

A.6 CODES FOR CREATING AND MANIPULATING SPECIES AND SPECIES GROUPS

Additional species and groups are added by this code component. Individual species are informative, but groups of species (e.g. scoters) rather than individual species are both informative and help to determine which groups might best be ignored for statistical models.

Groupings selection is shown in the code below. On the left hand side of the tilde (~) are the species codes for the group on the right hand side. For example, the only Gannet is Northern Gannet, and it forms a unique group. Cormorants are a group in which there are two species, DCCO and GRCO.

```

## these groups need to be exclusive (as the code is currently written)
## we can easily still do analyses of individuals species, if we want
fd.df <- fd.df %>%
  mutate(
    sp.grp = case_when(
      spcd %in% c("BLKI", "GBBG", "GULL", "HEGU", "ICGU", "LAGU", "LBBG", "ME
GU",
                 "RBGU") ~ "Gull",
      spcd %in% c("ALCID", "ATPU", "COMU", "DOVE", "RAZO", "TBMU") ~ "Alcid",
      ## no BLGU (Patrick)
      spcd %in% c("BLGU") ~ "BLGU",
      spcd %in% c("COEI", "COGO", "HADU", "KIEI", "LTDU", "RBME") ~ "Seaduck"
    ),
    spcd %in% c("BLSC", "SUSC", "WWSC", "SCOTER") ~ "Scoter",
    spcd %in% c("ABDU", "BWTE", "BUFF", "CAGO", "COME", "GWTE", "HOME",
                 "MALL", "NSHO", "SNGO") ~ "OtherDuck",
    spcd %in% c("HOGR", "RNGR") ~ "Grebe",

```

```

spcd %in% c("NOGA") ~ "NOGA",
spcd %in% c("ARLO", "COLO", "LOON", "PALO", "RTLO" ) ~ "Loon",
spcd %in% c("BBPL", "GRYE", "LESA", "LEYE", "PUSA", "REPH", "RUTU", "SAND",
           "SESA", "SPPL", "SPSA" ) ~ "Shorebird",
spcd %in% c("DCCO", "GRCO") ~ "Cormorant",
spcd %in% c("COSH", "GRSH", "SOSH") ~ "Shearwater",
spcd %in% c("BAEA", "BLTE", "GBHE", "NOFU", "NOHA", "OSPR",
           "PEFA", "RNPH", "WISP", "TUVU") ~ "Other",
TRUE ~ "Other"
)
)

```

A.7 CODES TO GROUP AND UNGROUP SPECIES GROUPS FOR WORKING MATRIX COMPILATION

After having ungrouped the data, which involved removing the zeros, the zeros must be reinserted, since they are a critical part of the dataset. This is done by taking the long data (one observation per species period), making it wide (and filling the missing spots with zeros), then making it long again (retaining the zeros).

Note that when done this way, any surveys and periods where absolutely no birds were seen are ignored. This condition should be checked to see if and how often this occurred.

```

## the following syntax spreads across all survey periods, making NA
## equal zero (so adding zeroes for all species in all survey periods)
## it then gathers that back up into the original format, and joins in the
## rest of the metadata originally in fd.df

tmp <- fd.df %>%
  select(survey, period, date, spcd, total.a, total.b, total.br, total.tl, to
tal.c) %>%
  arrange(spcd)

total.a <- tmp %>% select(survey:spcd, total.a) %>%
  pivot_wider(names_from = spcd, values_from = total.a, values_fill = list(to
tal.a = 0)) %>%
  pivot_longer(cols = ABDU:WWSC, names_to = "spcd", values_to = "count") %>%
  mutate(loc = "All except Black Rock")

total.b <- tmp %>% select(survey:spcd, total.b) %>%
  pivot_wider(names_from = spcd, values_from = total.b, values_fill = list(to
tal.b = 0)) %>%
  pivot_longer(cols = ABDU:WWSC, names_to = "spcd", values_to = "count") %>%
  mutate(loc = "All")

total.br <- tmp %>% select(survey:spcd, total.br) %>%

```

```
  pivot_wider(names_from = spcd, values_from = total.br, values_fill = list(t
otal.br = 0)) %>%
  pivot_longer(cols = ABDU:WWSC, names_to = "spcd", values_to = "count") %>%
  mutate(loc = "Black Rock")

total.tl <- tmp %>% select(survey:spcd, total.tl) %>%
  pivot_wider(names_from = spcd, values_from = total.tl, values_fill = list(t
otal.tl = 0)) %>%
  pivot_longer(cols = ABDU:WWSC, names_to = "spcd", values_to = "count") %>%
  mutate(loc = "Tidal Lease")

total.c <- tmp %>% select(survey:spcd, total.c) %>%
  pivot_wider(names_from = spcd, values_from = total.c, values_fill = list(to
tal.c = 0)) %>%
  pivot_longer(cols = ABDU:WWSC, names_to = "spcd", values_to = "count") %>%
  mutate(loc = "Not BR or Tidal Lease")

## get a list of species information here
sp.tmp <- fd.df %>% select(spcd, species, sp.grp) %>%
  filter(!is.na(species)) %>%
  distinct()

## combine all of the files and join in the species information
fd.df.up <- bind_rows(total.a, total.b, total.c, total.br, total.tl) %>%
  left_join(sp.tmp) %>%
  left_join(ed.df, by = c("survey", "period", "date"))

rm(tmp, sp.tmp) ## don't need these any more
```

The following code produces a summary, for every species group, in every survey period. The same data frame could be used to directly analyse a single species.

```
## sums up for every species group, each survey period
## this is the main data set that we need.

## we 'cheat' a little by also grouping by the various environmental
variables,
## so that we retain them in the final summary data set.

## because we group on the 'loc' variable, we retain the individual counts
for each
## of the locations, even though there is overlap among the groups. Shoud
check that
## this has been done correctly (by just doing some of the sums across groups
by hand)
```

```
## for now, keep just the EC weather data
sum.df <- fd.df.up %>%
  group_by(survey, period, date, year, hour, doy, sp.grp, start, htht, ttss,
    tssr,
    beaufort, bpress, temp, wind.dir, wind.spd, wind.x, wind.y, loc)
%>%
  summarize(count = sum(count)) %>%
  mutate(week = week(date)) %>% ## why do I need this? (probably don't)
  filter(!is.na(start)) %>% ## still missing some (not any more; 23 Nov
2019)
  ungroup()

## and then just a few select species
sum.sp.df <- fd.df.up %>%
  filter(spcd %in% c("ABDU", "BLSC", "COEI", "COLO", "DCCO", "GBBG",
    "HADU", "HEGU", "LTDU", "NOGA", "PUSA", "RAZO",
    "RBGU", "RNGR", "RTLO")) %>%

  group_by(survey, period, date, year, hour, doy, spcd, start, htht, ttss,
    tssr,
    beaufort, bpress, temp, wind.dir, wind.spd, wind.x, wind.y, loc)
%>%
  summarize(count = sum(count)) %>%
  mutate(week = week(date),
    sp.grp = spcd) %>%
  ungroup()

## combine these
sum.df <- bind_rows(sum.df, sum
```

A.8 CODE TO PRODUCE SPECIES BY TIME OF YEAR PLOTS (See main text, Figure 1)

The code below plots a partial set of the data, because there is overlap in the categories. To produce an overall plot, the location “All” can be used. At this point the data must be adjusted for the numbers of survey periods per survey. The current test analysis doesn’t do that, and is determined per survey. However this adjustment can be readily made in the R code.

The R code below produces a data frame with all combinations of species, species groups, and locations, that can be used for visualization and analysis.

The analysis below uses the resulting data frame to look at the patterns comparing Black Rock to the Tidal Lease for the most common species.

```
tmp.df <- sum.df %>% filter(loc == "All") %>%
  mutate(tmp.date = dmy("1-1-1900") + week*7) %>%
  group_by(survey, sp.grp, loc, date, tmp.date) %>%
  summarize(count = mean(count))

p <- ggplot(data=tmp.df, aes(tmp.date, count+1, group=format(as.Date(tmp.date), "%W"))))
p + geom_boxplot() + scale_y_log10() +
  facet_wrap(~sp.grp, ncol = 3) +
  ylab("Count per period") +
  xlab("Time of Year") +
  theme(axis.text.x = element_text(size=7, angle=90)) +
  scale_x_date(date_breaks = "4 weeks",
               date_labels = "%b %d")
```

A.9 CODE TO PRODUCE REDUCED SET OF SPECIES BY TIME OF YEAR PLOTS (See main text, Figure 2)

The analysis below uses the data frame generated in A.8 above to look at the patterns comparing Black Rock to the Tidal Lease for a reduced set of species.

```
tmp.df <- sum.df %>%
  mutate(tmp.date = dmy("1-1-1900") + week*7) %>%
  filter((sp.grp %in% c("ABDU", "BLGU", "BLSC", "COEI", "COLO",
                      "DCCO", "GBBG", "HEGU", "LTDU", "RBGU", "RTLO")),
         loc %in% c("Black Rock", "Tidal Lease", "Not BR or Tidal Lease"))

p <- ggplot(data=tmp.df, aes(tmp.date, count+1, group=format(as.Date(tmp.date), "%W"))))
p + geom_boxplot() + scale_y_log10() +
```

```
facet_wrap(~sp.grp, ncol = 3) +
ylab("Count per period") +
xlab("Time of Year") +
theme(axis.text.x = element_text(size=7, angle=90)) +
scale_x_date(date_breaks = "4 weeks",
             date_labels = "%b %d")
```

A.10 CODE TO PRODUCE A FOCUSED SET OF SPECIES BY TIME OF YEAR PLOTS (See main text, Figure 3)

This code looks at the patterns comparing Black Rock to the Tidal Lease for the most common species.

Using the data frame with all combinations of species, species groups, and locations, a plot in the same layout as for Figure 2, can be produced, but split by the independent locations (Black Rock, Tidal Lease, Other (not BR or Tidal Lease)).

```
tmp.df <- sum.df %>%
  mutate(tmp.date = dmy("1-1-1900") + week*7,
         pres = ifelse(count == 0, 0, 1)) %>%
  filter((sp.grp %in% c("ABDU", "BLGU", "BLSC", "COEI", "COLO",
                      "DCCO", "GBBG", "HEGU", "LTDU", "RBGU", "RTLO")),
         loc %in% c("Black Rock", "Tidal Lease", "Not BR or Tidal Lease"))

p <- ggplot(data=tmp.df, aes(tmp.date, count+1, group=format(as.Date(tmp.date), "%W"))
) + geom_boxplot() + scale_y_log10() +
  facet_grid(sp.grp~loc) +
  ylab("Count per period") +
  xlab("Time of Year") +
  theme(axis.text.x = element_text(size=7, angle=90)) +
  scale_x_date(date_breaks = "4 weeks",
              date_labels = "%b %d")
```

A.11 CODE FOR PRODUCING SUMMARY TABLE OF PROPORTIONS OF SPECIES OCCURRING IN AREAS (See main text, Table 1)

The data shows that there are effects of location that differ for the various species. To assist in the assessment, this code produces a table showing the number of sampling periods where the species was present, for Black Rock, The Tidal Lease, or neither.


```
## at some point code in the 737 here, so it can vary depending on the input  
with(tmp.df, trunc(table(pres, sp.grp, loc)/737*100)[2,,])
```

A.12 CODE FOR PRODUCING SUMMARY TABLE OF SAMPLING INTENSITY (NUMBER OF PERIODS) BY YEAR FOR DATASET (See main text, Table 2)

This code summarizes the number of survey periods throughout the FORCE baseline studies and Environmental Effects Monitoring Program (EEMP).

```
obs.sum <- fd.df.up %>%  
  select(survey, period, date, doy, start, htth) %>%  
  distinct() %>%  
  mutate(htth = trunc(htth),  
         hr = trunc(hour(start)),  
         month = month(date),  
         year = year(date)) %>%  
  group_by(date, period, month, year) %>%  
  tally()  
  
with(obs.sum, table(year, month))
```

A.13 CODE FOR PRODUCING SUMMARY GRAPH OF SPECIES MEAN COUNT PER SURVEY PERIOD SUMMARIZED BY WEEK (See main text, Figure 4)

This code provides an additional way of visualizing the data, summarizing counts over week of the year (taking the mean count per survey period).

```
sum2.df <- sum.df %>% group_by(loc, sp.grp, week) %>%  
  summarize(mn.count = mean(count))
```

The following code produces the graph output in Figure 4.

```
tmp.df <- sum2.df %>%  
  filter((sp.grp %in% c("COEI", "DCCO", "GBBG", "BLGU",  
                      "HEGU", "NOGA", "RTLO", "Scoter")),  
         loc %in% c("Black Rock", "Tidal Lease"))  
  
p <- ggplot(data=tmp.df, aes(week, mn.count+0.01, colour=loc))  
  
p + geom_jitter(size=0.8, height=0.01) +
```

```
geom_line() +  
scale_y_log10() +  
facet_wrap(~sp.grp) +  
xlab("Week of Year") +  
ylab("Log10 of mean count per weekly period") +  
theme(axis.text.x = element_text(size=5, angle=45))
```

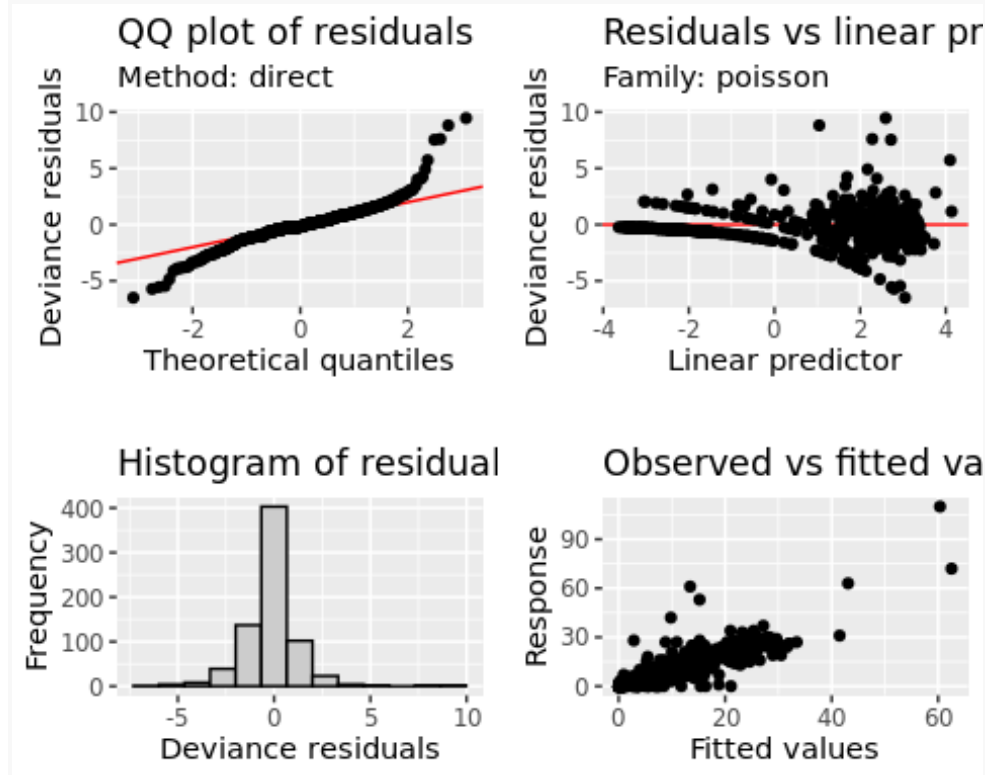
A.14 CODE FOR AN EXAMPLE OF APPLYING A MODEL DISTRIBUTION TO A SINGLE SPECIES (GREAT BLACK-BACKED GULL, AND FITTING THE MODEL (SEE FIGURES 5 & 6)

This is a sample analysis of Great Black-backed Gull. 'Survey' is used as a random effect in the GAM models, to account for at least some of the unobserved variability.

```
tmp.df <- filter(sum.df, sp.grp == "GBBG",  
                loc == "All") %>%  
  ## some of this I don't use ....  
  mutate(year.fac = factor(year < 2016),  
         week.fac = factor(week),  
         loc.fac = factor(loc),  
         season = case_when(doy > 340 | doy < 50 ~ "Winter",  
                             doy >= 50 & doy < 135 ~ "Spring",  
                             doy >= 135 & doy < 250 ~ "Summer",  
                             TRUE ~ "Fall"),  
         season = factor(season),  
         survey = factor(survey),  
         pres = ifelse(count == 0, 0, 1)) %>% ## could consider separate pres  
/absence models  
  filter(!is.na(temp))  
  
## fit a count/poisson model first  
tmp1.gam <- gam(count ~ s(doy, bs = "cc", k = 25) +  
                s(tssr, bs = "cr", k = 5) +  
                s(htht, bs = "cc", k = 5) +  
                s(wind.dir, bs = "cc", k = 5) +  
                s(log10(wind.spd), k = 5) +  
                s(temp, k = 5) +  
                s(bpress, k = 5) +  
                s(survey, bs = "re"),  
                family = poisson,  
                data = tmp.df,  
                method = "REML")
```

In this step, the model properties are checked.

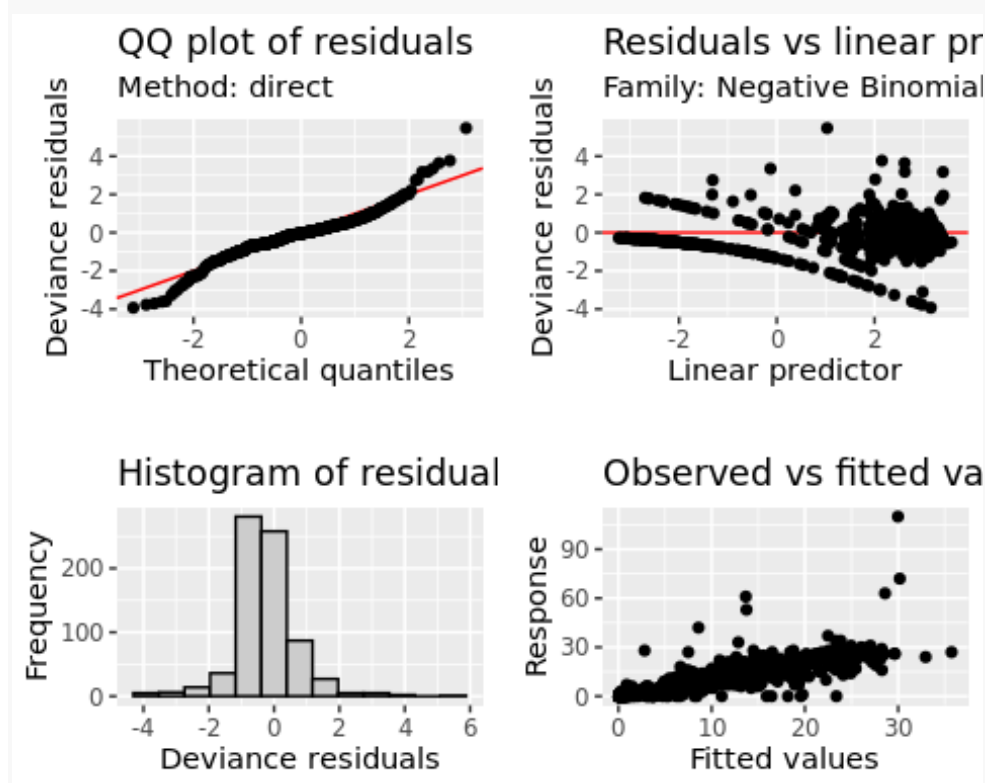
`appraise(tmp1.gam)`



The plots show over-dispersion, and the model is changed to negative-binomial and re-run.

```
tmp2.gam <- gam(count ~ s(doy, bs = "cc", k = 25) +  
  s(tssr, bs = "cr", k = 5) +  
  s(htht, bs = "cc", k = 5) +  
  s(wind.dir, bs = "cc", k = 5) +  
  s(log10(wind.spd), k = 5) +  
  s(temp, k = 5) +  
  s(bpress, k = 5) +  
  s(survey, bs = "re"),  
  family = nb(),  
  data = tmp.df,  
  method = "REML")
```

```
appraise(tmp2.gam)
```



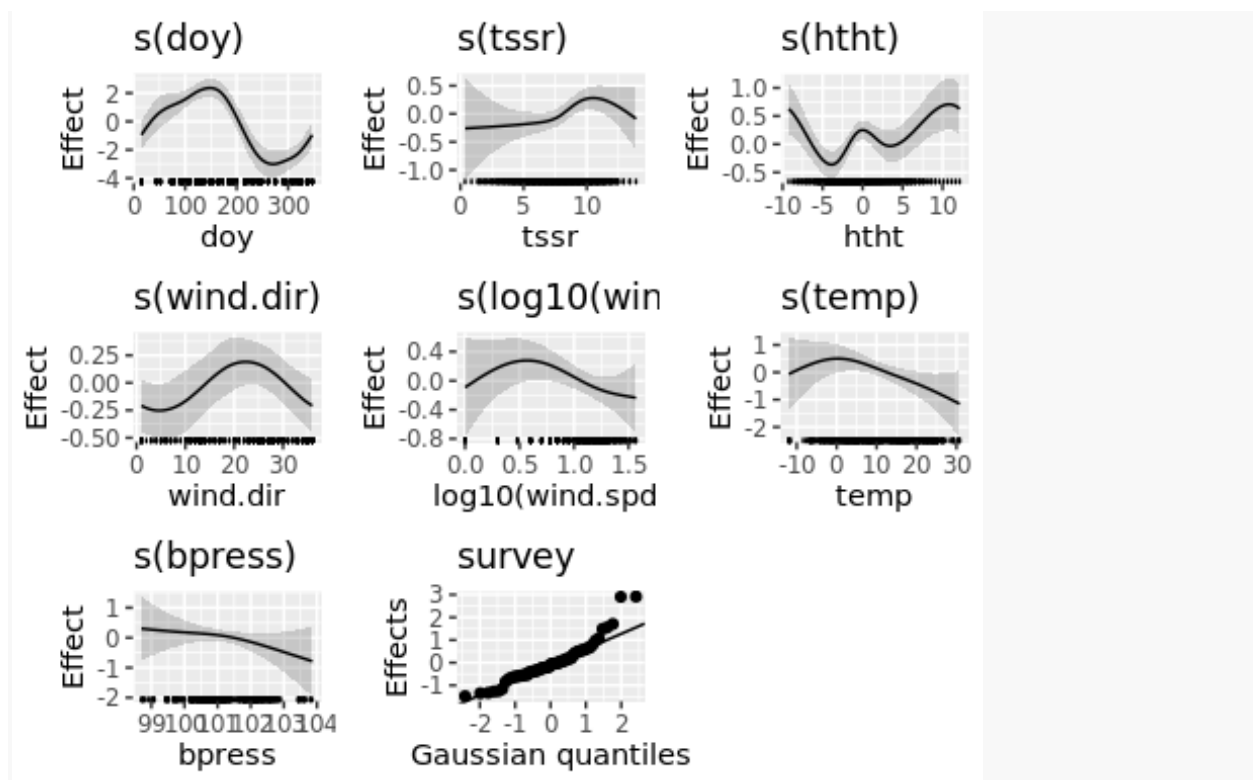
The negative-binomial shows a better overall fit (see the QQ plot of residuals) but there are some high counts that aren't estimated well. That could make the model less suitable (given the paucity of the data, and the resulting lack of high counts in the dataset to be used in modeling. For this example, this problem is not solved and the issue is left for future consideration. In the interim however, these two models are compared using the Akaike Information Coefficient (AIC). The negative binomial is shown to be superior by the lower value of the AIC.

```
AIC(tmp1.gam, tmp2.gam)
```

```
##           df      AIC
## tmp1.gam 78.97511 3416.654
## tmp2.gam 74.44106 3125.830
```

A.15 SUMMARY STATISTICS GENERATED FROM THE GREAT BLACK-BACKED GULL DATASET.

```
draw(tmp2.gam)
```



A.16 SIGNIFICANCE STATISTICS PRODUCED FOR GREAT BLACK-BACKED GULL DATASET.

Significance statistics are produced for the environmental variables in relation to Great Black-backed Gull annual abundance. The significant parameters are day of year, sunrise time, wind-direction and survey.

```
summary(tmp2.gam)

##
## Family: Negative Binomial(4.031)
## Link function: log
##
## Formula:
## count ~ s(doy, bs = "cc", k = 25) + s(tssr, bs = "cr", k = 5) +
##       s(htht, bs = "cc", k = 5) + s(wind.dir, bs = "cc", k = 5) +
##       s(log10(wind.spd), k = 5) + s(temp, k = 5) + s(bpress, k = 5) +
##       s(survey, bs = "re")
##
## Parametric coefficients:
##               Estimate Std. Error z value Pr(>|z|)
## (Intercept)   0.6230     0.1488   4.187 2.83e-05 ***
## ---
## Signif. codes:  0 '***' 0.001 '**' 0.01 '*' 0.05 '.' 0.1 ' ' 1
```

```
##
## Approximate significance of smooth terms:
##           edf Ref.df   Chi.sq p-value
## s(doy)      5.170 23.000 17156.682 < 2e-16 ***
## s(tssr)     3.374  3.771   11.976 0.00820 **
## s(htht)     2.886  3.000   141.481 0.10360
## s(wind.dir) 1.723  3.000   176.614 0.00744 **
## s(log10(wind.spd)) 2.543  3.088    6.950 0.09557 .
## s(temp)     2.535  2.950    5.985 0.09515 .
## s(bpress)   1.505  1.701    1.436 0.30989
## s(survey)   45.191 63.000   387.500 < 2e-16 ***
## ---
## Signif. codes:  0 '***' 0.001 '**' 0.01 '*' 0.05 '.' 0.1 ' ' 1
##
## R-sq.(adj) = 0.646   Deviance explained = 83.3%
## -REML = 1623.3   Scale est. = 1           n = 727
```

A.17 ASSESSING GREAT BLACK-BACKED GULL ABUNDANCE LOCALLY IN THE STUDY AREA AT BLACK ROCK, NOT ON BLACK ROCK AND FOR THE TIDAL LEASE.

The Tidal Lease would be a suitable area for assessing the abundance pattern; however there are few observations of Great Black-backed Gull in the Tidal Lease (A.16 above), so a local comparison was conducted of abundance of birds on Black Rock to Not Black Rock or to those observed in the Tidal Lease. The significant parameters are day of year, sunrise time, wind-direction and survey. Based on this analysis, the model was simplified to look for effects of location.

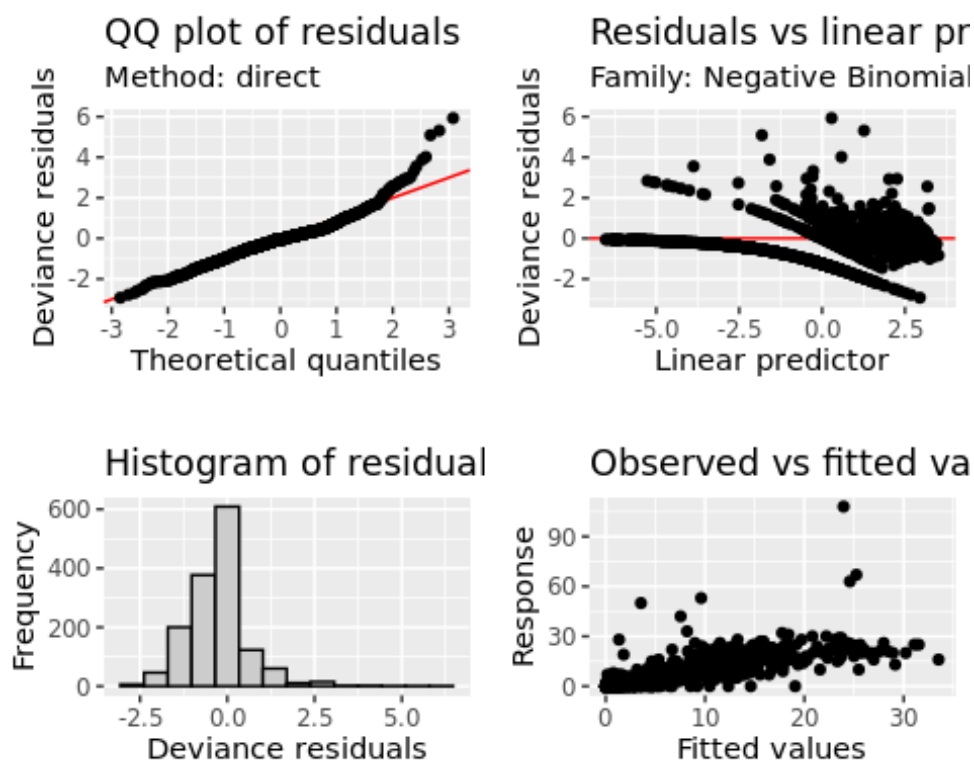
```
tmp.df <- filter(sum.df, sp.grp == "GBBG",
                 loc %in% c("Black Rock", "Not BR or Tidal Lease")) %>%
  mutate(year.fac = factor(year < 2016),
         week.fac = factor(week),
         loc.fac = factor(loc),
         season = case_when(doy > 340 | doy < 50 ~ "Winter",
                           doy >= 50 & doy < 135 ~ "Spring",
                           doy >= 135 & doy < 250 ~ "Summer",
                           TRUE ~ "Fall"),
         season = factor(season),
         survey = factor(survey),
         pres = ifelse(count == 0, 0, 1)) %>%
  filter(!is.na(temp))

tmp3.gam <- gam(count ~ loc.fac +
               s(doy, bs = "cc", k = 25) +
               s(tssr, bs = "cr", k = 5, by = loc.fac) +
               s(htht, bs = "cc", k = 5, by = loc.fac) +
               s(wind.dir, bs = "cc", k = 5, by = loc.fac) +
               s(survey, bs = "re"),
```

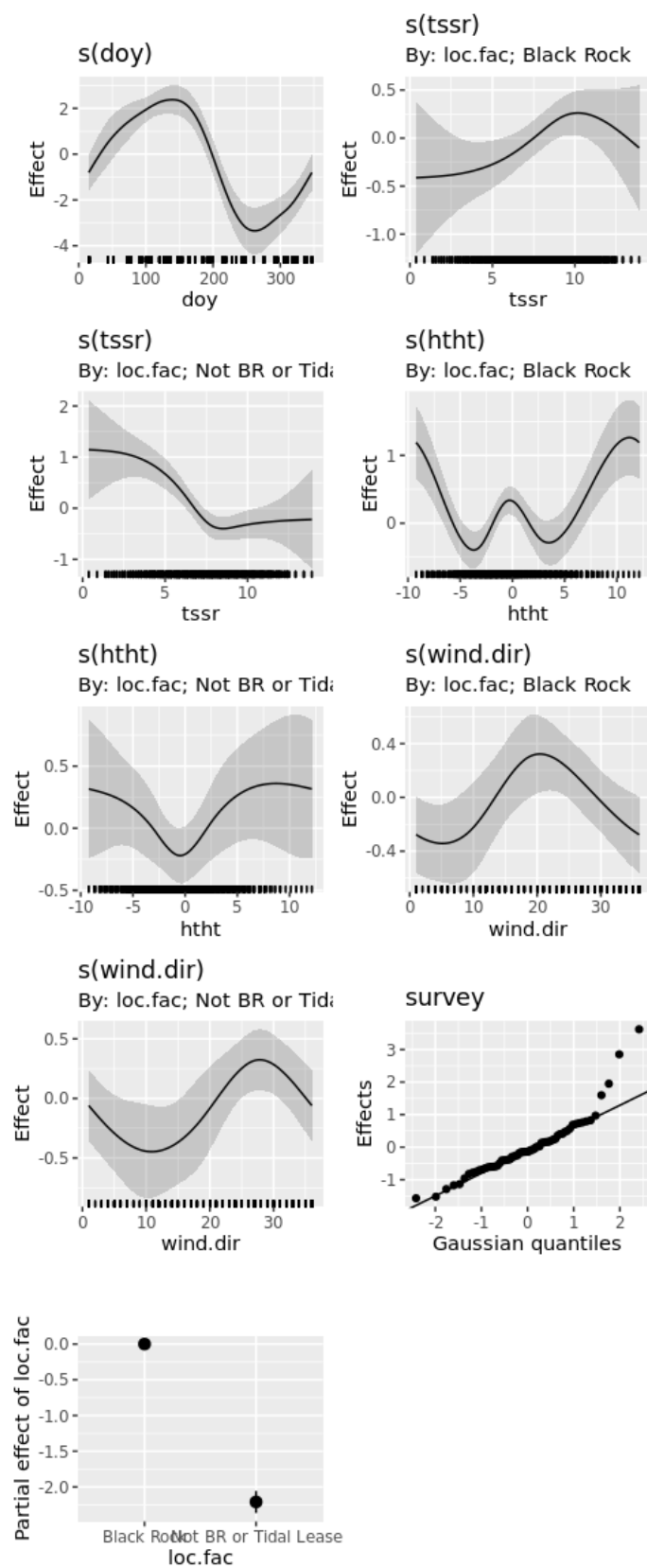
```
family = nb(),  
data = tmp.df,  
method = "REML")
```

The results of this analysis (below) suggest that tide height and time of day influence the counts differently at the two locations, but that wind direction doesn't have a similar effect.

```
appraise(tmp3.gam)
```



```
draw(tmp3.gam, ncol=2)
```

Those

The model above can then be tweaked (see below) to determine if a better fit can be obtained. To simplify the model, the 'by' term was dropped for each of tide and sunrise time, and the fit tested using Akaike Information Criterion, AIC. The result presented below suggests that the fit isn't improved enough to suggest that tide height or time of day have an effect on the differences in counts differ between these two locations. There may well be differences, but the data may be insufficient to detect them (which is another way of saying there is so much variability in the system to begin with, these environmental effects are difficult to detect).

```
tmp4.gam <- gam(count ~ loc.fac +
  s(doy, bs = "cc", k = 25) +
  s(tssr, bs = "cr", k = 5) +
  s(htht, bs = "cc", k = 5, by = loc.fac) +
  s(wind.dir, bs = "cc", k = 5) +
  s(survey, bs = "re"),
  family = nb(),
  data = tmp.df,
  method = "REML")

tmp5.gam <- gam(count ~ loc.fac +
  s(doy, bs = "cc", k = 25) +
  s(tssr, bs = "cr", k = 5, by = loc.fac) +
  s(htht, bs = "cc", k = 5) +
  s(wind.dir, bs = "cc", k = 5) +
  s(survey, bs = "re"),
  family = nb(),
  data = tmp.df,
  method = "REML")

AIC(tmp3.gam, tmp4.gam, tmp5.gam)

##           df      AIC
## tmp3.gam 74.30237 4421.188
## tmp4.gam 67.86697 4482.470
## tmp5.gam 68.89730 4463.477
```

A.18 ANALYSIS FOR RED-THROATED LOON

Analysis of Red-throated Loon abundance in the example assumes that the negative binomial distribution is suitable, as it was for Great Black-backed Gull, without going through the process of testing for the distribution. The next step in the process involves loading the data.

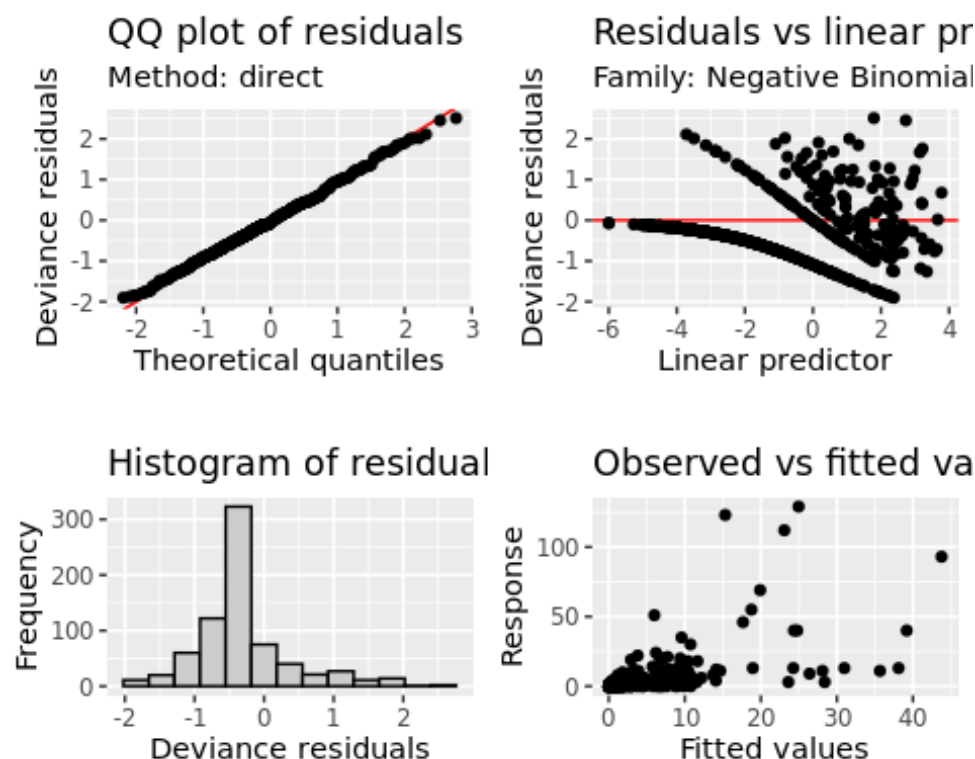
```
tmp.df <- filter(sum.df, sp.grp == "RTLO",
  loc == "All") %>%
  mutate(year.fac = factor(year < 2016),
```

```
week.fac = factor(week),
loc.fac = factor(loc),
season = case_when(doy > 340 | doy < 50 ~ "Winter",
                  doy >= 50 & doy < 135 ~ "Spring",
                  doy >= 135 & doy < 250 ~ "Summer",
                  TRUE ~ "Fall"),
season = factor(season),
survey = factor(survey),
pres = ifelse(count == 0, 0, 1)) %>%
filter(!is.na(temp))

tmp1.gam <- gam(count ~ s(doy, bs = "cc", k = 25) +
               s(tssr, bs = "cr", k = 5) +
               s(htht, bs = "cc", k = 5) +
               s(wind.dir, bs = "cc", k = 5) +
               s(log10(wind.spd), k = 5) +
               s(temp, k = 5) +
               s(bpress, k = 5) +
               s(survey, bs = "re"),
               family = nb(),
               data = tmp.df,
               method = "REML")
```

The model for Red-throated Loon is checked to look for the effectiveness of the negative binomial transformation, and other features (e.g. the distribution of residuals). The checking process shows that the negative binomial distribution partially deals with the extreme counts, but not as well as in the test analysis for the Great Black-backed Gull model. There are some unexpectedly high counts of Red-throated Loon during the summer (4 July 2012 survey) that may be the cause. We likely need other information, and may need to fit these models in a different framework, to account for those extreme points.

```
appraise(tmp1.gam)
```



Summary statistics are generated below to show the influence of various environmental factors. Factors which have a particular effect (i.e. show a significant effect) are day of year (Julian Day), sunrise time, wind direction and speed, and survey.

```
summary(tmp1.gam)

##
## Family: Negative Binomial(0.624)
## Link function: log
##
## Formula:
## count ~ s(doy, bs = "cc", k = 25) + s(tssr, bs = "cr", k = 5) +
##       s(htht, bs = "cc", k = 5) + s(wind.dir, bs = "cc", k = 5) +
##       s(log10(wind.spd), k = 5) + s(temp, k = 5) + s(bpress, k = 5) +
##       s(survey, bs = "re")
##
## Parametric coefficients:
##               Estimate Std. Error z value Pr(>|z|)
## (Intercept)  -1.276      0.193   -6.609 3.86e-11 ***
## ---
## Signif. codes:  0 '***' 0.001 '**' 0.01 '*' 0.05 '.' 0.1 ' ' 1
##
## Approximate significance of smooth terms:
```

```
##              edf Ref.df  Chi.sq  p-value
## s(doy)        7.188e+00 23.000  543.309 4.81e-06 ***
## s(tssr)       3.734e+00  3.944   15.012 0.002506 **
## s(htht)       6.268e-05  3.000    0.000 0.829663
## s(wind.dir)   2.463e+00  3.000   93.305 6.98e-05 ***
## s(log10(wind.spd)) 3.505e+00  3.829   23.053 0.000116 ***
## s(temp)      2.420e+00  2.802    5.705 0.079309 .
## s(bpress)    1.550e+00  1.731    4.939 0.054262 .
## s(survey)    3.185e+01 63.000  114.823 < 2e-16 ***
## ---
## Signif. codes:  0 '***' 0.001 '**' 0.01 '*' 0.05 '.' 0.1 ' ' 1
##
## R-sq.(adj) = 0.314  Deviance explained = 73.5%
## -REML = 842.89  Scale est. = 1          n = 727
```

This part of the analysis for Red-throated Loon is simplified and rerun, after dropping the unimportant terms (i.e. terms with a significance code of 0.1 or 1) from the analysis. The Akaike Information Criterion (AIC) shows that the change does not affect the fit of the model (i.e. the AIC for both models is virtually identical).

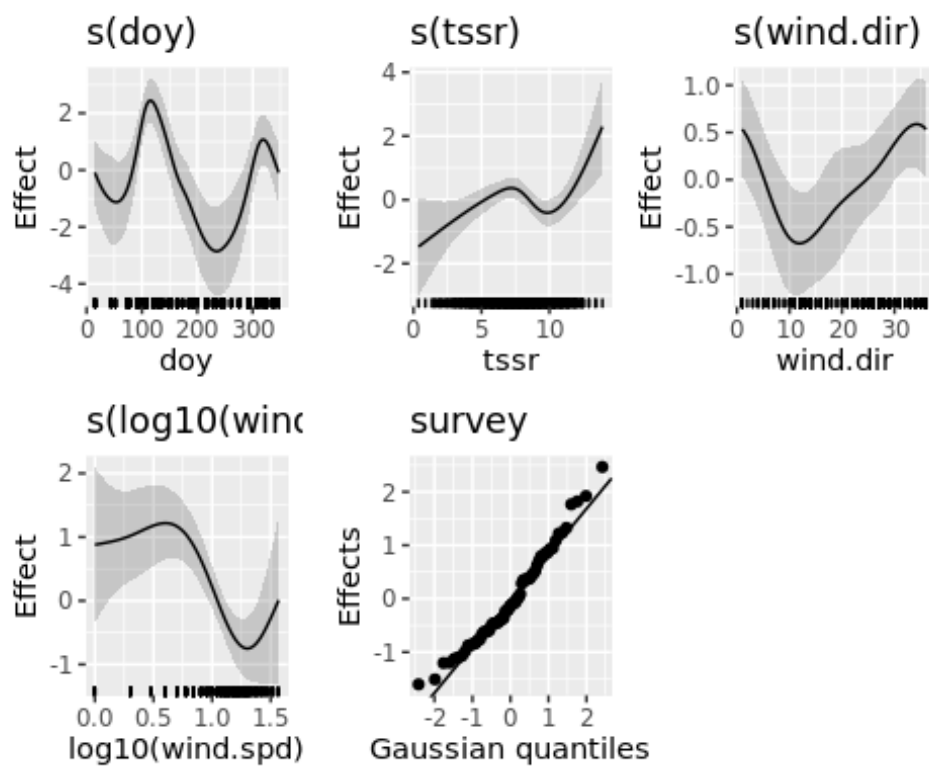
```
tmp2.gam <- gam(count ~ s(doy, bs = "cc", k = 25) +
  s(tssr, bs = "cr", k = 5) +
  s(wind.dir, bs = "cc", k = 5) +
  s(log10(wind.spd), k = 5) +
  s(survey, bs = "re"),
  family = nb(),
  data = tmp.df,
  method = "REML")
```

```
AIC(tmp1.gam, tmp2.gam)
```

```
##              df      AIC
## tmp1.gam 60.41903 1633.016
## tmp2.gam 58.36250 1633.462
```

The code below generates the summary analysis for Red-throated Loon.

```
draw(tmp2.gam)
```



Appendix B – FORCE Seabird Database Data Structure

August 2019

Introduction

This report provides a brief overview of the database of occurrence and abundance of seabirds and other water-associated birds obtained in shore-based, baseline and environmental monitoring surveys at the FORCE tidal energy demonstration site in Minas Passage, Nova Scotia, in 2010-2012 and 2016-2019. Data and analyses for the seabird surveys are presented in a series of reports which are available online from FORCE and from EnviroSphere Consultants Limited, Windsor, Nova Scotia, whose personnel and subcontractors conducted the surveys. The data was required to support contracts for seabird surveys conducted to support regulatory requirements for environmental monitoring at the FORCE Minas Passage Tidal Energy Demonstration Site¹⁰. Initially, *Microsoft Excel* spreadsheets were used to track the information. As the number of surveys grew, we recognized that additional flexibility was needed and a generic database structure was developed in *Microsoft Access*. The earlier information (2010-2012) was transferred to the database beginning in 2017. The most recent observations continued to late 2018 when the program was interrupted¹¹; however several surveys were conducted in April 2019 to capture part of the spring migration. All observations were made by Mr. Fulton Lavender, Halifax, Nova Scotia, an experienced professional bird observer, with field support from biologists and technicians from EnviroSphere Consultants.

Platform

The database has been compiled using *MicroSoft (MS) Excel* and *MS Access*. It is provided in the form of a *MS Access* database; and also as *MS Excel* versions of all the tables in the *MS Access* database.

Design

General: 1) Point surveys for coastal birds at the FORCE site began in May, 2010, as a *baseline monitoring* requirement for environmental assessment approvals of this tidal energy demonstration site on Minas Passage. The goal initially was to look at migratory periods; however in subsequent years (2011 & 2012) observations were completed capturing remaining periods of the year except mid-winter

¹⁰ Information on seabird abundance and distribution obtained on *vessel-based* baseline surveys conducted for FORCE in Minas Basin, Minas Passage and Minas Channel in 2009-2011 are available in project reports available from FORCE. Digital records including copies of original data recording forms were transferred to, and are archived with, the Canadian Wildlife Service, Dartmouth, Nova Scotia.

¹¹ A turbine installed by one of the providers (Cape Sharp Tidal Energy Development) in June 2018 was abandoned shortly thereafter and subsequently ceased to operate. FORCE decided in December 2018 to discontinue seabird observations until an operational turbine was in place, to uphold its mandate to examine turbine effects.

and late-summer. Monitoring in the second phase (*environmental effects monitoring* beginning May 2016) included observations throughout the year, with emphasis (i.e. increased sampling intensity) on migratory periods. Two and a half year's surveys under the FORCE program (May 2016-December 2018); and four surveys during spring migration (April 2019) conducted independently by EnviroSphere Consultants have been completed to date. 2) The program was begun in May 2010 without a standard design, except to survey on successive half-hour periods, starting from approximately high tide around mid-day (i.e. typically 12 periods per outgoing tide), to count and identify birds occurring in open water at the site. General principles were to broadly locate birds spatially in relation to the known areas proposed for tidal turbines. 3) An approach was developed over the first three surveys (May 1, 13 & 27, 2010), and subsequently followed closely. In addition to open water areas, the survey from the onset included an accounting of birds on Black Rock, a prominent island at the site and used by birds. The latest phase (2016 onward) refined the approach by including a more detailed grid of locations in the study area to which observations could be assigned, and added information on bird behaviour.

Initial Survey Phase: 2010-2012: 1) Listed species and stage, whether it was adult (three codes, B=breeding; U=undetermined, NB=non-breeding) or juvenile (1C, 2C, 3C, or 4C if relevant to the species, and these stages mostly concerned gulls or cormorants); 2) Sex was not recorded for sightings. 3) Listed activity in relation to activities which could interact (or not) with turbines (FL=flying; OW=on water; BR=on Black Rock; FD=feeding area (if OW, whether the bird was in the "turbine area" (I) or on the water "outside turbine area", (O)). The observer provided a separate breakdown for the "O" birds from 2011 to 2012, which placed them in the areas either "Inside Black Rock" or "Outside Black Rock". Unfortunately this breakdown (i.e. inside or outside BR. etc.) was done secondarily to information recorded on the original data forms, and consequently only the combined open water area ("O") is listed in the database. However, the secondary information is recorded in the database in a separate field in which the breakdown of "inside Black Rock" versus outside is recorded as a ratio. This allows an additional level of information to be extracted from the database if needed. In the database and to be consistent with the records from 2016-2019, the code in the 2010-2012 records for "Turbine area" was changed to "CLT" to reflect that it focused on part of the "Crown Lease" where tidal energy devices potentially would be installed; and to allow the CL area to be searched over the entire dataset. 4) In first survey, there was confusion about the code for NB (non-breeder) and sometimes it was applied incorrectly to juveniles, which caused a double-counting of some birds (which has been corrected in the database). The distinction between B and NB codes has some ambiguity, since both refer to adults and both usually refer to whether the bird has the required appearance and is seen in the breeding season (B) or not (NB), and not so much whether there is a specific plumage, although some birds definitely are breeding by their activities (e.g. Black Guillemot and Herring Gull). Uncertainty over whether flying birds ("FL") needed to be indicated as being in the "turbine" area also occurred in the first survey phase and some records were edited in the beginning (this also been corrected in the database).

Field Data Recording

The current field reporting form used in recording the data is presented in Appendix B. Forms allow recording of both bird observations and environmental data (e.g. windspeed, temperature, seastate) for each 30-minute observation period. The data recording form and use has evolved over the course of the monitoring studies at the FORCE site. For the first several surveys in 2010-2012, sightings were recorded

in a notebook by both the field assistant and observer, and later organized into a table format at the end of each survey. From the third survey onward, however, a field data recording form was developed, but the approach continued to involve recording birds in a notebook, and transcribing the counts into the data sheets at the end of the survey. During the 2010-2012 period, environmental conditions were recorded only incidentally for the survey date as a whole. Starting with the May 2016 survey, field recording forms were used as the only means of capturing data and included detailed environmental data. The observer focused on locating and identifying birds and the field assistant recorded the sightings and environmental data on the field data forms. By this time, FORCE had an operating weather station to provide information on conditions; however the weather station is sheltered from winds from the northern quadrant (NW, N, and NE) and temperatures also reflect nearshore and upland conditions.

Data from both survey periods (2010-2012 & 2016-2019) was entered into spreadsheets in *MS Excel*. *Excel* spreadsheets matched the structure of the data recording forms. During the analysis phase of the 2016-2017 survey only, some of the analyses were conducted exclusively in *Excel*. This was found to be unsatisfactory for long-term use, and the early data from spreadsheets was transferred from *Excel* into *Access* in the summer of 2017. For 2017-2019, all data has been routinely entered in *Excel* as a step in transferring information to *Access*, and all analyses for the period were conducted on data (i.e. in spreadsheets) produced from the *Access* database. Also in 2017, the original data from the 2010-2012 surveys, which was in a format incompatible with the newer structure, was carefully transferred from the original data recording forms and field notes as well as spreadsheets. The resulting spreadsheets compatible with the current database structure, were transferred into the current *MS Access* database.

Information forming the database has always been carefully checked: 1) first to detect field recording errors on the original field reporting form to ensure consistency and to ensure that the form was correctly filled out; and 2) the data transcription from reporting forms into *Excel* spreadsheets was checked for consistency and accuracy. All data entry was double-checked initially as a step in the data entry process; and then checked by a second individual, before being transferred into the *MS Access* database.

Main Data Table

Data on bird occurrence in the database are contained in two tables for the two periods of the survey, 2010-2012 and 2016-2019. The tables are called: *Fundy Data 2010-2012* & *Fundy Data 2016-2019*.

The structure of the main data tables is as follows:

Field Name	Type	Field Length	Contents
ID	AutoNumber	Long Integer	Sequential key assigned by the database
SURVEY	Text	255	Surveys in order, coded by year and number of survey. Example: 2012-01 for the first survey in 2012.
PERIOD	Text	255	Identifier for up to 13, half hour periods per day, in time sequence
SUB_PERIOD	Text	50	Used to break down the 30-minute survey period for test purposes. From 2010 to September 2017, always 1. Starting in October 2017, 1, 2, 3 or 4, with 1 and 3 snapshots at the beginning and mid-way through the period, and 2 and 4, birds seen between the two snapshots. The code 9 is included to indicate a species which occurred in sub-period 3, but not in any other period, and is a means of capturing such sightings. The sum of counts in sub-periods 1, 2, 4 and 9 is equivalent to the total for the period observed in the 2010-2012 surveys.
DATE_TXT	Text	255	Date spelled out. e.g. "October 23, 2010"
DATE_DMY	Text	50	Date as text in D/M/Y format required by MS Access
TOTAL_PERIODS	Text	255	Total number of 30-minute periods per survey.
AREA	Text	255	Code for geographic subdivision of study site. For 2010-2012, codes are: BR = Black Rock; CLT=Crown Lease / "Turbine Area"; O=all other areas. For 2016-2019, codes refer to subdivisions: BR= Black Rock; CL (can be CL1 to CL4)=Crown Lease; OB (OB1 to OB3)= Outside Black Rock; IB (IB1 & IB2)=Inside Black Rock; and FF (FF1 to FF3) = Farfield. Also includes LAND, where a non-seabird species such as a peregrine falcon occurs over land at the site.
SPECIES	Text	255	Four-letter Species Code. Includes codes for non-aquatic species (e.g. Bald Eagle) and marine mammals (e.g. Harbour Porpoise).
B	Number	Integer	Adult bird category: B= Breeding. Contains counts of individuals in each 30-minute period.
U	Number	Integer	Adult bird category: U= Undetermined Breeding Status. Counts.
NB	Number	Integer	Adult bird category: NB= Non-Breeding. Counts
MOULT	Number	Integer	Adult bird category: M= Moulting (this category has never been used).
SEX	Text	255	M or F, if known; U if not. Usually only for eiders.

Field Name	Type	Field Length	Contents
1C	Number	Integer	Immature bird category: 1C= first cycle (i.e. less than 1-year).
2C	Number	Integer	Immature bird category: 2C= second cycle (1- to 2 years).
3C	Number	Integer	Immature bird category: 3C= third cycle (2- to 3 years).
4C	Number	Integer	Immature bird category: 4C= fourth cycle (3- to 4 years).
OW	Number	Integer	Count of number of those counted which were on water.
FL	Number	Integer	Count of number of those counted which were flying.
DIR	Text	255	Direction (alphabetical, i.e. N, W, S, etc). Also applies to "OTHER" below which can include "Drifting". Includes "C" for circling and "H" or "O" for holding position.
DIVE_AIR	Text	255	Number of the birds recorded which were diving from the air to feed.
DIVE_WATER	Text	255	Number of the birds recorded which were diving from the from the water surface to feed.
FEEDING	Text	255	Number feeding. The field hasn't been used as the comment has been always placed in the "OTHER" field.
OTHER	Text	255	Field which includes miscellaneous codes: "DRIFTING", "CIRCLING" OR "C", "FEEDING", "MM" or Marine Mammal, "NBR" for birds near Black Rock.
COMMENT	Text	255	Any other information recorded at the time. "Location Estimated" (only in the 2010-2012 data) refers to records where there was ambiguity in the area code for the record and a 'best guess' was applied. Although the location was ambiguous, the total count for the record, period, survey, remains correct.

Data Management Approach (from 2016-2019)

After each survey, the field data form is checked carefully for consistency and completeness, by both the observer/recorder and by a separate staff person. After correction, separate back-up photocopies of the data sheets are made. The data is then transcribed to an *Excel* spreadsheet template. The data entered into the spreadsheet is double-checked and reviewed against the field data form, and the spreadsheet archived. This spreadsheet is then imported into the *MS Access* database. The database is itself backed up before the new data is added, by saving an *Excel* version of the whole database, and storing a backup version of the database. From the *MS Access* database, the data can be exported as *Excel* spreadsheets or text files which can be used for analyses.

Other Tables in Database

Julian Date: A table in *Excel* and in *MS Access* is maintained with the survey number, the text version of the date, and the Julian date (a sequential number from 1 to 365) to be used in data analysis and modeling.

Species Codes: A table is maintained which has the 4-letter species code for all species which have been recorded in our surveys at the site, and the corresponding common and scientific names. This table also includes: 1) Some terrestrial / coastal species of importance including: Bald Eagle, Peregrine Falcon, Osprey, Turkey Vulture, Great Blue Heron, and Northern Harrier; and 2) marine mammals, including: Harbour Porpoise, Harp Seal, Harbour Seal, and Grey Seal. It also has the American Ornithological Society (AOS) order, which we derived as the row number of the species in the AOS list, which is a taxonomically-oriented system.

Errors Found and Corrections: If, in the process of using the data, errors are discovered, they are formally noted and passed on to the database manager, who ensures that the corrections are implemented in the tables in the database. When a change is made, a note of the change, the data, the database table affected, and the person making the change, is made in the “Errors Found and Corrections” table.

Environmental Data: A table contains all available information on weather, time, time zone (AST or ADT) and tide state for each period in the survey. Fields are presented below (High tide time is also noted):

Field Name	Type	Field Length	Contents
SURVEY	Text	255	Survey Number
PERIOD	Text	255	Period
DATE_TXT	Text	255	Text version of Date
DATE_DMY	Text	255	“D/M/Y”
START_TIME	Text	255	Start time of Period
END_TIME	Text	255	End Time of Period
TIME_ZONE	Text	255	Time Zone (AST or ADT)
HIGH_TIDE	Text	255	High Tide (at either Cape Sharp or Diligent River)
OBSERVER	Text	255	Initials of Observer
ASSISTANT	Text	255	Initials of Assistant
CLOUD_PCT	Text	255	‘% cloud cover’

Field Name	Type	Field Length	Contents
WIND_KPH	Text	255	Wind speed (KPH)
DIR_NOM	Text	255	Direction (N,S,E,W)
DIR_DEG	Text	255	Direction (degrees)
WAVES_M	Text	255	Wave Height (m)
BEAUFORT	Text	255	Beaufort Wind Scale estimate
T_DEG_C	Text	255	Air Temperature (° C.) at FORCE
PAGE	Text	255	Field Sheet (i.e. consecutive period)
COMMENT	Text	255	Notes on local conditions in relation to survey

Other Features of Database

MS Access is database produce sold by *MicroSoft* and compatible with its Windows® operating system. The FORCE database as provided contains only the data tables and a few simple sample ‘queries’ designed to illustrate the basic functioning of queries in the software.

Species Table

All the species, their species codes and the AOS (American Ornithological Society) codes are in a single table. This is to allow 1) filling in tables with the correct common name manually; and 2) to allow arranging the data in groups (i.e. loons, sea ducks, etc.) automatically to save time. Sometimes this is useful for analysis where you want a group data total (i.e. totals for gulls).

- The table has all the species to date (i.e. up to the end of the 2017-2018 period (May 10, 2018)).
- For any new species, add them to the end of the list. Find the AOS order on the website or on the list we have downloaded. The ‘AOS Order’ is the row number in the table. Note that there are also ‘AOS Codes’ or Identifiers in the database, which are unique numbers assigned to each species. These are not in taxonomic order.
- A “Join” query takes information from one database table and adds it to another. In this case, the species table has the same “species code” (i.e. NOGA, HEGU, etc.) as in our database table. So when we run this type of query, it will fill out a table having the species codes, with the species names as well. This saves time and ensures that the spelling, etc. is always correct.

Sample of Information in Species Code Table				
ID	SPECIES	COMMON_NAME	SCIENTIFIC_NAME	AOS_ORDER
1	ABDU	American Black Duck	Anas rubripes	0049
2	ALCID	Alcid Unidentified	Alcidae	8880
3	ARLO	Arctic Loon	Gavia arctica	0627
4	ATPU	Atlantic Puffin	Fratercula arctica	0562
5	BAEA	American Bald Eagle	Haliaeetus leucocephalus	0782
6	BBPL	Black-Bellied Plover	Pluvialis squatarola	0450
7	BLGU	Black Guillemot	Cephus grylle	0547
8	BLKI	Black-Legged Kittiwake	Rissa tridactyla	0566
9	BLSC	Black Scoter	Melanitta nigra	0070
10	BLTE	Black Tern	Chlidonias niger	0610

Appendix C1 – Polynomial Regression Equations (Abundance versus Julian Day) for Dominant Seabirds or Seabird Groups, 2010-2018.

Note: Log transformations when applied were $\log_{10}(x + 1)$. y = abundance. Periods were: spring from February 13 to July 18; summer from May 13 to September 6; and fall-winter from September 18 to December 13.

Polynomial Regression Equations		
Waterbird Abundance at site		
Total	Spring	$y = 2E-06x^4 - 0.0011x^3 + 0.1667x^2 - 9.2657x + 169.8$ $R^2 = 0.1896$
	Summer	$y = -2E-06x^4 + 0.0013x^3 - 0.4153x^2 + 55.838x - 2688.1$ $R^2 = 0.6026$
	Fall	$y = 4E-06x^4 - 0.0056x^3 + 2.6696x^2 - 558.26x + 43524$ $R^2 = 0.1043$
COEI	Spring	$y = 7E-08x^4 - 2E-05x^3 + 0.0008x^2 + 0.2886x - 12.328$ $R^2 = 0.0856$
	Summer	$y = 3E-07x^4 - 0.0002x^3 + 0.0513x^2 - 6.0401x + 273.49$ $R^2 = 0.2555$
	Fall	$y = -2E-07x^4 + 0.0002x^3 - 0.0929x^2 + 15.343x - 912.9$ $R^2 = 0.0832$
Cormorants (DCCO + GRCO)	Spring	$y = 9E-07x^4 - 0.0004x^3 + 0.0692x^2 - 4.1604x + 78.841$ $R^2 = 0.1134$
	Summer	$y = -4E-07x^4 + 0.0003x^3 - 0.0938x^2 + 11.706x - 530.84$ $R^2 = 0.1977$
	Fall	$y = 3E-07x^4 - 0.0003x^3 + 0.1606x^2 - 34.508x + 2780.2$ $R^2 = 0.9289$
Black Guillemot	Spring	$y = 4E-08x^4 - 2E-05x^3 + 0.0034x^2 - 0.2267x + 4.6674$ $R^2 = 0.4952$
	Summer	$y = 6E-07x^4 - 0.0004x^3 + 0.1257x^2 - 15.495x + 704.07$ $R^2 = 0.451$
	Fall	$y = 7E-08x^4 - 9E-05x^3 + 0.0428x^2 - 8.8002x + 675.22$ $R^2 = 0.118$
Gulls (GBBG, HEGU)	Spring	$y = 1E-07x^4 - 0.0001x^3 + 0.026x^2 - 1.8273x + 49.045$ $R^2 = 0.3718$
	Summer	$y = -1E-06x^4 + 0.001x^3 - 0.3008x^2 + 39.965x - 1895.1$ $R^2 = 0.7175$
	Fall	$y = -2E-06x^4 + 0.002x^3 - 0.893x^2 + 175.34x - 12871$ $R^2 = 0.0796$
Migrants 2 (RBGU, COLO, ABDU)	Spring	$y = 2E-09x^4 + 2E-06x^3 - 0.001x^2 + 0.1204x - 3.3838$ $R^2 = 0.2008$

Appendix C1 –Polynomial Regression Equations for Selected Seabirds

	Summer	$y = -8E-07x^4 + 0.0006x^3 - 0.164x^2 + 19.541x - 859.41$ $R^2 = 0.5173$
	Fall	$y = 3E-07x^4 - 0.0004x^3 + 0.1841x^2 - 37.72x + 2886.3$ $R^2 = 0.0369$
Migrants 3 (BLKI, RAZO, ATPU)	Spring	$y = 8E-09x^4 - 4E-06x^3 + 0.0006x^2 - 0.0368x + 0.7196$ $R^2 = 0.087$
	Summer	$y = 0$ $R^2 = \#N/A$
	Fall	$y = 2E-07x^4 - 0.0002x^3 + 0.1262x^2 - 28.62x + 2383.6$ $R^2 = 0.174$
Migrants 4 (COMU, TBMU)	Spring	$y = 5E-09x^4 - 2E-06x^3 + 0.0004x^2 - 0.0238x + 0.4752$ $R^2 = 0.047$
	Summer	$y = 0$ $R^2 = \#N/A$
	Fall	$y = 1E-07x^4 - 0.0001x^3 + 0.0652x^2 - 13.474x + 1038.7$ $R^2 = 0.1951$
Migrants 5 (RTLO, SCOTER, NOGA)	Spring	$y = 1E-06x^4 - 0.0006x^3 + 0.0832x^2 - 4.5473x + 77.722$ $R^2 = 0.2212$
	Summer	$y = 2E-07x^4 - 0.0001x^3 + 0.0417x^2 - 5.1885x + 243.63$ $R^2 = 0.3408$
	Fall	$y = 3E-06x^4 - 0.0042x^3 + 1.9581x^2 - 403.09x + 30951$ $R^2 = 0.0913$
RTLO	Spring	$y = 3E-07x^4 - 0.0002x^3 + 0.0226x^2 - 1.2578x + 22.108$ $R^2 = 0.2097$
	Summer	$y = 2E-08x^4 - 2E-05x^3 + 0.0045x^2 - 0.519x + 23.223$ $R^2 = 0.1419$
	Fall	$y = 2E-06x^4 - 0.002x^3 + 0.9759x^2 - 208.53x + 16557$ $R^2 = 0.1457$
Scoters	Spring	$y = 9E-07x^4 - 0.0004x^3 + 0.0587x^2 - 3.1526x + 52.654$ $R^2 = 0.1949$
	Summer	$y = 8E-08x^4 - 6E-05x^3 + 0.0189x^2 - 2.4912x + 122$ $R^2 = 0.4108$
	Fall	$y = 2E-06x^4 - 0.0025x^3 + 1.1125x^2 - 220.57x + 16335$ $R^2 = 0.044$
NOGA	Spring	$y = 1E-08x^4 - 9E-06x^3 + 0.0018x^2 - 0.1306x + 2.8617$ $R^2 = 0.1293$
	Summer	$y = 9E-08x^4 - 7E-05x^3 + 0.0183x^2 - 2.1784x + 98.404$ $R^2 = 0.1624$
	Fall	$y = 1E-08x^4 - 1E-05x^3 + 0.0066x^2 - 1.3697x + 106.21$ $R^2 = 0.0816$
HEGU	Spring	$y = 3E-07x^4 - 0.0001x^3 + 0.0272x^2 - 2.1787x + 70.952$ $R^2 = 0.2038$
	Summer	$y = 3E-06x^4 - 0.0019x^3 + 0.5407x^2 - 65.563x + 2921.7$ $R^2 = 0.2744$

Appendix C1 –Polynomial Regression Equations for Selected Seabirds

	Fall	$y = 3E-06x^4 - 0.0033x^3 + 1.4909x^2 - 296.29x + 22008$ $R^2 = 0.1577$
GBBG	Spring	$y = 8E-08x^4 - 7E-05x^3 + 0.0137x^2 - 0.936x + 27.245$ $R^2 = 0.4919$
	Summer	$y = -5E-07x^4 + 0.0004x^3 - 0.1345x^2 + 17.944x - 845.06$ $R^2 = 0.7998$
	Fall	$y = 7E-08x^4 - 8E-05x^3 + 0.0359x^2 - 6.7177x + 462.83$ $R^2 = 0.039$
Abundance of Waterbirds over Open Water (i.e. excluding Black Rock)		
Total excluding Black Rock	Spring	$y = 2E-06x^4 - 0.0007x^3 + 0.0959x^2 - 4.6598x + 69.487$ $R^2 = 0.1877$
	Summer	$y = -2E-07x^4 + 0.0002x^3 - 0.0709x^2 + 10.473x - 546.08$ $R^2 = 0.2308$
	Fall	$y = 7E-06x^4 - 0.0087x^3 + 4.0451x^2 - 831.62x + 63808$ $R^2 = 0.0996$
COEI excluding Black Rock	Spring	$y = 2E-07x^4 - 6E-05x^3 + 0.0058x^2 + 0.0212x - 7.8413$ $R^2 = 0.1043$
	Summer	$y = -3E-08x^4 + 2E-05x^3 - 0.0065x^2 + 0.8438x - 38.391$ $R^2 = 0.7031$
	Fall	$y = 1E-07x^4 - 0.0002x^3 + 0.0896x^2 - 18.714x + 1459.9$ $R^2 = 0.1176$
Cormorants excluding Black Rock	Spring	$y = 2E-07x^4 - 9E-05x^3 + 0.014x^2 - 0.8151x + 14.982$ $R^2 = 0.0618$
	Summer	$y = -1E-07x^4 + 1E-04x^3 - 0.0286x^2 + 3.7095x - 175.58$ $R^2 = 0.2395$
	Fall	$y = -3E-08x^4 + 3E-05x^3 - 0.0122x^2 + 1.6188x - 51.621$ $R^2 = 0.7928$
BLGU excluding Black Rock	Spring	$y = 3E-08x^4 - 1E-05x^3 + 0.0023x^2 - 0.1436x + 2.8328$ $R^2 = 0.4601$
	Summer	$y = 5E-07x^4 - 0.0004x^3 + 0.1017x^2 - 12.37x + 552.16$ $R^2 = 0.4538$
	Fall	$y = 7E-08x^4 - 9E-05x^3 + 0.0428x^2 - 8.8002x + 675.22$ $R^2 = 0.118$
Gulls excluding Black Rock	Spring	$y = 6E-09x^4 - 3E-05x^3 + 0.0074x^2 - 0.5382x + 14.16$ $R^2 = 0.1914$
	Summer	$y = -7E-07x^4 + 0.0006x^3 - 0.185x^2 + 24.787x - 1195.5$ $R^2 = 0.4978$
	Fall	$y = -2E-06x^4 + 0.002x^3 - 0.8735x^2 + 171.53x - 12593$ $R^2 = 0.0764$
HEGU excluding Black Rock	Spring	$y = -1E-07x^4 + 6E-05x^3 - 0.0086x^2 + 0.5241x - 9.2037$ $R^2 = 0.1749$
	Summer	$y = 2E-07x^4 - 0.0001x^3 + 0.0267x^2 - 2.8018x + 110.71$ $R^2 = 0.1115$
	Fall	$y = 1E-06x^4 - 0.0012x^3 + 0.5603x^2 - 116x + 8960.8$ $R^2 = 0.2417$

Appendix C1 –Polynomial Regression Equations for Selected Seabirds

GBBG excluding Black Rock	Spring	$y = -5E-08x^4 + 2E-05x^3 - 0.0041x^2 + 0.3027x - 6.6424$ $R^2 = 0.1195$
	Summer	$y = -6E-08x^4 + 5E-05x^3 - 0.0187x^2 + 2.7652x - 145.48$ $R^2 = 0.5372$
	Fall	$y = 1E-07x^4 - 0.0001x^3 + 0.0555x^2 - 10.528x + 740.85$ $R^2 = 0.0437$
Abundance of Waterbirds on Black Rock		
COEI on Black Rock	Spring	$y = -2E-07x^4 + 9E-05x^3 - 0.0123x^2 + 0.6922x - 12.889$ $R^2 = 0.4339$
	Summer	$y = -7E-07x^4 + 0.0006x^3 - 0.1712x^2 + 22.493x - 1085.5$ $R^2 = 0.3873$
	Fall	$y = 1E-06x^4 - 0.0015x^3 + 0.7092x^2 - 145.82x + 11213$ $R^2 = 0.0888$
Cormorants on Black Rock (DCCO +GRCO)	Spring	$y = 7E-07x^4 - 0.0003x^3 + 0.0533x^2 - 3.2429x + 62.136$ $R^2 = 0.1222$
	Summer	$y = -3E-07x^4 + 0.0003x^3 - 0.0746x^2 + 9.1327x - 405.59$ $R^2 = 0.1714$
	Fall	$y = 4E-07x^4 - 0.0005x^3 + 0.2214x^2 - 46.046x + 3586.9$ $R^2 = 0.8563$
GBBG on Black Rock	Spring	$y = 2E-07x^4 - 0.0001x^3 + 0.0198x^2 - 1.3922x + 37.235$ $R^2 = 0.2308$
	Summer	$y = -6E-08x^4 + 5E-05x^3 - 0.0187x^2 + 2.7652x - 145.48$ $R^2 = 0.5372$
	Fall	$y = 2E-07x^4 - 0.0002x^3 + 0.0971x^2 - 18.742x + 1346.8$ $R^2 = 0.0578$
BLGU on Black Rock	Spring	$y = 1E-07x^4 - 7E-05x^3 + 0.0141x^2 - 0.9584x + 20.482$ $R^2 = 0.1715$
	Summer	$y = -5E-07x^4 + 0.0004x^3 - 0.1302x^2 + 16.775x - 781.98$ $R^2 = 0.5137$
	Fall	$y = -3E-06x^4 + 0.0034x^3 - 1.5267x^2 + 305.26x - 22809$ $R^2 = 0.1335$
Gulls on Black Rock (HEGU + GBBG)	Spring	$y = 2E-07x^4 - 0.0001x^3 + 0.0294x^2 - 2.0796x + 54.69$ $R^2 = 0.3854$
	Summer	$y = -1E-06x^4 + 0.0009x^3 - 0.2821x^2 + 37.2x - 1749.6$ $R^2 = 0.7251$
	Fall	$y = -2E-06x^4 + 0.0021x^3 - 0.9484x^2 + 185.87x - 13612$ $R^2 = 0.0866$
HEGU on Black Rock	Spring	$y = 1E-07x^4 - 7E-05x^3 + 0.0141x^2 - 0.9584x + 20.482$ $R^2 = 0.1715$
	Summer	$y = -5E-07x^4 + 0.0004x^3 - 0.1302x^2 + 16.775x - 781.98$ $R^2 = 0.5137$
	Fall	$y = -3E-06x^4 + 0.0034x^3 - 1.5267x^2 + 305.26x - 22809$ $R^2 = 0.1335$

Polynomial Regression Equations (log ₁₀)		
Overall Waterbird Abundance at Site (Log ₁₀)		
Total	Spring	$y = -2E-10x^4 + 1E-07x^3 - 3E-05x^2 + 0.0034x + 0.3156$ $R^2 = 0.9999$
	Summer	$y = -2E-11x^4 + 2E-08x^3 - 6E-06x^2 + 0.0015x + 0.3805$ $R^2 = 1$
	Fall	$y = -2E-12x^4 + 3E-09x^3 - 2E-06x^2 + 0.0008x + 0.418$ $R^2 = 1$
COEI	Spring	$y = -8E-09x^4 + 4E-06x^3 - 0.0008x^2 + 0.0759x - 1.9663$ $R^2 = 0.2162$
	Summer	$y = -5E-09x^4 + 5E-06x^3 - 0.0019x^2 + 0.2849x - 14.174$ $R^2 = 0.4116$
	Fall	$y = 8E-09x^4 - 1E-05x^3 + 0.0058x^2 - 1.2587x + 101.19$ $R^2 = 0.0445$
Cormorants (DCCO + GRCO)	Spring	$y = 4E-08x^4 - 2E-05x^3 + 0.0031x^2 - 0.1918x + 3.7645$ $R^2 = 0.3364$
	Summer	$y = -5E-08x^4 + 4E-05x^3 - 0.012x^2 + 1.5127x - 69.469$ $R^2 = 0.1528$
	Fall	$y = -5E-09x^4 + 4E-06x^3 - 0.0009x^2 - 0.0597x + 26.263$ $R^2 = 0.8451$
Black Guillemot	Spring	$y = 8E-09x^4 - 4E-06x^3 + 0.0007x^2 - 0.0492x + 1.0147$ $R^2 = 0.593$
	Summer	$y = 7E-08x^4 - 5E-05x^3 + 0.0146x^2 - 1.8229x + 83.716$ $R^2 = 0.645$
	Fall	$y = 3E-08x^4 - 3E-05x^3 + 0.0148x^2 - 3.0334x + 231.93$ $R^2 = 0.1209$
Gulls (GBBG + HEGU)	Spring	$y = 7E-09x^4 - 4E-06x^3 + 0.0008x^2 - 0.0534x + 2.1664$ $R^2 = 0.5265$
	Summer	$y = 2E-09x^4 + 4E-07x^3 - 0.0006x^2 + 0.1298x - 6.6537$ $R^2 = 0.861$
	Fall	$y = -4E-09x^4 - 2E-06x^3 + 0.0039x^2 - 1.3678x + 146.13$ $R^2 = 0.156$
HEGU	Spring	$y = 2E-08x^4 - 1E-05x^3 + 0.0017x^2 - 0.1269x + 4.1915$ $R^2 = 0.227$
	Summer	$y = 8E-08x^4 - 6E-05x^3 + 0.0183x^2 - 2.2748x + 104.24$ $R^2 = 0.4473$
	Fall	$y = 3E-07x^4 - 0.0003x^3 + 0.1537x^2 - 30.592x + 2276.2$ $R^2 = 0.1892$
GBBG	Spring	$y = 1E-09x^4 - 2E-06x^3 + 0.0004x^2 - 0.0278x + 1.5236$ $R^2 = 0.6059$
	Summer	$y = 3E-08x^4 - 2E-05x^3 + 0.0043x^2 - 0.4206x + 15.961$ $R^2 = 0.9376$

Appendix C1 –Polynomial Regression Equations for Selected Seabirds

Migrants 2 (RBGU, COLO, ABDU)	Fall	$y = -1E-08x^4 + 2E-05x^3 - 0.0074x^2 + 1.5366x - 119.63$ $R^2 = 0.029$
	Spring	$y = -2E-09x^4 + 1E-06x^3 - 0.0003x^2 + 0.0352x - 0.913$ $R^2 = 0.2534$
	Summer	$y = -1E-07x^4 + 9E-05x^3 - 0.0255x^2 + 3.0558x - 135.01$ $R^2 = 0.6568$
Migrants 3 (BLKI, RAZO, ATPU)	Fall	$y = 6E-08x^4 - 8E-05x^3 + 0.0355x^2 - 7.3776x + 572.82$ $R^2 = 0.0388$
	Spring	$y = 3E-09x^4 - 1E-06x^3 + 0.0002x^2 - 0.0116x + 0.2258$ $R^2 = 0.0865$
	Summer	$y = 0$ $R^2 = \#N/A$
Migrants 4 (COMU, TBMU)	Fall	$y = 5E-08x^4 - 6E-05x^3 + 0.0316x^2 - 6.8448x + 549.47$ $R^2 = 0.2207$
	Spring	$y = 2E-09x^4 - 8E-07x^3 + 0.0001x^2 - 0.0079x + 0.1581$ $R^2 = 0.047$
	Summer	$y = 0$ $R^2 = \#N/A$
Migrants 5 (RTLO, SCOTER, NOGA)	Fall	$y = 4E-08x^4 - 4E-05x^3 + 0.0208x^2 - 4.3045x + 332.59$ $R^2 = 0.2067$
	Spring	$y = 6E-08x^4 - 3E-05x^3 + 0.0038x^2 - 0.2115x + 3.774$ $R^2 = 0.4722$
	Summer	$y = 5E-08x^4 - 4E-05x^3 + 0.011x^2 - 1.363x + 63.547$ $R^2 = 0.363$
RTLO	Fall	$y = 2E-07x^4 - 0.0002x^3 + 0.1058x^2 - 21.672x + 1655.4$ $R^2 = 0.1442$
	Spring	$y = 4E-08x^4 - 2E-05x^3 + 0.0025x^2 - 0.1495x + 2.8366$ $R^2 = 0.3464$
	Summer	$y = 1E-09x^4 - 5E-07x^3 + 6E-05x^2 - 0.0029x + 0.3289$ $R^2 = 0.2292$
Scoters	Fall	$y = 1E-07x^4 - 0.0001x^3 + 0.0662x^2 - 14.155x + 1124.4$ $R^2 = 0.2672$
	Spring	$y = 5E-08x^4 - 2E-05x^3 + 0.0031x^2 - 0.162x + 2.61$ $R^2 = 0.504$
	Summer	$y = 3E-08x^4 - 2E-05x^3 + 0.006x^2 - 0.7885x + 38.244$ $R^2 = 0.4573$
NOGA	Fall	$y = 2E-07x^4 - 0.0002x^3 + 0.1075x^2 - 21.153x + 1554.2$ $R^2 = 0.0715$
	Spring	$y = 8E-09x^4 - 4E-06x^3 + 0.0008x^2 - 0.0501x + 1.033$ $R^2 = 0.143$
	Summer	$y = 3E-08x^4 - 3E-05x^3 + 0.0072x^2 - 0.904x + 42.28$ $R^2 = 0.214$
	Fall	$y = 4E-09x^4 - 6E-06x^3 + 0.0026x^2 - 0.5502x + 42.661$ $R^2 = 0.0816$
Abundance of Waterbirds over Water (i.e. excluding Black Rock) (Log₁₀)		

Appendix C1 –Polynomial Regression Equations for Selected Seabirds

Total excluding Black Rock	Spring	$y = 2E-08x^4 - 8E-06x^3 + 0.001x^2 - 0.0376x + 0.8061$ $R^2 = 0.302$
	Summer	$y = -1E-08x^4 + 1E-05x^3 - 0.0033x^2 + 0.4411x - 20.689$ $R^2 = 0.2037$
	Fall	$y = 3E-07x^4 - 0.0004x^3 + 0.1782x^2 - 36.406x + 2779.2$ $R^2 = 0.1189$
COEI excluding Black Rock	Spring	$y = -8E-09x^4 + 5E-06x^3 - 0.0009x^2 + 0.0683x - 1.0089$ $R^2 = 0.3032$
	Summer	$y = 6E-08x^4 - 5E-05x^3 + 0.0133x^2 - 1.6999x + 79.418$ $R^2 = 0.3728$
	Fall	$y = -2E-07x^4 + 0.0003x^3 - 0.1424x^2 + 29.762x - 2319.4$ $R^2 = 0.4264$
Cormorants excluding Black Rock	Spring	$y = 2E-08x^4 - 9E-06x^3 + 0.0014x^2 - 0.0898x + 1.7733$ $R^2 = 0.168$
	Summer	$y = -2E-08x^4 + 2E-05x^3 - 0.0059x^2 + 0.771x - 36.6$ $R^2 = 0.2133$
	Fall	$y = -2E-08x^4 + 2E-05x^3 - 0.0066x^2 + 1.1249x - 67.407$ $R^2 = 0.7536$
BLGU excluding Black Rock	Spring	$y = 2E-09x^4 - 9E-07x^3 + 0.0002x^2 - 0.0114x + 0.2309$ $R^2 = 0.5842$
	Summer	$y = 1E-08x^4 - 1E-05x^3 + 0.0031x^2 - 0.3819x + 17.202$ $R^2 = 0.7079$
	Fall	$y = 1E-08x^4 - 1E-05x^3 + 0.0059x^2 - 1.2143x + 92.705$ $R^2 = 0.1216$
Gulls excluding Black Rock (GBBG + HEGU)	Spring	$y = 8E-09x^4 - 5E-06x^3 + 0.0009x^2 - 0.0561x + 1.7678$ $R^2 = 0.4358$
	Summer	$y = -1E-08x^4 + 9E-06x^3 - 0.003x^2 + 0.4034x - 18.647$ $R^2 = 0.6719$
	Fall	$y = -2E-09x^4 - 5E-06x^3 + 0.0051x^2 - 1.6145x + 163.98$ $R^2 = 0.1531$
HEGU excluding Black Rock	Spring	$y = -1E-08x^4 + 5E-06x^3 - 0.0007x^2 + 0.0461x - 0.5884$ $R^2 = 0.1441$
	Summer	$y = 2E-08x^4 - 2E-05x^3 + 0.005x^2 - 0.5991x + 27.405$ $R^2 = 0.0867$
	Fall	$y = 2E-07x^4 - 0.0002x^3 + 0.106x^2 - 21.856x + 1681.8$ $R^2 = 0.336$
GBBG excluding Black Rock	Spring	$y = 4E-09x^4 - 1E-06x^3 + 0.0001x^2 - 0.01x + 0.8303$ $R^2 = 0.3581$
	Summer	$y = 4E-08x^4 - 3E-05x^3 + 0.0085x^2 - 1.0648x + 48.583$ $R^2 = 0.3493$
	Fall	$y = -6E-08x^4 + 8E-05x^3 - 0.0413x^2 + 8.996x - 727.59$ $R^2 = 0.4074$
Abundance of Waterbirds on Black Rock (Log₁₀)		
COEI on Black Rock	Spring	$y = -2E-08x^4 + 7E-06x^3 - 0.0009x^2 + 0.0466x - 0.8182$ $R^2 = 0.4791$

Appendix C1 –Polynomial Regression Equations for Selected Seabirds

	Summer	$y = -9E-08x^4 + 7E-05x^3 - 0.0219x^2 + 2.8271x - 133.88$ $R^2 = 0.3732$
	Fall	$y = 2E-07x^4 - 0.0003x^3 + 0.1285x^2 - 26.395x + 2027.8$ $R^2 = 0.1162$
Cormorants on Black Rock	Spring	$y = 3E-08x^4 - 2E-05x^3 + 0.0027x^2 - 0.1715x + 3.3577$ $R^2 = 0.2581$
	Summer	$y = -5E-08x^4 + 4E-05x^3 - 0.0112x^2 + 1.3809x - 62.339$ $R^2 = 0.1149$
	Fall	$y = 5E-08x^4 - 7E-05x^3 + 0.0307x^2 - 6.4268x + 504.01$ $R^2 = 0.8083$
GBBG on Black Rock	Spring	$y = -4E-10x^4 - 8E-07x^3 + 0.0003x^2 - 0.0268x + 1.5598$ $R^2 = 0.2345$
	Summer	$y = -6E-08x^4 + 5E-05x^3 - 0.0144x^2 + 1.9094x - 92.092$ $R^2 = 0.7689$
	Falls	$y = 2E-08x^4 - 2E-05x^3 + 0.008x^2 - 1.509x + 104.74$ $R^2 = 0.0363$
BLGU on Black Rock	Spring	$y = 2E-08x^4 - 9E-06x^3 + 0.0016x^2 - 0.1041x + 2.4049$ $R^2 = 0.4103$
	Summer	$y = -2E-08x^4 + 2E-05x^3 - 0.0042x^2 + 0.5037x - 21.17$ $R^2 = 0.7078$
	Fall	$y = -2E-07x^4 + 0.0003x^3 - 0.1232x^2 + 24.591x - 1834.8$ $R^2 = 0.1536$
Gulls on Black Rock (HEGU, GBBG)	Spring	$y = 8E-09x^4 - 5E-06x^3 + 0.0009x^2 - 0.0587x + 2.2858$ $R^2 = 0.5297$
	Summer	$y = -3E-10x^4 + 2E-06x^3 - 0.0009x^2 + 0.1636x - 7.9185$ $R^2 = 0.8562$
	Fall	$y = -2E-08x^4 + 1E-05x^3 - 0.0018x^2 - 0.3142x + 72.836$ $R^2 = 0.1688$
HEGU on Black Rock	Spring	$y = 3E-09x^4 - 2E-06x^3 + 0.0003x^2 - 0.0233x + 0.5054$ $R^2 = 0.1444$
	Summer	$y = 3E-08x^4 - 2E-05x^3 + 0.006x^2 - 0.7733x + 36.837$ $R^2 = 0.2695$
	Fall	$y = 0$ $R^2 = \#N/A$

Appendix C2 – Polynomial Regression Relationships of Dominant Waterbirds Species and Groups, 2010-2019

Note: Log transformations when applied were $\log_{10}(x + 1)$.

TOTAL BIRDS

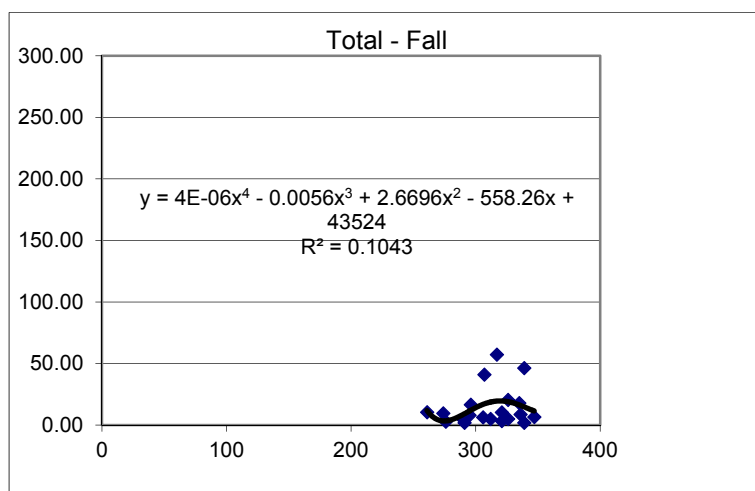
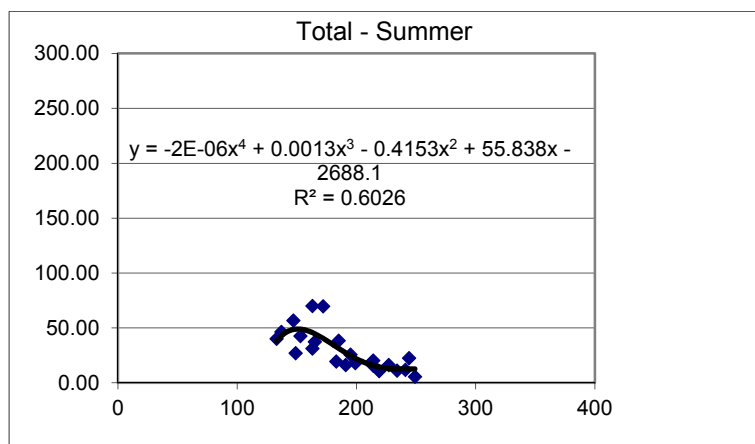
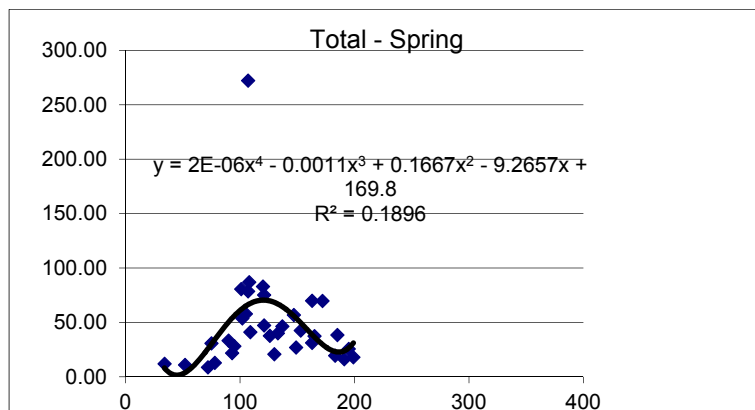


Figure C1. Abundance of Waterbirds (number/30 minutes) versus Julian day, 2010-2019, with polynomial regression line and regression parameters.

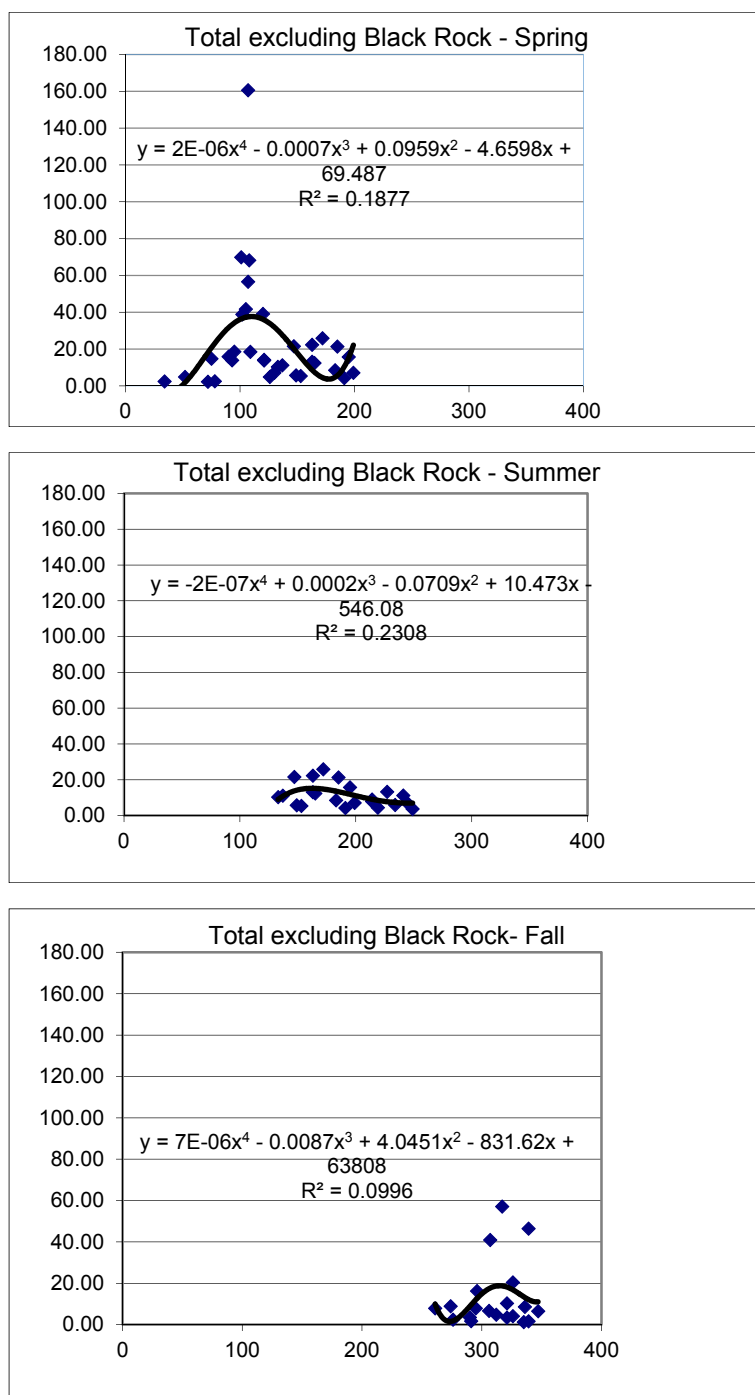


Figure C2. Abundance of Waterbirds (number/30 minutes) excluding Black Rock versus Julian day, 2010-2019, with polynomial regression line and regression parameters.

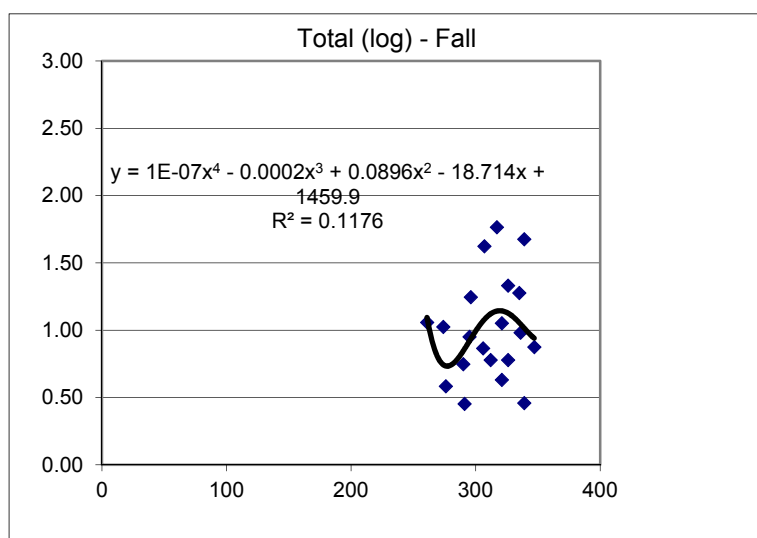
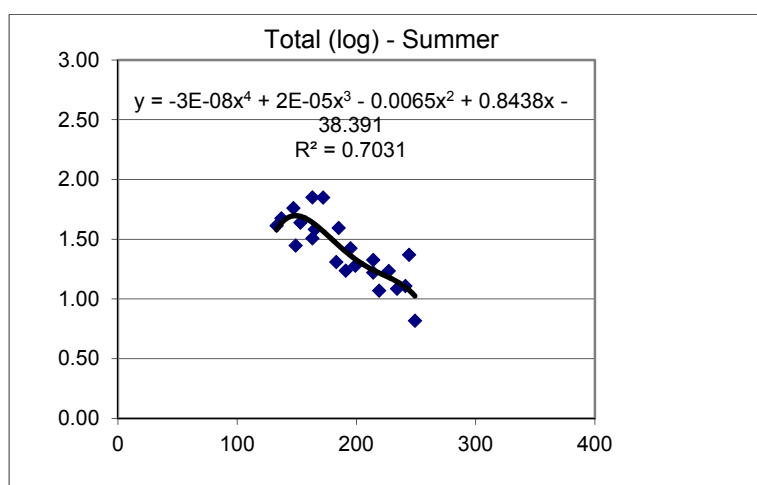
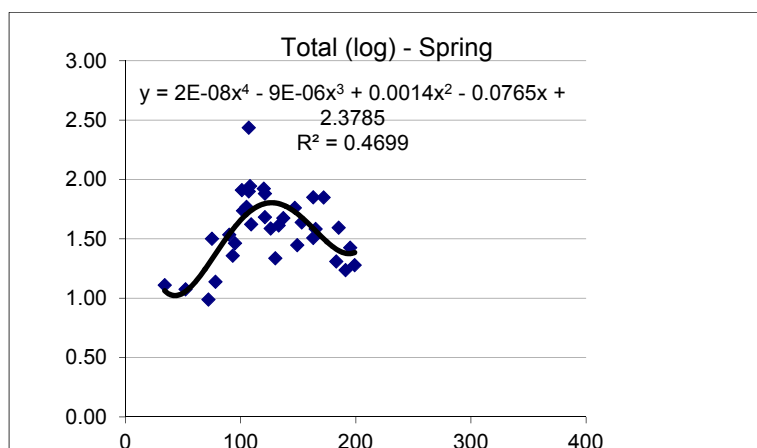


Figure C3. Abundance of Waterbirds (number/30 minutes) (\log_{10} transformed) versus Julian day, 2010-2019, with polynomial regression line and regression parameters.

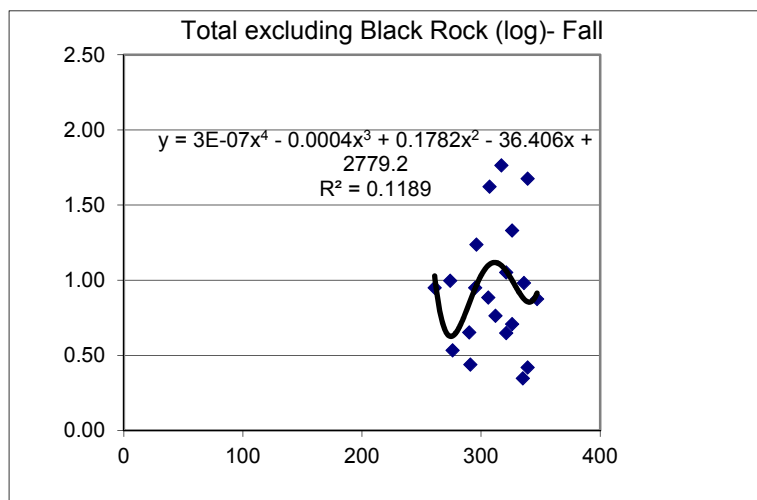
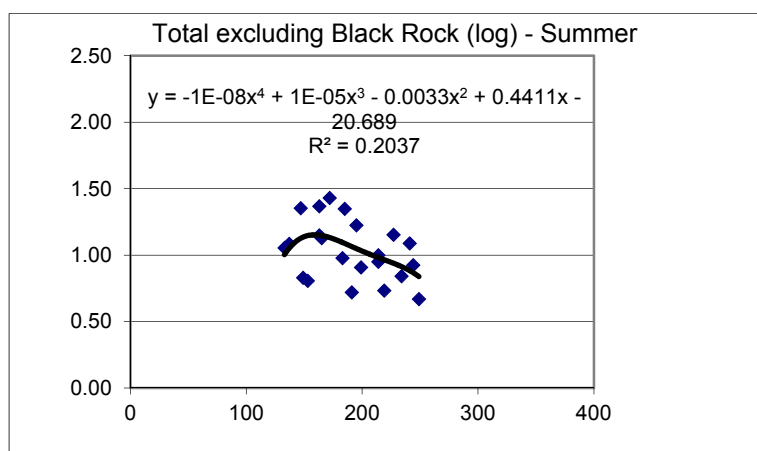
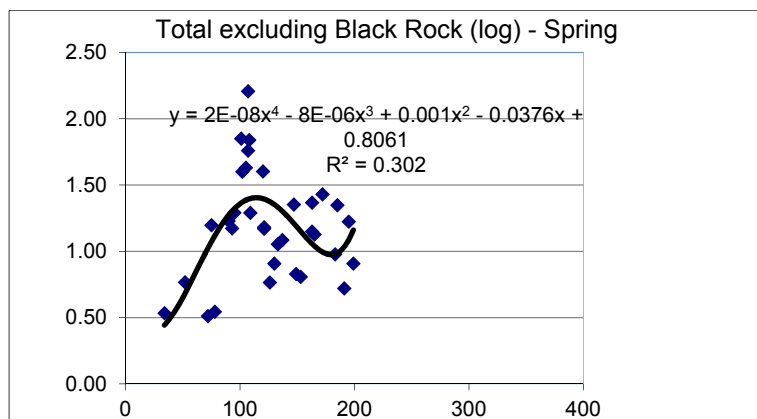


Figure C4. Abundance of Waterbirds (number/30 minutes) excluding Black Rock (\log_{10} transformed) versus Julian day, 2010-2019, with polynomial regression line and regression parameters.

GREAT BLACK-BACKED GULL

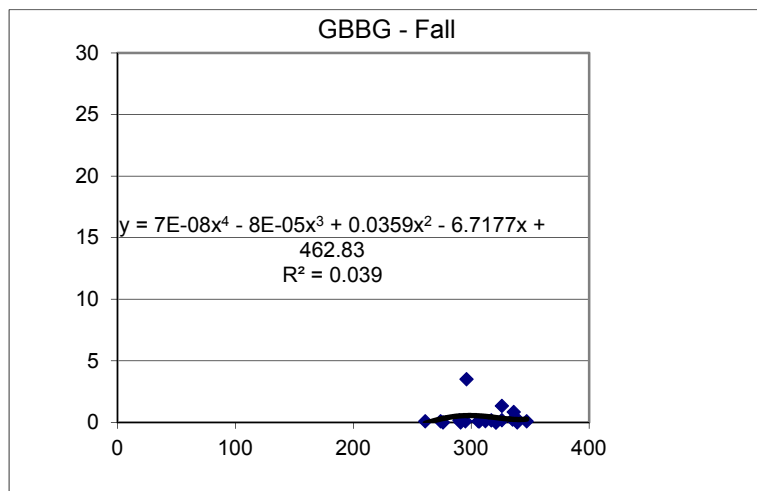
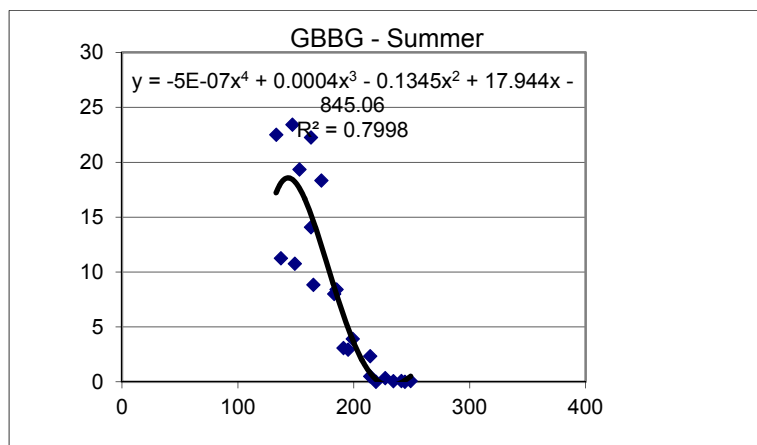
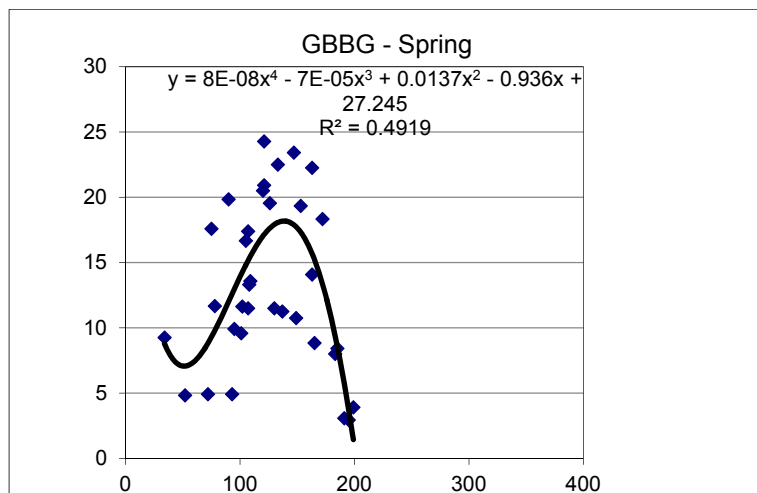


Figure C5. Abundance of Great Black-backed Gull (number/30 minutes) versus Julian day, 2010-2019, with polynomial regression line and regression parameters.

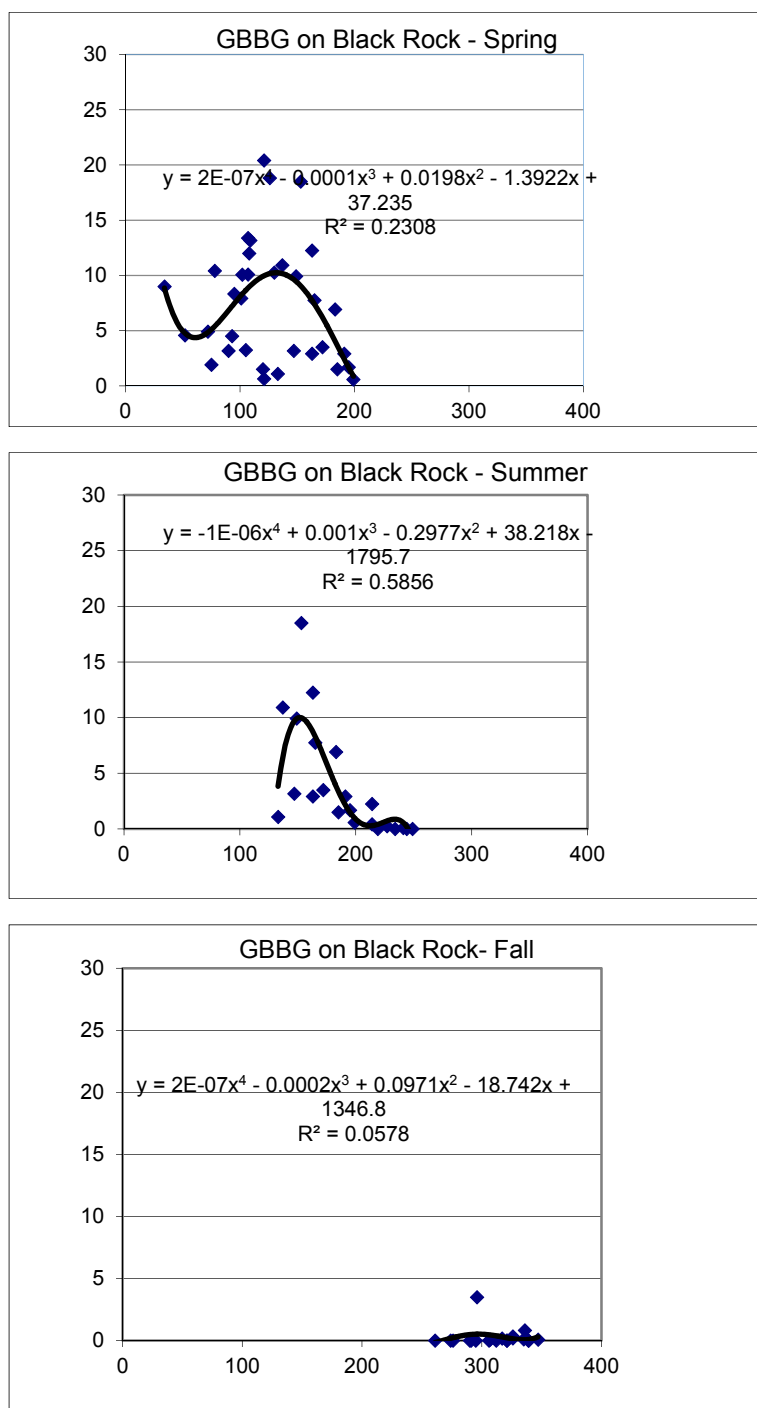


Figure C6. Abundance of Great Black-backed Gull (number/30 minutes) on Black Rock versus Julian day, 2010-2019, with polynomial regression line and regression parameters.

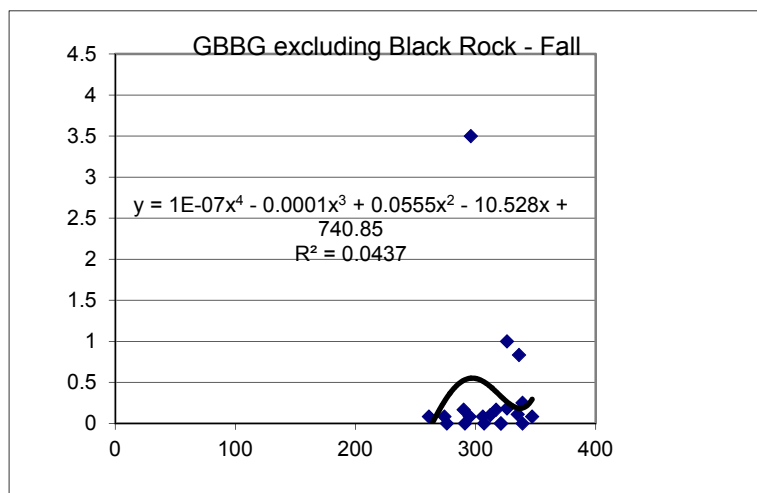
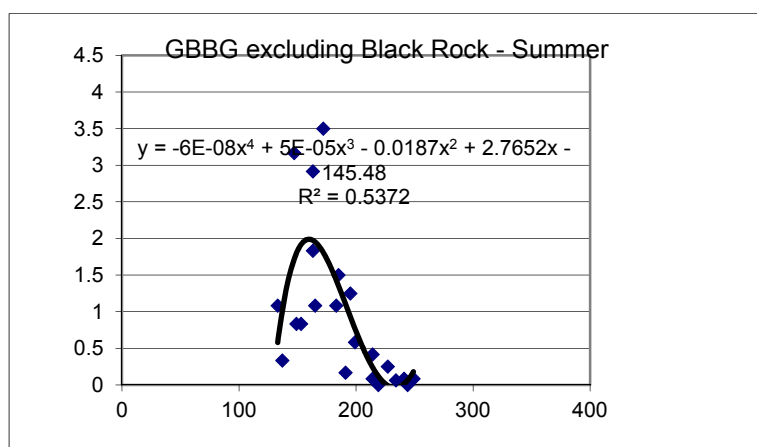
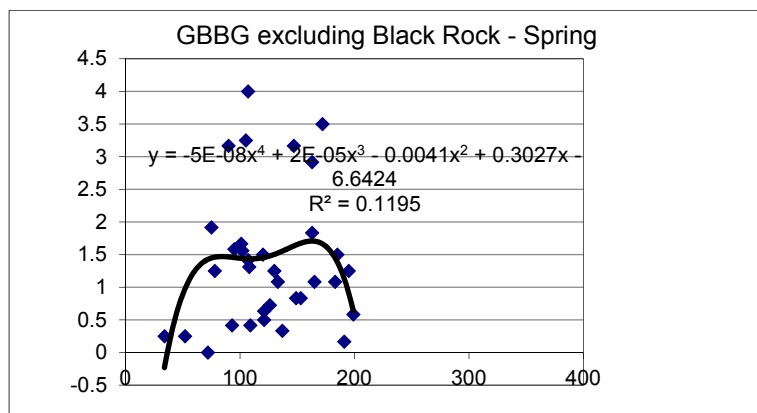


Figure C7. Abundance of Great Black-backed Gull (number/30 minutes) excluding Black Rock versus Julian day, 2010-2019, with polynomial regression line and regression parameters.

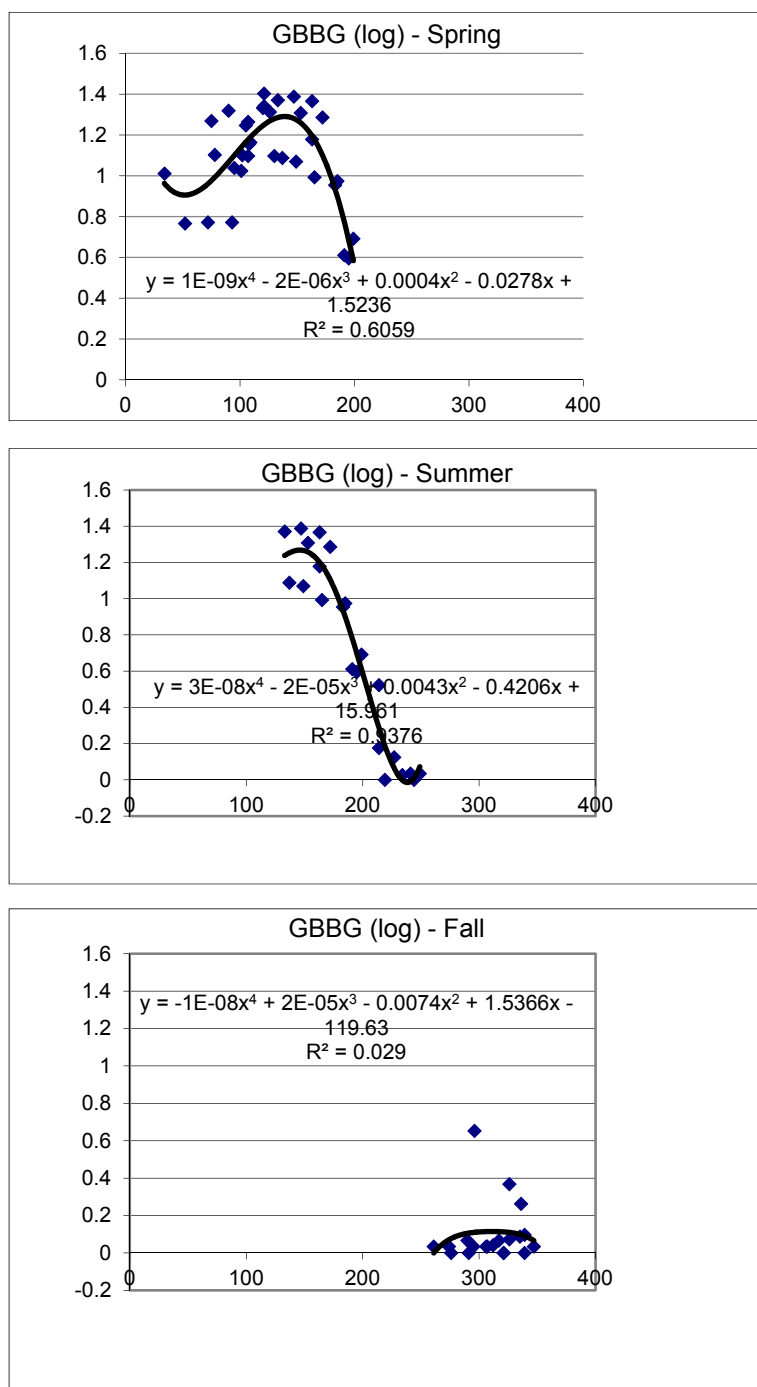


Figure C8. Abundance of Great Black-backed Gull (number/30 minutes) (\log_{10} transformed) versus Julian day, 2010-2019, with polynomial regression line and regression parameters.

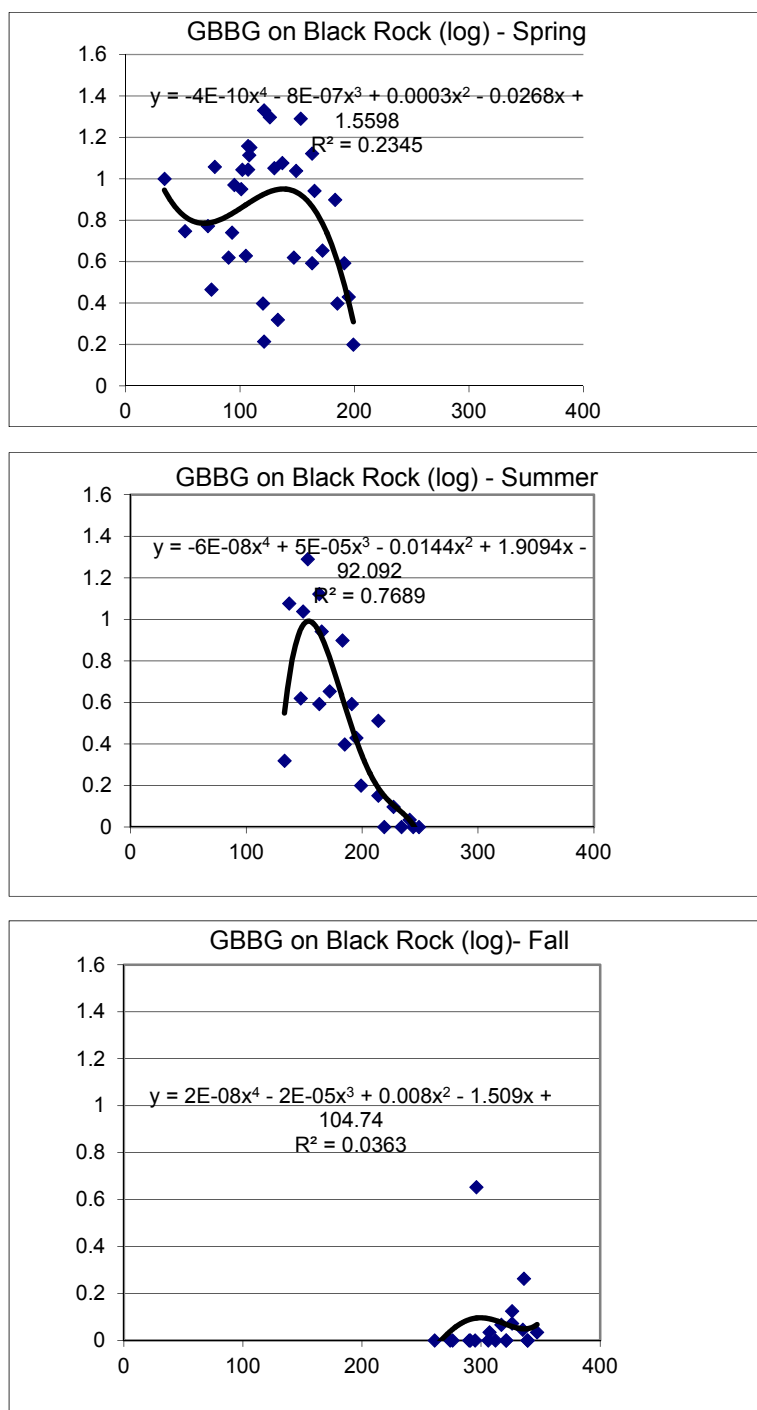


Figure C9. Abundance of Great Black-backed Gull (number/30 minutes) on Black Rock (\log_{10} transformed) versus Julian day, 2010-2019, with polynomial regression line and regression parameters.

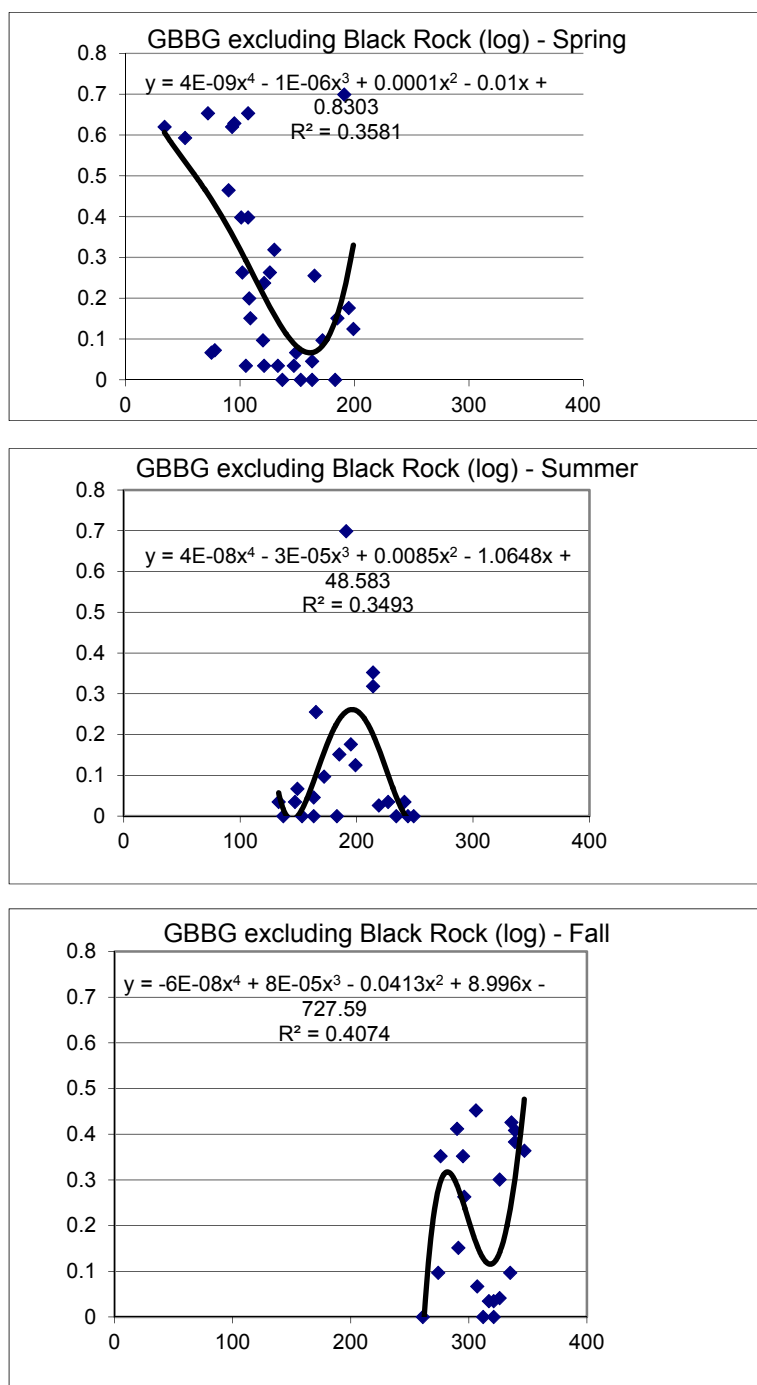


Figure C10. Abundance of Great Black-backed Gull (number/30 minutes) excluding Black Rock (\log_{10} transformed) versus Julian day, 2010-2019, with polynomial regression line and regression parameters.

HERRING GULL

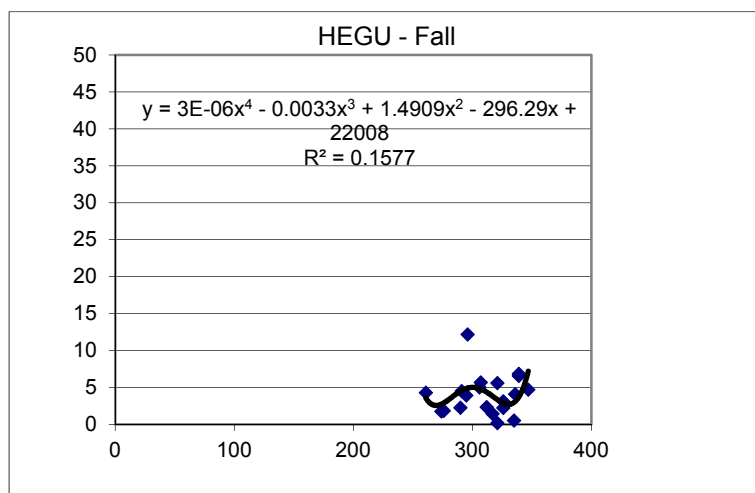
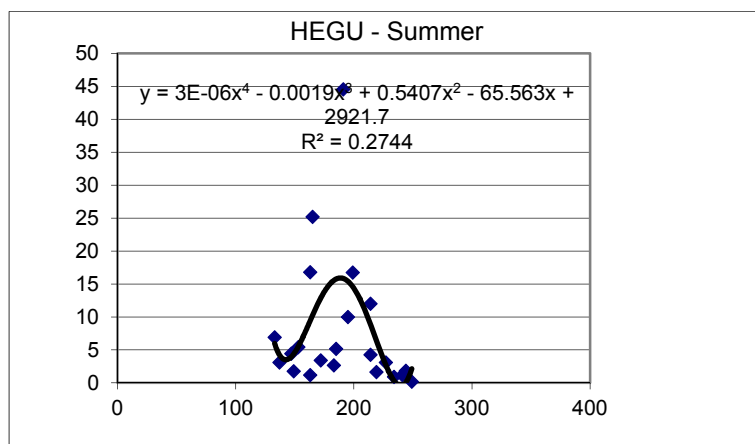
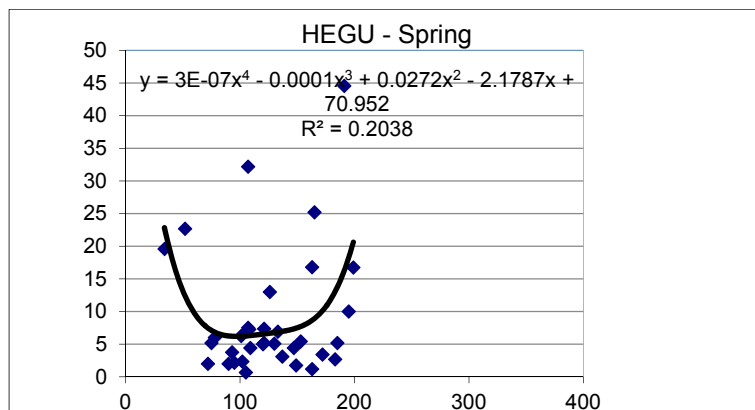


Figure C11. Abundance of Herring Gull (number/30 minutes) versus Julian day, 2010-2019, with polynomial regression line and regression parameters.

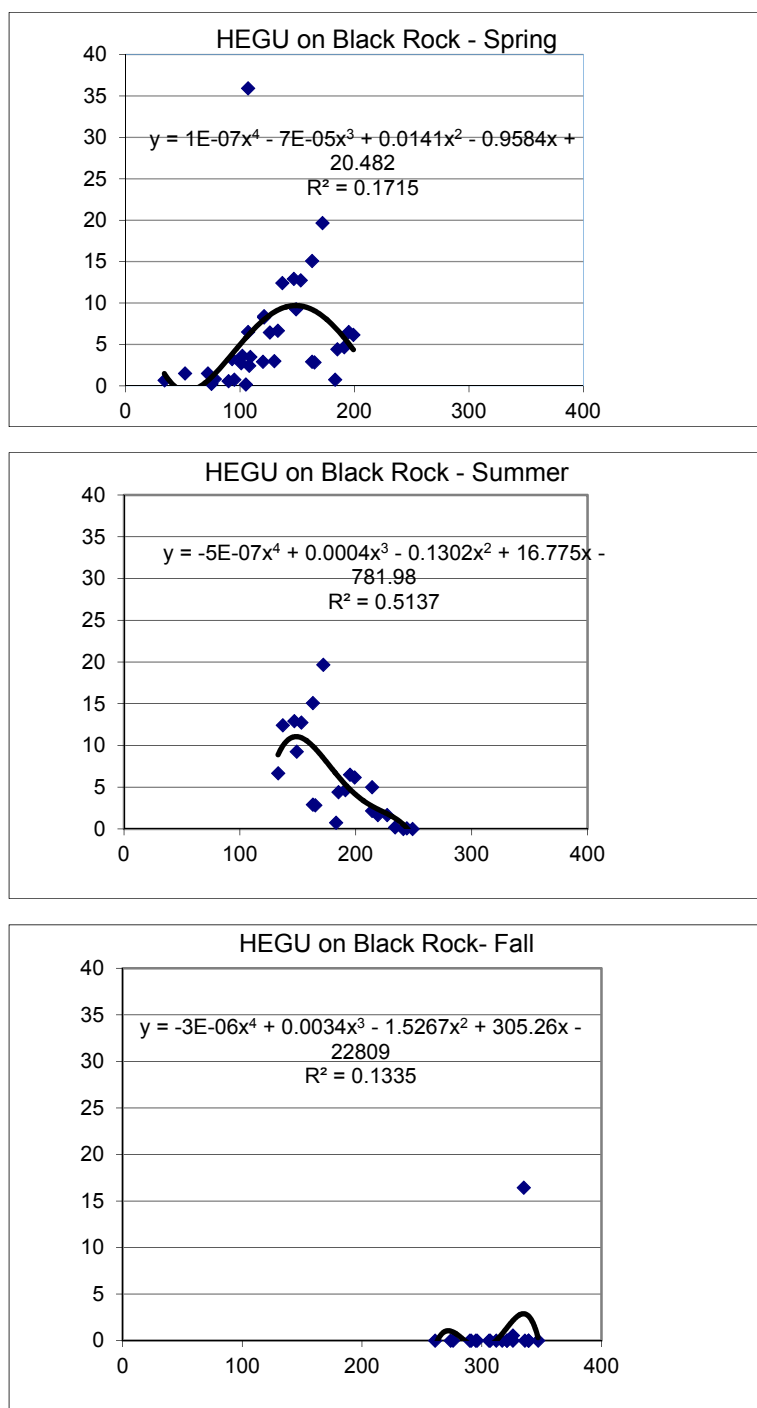


Figure C12. Abundance of Herring Gull (number/30 minutes) on Black Rock versus Julian day, 2010-2019, with polynomial regression line and regression parameters.

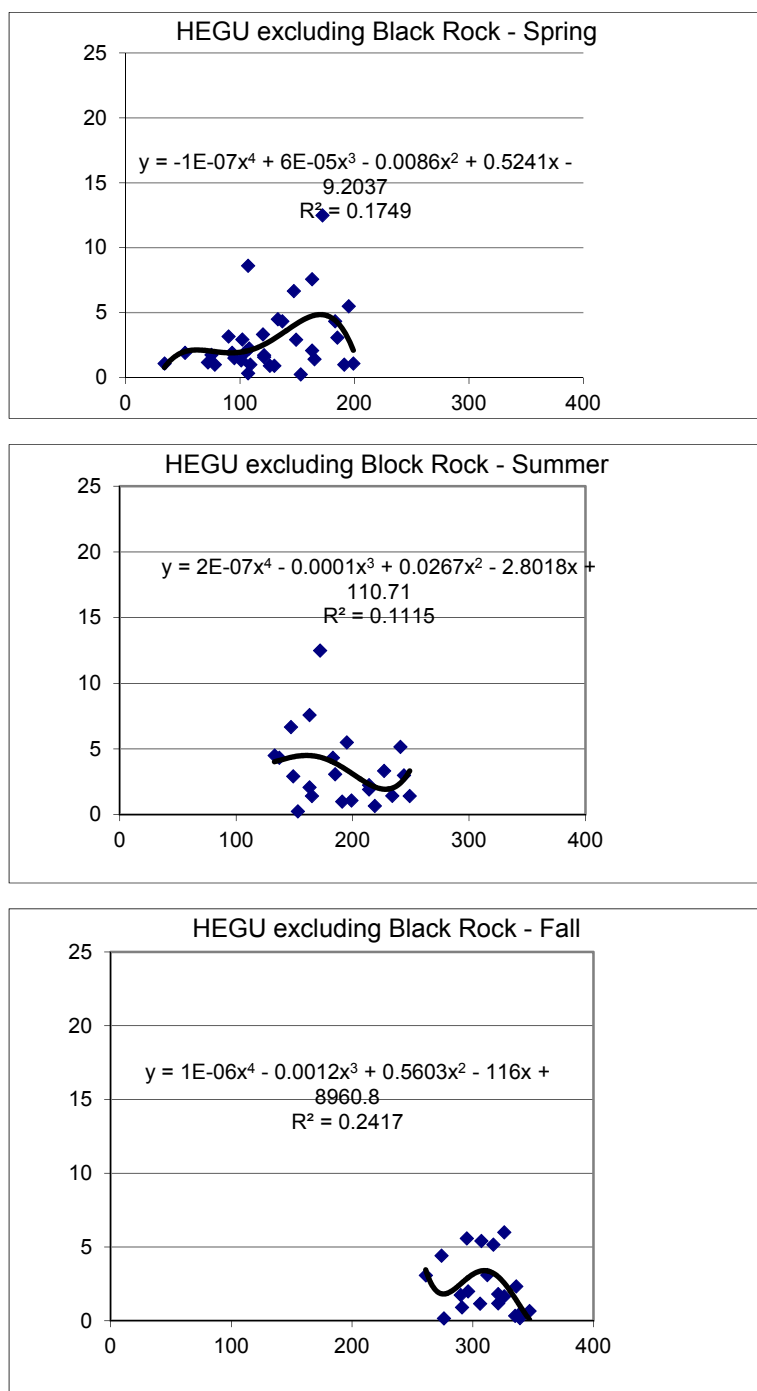


Figure C13. Abundance of Herring Gull (number/30 minutes) excluding Black Rock versus Julian day, 2010-2019, with polynomial regression line and regression parameters.

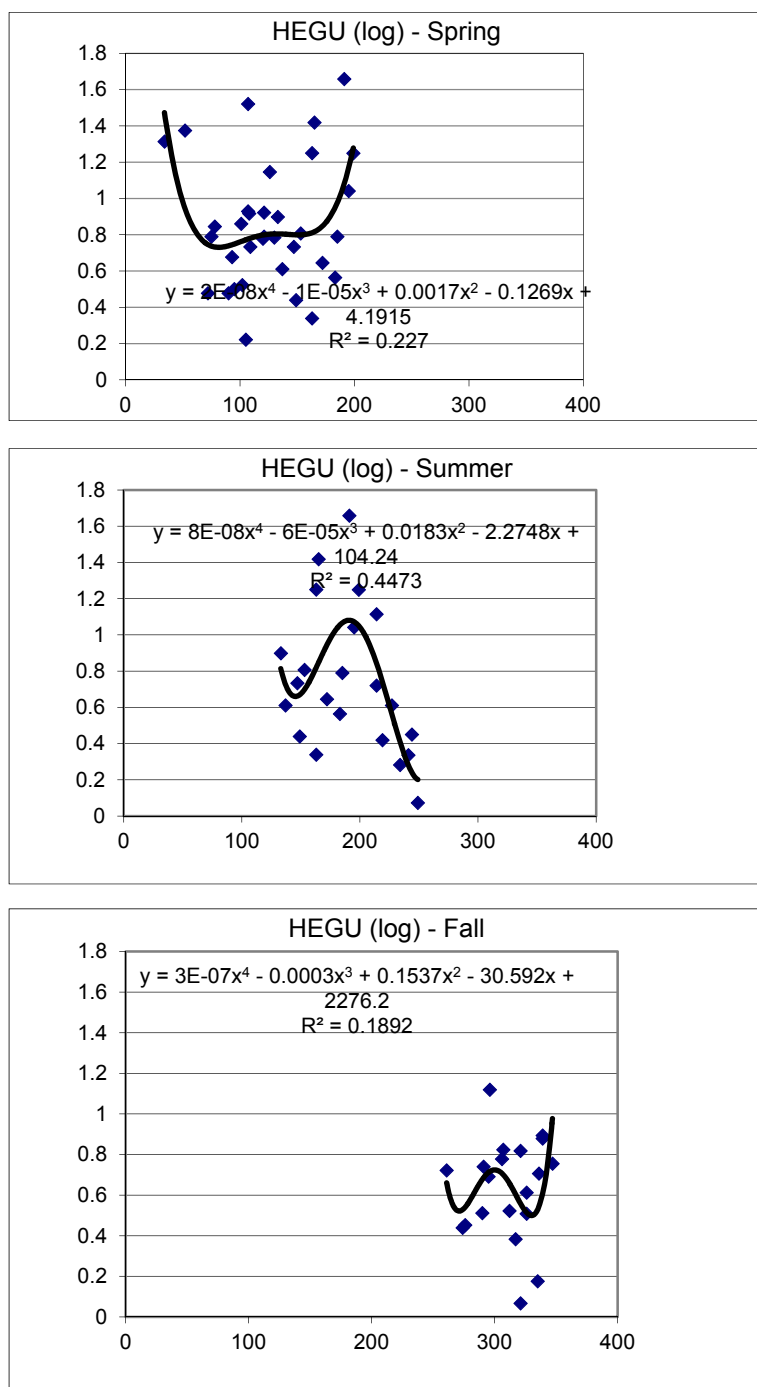


Figure C14. Abundance of Herring Gull (number/30 minutes) (\log_{10} transformed) versus Julian day, 2010-2019, with polynomial regression line and regression parameters.

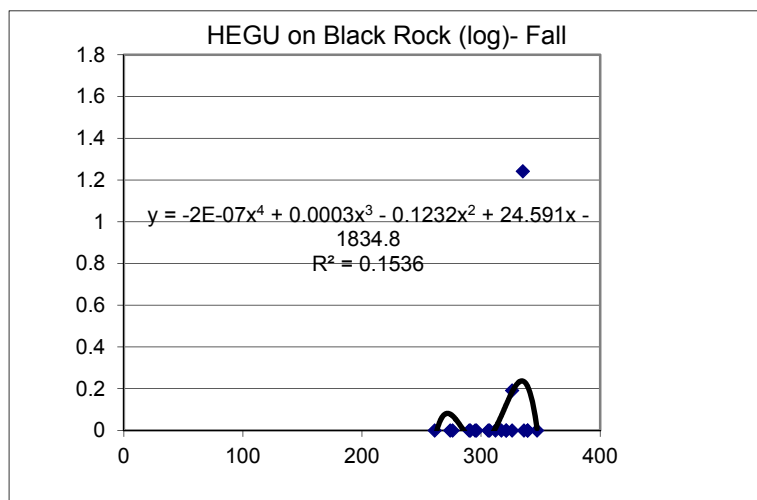
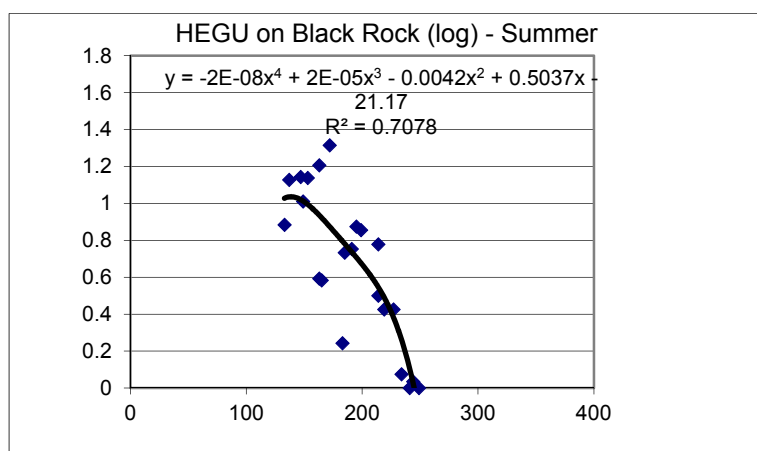
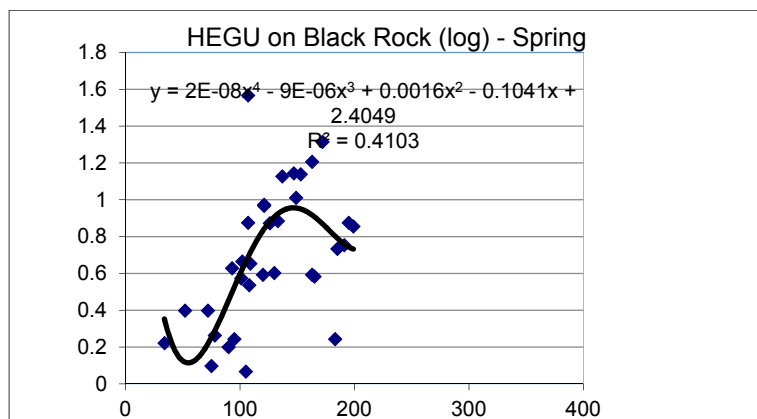


Figure C15. Abundance of Herring Gull (number/30 minutes) on Black Rock (\log_{10} transformed) versus Julian day, 2010-2019, with polynomial regression line and regression parameters.

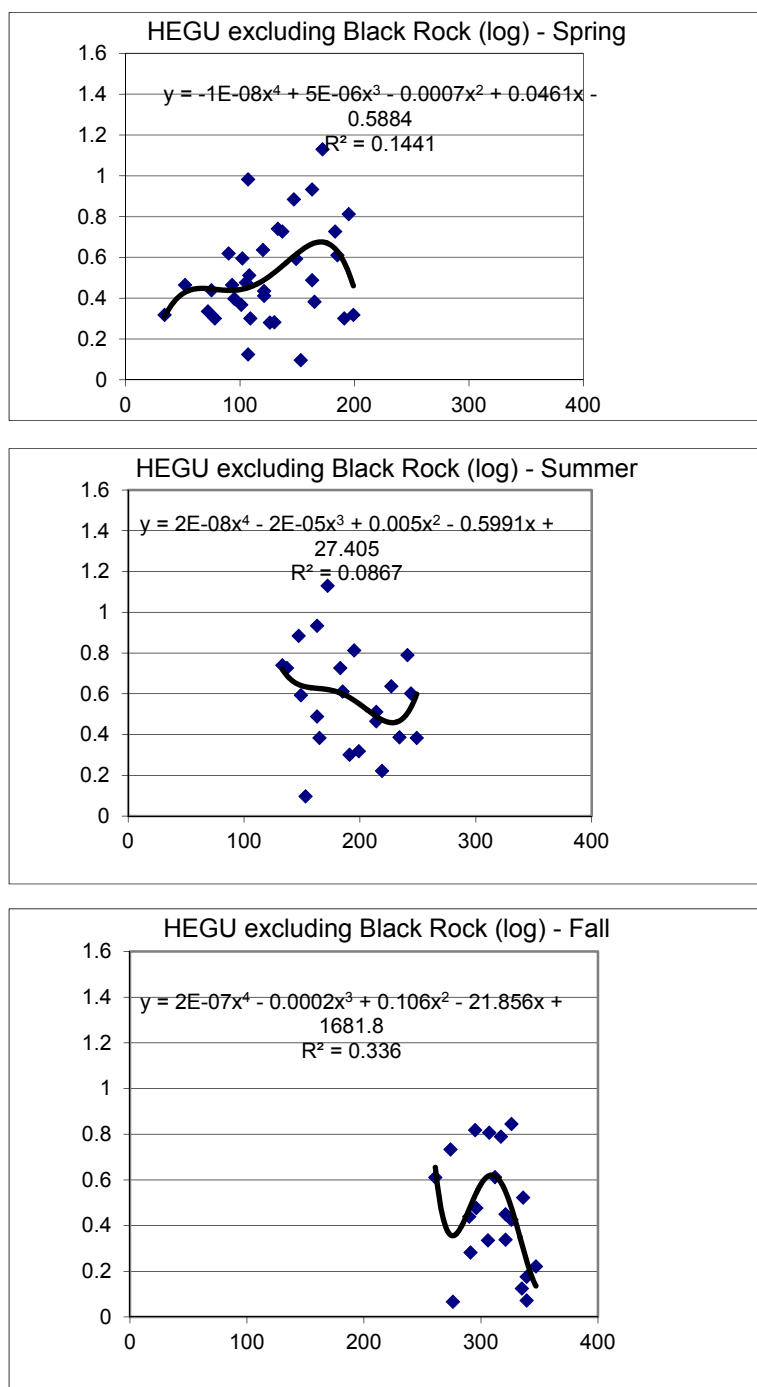


Figure C16. Abundance of Herring Gull (number/30 minutes) (\log_{10} transformed) versus Julian day, 2010-2019, with polynomial regression line and regression parameters.

CORMORANTS

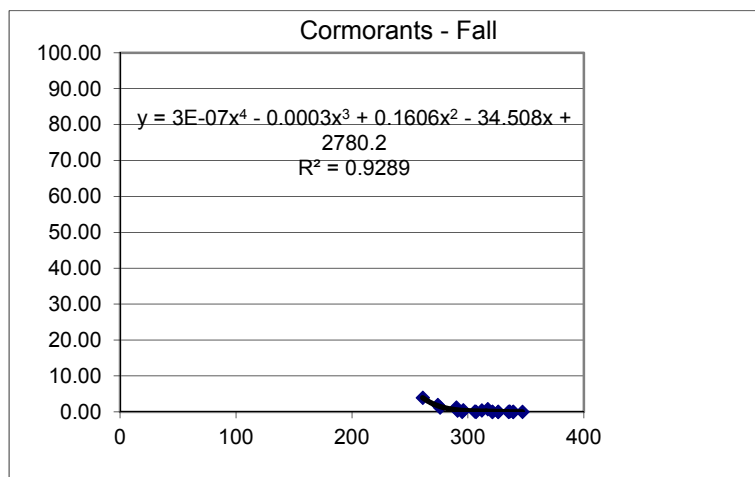
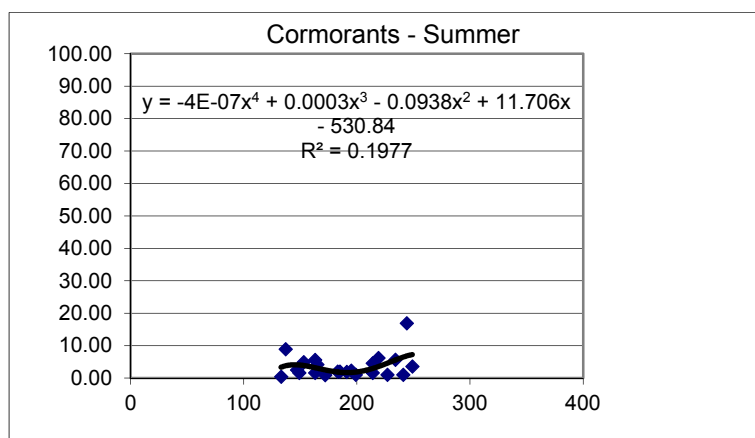
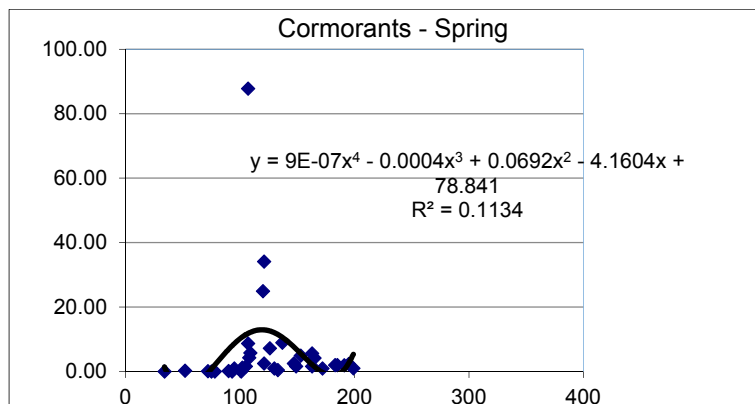


Figure C17. Abundance of cormorants (number/30 minutes) versus Julian day, 2010-2019, with polynomial regression line and regression parameters.

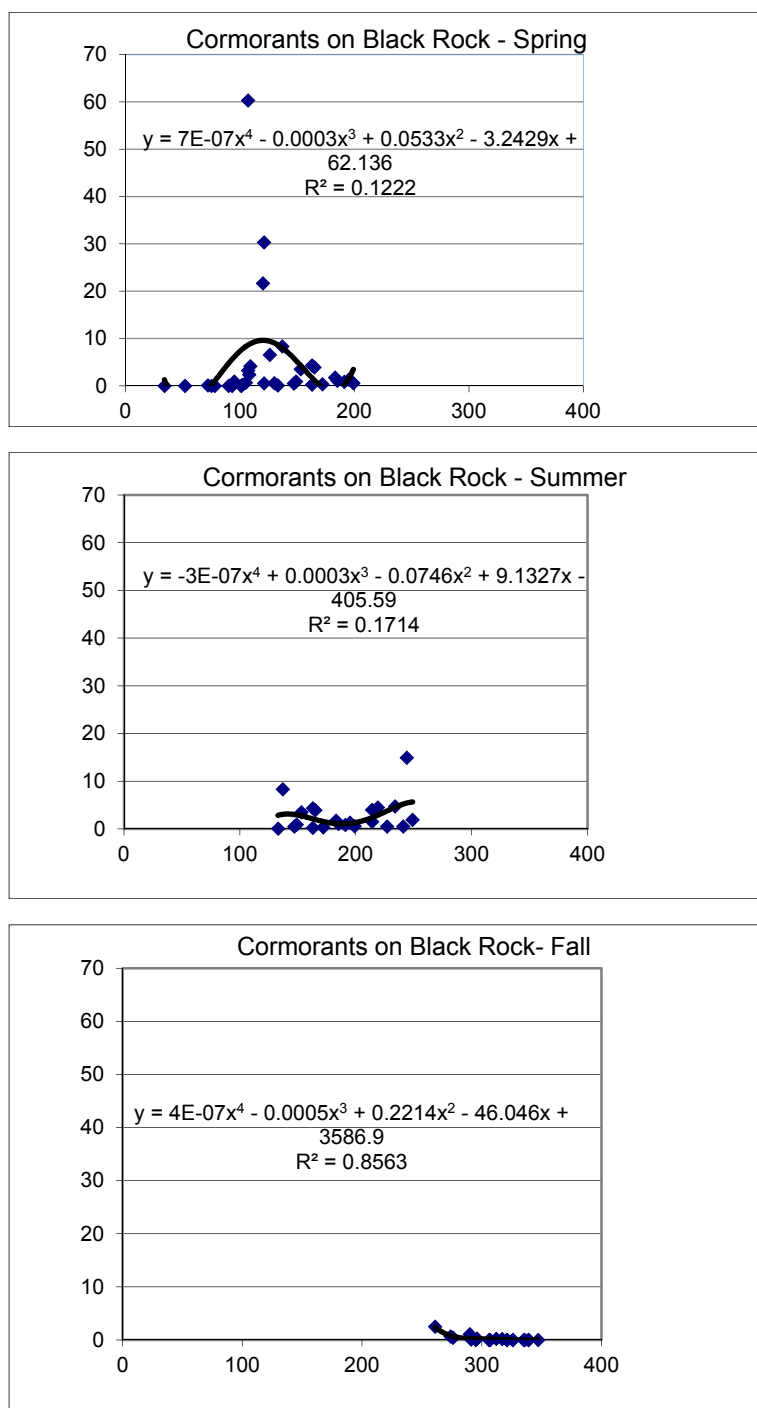


Figure C18. Abundance of cormorants (number/30 minutes) on Black Rock versus Julian day, 2010-2019, with polynomial regression line and regression parameters.

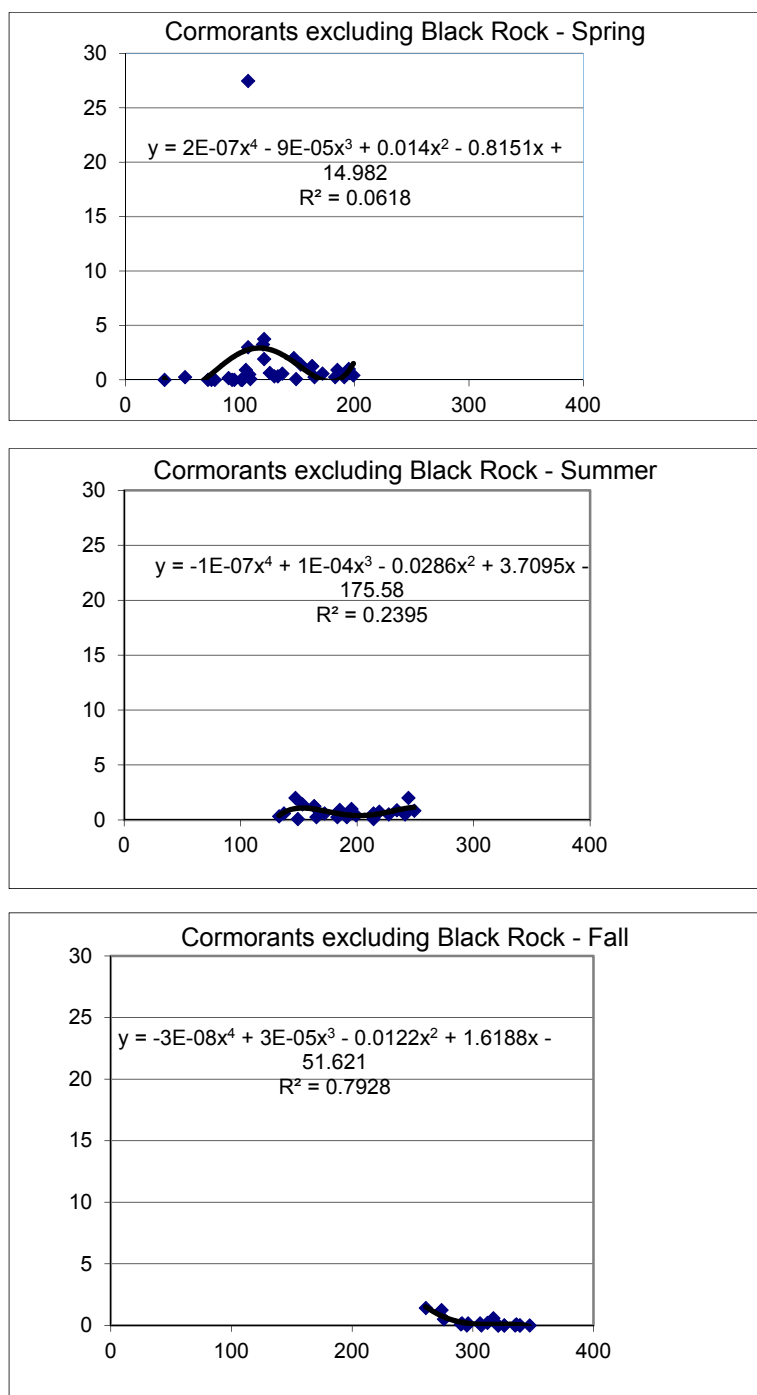


Figure C19. Abundance of cormorants (number/30 minutes) excluding Black Rock versus Julian day, 2010-2019, with polynomial regression line and regression parameters.

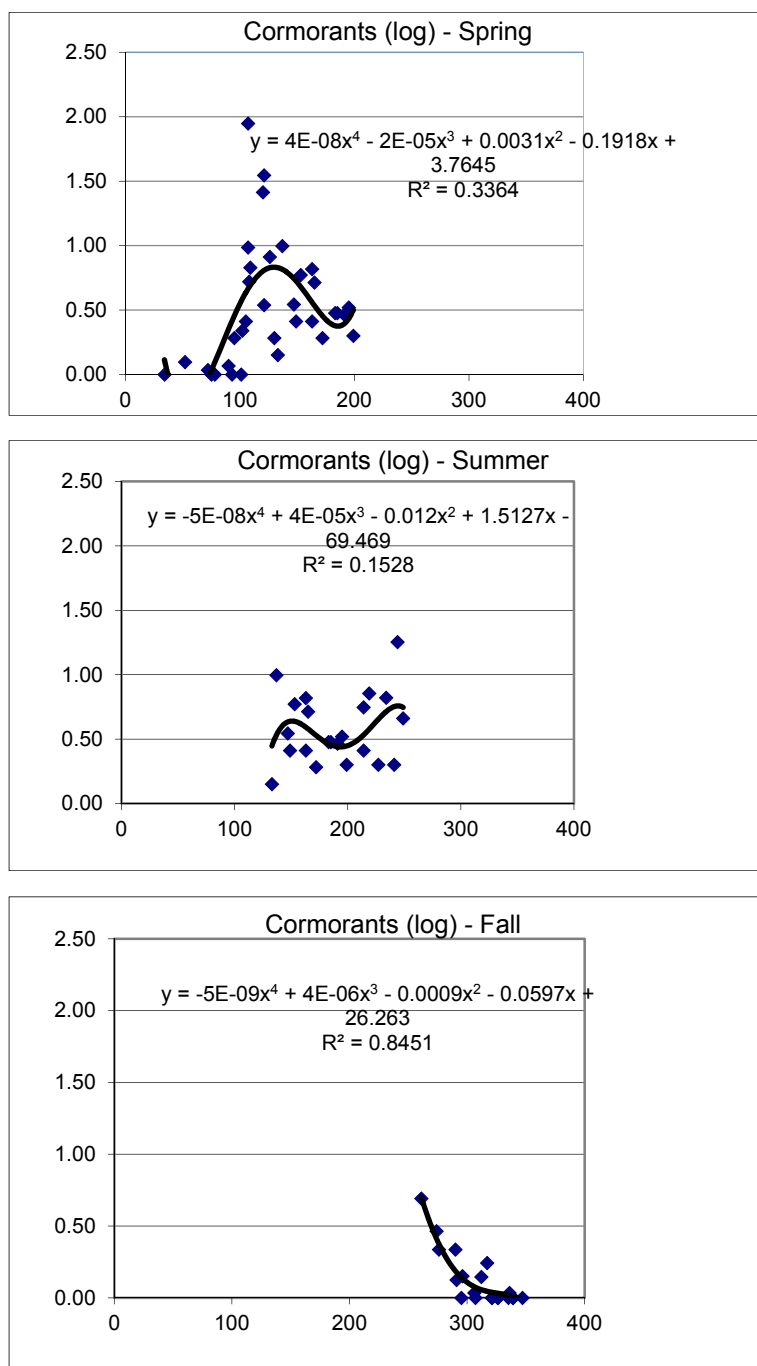


Figure C20. Abundance of cormorants (number/30 minutes) (\log_{10} transformed) versus Julian day, 2010-2019, with polynomial regression line and regression parameters.

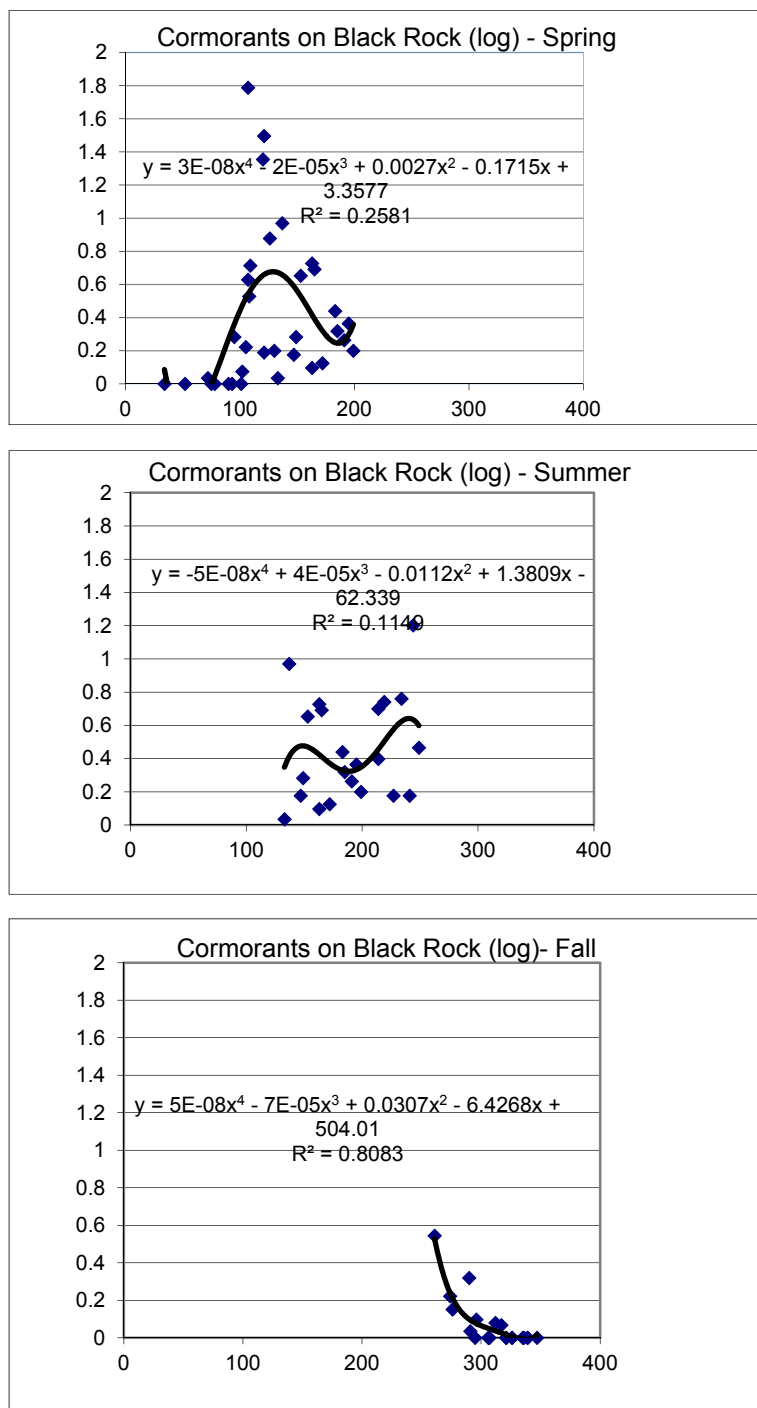


Figure C21. Abundance of cormorants (number/30 minutes) on Black Rock (log₁₀ transformed) versus Julian day, 2010-2019, with polynomial regression line and regression parameters.

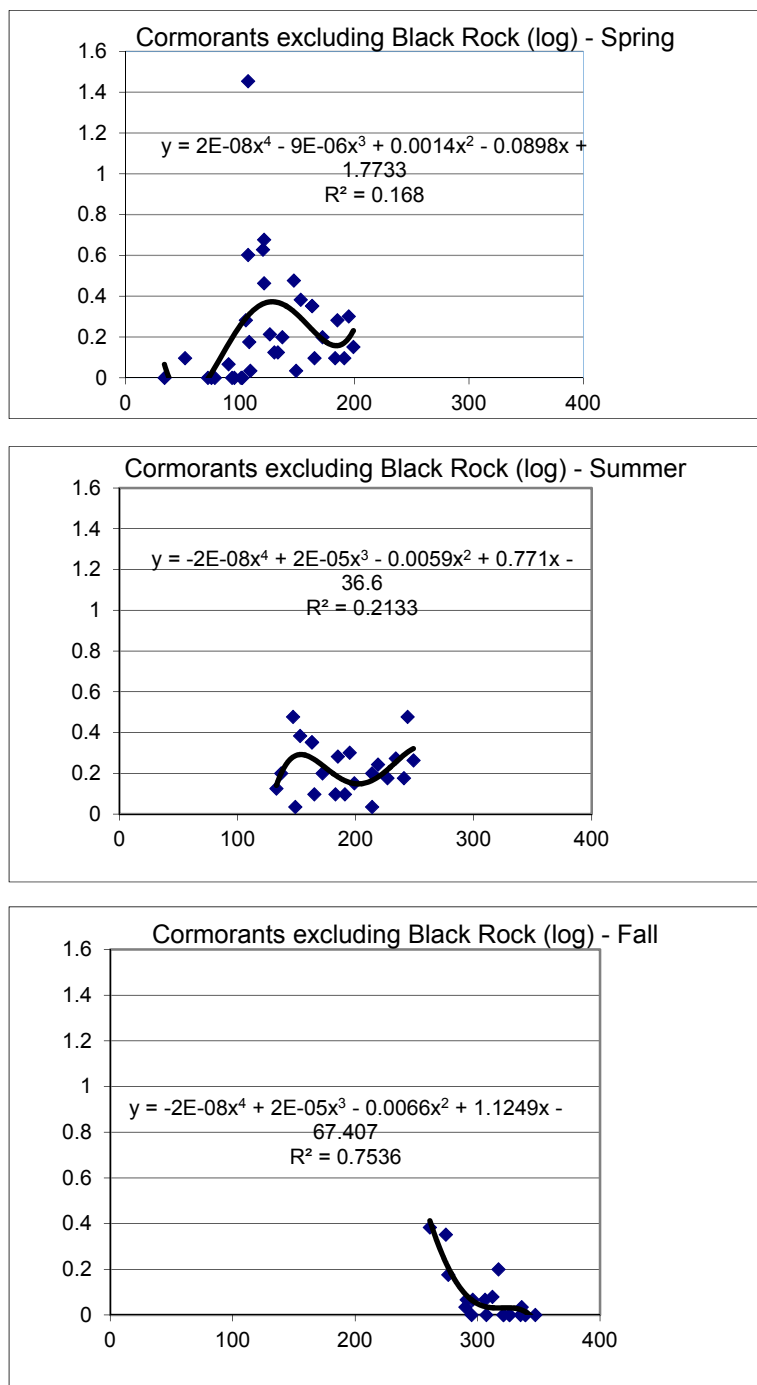


Figure C22. Abundance of cormorants (number/30 minutes) excluding Black Rock (\log_{10} transformed) versus Julian day, 2010-2019, with polynomial regression line and regression parameters.

BLACK GUILLEMOT

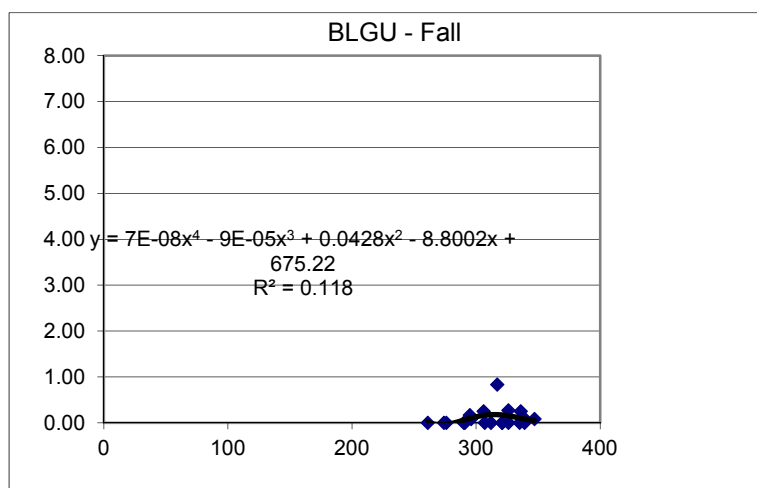
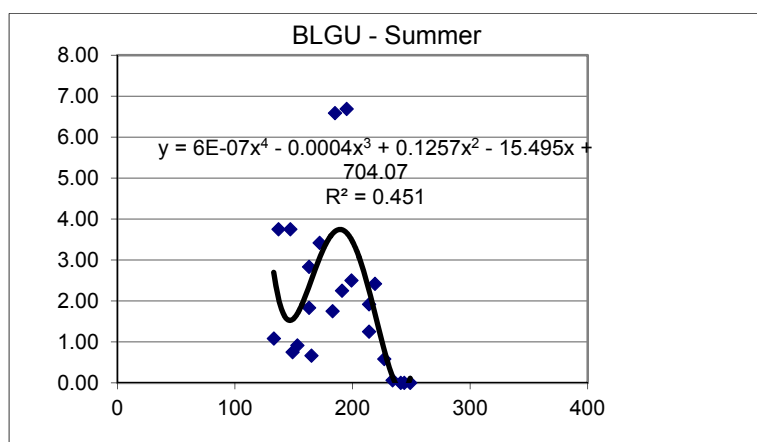
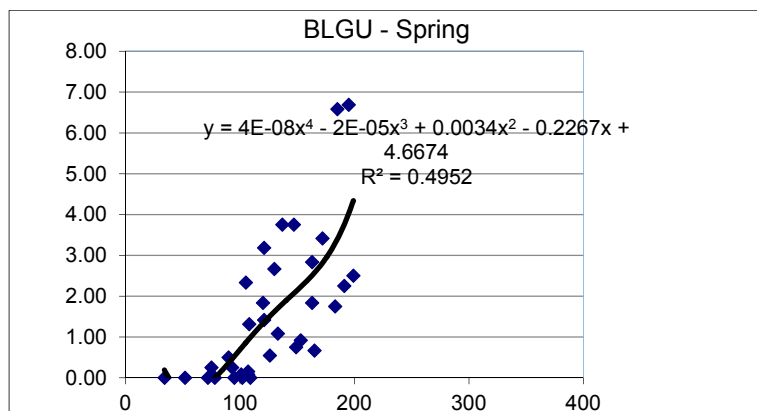


Figure C23. Abundance of Black Guillemot (number/30 minutes) versus Julian day, 2010-2019, with polynomial regression line and regression parameters.

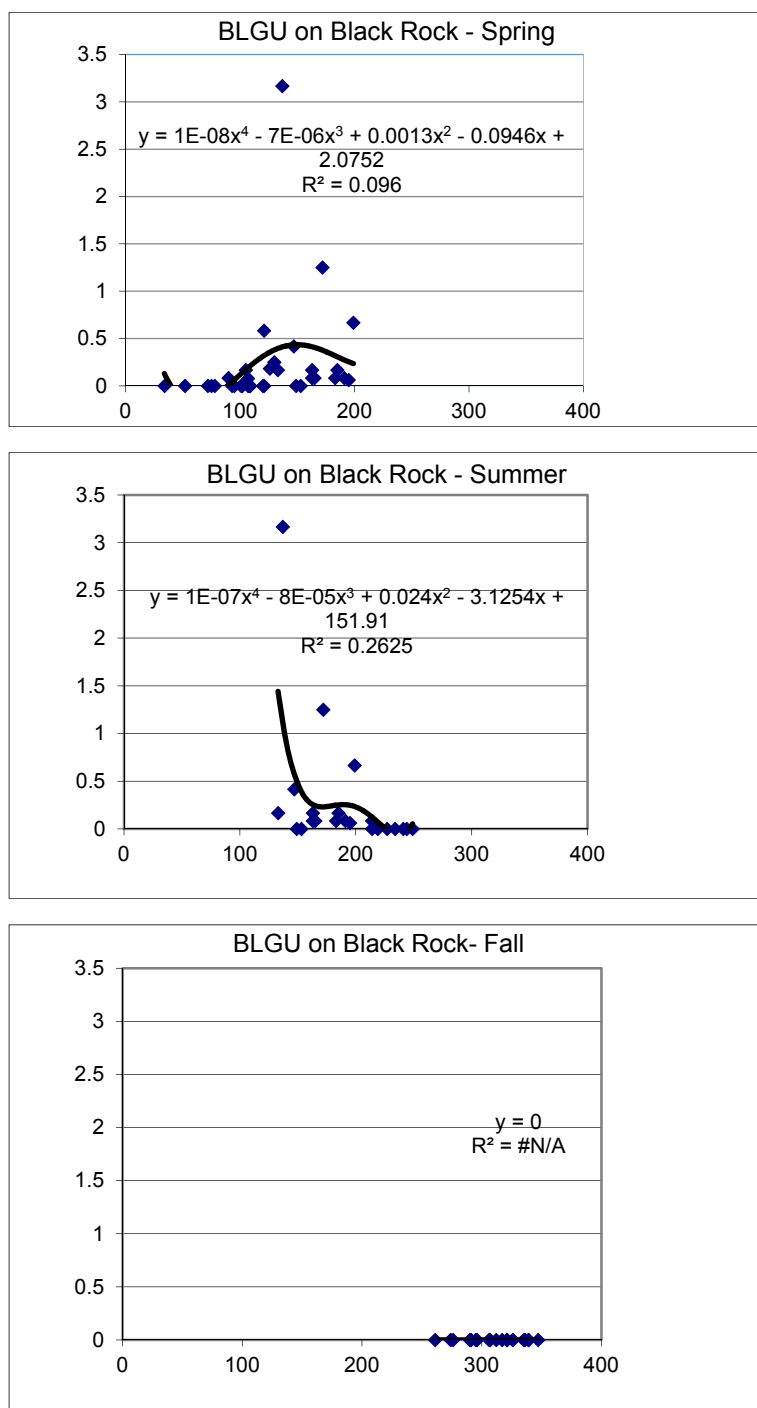


Figure C24. Abundance of Black Guillemot (number/30 minutes) on Black Rock versus Julian day, 2010-2019, with polynomial regression line and regression parameters.

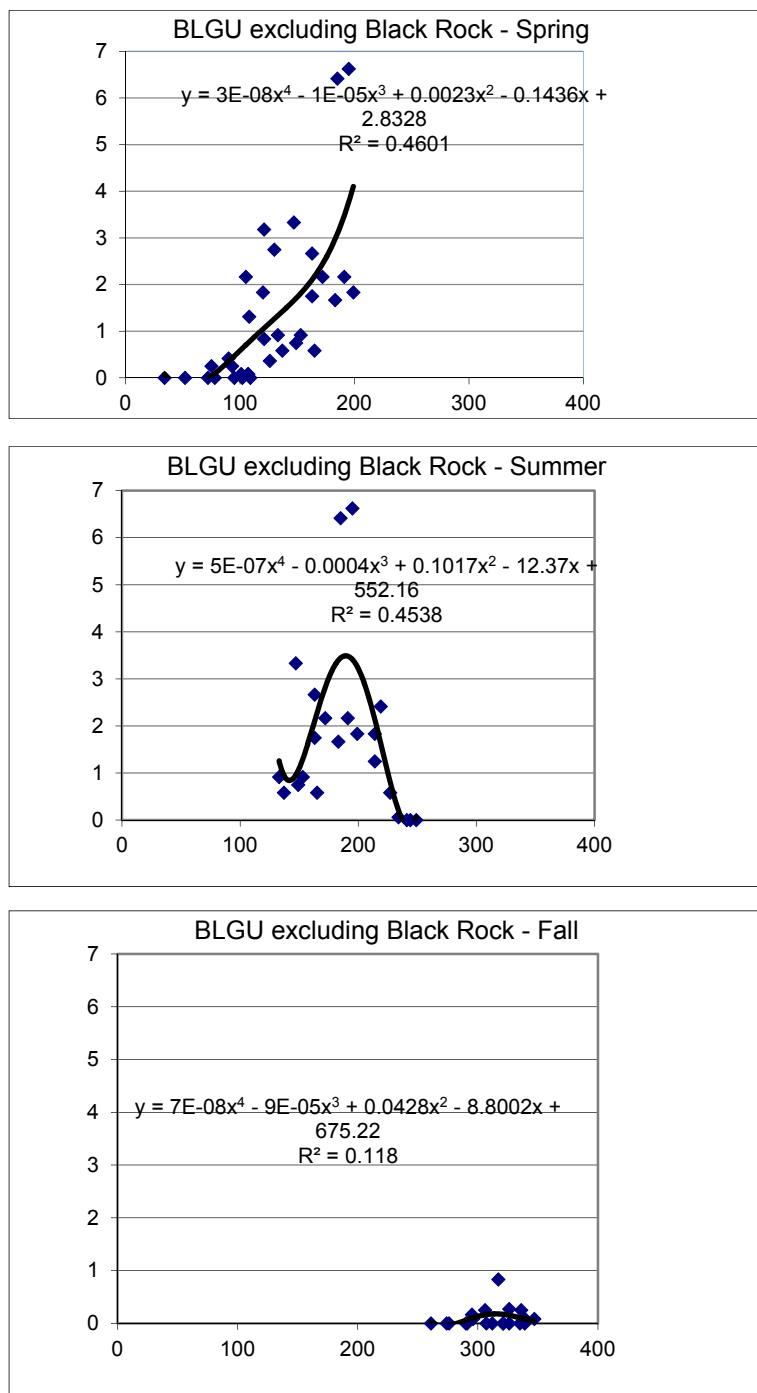


Figure C25. Abundance of Black Guillemot (number/30 minutes) excluding Black Rock versus Julian day, 2010-2019, with polynomial regression line and regression parameters.

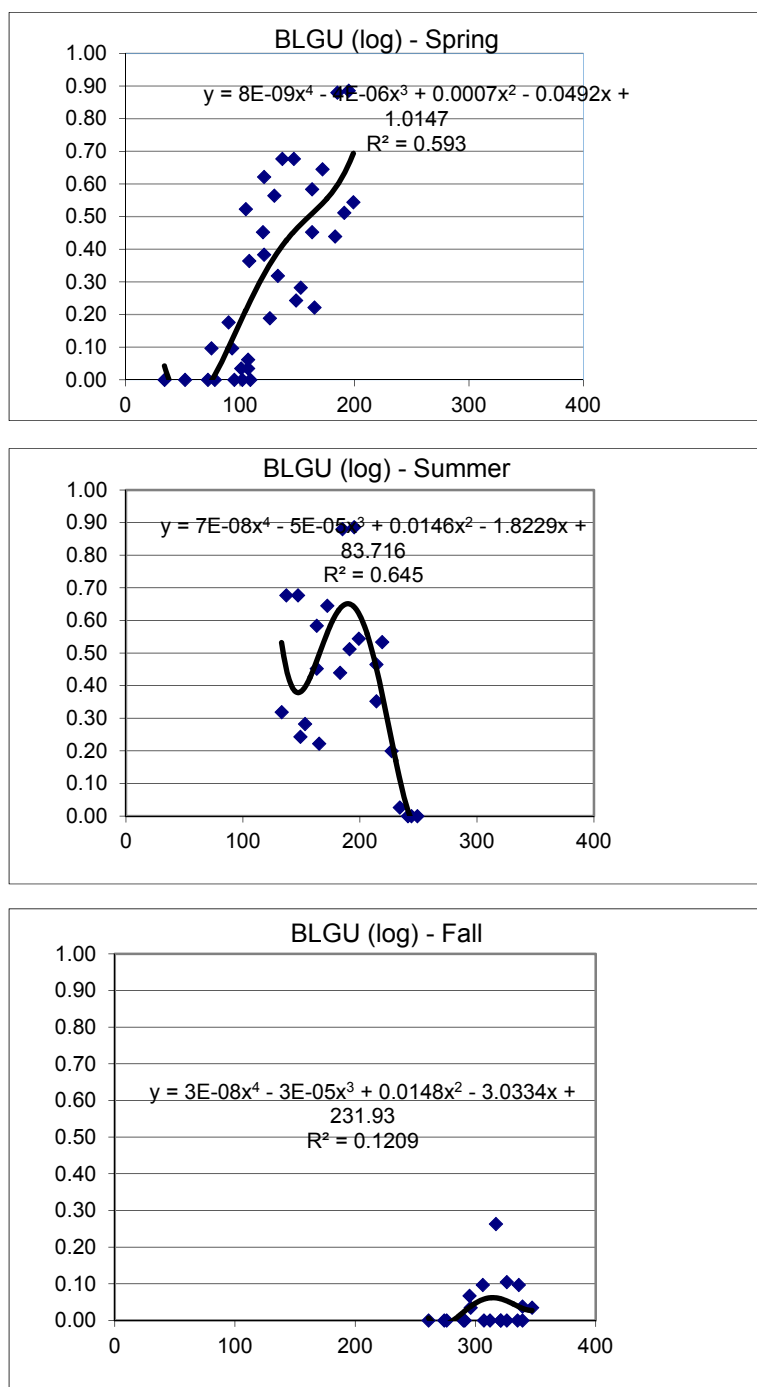


Figure C26. Abundance of Black Guillemot (number/30 minutes) (\log_{10} transformed) versus Julian day, 2010-2019, with polynomial regression line and regression parameters.

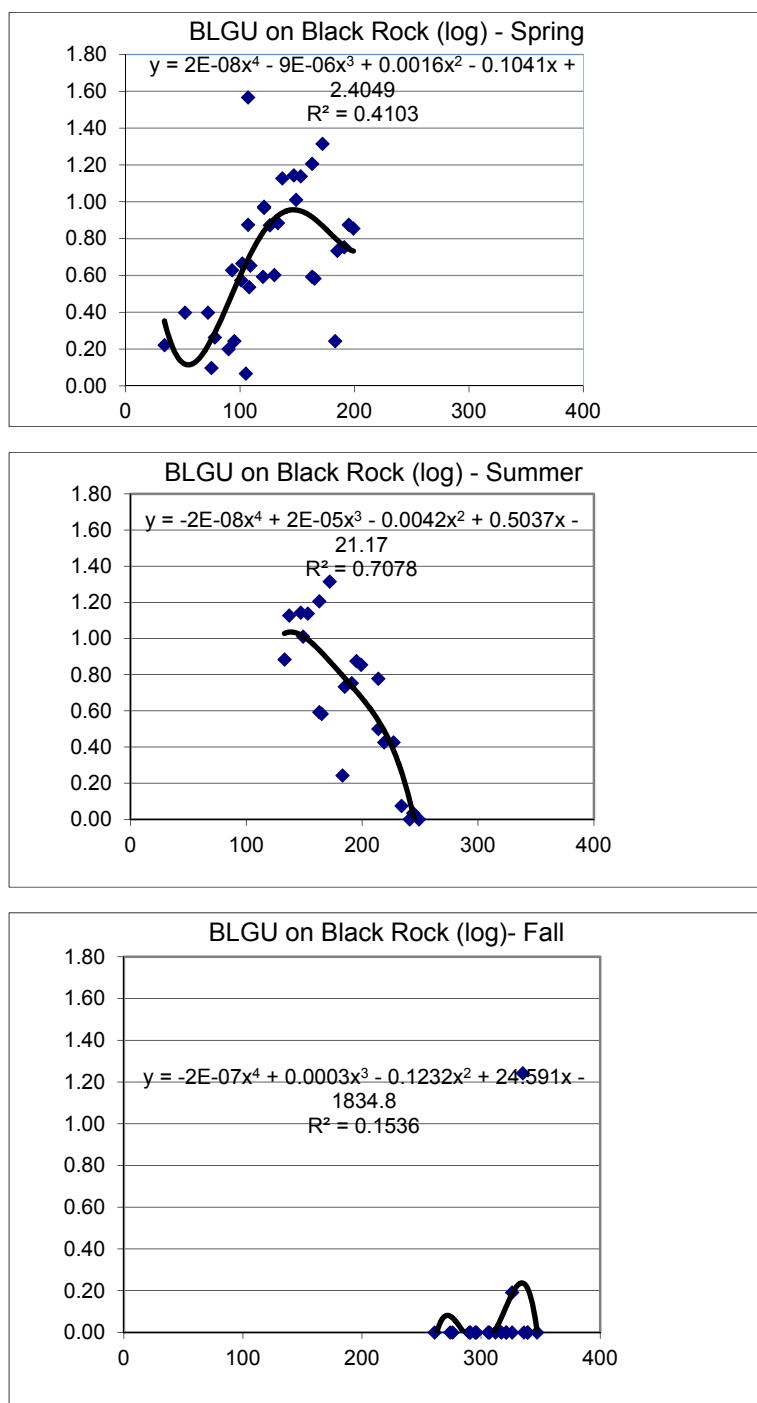


Figure C27. Abundance of Black Guillemot (number/30 minutes) on Black Rock (\log_{10} transformed) versus Julian day, 2010-2019, with polynomial regression line and regression parameters.

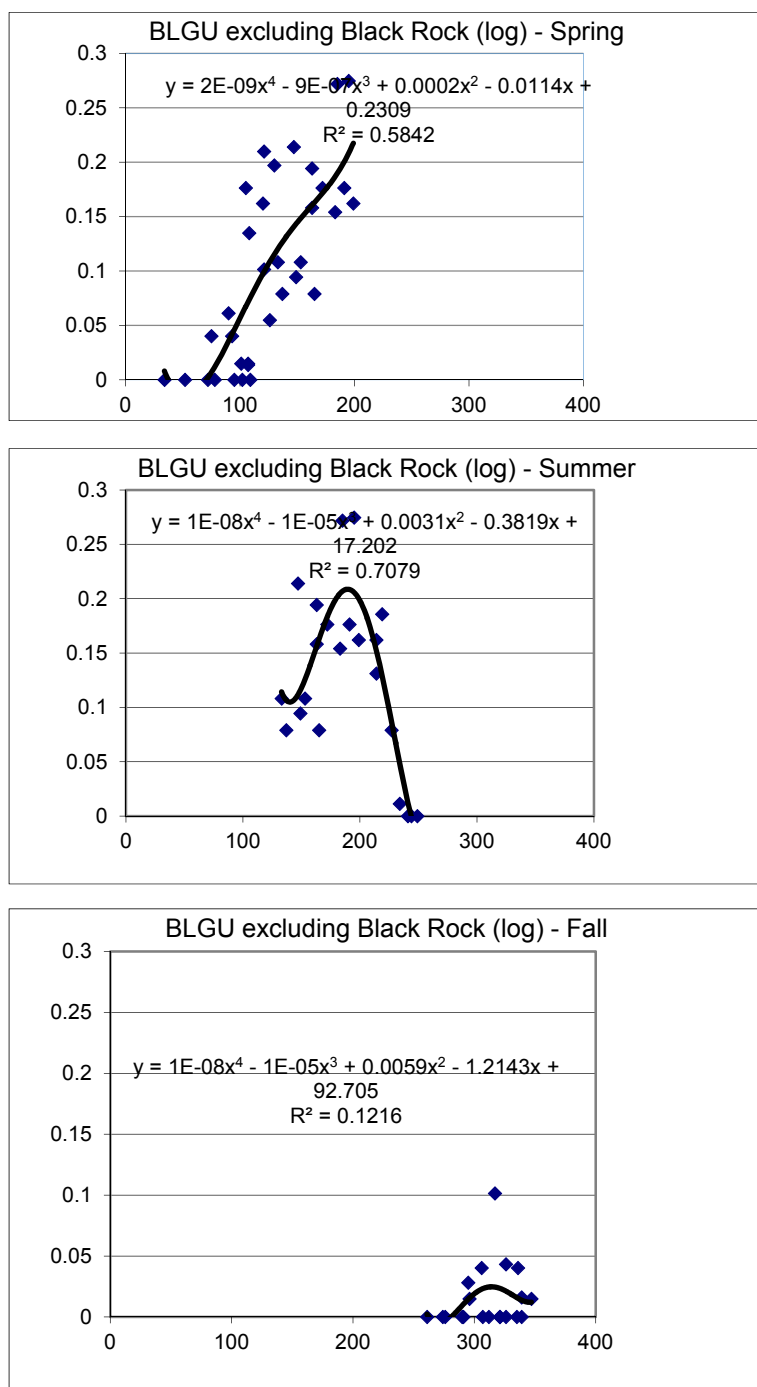


Figure C28. Abundance of Black Guillemot (number/30 minutes) excluding Black Rock (\log_{10} transformed) versus Julian day, 2010-2019, with polynomial regression line and regression parameters.

COMMON EIDER

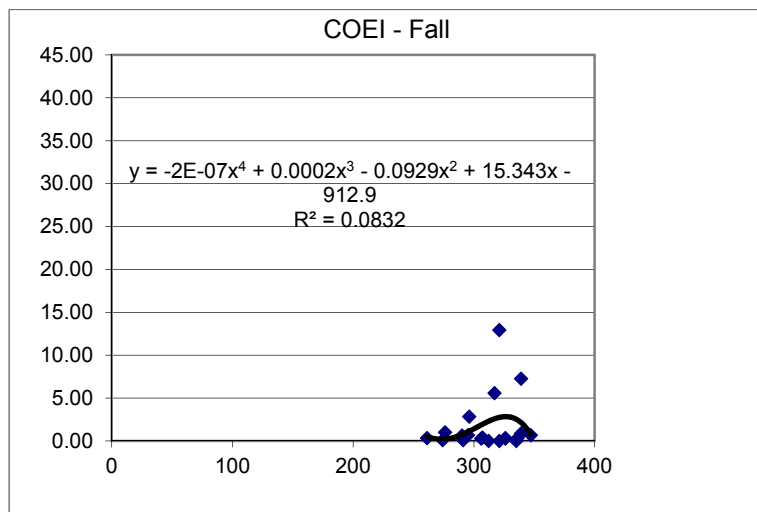
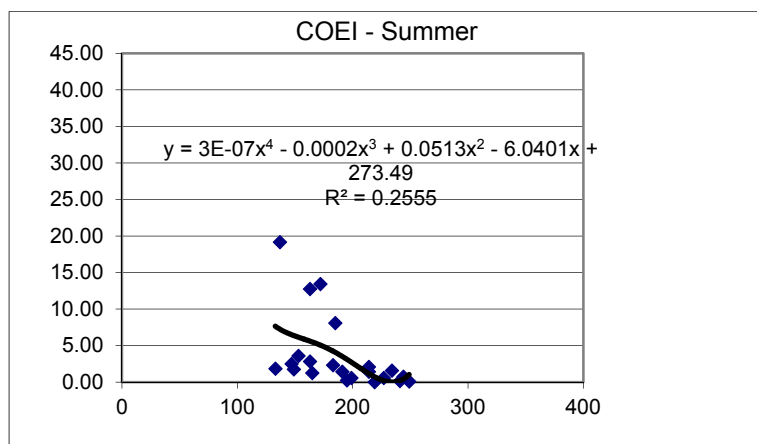
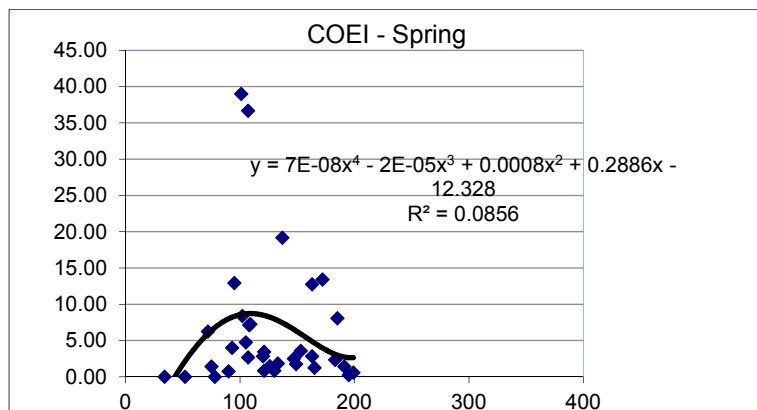


Figure C29. Abundance of Common Eider (number/30 minutes) versus Julian day, 2010-2019, with polynomial regression line and regression parameters.

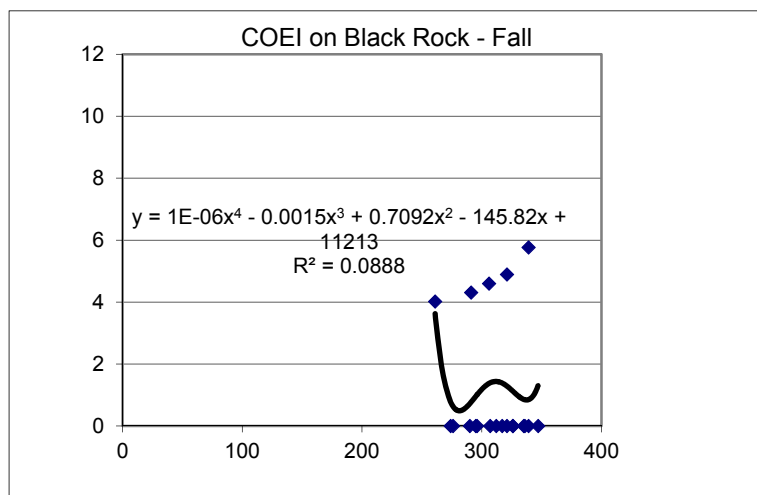
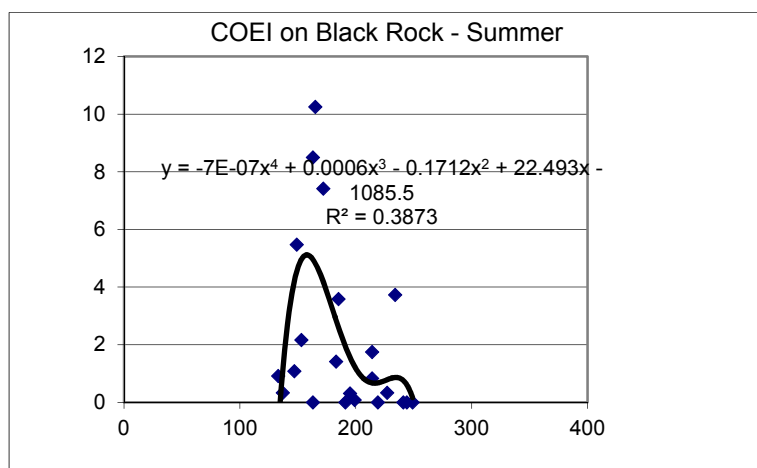
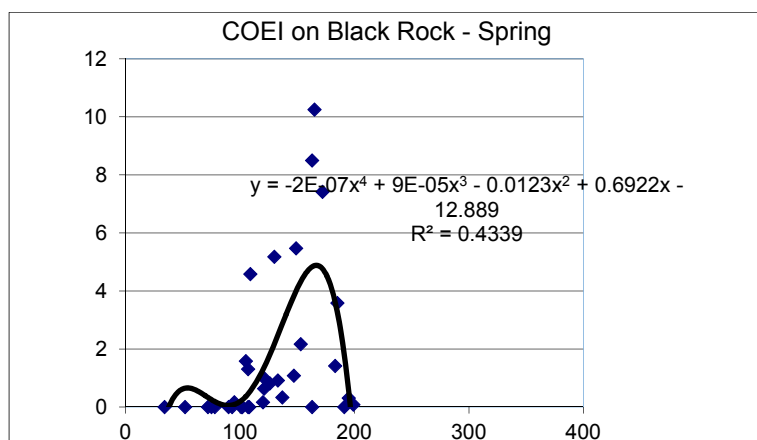


Figure C30. Abundance of Common Eider (number/30 minutes) on Black Rock versus Julian day, 2010-2019, with polynomial regression line and regression parameters.

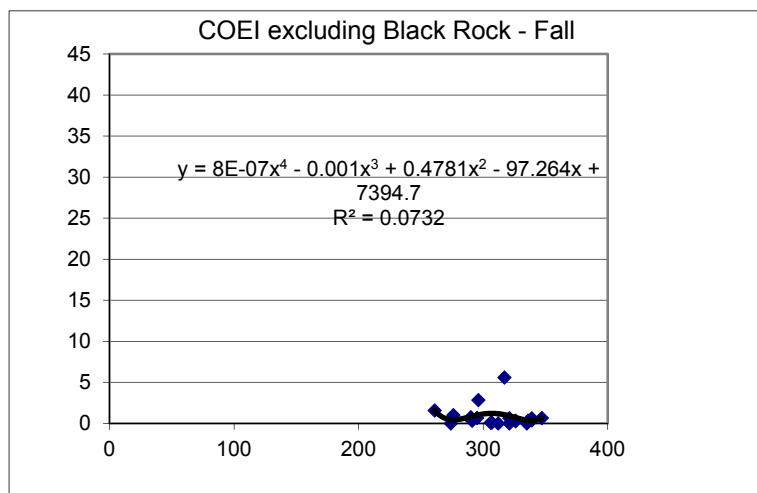
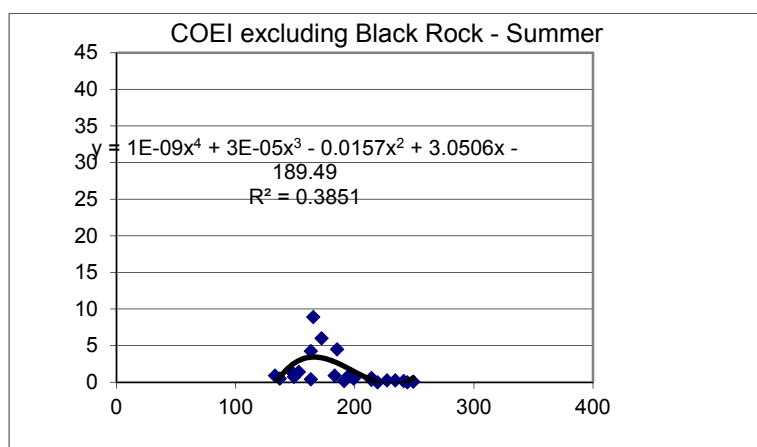
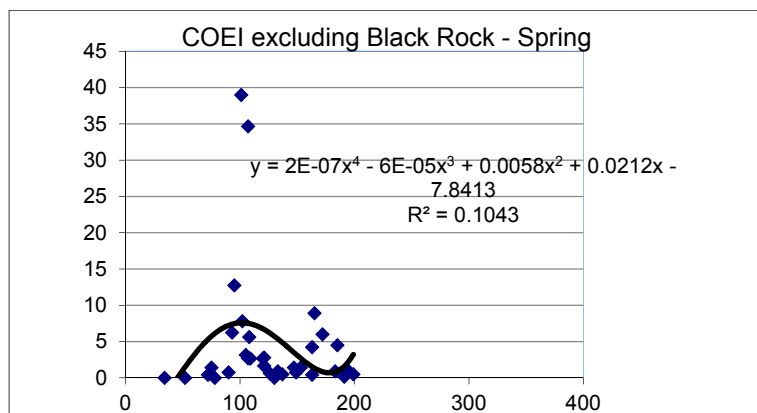


Figure C31. Abundance of Common Eider (number/30 minutes) excluding Black Rock versus Julian day, 2010-2019, with polynomial regression line and regression parameters.

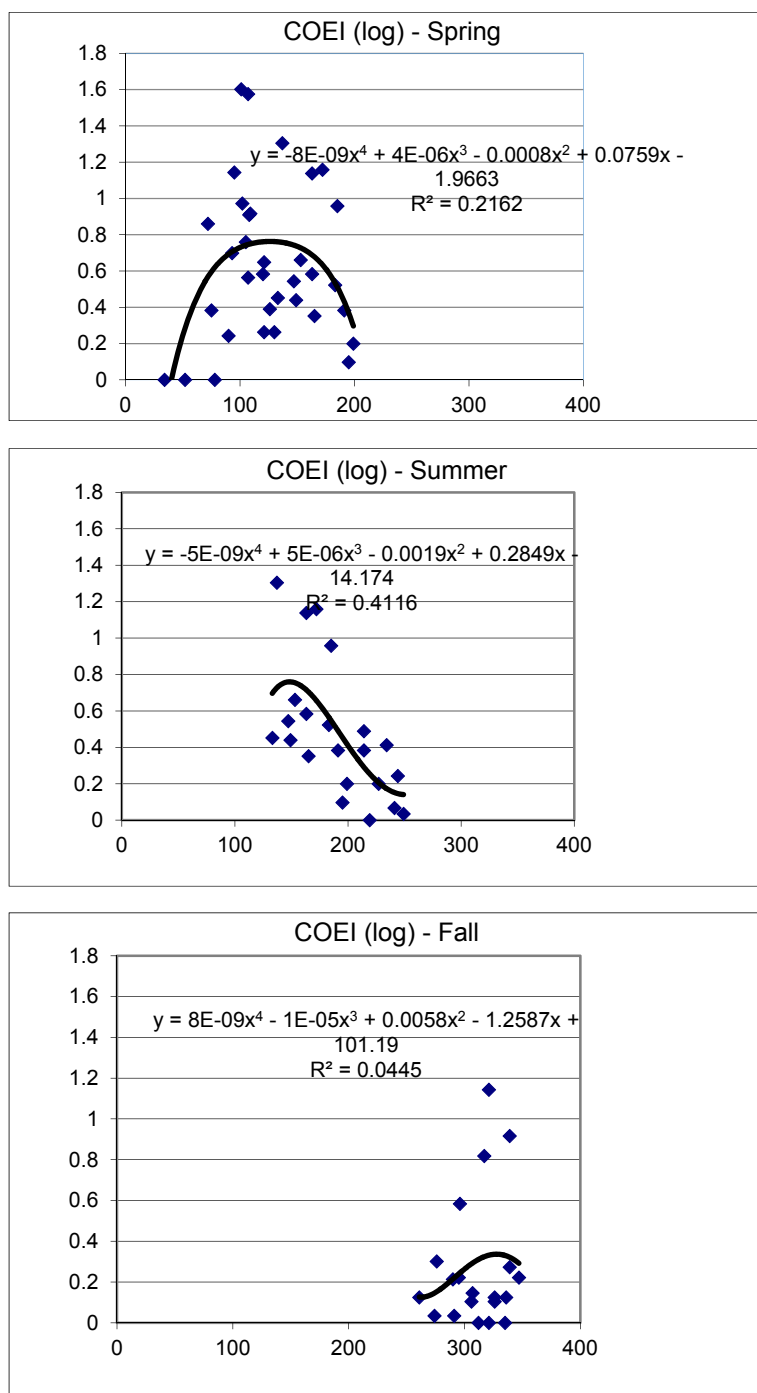


Figure C32. Abundance of Common Eider (number/30 minutes) (\log_{10} transformed) versus Julian day, 2010-2019, with polynomial regression line and regression parameters.

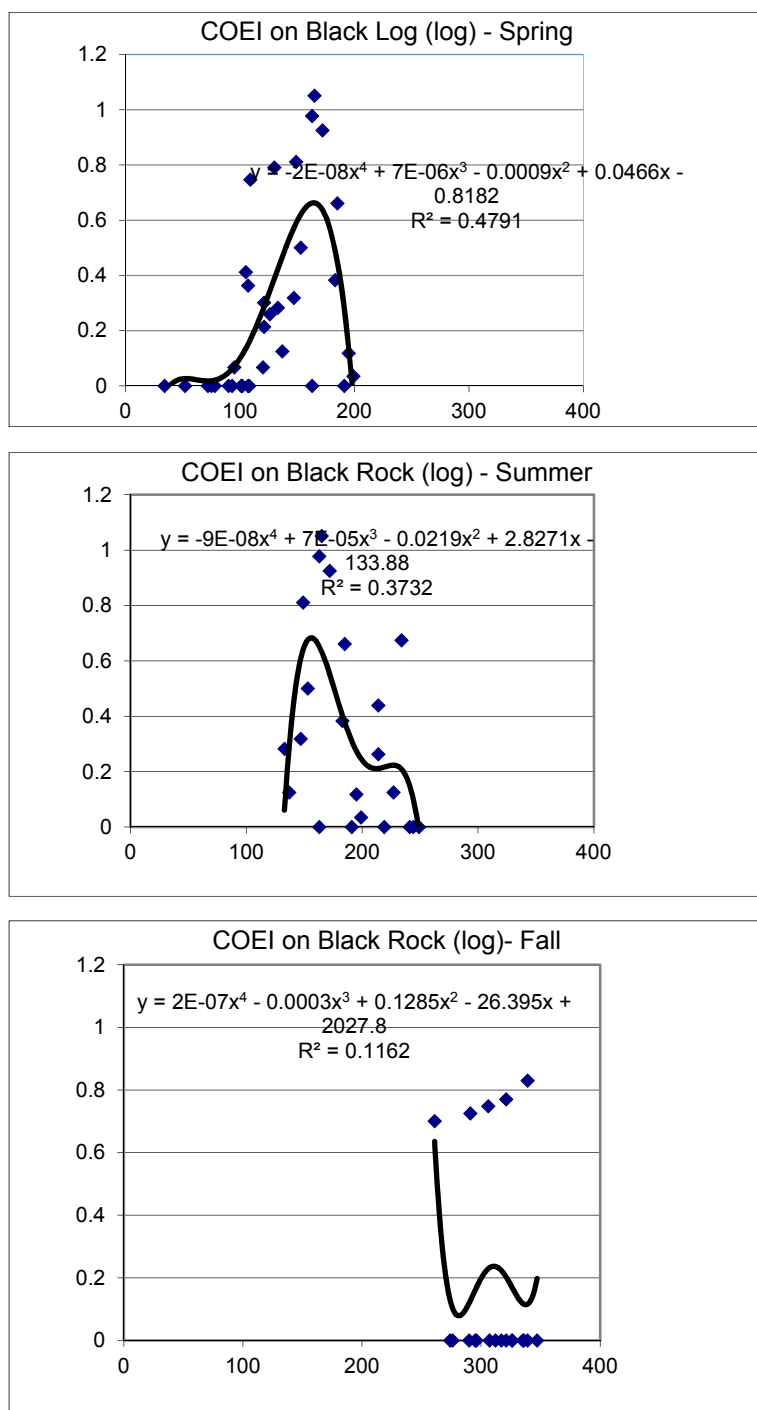


Figure C33. Abundance of Common Eider (number/30 minutes) on Black Rock (\log_{10} transformed) versus Julian day, 2010-2019, with polynomial regression line and regression parameters.

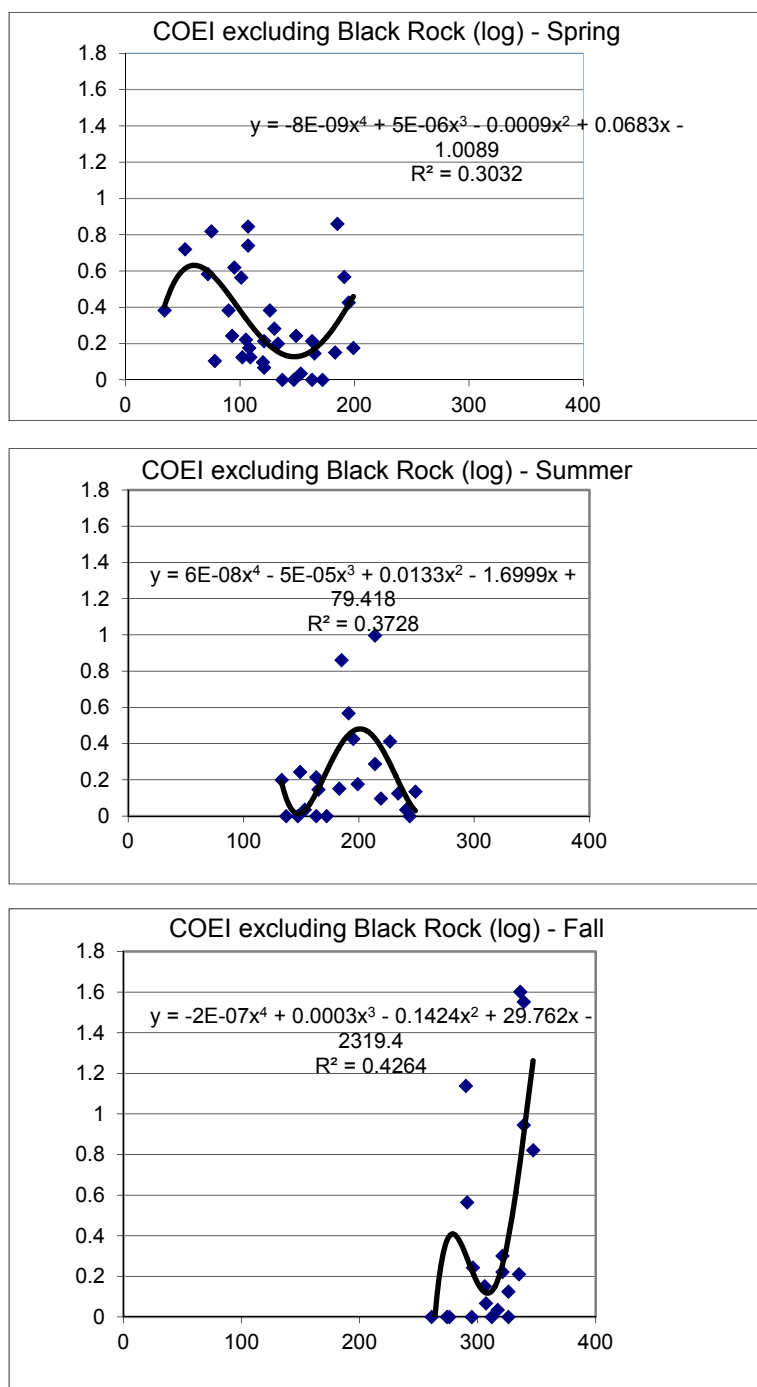


Figure C34. Abundance of Common Eider (number/30 minutes) excluding Black Rock (\log_{10} transformed) versus Julian day, 2010-2019, with polynomial regression line and regression parameters.

SCOTERS

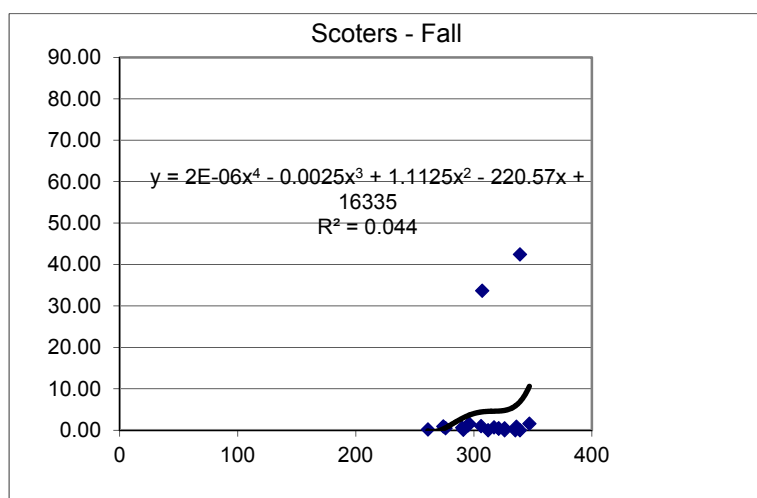
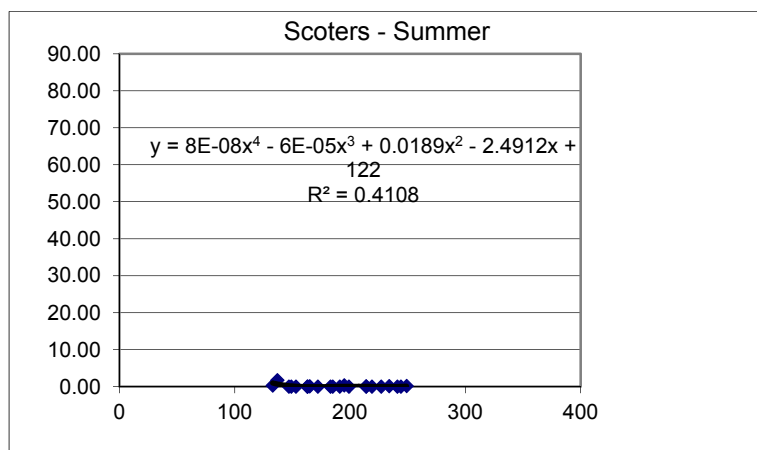
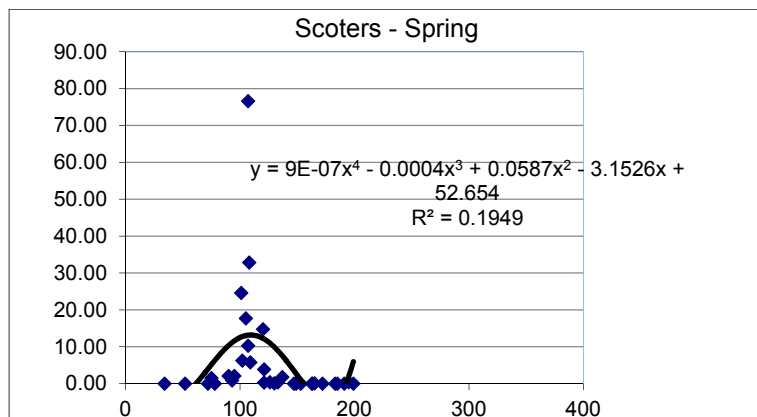


Figure C35. Abundance of scoters (number/30 minutes) (\log_{10} transformed) versus Julian day, 2010-2019, with polynomial regression line and regression parameters.

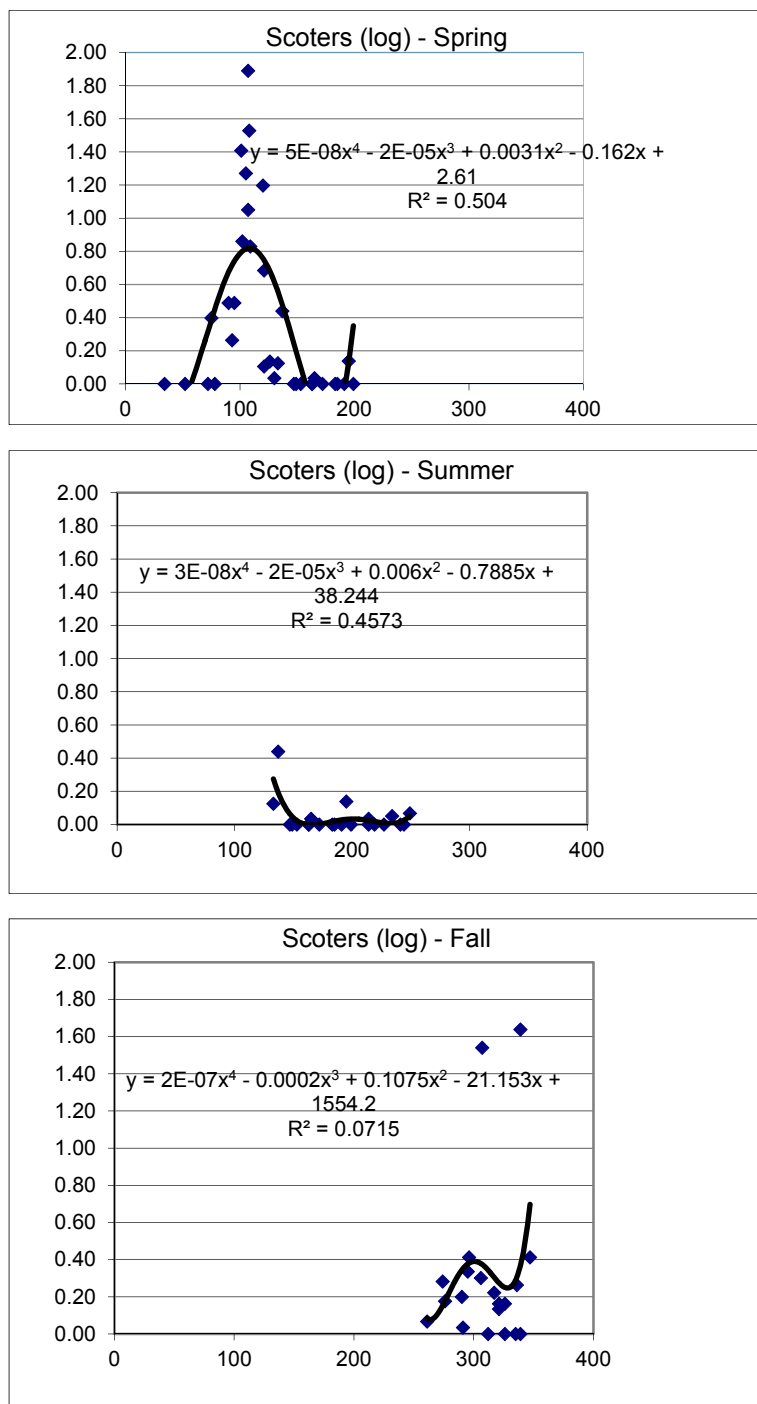


Figure C36. Abundance of scoters (number/30 minutes) (\log_{10} transformed) versus Julian day, 2010-2019, with polynomial regression line and regression parameters.

RED-THROATED LOON

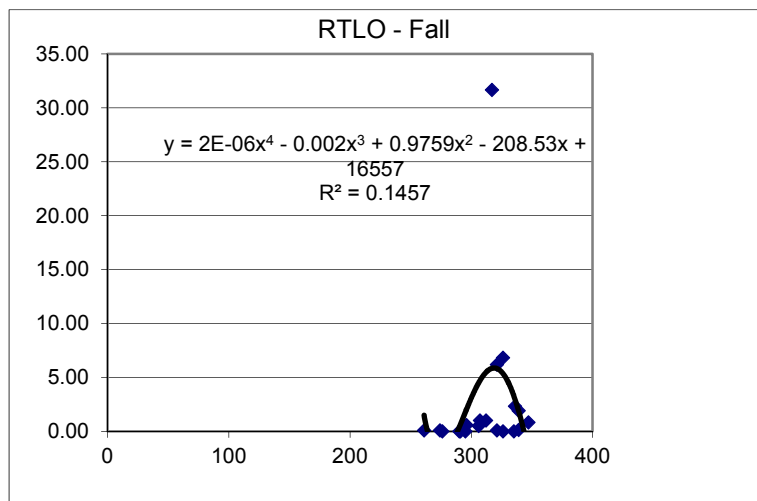
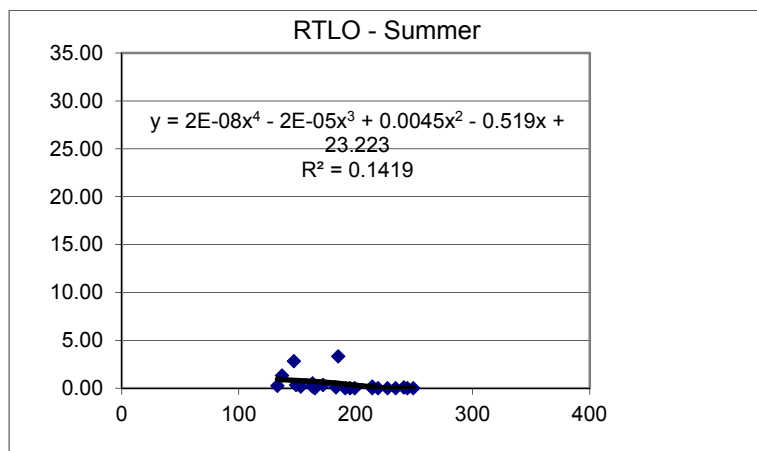
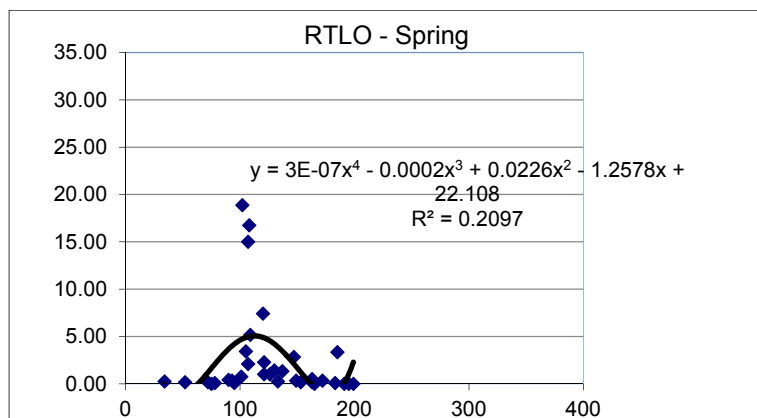


Figure C37. Abundance of Red-throated Loon (number/30 minutes) versus Julian day, 2010-2019, with polynomial regression line and regression parameters.

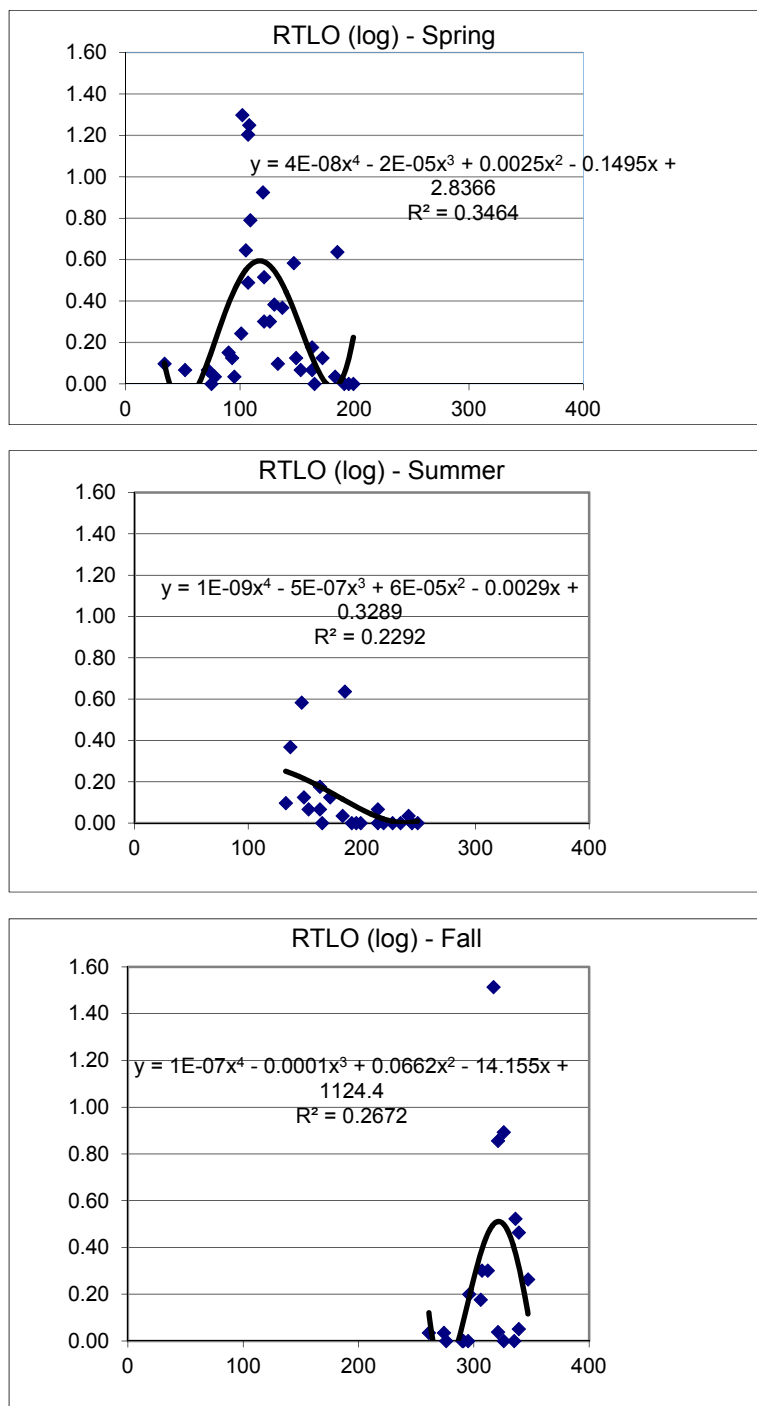


Figure C38. Abundance of Red-throated loon (number/30 minutes) (log₁₀ transformed) versus Julian day, 2010-2019, with polynomial regression line and regression parameters.

Integrating Hydroacoustic Approaches to Predict Fish Interactions with In-stream Tidal Turbines

Project number: 300-208

Start date: October 1, 2017

Reporting period: October 1, 2017 – December 31, 2019

Recipient name: Fundy Ocean Research Center for Energy (FORCE)

Project lead: Daniel J. Hasselman, FORCE Science Director

Prepared by:

Haley Viehman^{1*}, Dan Hasselman^{2£}, Tyler Boucher², Jessica Douglas², Lindsay Bennett²

¹ Echoview Software, Hobart, Tasmania

² Fundy Ocean Research Center for Energy, Halifax, NS

*Lead author: haley.viehman@echoview.com

£Corresponding author: dan.hasselman@fundyforce.ca

Submission date: December 31, 2019

Table of Contents

1. Executive Summary.....	2
2. Introduction and Objectives	3
3. Methodology.....	5
3.1. Mobile vessel surveys.....	6
3.2. Stationary platform deployments	6
3.2.1. Simrad EK80 WBAT	7
3.2.2. Nortek Signature 500 ADCP	7
3.2.3. Aanderaa SeaGuard RCM.....	8
3.3. Hydroacoustic data Processing	8
3.3.1. Data calibration.....	8
3.3.2. Noise removal	10
3.3.3. Data partitioning.....	14
3.3.4. Echo integration.....	15
3.4. Auxiliary data processing	15
3.4.1. Current speed and direction	15
3.4.2. Salinity and temperature	16
3.5. Data analysis.....	17
3.5.1 Spatial autocorrelation	17
3.5.2 Temporal autocorrelation.....	18
3.5.3 Comparison of mobile to stationary measurements.....	19
4. Results and Conclusions.....	19
4.1 Qualitative observations of acoustic datasets.....	19
4.1.1 Mobile data	19
4.1.2 Stationary data.....	23
4.2 Spatial autocorrelation	29
4.3 Temporal autocorrelation.....	32
4.4 Comparison of mobile to stationary measurements.....	35
5. Recommendations	37
Budget.....	39
Employment Summary	40
Bibliography	41
Performance measures (NR-Can)	45

1. Executive Summary

A key challenge facing the global marine renewable energy sector is the ability to effectively answer the critical question of the safety of in-stream tidal energy turbines for fish, a key component of the marine environment. Traditional fish sampling technologies, such as trawls, have limited application in high-flow environments. Novel approaches are required to provide the environmental data necessary to achieve public, regulatory, and industry confidence.

FORCE and its partners have been using hydroacoustics to collect information on fish use of the Minas Passage. Two data collection methods have been used: downward-looking, mobile surveys, and upward-looking, stationary surveys. The first method provides spatial coverage of the test site but only spans 24 hours at a time. Conversely, the upward-looking, stationary approach lacks spatial coverage but spans long periods of time (approximately 2 months). There is a need to understand the extent over which results from each survey type might be applied—that is, how much time is represented by the results from a single mobile survey, and how much space is represented by the results from the stationary surveys.

The goal of this project was to use each of these two complementary methods to inform our understanding of the results from the other. Specifically, the mobile acoustic survey data were used to provide an estimate the spatial representative range of the stationary results. The stationary data were be used to estimate the temporal representative range of the 24-hour mobile survey results. Concurrent data collected by the two methods were also compared to assess the challenges associated with each survey type, and to confirm whether both methods provide similar findings.

This assessment utilized backscatter data from repeated passes of one of the mobile transects, and from 3 of the two-month deployments of the stationary platform. The spatial representative range of the stationary results could not be determined using data from the single transect. However, the stationary dataset revealed strong tidal and diel periodicities in volume backscatter (roughly proportional to fish density) at this site, with greater variation occurring at these small time scales than over course of the year. This finding reinforces the importance of 24-hr data collection periods in ongoing monitoring efforts. Collecting at least 24 hours of data at a time allows this tidal and diel variability to be quantified and kept separate from the longer-term trends that we seek to monitor. The temporal representative range of a 24-hr survey was determined to be approximately 3 days. At the 24-hour scale, water column backscatter was comparable across the two survey types, but at shorter time scales, it was not.

Data from both survey types were subject to contamination by backscatter from entrained air in the water column—a common issue at tidal energy sites. All data had to be carefully scrutinized and cleaned, which was an extremely time-consuming process and highlights the need to develop more advanced backscatter classification tools.

2. Introduction and Objectives

The effects of in-stream tidal energy turbines on fish are of high concern to regulators, project developers, fishers, and other members of the public. While we are building our understanding of fish use of high-flow tidal areas, there is still much to be understood in terms of the biology, biophysical linkages, and the methods we are developing to study them. In Nova Scotia, this uncertainty has led to added monitoring requirements at the FORCE tidal test site, but there are limited existing best practices for predicting or detecting in-stream tidal turbine effects on fish and no standard approaches to environmental monitoring.

For an in-stream tidal turbine to affect fish, fish must interact with the device itself or with some part of its physical ‘footprint’ (e.g., electromagnetic fields, altered hydrodynamics, or acoustic output [1]). To assess the potential for an interaction with any of these components, spatial and temporal patterns in fish distribution in the area where turbine(s) are operating must be understood [2-9]. Though we are building our knowledge of fish use of very fast tidal environments, much remains to be known. In the upper Bay of Fundy, the turnover of species in Minas Channel and Minas Basin is relatively well understood based on studies at weirs and dams in these areas [10,11]. Fish must pass through the Minas Passage to enter or exit the Basin, but information on the presence and distribution of fish within Minas Passage itself is sparse. Data gathered to date indicate that fish presence in the Channel or the Basin does not necessarily reflect that of the Passage [12]. Moreover, fish behavior within the fast currents of the Passage has been found to differ from what is typically expected: Atlantic sturgeon (*Acipenser oxyrinchus*), a demersal species, were found to traverse the Passage pelagically [3], and Bay of Fundy striped bass (*Morone saxatilis*), previously thought to overwinter in fresh water, were found overwintering within the Passage [2]. Predicting the effects of tidal power development within the Passage – and effectively detecting any – requires a much more thorough understanding of where and when fish are within Minas Passage.

Sampling fish at tidal energy sites is a challenge, as traditional fish sampling techniques (e.g., trawls) are not workable in the fast currents and high turbulence. Hydroacoustics has been identified as one of the more suitable tools for monitoring fish with the necessary resolution and coverage (spatial and temporal) to understand their movements in these dynamic areas [4]. Hydroacoustics refers to sonar technology specialized for observing and monitoring underwater organisms [13,14], and can be used to continuously monitor organisms throughout the water column [4]. This technology has already proven useful for studying fish distribution at tidal energy sites, in a wide range of hydroacoustic survey strategies, e.g. mobile [15-21] or stationary [5,6] vessel-based surveys, and stationary surveys from autonomous [12,16,17,22-25] or shore-connected [26] seabed platforms. Mobile surveys cover large amounts of space, which is essential for understanding how fish and other animals use tidal passages and how likely they may be to encounter in-stream tidal turbines; however, these surveys typically occur over a shorter time period (e.g., one day at a time). In contrast, stationary surveys collect data at one point in space and typically run for a longer period of time (e.g., one month or more), which provides high-resolution records of

how fish presence and vertical distribution at a site vary over short and long time scales [12,22,25-28].

FORCE has been monitoring fish presence and distribution at the test site in Minas Passage using two different hydroacoustic approaches. One is a vessel-based mobile survey, which utilizes a down-facing echosounder to sample fish densities across the test site area [15]. The other is a platform-based, stationary survey, which deploys an echosounder on a bottom-mounted platform for long periods of time [12]. The mobile surveys are meant to track the long-term trends in fish density at the test site, and provide the opportunity to map the spatial distribution of fish in relation to potential locations of turbines. However, these surveys span only 24 hours at a time. The stationary surveys, on the other hand, deploy an autonomous platform on the seafloor to collect acoustic data for up to 2 months at a time, sampling every half hour. These surveys have very good temporal coverage, but only acquire data at one location. Given our limited understanding of fish spatial and temporal distribution at this site, it is unknown how representative the results from either survey are—that is, how much space is represented by readings from the stationary platform, located at one location, and how much time is represented by the short-term measurements from the vessel? A study examining spatially and temporally indexed data in Puget Sound, Washington defined this concept of “representative range” in space and time [16]. That study outlined several approaches to estimating these based on the point at which samples in each dataset cease to remain correlated with themselves. We sought to follow a similar line of investigation at the FORCE site, using spatial and temporal correlation metrics to understand the potential reach of each survey method. The specific questions we sought to answer were,

1. What is the spatial representative range of hydroacoustic data collected at one location in the FORCE test site?
2. What is the temporal representative range of hydroacoustic data collected over a short period of time at the FORCE test site?
3. Are concurrent results from the mobile and stationary datasets comparable to each other, and how did challenges differ across methods?

Integrating these two approaches to answer these questions will allow for a better understanding of fish use of the site, which will inform probability of encounter models in future [19]. The information gained through this integrated approach and evaluation of the strengths and weaknesses of each survey method will additionally inform recommendations of best practices for monitoring turbine effects.

3. Methodology

Hydroacoustic surveys of the FORCE site have been ongoing since 2016. This project utilized data collected by two main survey methods from December 2017 to November 2018, during which time several of the 24-hr mobile surveys overlapped with the long-term stationary data collection from the bottom-mounted platform (Table 1).

Table 1. Summary of overlapping stationary platform deployments and mobile vessel-based surveys.

Platform deployments (stationary)			Vessel surveys (mobile)	
Start date	End date	Location	Start date	End date
14 Dec 2017	22 Feb 2018	45°21'46.8" N 64°25'39.7" W	15 Feb 2018	16 Feb 2018
30 Mar 2018	23 May 2018	45°21'47.3" N 64°25'38.9" W	10 Apr 2018	11 Apr 2018
			08 May 2018	09 May 2018
15 Sep 2018	13 Dec 2018 (Data collected until 19 Nov 2018)	45°21'47.5" N 64°25'39.9" W	20 Sep 2018	21 Sep 2018
			21 Oct 2018	22 Oct 2018

Mobile vessel surveys were carried out as described in [15]. The stationary platform was deployed in the same area, close to transect 4 of the mobile surveys (Figure 1). For this reason, data from transect 4 were used in these analyses.

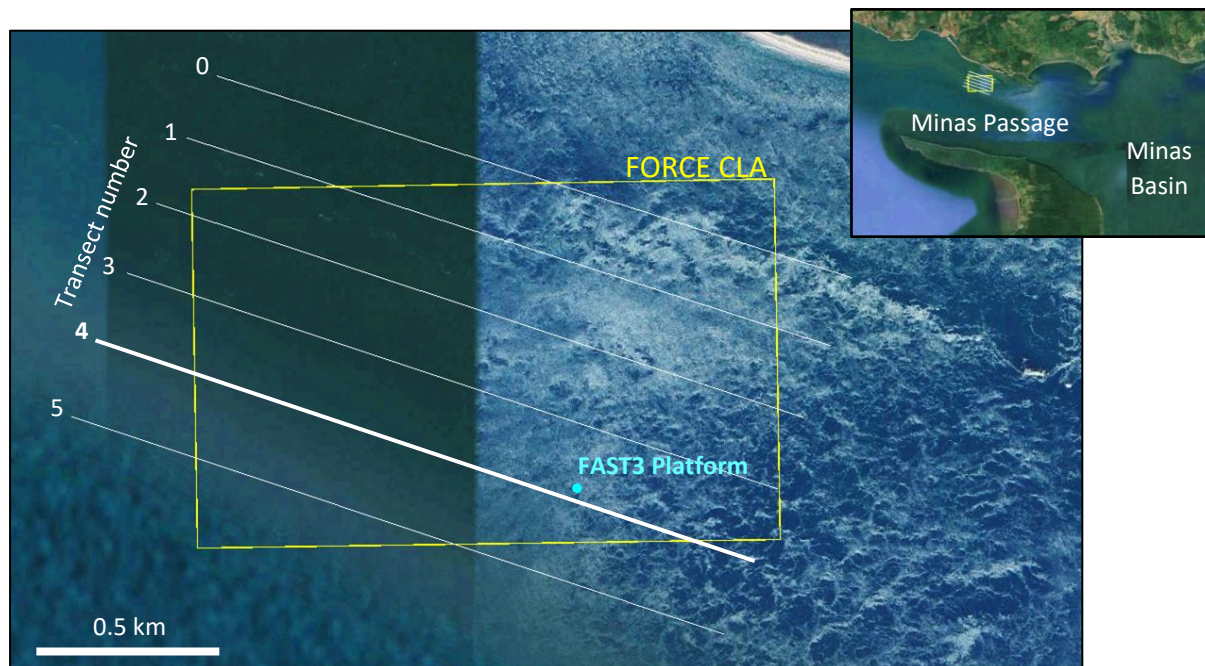


Figure 1. Stationary and mobile hydroacoustic survey locations at the FORCE crown lease area (CLA) in Minas Passage.

3.1. Mobile vessel surveys

The details relevant to this project are reviewed here, but full details may be found in the [15].

Transects were carried out aligned as closely as possible with the lines shown in Figure 1, which formed the northern grid of the survey. The vessel would sample this grid and another on the southern side of the passage once during each tidal stage, resulting in sampling each stage (ebb and flood) at each grid once during the day and once during the night. Each transect was repeated twice, with the vessel travelling with the current in one pass and against the current in the other.

Only data from transect 4 were used in this assessment, as this transect was closest to the FAST3 stationary platform (~40 m closest distance). All surveys were carried out on the neap tide in order to reduce variability related to the lunar cycle, as well as to reduce the detrimental effect of current speed on data quality.

The vessel was equipped with a Simrad EK80 WBT echosounder, with a 7° circular split-beam transducer mounted on a pole over the side and oriented downward. This echosounder pinged 2 times per second, at a frequency of 120 kHz (narrowband, “CW mode”) with a pulse duration of 1.024 ms and power output of 250 W.

Calibrations were carried out before each survey by suspending a 23 mm copper calibration sphere on monofilament line at least 2 m below the transducer face [29]. This was carried out at high tide while the vessel was dockside, prior to each survey [15].

3.2. Stationary platform deployments

This project utilised the Fundy Advanced Sensor Technology platform, FAST3 (Figure 2). This platform was equipped with two echosounders: a Simrad EK80 Wideband Autonomous Transceiver (WBAT), and an ASL Environmental Sciences Acoustic Zooplankton Fish Profiler (AZFP). The platform also included a Nortek Signature 500 ADCP and an Aanderaa SeaGuard Recording Current Meter (RCM). The WBAT, AZFP, and Signature 500 were operated in alternating intervals to avoid acoustic contamination across instruments. This project used acoustic data from the Simrad WBAT, and “auxiliary” data from the Signature 500 and RCM, as described in more detail below.



Figure 2. FAST3 platform prior to deployment at the FORCE test site. (a) ASL AZFP transducer; (b) Aanderaa SeaGuard RCM; (c) Nortek Signature 500; (d) Simrad EK80 WBAT transducer.

3.2.1. Simrad EK80 WBAT

The Simrad EK80 WBAT transducer was mounted to the platform with its face at 0.7 m height, facing upward. The transducer had a circular beam with a half-power beam angle of 7° . It operated at 120 kHz (narrowband, CW mode), with a nominal pulse duration of 0.128 ms, a ping rate of 1 Hz, and a power output of 125 W. The data collection range was limited to 60 m to reduce the required storage capacity and allow longer deployments. Data were collected for 1 minute in passive mode and 5 minutes in active mode every half-hour for the duration of each platform deployment. Passive data were collected to monitor system noise during the deployment, but were not used in the analyses presented here.

Calibration data were collected with the WBAT between deployments, on 6 March 2018 and 13 July 2018. These data were collected *ex situ* at the Dominion Diving wharf in Dartmouth, Nova Scotia, due to difficulty in positioning the sphere within the beam at the deployment location, where the water is constantly moving. Readings were obtained of a standard 23 mm copper calibration sphere was suspended at least 2 m below the transducer face [29]. Data were collected with the same settings used during deployments, and salinity and temperature during calibration were measured separately. Calibration data processing is described in section 3.3.1.

3.2.2. Nortek Signature 500 ADCP

The Nortek Signature 500 ADCP was mounted to the platform, facing upward, similarly to the WBAT transducer. This instrument sampled the water column for a 5 min period of time, every 15 minutes in the Dec 2017-Feb 2018 and Mar-May 2018 deployment, and every 30 minutes in the Sep-Nov 2018 deployment. The sample rate during each burst was 4 per second in Dec-Feb and Sep-Nov deployments, and 2 per second in the Mar-May deployment.

3.2.3. Aanderaa SeaGuard RCM

The Aanderaa SeaGuard RCM measured conductivity, temperature, turbidity, pressure, current speed, and current direction at the platform each half hour for all deployments except September 2018, when the instrument was not operational.

3.3. Hydroacoustic data Processing

Acoustic data collected at tidal energy sites require a large amount of processing prior to analysis. This is mainly due to the large quantities of air entrained into the upper water column by current-, wind-, and wave-induced turbulence, sometimes extending to the sea floor at this site. Data processing was carried out in Echoview® software (10.0, Myriax, Hobart, Australia), and consisted of calibration, noise removal, data partitioning, and echo integration.

Volume backscatter (S_V) data were used in these analyses. S_V is the total sound energy backscattered at a given range and normalized to a unit volume of water, and has units of dB re 1 m²m⁻³. S_V can be used as a rough index of fish density (though note that this is confounded by the different scattering properties of individual fish related to species, size, and orientation relative to the transducer) [13, 30].

3.3.1. Data calibration

Calibration parameters obtained from in- and ex-situ calibration data collection methods (sections 3.1 and 3.2.1) were applied to the data. These parameters included direct backscatter corrections (gain and S_a correction), as well as corrections for the environmental conditions experienced by the echosounder during data collection (e.g., temperature and salinity, which determined absorption coefficient, sound speed, and the corresponding adjustments to equivalent beam angle) [29].

For the mobile surveys, surface water temperature was measured from the vessel during each transect, and salinity was measured several times throughout the day via refractometer. The average temperature recorded for transect 4, and the average salinity for each survey, were used to calibrate the data used here (Table 2, Figure 3).

Measurements from the stationary platform revealed tidal variation in sound speed, meaning using a daily average sound speed could introduce error to acoustic backscatter values. However, this potential error was quite low (see below), and unlikely to affect the analyses presented here.

Table 2. Summary of environmental parameters during each mobile vessel survey. Sound speed was calculated using equations in references indicated.

Start date	End date	Temperature (°C)	Salinity (ppt)	Sound speed (m·s ⁻¹)
15 Feb 2018	16 Feb 2018	0	36	1451.5 [31]
10 Apr 2018	11 Apr 2018	2.7	36	1463.1 [32]
08 May 2018	09 May 2018	6.3	35	1476.7 [32]
20 Sep 2018	21 Sep 2018	15	33	1505.1 [32]
21 Oct 2018	22 Oct 2018	11.5	35	1495.9 [32]

The stationary datasets spanned approximately 2 months each and experienced a far greater range of environmental condition than each 24-hour mobile survey. The stationary

dataset therefore required a different approach to determining environmental parameters for calibration. Sound speed could change by as much as $36 \text{ m}\cdot\text{s}^{-1}$ from the start of a deployment to the end (Figure 3; see section 3.4.2 for calculations). As sound speed is used in the calculation of backscatter values, one value could not be used for an entire deployment. Sound speed could vary by as much as $\pm 4.5 \text{ m}\cdot\text{s}^{-1}$ over the course of a tidal cycle due to changes in temperature (primarily) and salinity, which correlates to approximately $\pm 2.5\%$ error in volume backscatter. To keep backscatter error within the bounds of this tidal variation, the stationary acoustic datasets were split whenever the cumulative change in the 12-hr average sound speed exceeded $4.5 \text{ m}\cdot\text{s}^{-1}$ (Figure 3). The average temperature, salinity, sound speed, and absorption coefficient were calculated for and applied to each of these data subsets, and used to correct the equivalent beam angle from its factory value [29].

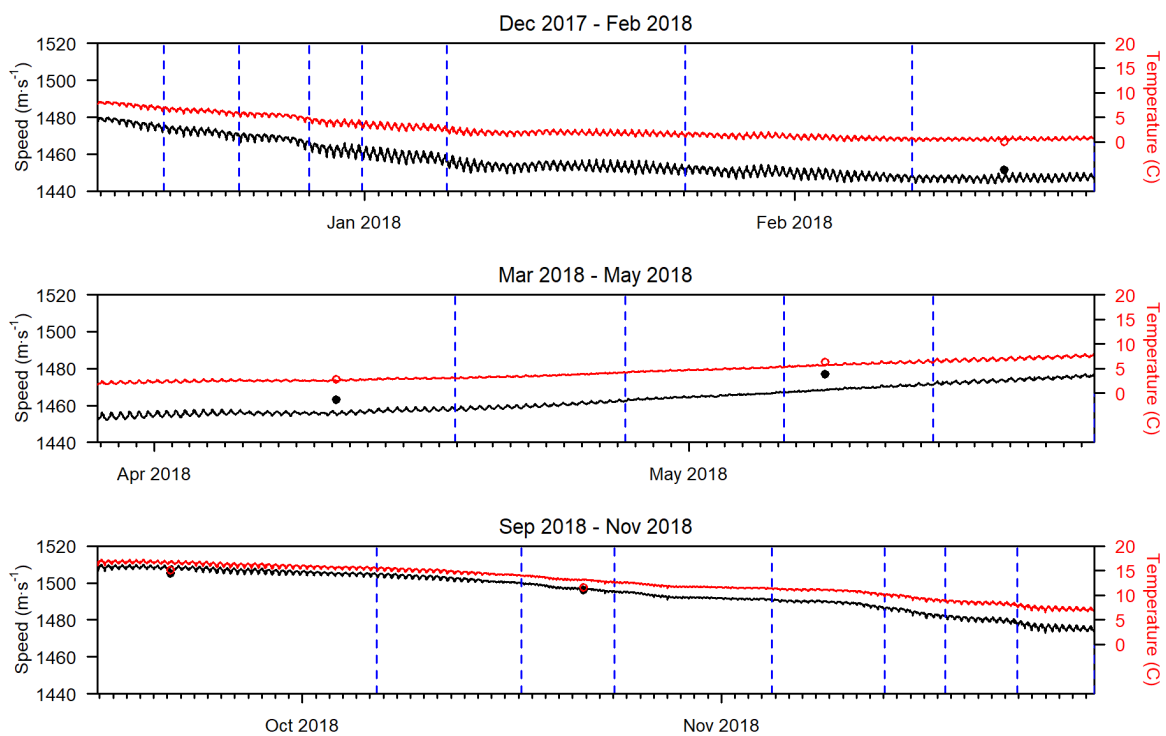


Figure 3. Sound speed and temperature used to calibrate stationary (lines) and mobile (points) acoustic data. Black indicates sound speed and red indicates temperature. Vertical dashed lines indicate calibration subsets of the stationary datasets.

The vessel-based measurements of salinity and temperature differed slightly from the simultaneous platform measurements (Figure 3), and therefore sound speed values were somewhat different for the mobile and stationary datasets, particularly for the April and May mobile surveys. This difference could be related to the different instruments and conversion factors in use, or potentially to differences in surface- and bottom-water parameters (though the water column is generally well-mixed). Direct comparisons of measurements of the same volume of water by each instrument would be helpful in determining the source of this difference in future.

The other necessary Simrad calibration parameters, gain and S_a correction, were calculated for each dataset using Echoview software, measurements of the standard calibration sphere (collected as described in section 3.2.1), and equations from [29].

3.3.2. Noise removal

Once data were calibrated, a minimum S_V threshold of -70 dB re $1 \text{ m}^2 \text{ m}^{-3}$ was applied in both the mobile and stationary datasets. This threshold removed backscatter from weak acoustic targets, more likely to be from non-fish targets (e.g. zooplankton, debris, sediment, and low-amplitude “background” noise). Any remaining unwanted backscatter was then identified and removed. This unwanted backscatter included backscatter from within $2x$ the transducer’s nearfield (calculated to be 1.4 m) [14,29], the bottom (down-looking data collection) or surface (up-looking data collection), several types of distinct water column artefacts, and what we are describing as “transient noise,” similar in appearance to that described in [33]. More detail on each type of noise and how it was removed is provided below.

3.3.2.1 Surface and bottom

Echoview’s bottom detection algorithm was used in both datasets to detect the surface (stationary, up-looking dataset) or bottom (mobile, down-looking dataset). The algorithm parameters were optimized by eye, and any necessary corrections were applied manually.

3.3.2.2 Entrained air

A threshold offset line was used to delineate the lower limit of the entrained air extending downward from the surface in each dataset (Figure 4). Prior to line detection, the data were blurred somewhat with a $13 \text{ sample} \times 13 \text{ ping}$ convolution, which enhanced the entrained air backscatter and made the threshold detection line more effective at removing air backscatter near the edges of the plumes. The entrained air line was then manually edited to ensure it removed as much backscatter from entrained air, and as little backscatter likely to be from fish, as possible.

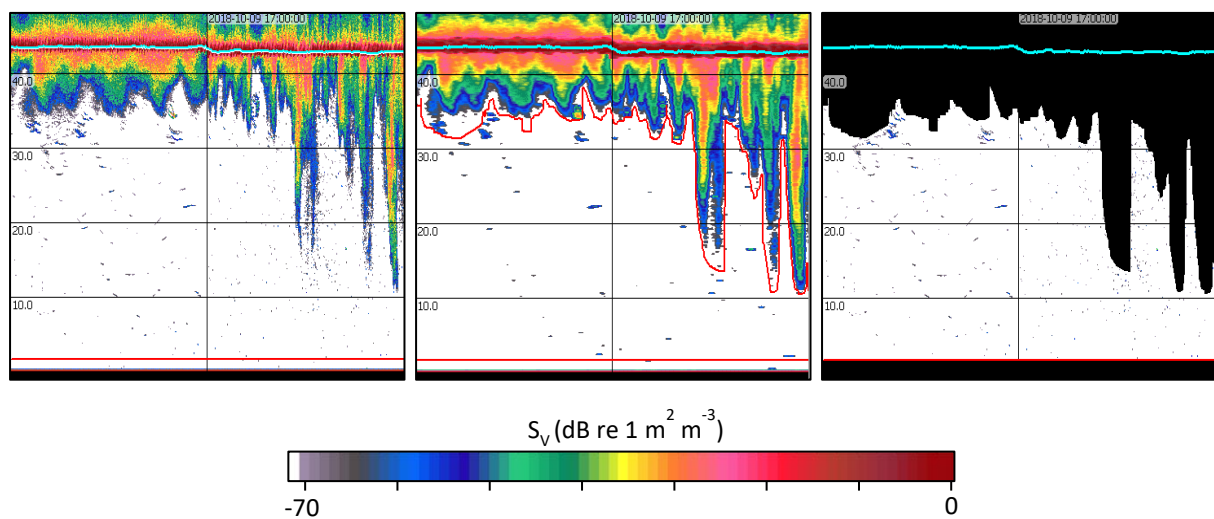


Figure 4. Detection and removal of entrained air from S_V data from the stationary dataset. Left: original S_V data, showing the nearfield (flat red line) and detected surface (thick cyan line). Middle: 13×13 convolution filter of original data, with threshold offset line delineating the entrained air (upper red line). Right: original S_V data with entrained air, nearfield, and surface backscatter removed.

3.3.2.3 Distinct water column artefacts

Several visually distinct acoustic signals, unlikely to be from fish, were present in the data and had to be manually removed. These were:

- a) *Interference from other acoustic instruments.* This noise typically appeared as individual contaminated pings, or a few in a row, and most often was likely due to a vessel passing nearby (Figure 5). It occurred rarely and was removed manually by defining bad data (no data) regions.

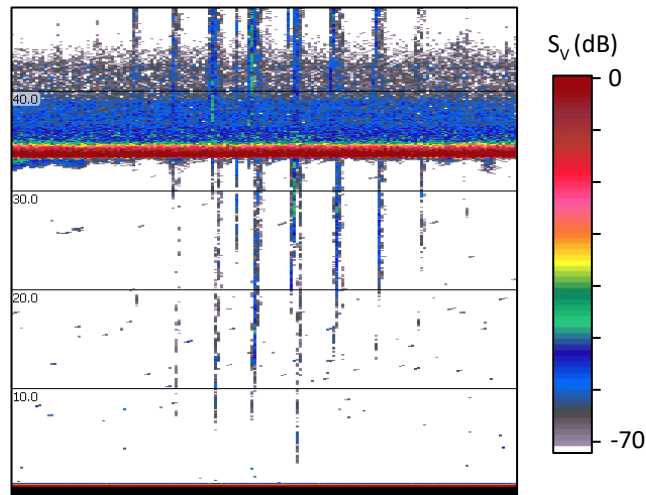


Figure 5. Example of acoustic interference from vessel echosounder in stationary dataset.

- b) *Very strong backscatter.* In the stationary dataset, every so often, backscatter from just one or two targets in an analysis cell would be much stronger than all other backscatter. The backscatter from these targets strongly skewed the average S_v reported for the cell, causing it to no longer be representative the majority of the 5-min interval. These samples were identified and inspected, and if determined unlikely to be from individual fish or fish aggregations, they were removed from analysis with a bad data (no data) region (Figure 6).

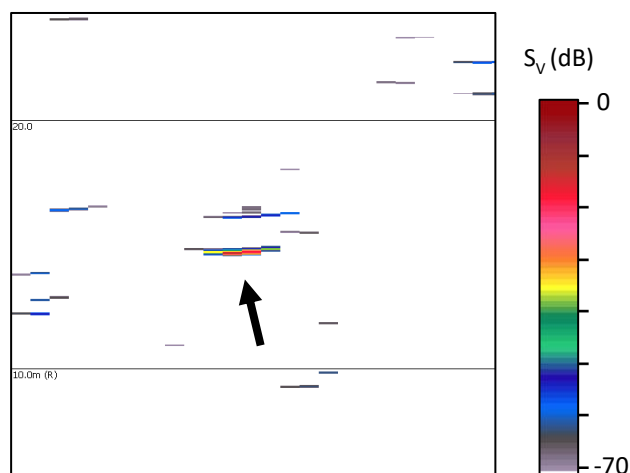


Figure 6. Example of “very strong backscatter” in stationary S_v data. This target had a target strength of -18 dB re 1 m^2 , and raised the mean S_v of the 5-min sampling period by 13 dB.

Some of these strong samples appeared to be from an object moving through the beam (i.e., could be tracked across consecutive pings). Others were more difficult to identify, particularly at high current speeds, when any object moving with the current would likely only be detected in just one or two pings, and therefore could appear similar to interference from acoustic instruments.

The target strengths of these artefacts was in the area of -20 dB re 1 m^2 or more. This could be expected from marine mammals passing through the beam [34]. Large fish, such as striped bass, are another possibility, though according to the dorsal-aspect TS-length relationships found in the literature, -20 dB could correspond to a 2 m striped bass [35], whereas most striped bass tagged in the Minas Passage area have been under 1 m in length [2,9,10]. There is not much information available on the ventral TS of these organisms, but it is possible that it differs from the dorsal aspect [14].

Removing these targets meant the remaining backscatter was more representative of the majority of targets present. However, in future, other data may help determine what these targets are and if their presence is of interest (e.g. concurrent acoustic recordings of marine mammals, or detections of acoustically tagged fish by receivers).

- c) *Cascading water column backscatter.* A very distinct phenomenon was visible nearly every slack tide, and was decided to be more likely related to physical processes than biological ones. This was in the form of a cloud of backscatter, often of a similar strength as fish-like targets, appearing to either rise or sink through the water column (Figure 7). This noise was in all stationary datasets but was much more prevalent during the Dec 2017-Feb 2018 dataset. It was not seen in the passes of transect 4 from the mobile dataset that were analyzed here, possibly because transects were not carried out near slack tide. The source of this backscatter is unknown but may be related to, for example, air or sediment entrained into the water column upstream of the echosounder. Data segments that were contaminated by this noise needed to be manually identified and removed using bad data (no data) regions.

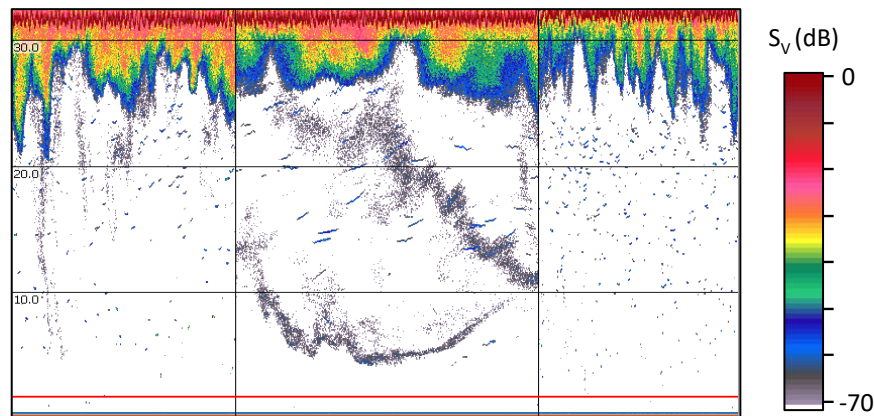


Figure 7. Example of “cascading” water column backscatter in S_v data from the stationary dataset, in this case occurring after a high slack tide.

3.3.2.3 “Transient” noise

In all stationary datasets, but not in the mobile dataset, there was a periodic increase in above-threshold backscatter spread throughout the water column (Figure 8). The source of this backscatter is unknown, though it was sometimes correlated with high current speed and/or entrained air depth. It did not appear biological in nature, given its even distribution throughout the water column. This noise tended to span two or three sequential 5-minute recording periods at each appearance. Affected cells were identified manually and omitted from the dataset.

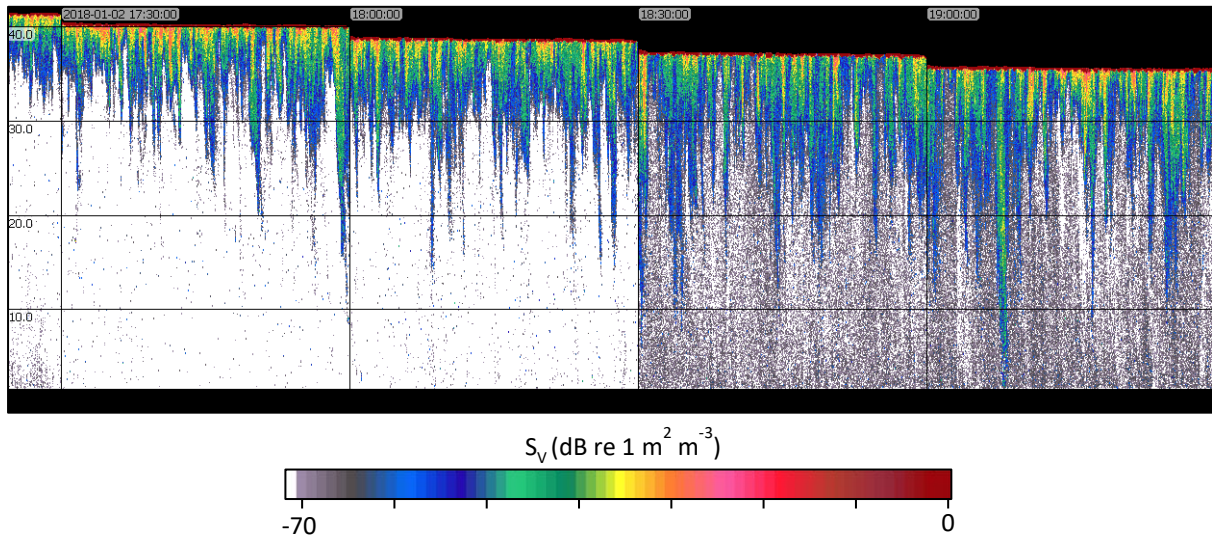


Figure 8. Example of “transient” noise in S_v data from the stationary dataset, visible in the two recording periods at the right.

Each tidal stage had a unique transient noise “profile.” Slack tides were generally unaffected by transient noise. Ebb and flood tides were both more contaminated, but in different ways. During flood tides, entrained air depth and current speed were highly correlated with transient noise once current speed exceeded $2 \text{ m}\cdot\text{s}^{-1}$. During ebb tide, there was little correlation of entrained air depth or transient noise occurrence with current speed. It is possible that the interaction of current speed and direction with local bathymetry caused these differences. During ebb tide, current speed is noticeably more variable than flood tide, and direction more variable at speeds over $1 \text{ m}\cdot\text{s}^{-1}$ (Figure 9). This likely reflects the fact that many more eddies form and pass through the platform’s location during the ebb tide, whereas the flow is less modified during the flood tide (see section 3.4.1 for more information on ADCP data processing).

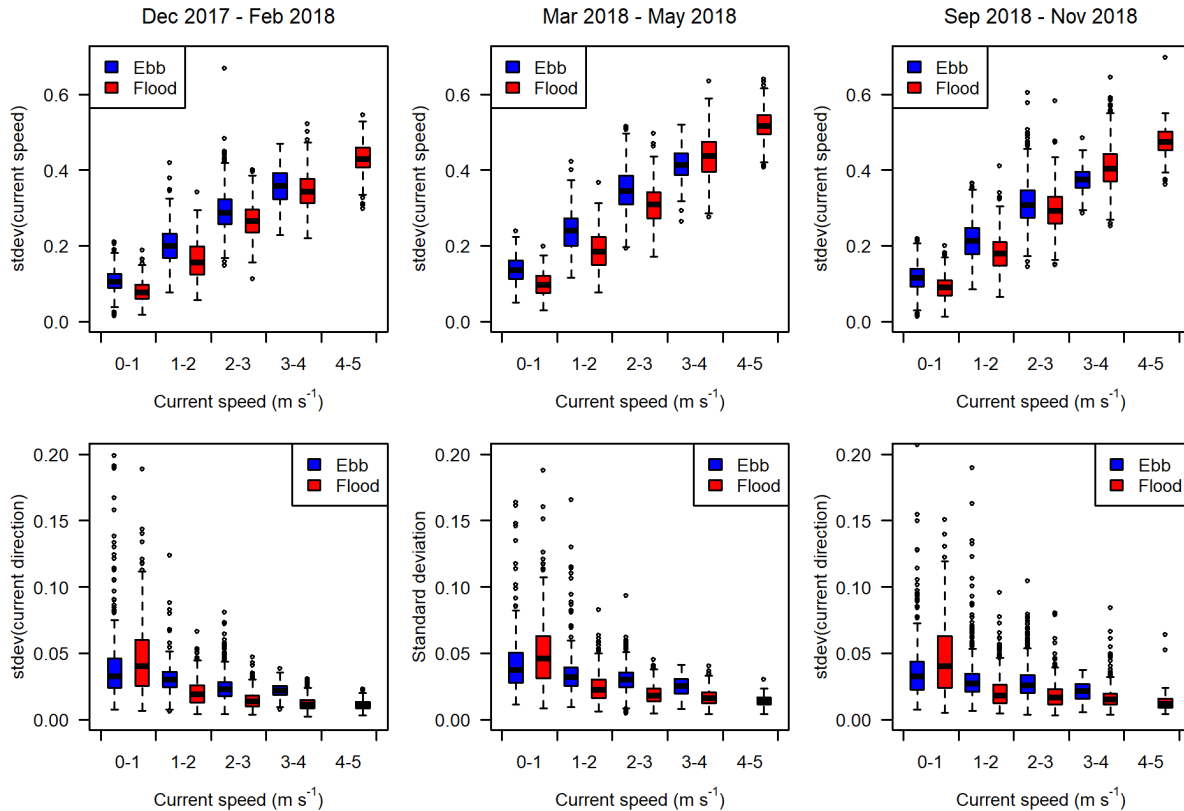


Figure 9. Standard deviation in current speed (top) and direction (bottom) for each stationary dataset, grouped by tide and speed range. Current speed and direction data were collected by the ADCP on the stationary platform and averaged for the water column. The horizontal black line is the median value, boxes span the interquartile range, whiskers extend to 1.5x the interquartile range, and points are the data falling outside of the range of the whiskers. This applies to all following boxplots.

3.3.3. Data partitioning

Once cleaned, the data were partitioned into bins with sizes chosen for the different analyses carried out, which differed by dataset.

3.3.3.1. Mobile acoustic data

Data from each pass of transect 4 were first split into equal-length distance bins that spanned the entire vertical water column. These bins measured 10 m along-track, which ensured high spatial resolution along the transect (average transect length of 1.9 km meant approximately 190 bins obtained per transect), and that every distance bin contained at least one ping (7 pings per bin on average, varying with vessel speed over ground). The echo integration results from each bin were exported from Echoview to determine the distance at which water column S_v became independent (see section 3.5.1).

The data were to then be partitioned by this distance to ensure independent samples were used in further analyses, including comparison to measurements from the stationary platform. However, it was found that water column mean S_v was already independent at the 10 m scale (details in section 3.5), so the distance bin was not adjusted.

For assessing the vertical distribution of fish, the 10-m bins were additionally partitioned into layers 1 m thick, measured upward from the sea floor.

3.3.3.2. Stationary acoustic data

Data collected from the stationary platform were partitioned first by 1-ping (1 sec) intervals, to assess at what temporal scale samples could be considered independent. This time was then used to partition each 5-minute data collection period into bins, in order to obtain a mean and variance estimate for each period.

Stationary data that were collected concurrently with each pass of transect 4 of the mobile surveys were isolated for comparisons of mean S_V and fish vertical distribution across survey methods. To assess vertical distribution, data binned by time were further partitioned into layers 1 m thick, measured upward from the sea floor.

3.3.4. Echo integration

Partitioned data were echo integrated and exported from Echoview for further analysis in R software (v3.6.2) [36]. The metric exported for use in the following analyses was mean S_V , the average volume backscatter from within the given analysis domain, in dB re $1 \text{ m}^2 \text{ m}^{-3}$.

3.4. Auxiliary data processing

3.4.1. Current speed and direction

Nortek Signature 500 ADCP data were converted from the Nortek ad2cp file format to csv format using the Nortek Signature Deployment software (v3.4.17.0). Data were exported in SDU coordinates (speed, direction, up) for further processing in R. This format provided measurements of current speed and direction (horizontal and vertical), as well as the amplitude of backscattering from the upward-facing beam of the ADCP. Average measurements were obtained for each 5-minute sampling burst. The range of the maximum amplitude from each burst was used to approximate the range of the surface, which was confirmed against acoustic data. Data in the upper 10% of the water column were then omitted from analyses to avoid any interference from side lobes (SignatureViewer v1.01.17, Nortek) (Figure 10).

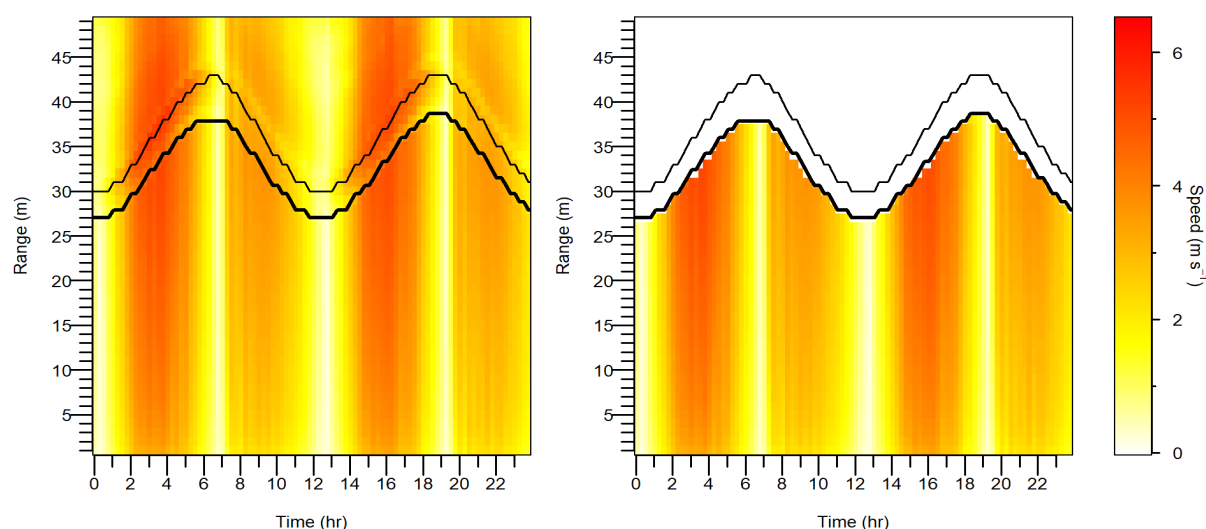


Figure 10. Example ADCP data, before and after surface backscatter removal. The thin black line is the estimated location of the surface, and the thick black line is the 10% offset from the surface.

Current direction readings were then corrected for magnetic declination (-17.22°). Water column averages of speed and direction were obtained for each burst, and were used for defining the start and end times of each tidal stage. Slack tides were defined as periods of time when average water column current speed was less than $0.5 \text{ m}\cdot\text{s}^{-1}$. The water column average current speed and direction are summarized for each deployment in Table 3 and Figure 11. Tidal stage times determined from the FAST3 ADCP data were used for both the mobile and stationary datasets.

Table 3. Summary of water column average current speed and direction during each platform deployment.

Dataset	Current direction (degrees)		Maximum current speed ($\text{m}\cdot\text{s}^{-1}$)	
	Flood tide	Ebb tide	Flood tide	Ebb tide
Dec 2017 – Feb 2018	118	291	4.7	3.5
Mar 2018 – May 2018	121	295	4.5	3.4
Sep 2017 – Dec 2017	118	292	4.4	3.3

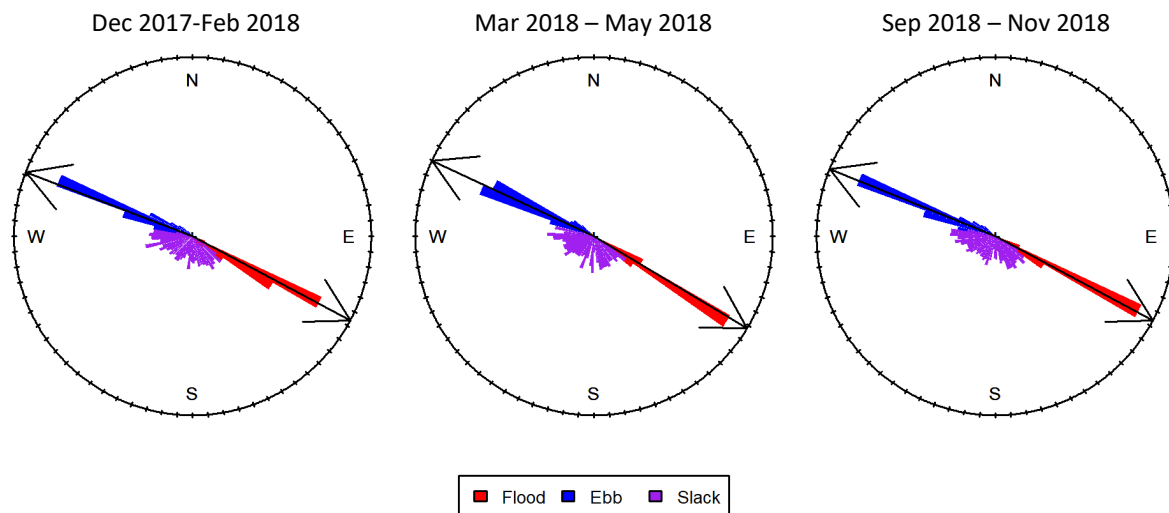


Figure 11. Average water column current direction during the three stationary platform deployments. Bar length indicates the frequency of current speed measurements within each 5-degree direction bin.

3.4.2. Salinity and temperature

Only temperature and conductivity data from the Aanderaa SeaGuard RCM were needed for the purposes of this report. Conductivity and temperature were used to calculate salinity using the code found at [37]. For the September 2018 deployment, when the SeaGuard was not functional, salinity was assumed equal to 31.5 psu, based on the range in salinity during the other two surveys, as well as salinity data from September of the previous year (note that salinity varies by approximately ± 0.5 psu over the course of a tidal cycle).

Temperature and salinity were used to calculate the sound speed and absorption coefficient, using the equations developed by [31,32,38]. These quantities were necessary for calibrating the acoustic data (see section 3.3.1).

3.5. Data analysis

3.5.1 Spatial autocorrelation

Empirical variograms were calculated for data from each repetition of transect 4 in the mobile dataset, which were echo-integrated at 10 m resolution. Variograms plot the semivariance of points within a dataset as a function of separation distance. Semivariance is calculated as

$$\gamma(d) = \frac{1}{2n(d)} \sum_i^{n(d)} [(y(x_i) - y(x_i + d))]^2$$

where y is the value of the data at location x_i , and $n(d)$ is the number of pairs of data points separated by distance d [39].

Small values of the semivariance indicate strong spatial dependence, whereas larger values indicate weaker dependence. A typical variogram would be expected to have a shape similar to Figure 12, in which the semivariance increases with distance until it levels off at the “sill”. After this transition point, samples are no longer spatially correlated, and the distance at which this occurs can approximate the distance to which information from a point measurement may be assumed representative [16,39]. The intercept of the variogram at 0 distance is the “nugget”, which indicates the level of variation occurring at smaller spatial scales than were measured.

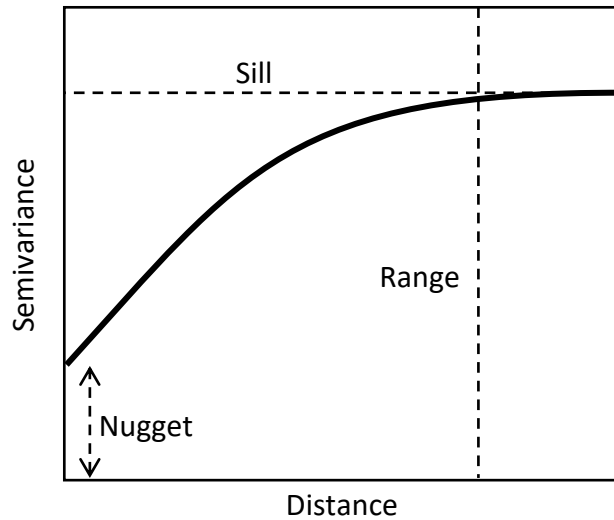


Figure 12. Theoretical shape of a variogram, showing the nugget, sill, and the distance at which samples are no longer spatially correlated.

Empirical variograms were calculated in R with the package *geoR* (v1.7-5.2.1) [40]. Null envelopes were generated for each variogram using 1000 Monte Carlo permutations. The null envelope indicates the expected variance as a function of distance, assuming spatial randomness. Points of the variogram that fall outside of this envelope indicate possible spatial dependence.

The goal was to determine the distance at which measurements became independent and to adjust the horizontal bin accordingly. However, when variograms were generated for all

transects, they were found to be nearly flat, with little evidence of the initial slope that would typically be expected (see section 4.2). This indicated a lack of spatial correlation at 10 m resolution, so bin size was kept at 10 m (but see section 4.2 for further discussion). Mean S_v measurements from these bins were assumed to be independent of each other, and were used in comparisons of mobile results to stationary.

3.5.2 Temporal autocorrelation

Temporal autocorrelation is the correlation of a time series with itself, when offset by some number of samples in time (lag). The autocorrelation coefficient, r_h , for a time series, y , at lag h , is given by

$$r_h = \frac{\sum_{t=1}^{N-h} (y_t - \bar{y})(y_{t+h} - \bar{y})}{\sum_{t=1}^N (y_t - \bar{y})^2}$$

where N is the number of samples in the series and \bar{y} is the series' mean [41]. The autocorrelation coefficient will be 1 for a lag of 0, when the series is aligned perfectly with itself (Figure 13). Assuming time dependence in the data, a confidence band for a significance level α can be calculated as:

$$\pm z_{1-\alpha/2} \sqrt{\frac{1}{N} \left(1 + 2 \sum_{i=1}^k r_i^2 \right)}$$

where z is the quantile function of a standard normal distribution. When the autocorrelation coefficient falls within this band, samples are assumed independent.

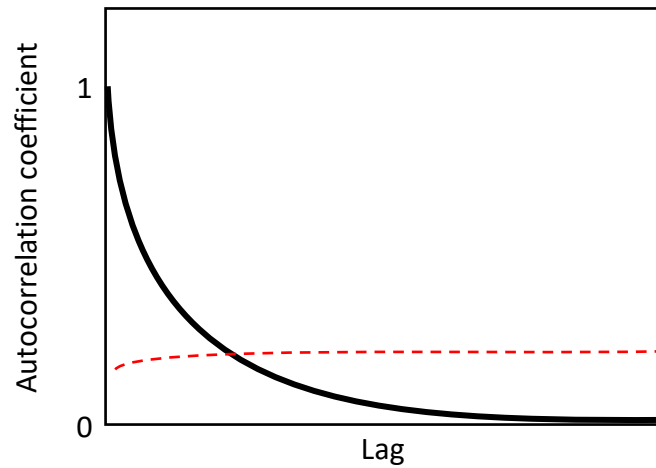


Figure 13. Theoretical shape of an autocorrelation function (ACF) of a time series, showing the 95% confidence interval.

For each of the three stationary datasets, the autocorrelation function (ACF) was calculated for every 5-minute recording period using the mean S_v values exported from Echoview in 1-ping (1 second) bins. An average ACF was calculated for each dataset, which indicated that water column mean S_v became independent at a lag of 6 seconds in each dataset (see section 4.3).

Stationary data were then partitioned into bins 6 seconds long and echo integrated. S_v mean values from these bins was used to calculate an estimate of the mean and variance for each 5-minute recording period, resulting in a new time series with half-hour resolution for each stationary dataset.

3.5.3 Comparison of mobile to stationary measurements

Stationary data collected concurrently to passes of transect 4 in the mobile surveys were identified and isolated. As stationary data were collected every half hour, measurements did not always align exactly in time, and so the nearest point in time was chosen for comparison to each mobile transect. The temporally indexed mean and variance was then compared to the mean and variance obtained for the corresponding passes of transect 4.

4. Results and Conclusions

Below are qualitative observations of the acoustic data used in this assessment, followed by a discussion of the spatial correlation of the mobile data (spatial representative range), the temporal correlation of the stationary data (temporal representative range), and the direct comparison of results from each study type.

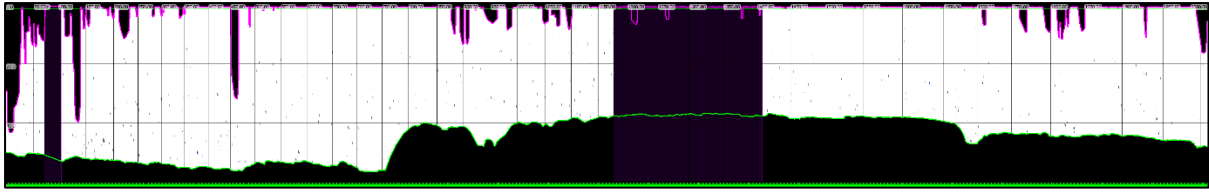
4.1 Qualitative observations of acoustic datasets

4.1.1 Mobile data

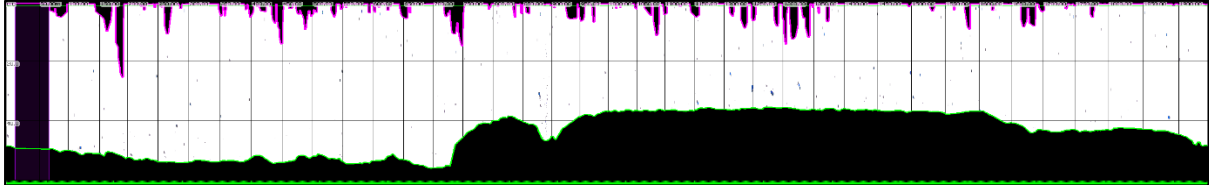
The mobile dataset used here consisted of 36 passes of transect 4 that overlapped with stationary data collection periods. These came from 5 different mobile surveys of the FORCE test site, in Feb, Apr, May, Sep, and Oct 2018. Example echograms from each survey are shown in Figure 14. Some qualitative differences between the individual passes of transect 4 were apparent. For example, backscatter in the Feb, Apr, and May surveys consisted of mainly individual targets scattered throughout the water column. There was noticeably more backscatter in the water column during the Sep and Oct surveys. Some aggregations were visible mid-water-column in the Sep survey during the day. These differences are likely related to seasonal changes in species composition and abundance in Minas Passage [2,3,9-12].

The amount of entrained air varied by survey and was greatest in the Oct survey, which was cut short due to poor weather conditions. Most mobile data were relatively clean, but transect passes missing more than 10% of their distance bins due to contamination from entrained air or other noise were omitted from spatial analysis. This included 3 passes in the Feb survey and 1 in the May survey.

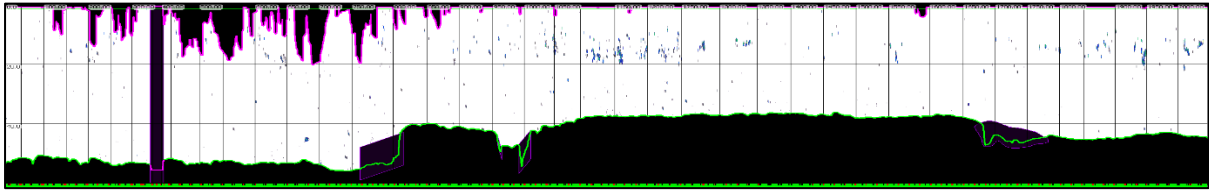
Feb, day, ebb, against-current



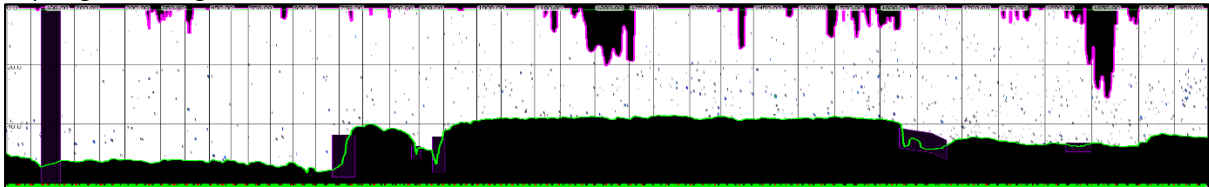
May, day, ebb, against-current



Sep, day, ebb, against-current



Sep, night, ebb, against-current



Oct, night, ebb, against-current

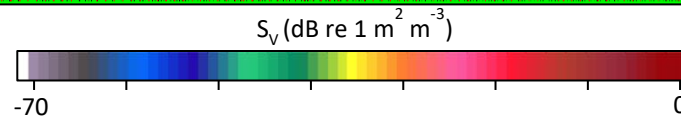
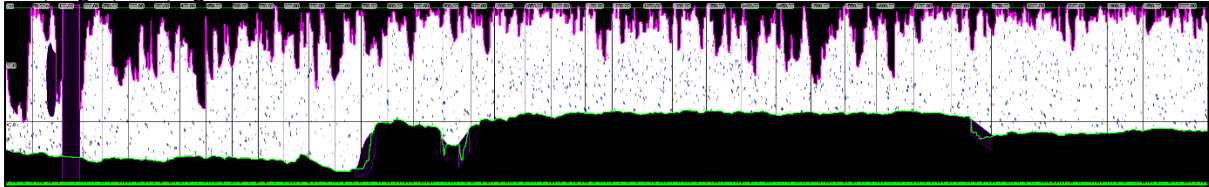


Figure 14. Example echograms from passes of Transect 4 carried out in 2018. The horizontal grid lines show depth increments of 20 m, measured from the surface downward. The vertical grid lines show distance increments of 50 m, measured along-transect. Volume backscatter (S_v) is shown, with units of $\text{dB re } 1 \text{ m}^2 \text{ m}^{-3}$. Black areas are data that were omitted (e.g., contaminated by entrained air, or below the bottom). Note that the number of targets at greater ranges will appear greater due to the beam widening with range, which is accounted for in calculations but not when viewing echograms.

Water column backscatter generally increased from Feb to Oct surveys (Figure 15). This trend is not easily seen when including the distance bins that contained empty water column. These data segments had no above-threshold backscatter in the water column, and therefore have a value of -999 dB (Figure 15a), which strongly skew the means. The trend does become apparent when the empty bins are omitted (Figure 15b). This upward trend is generally in agreement with the trends seen in the stationary dataset (section 4.1.2).

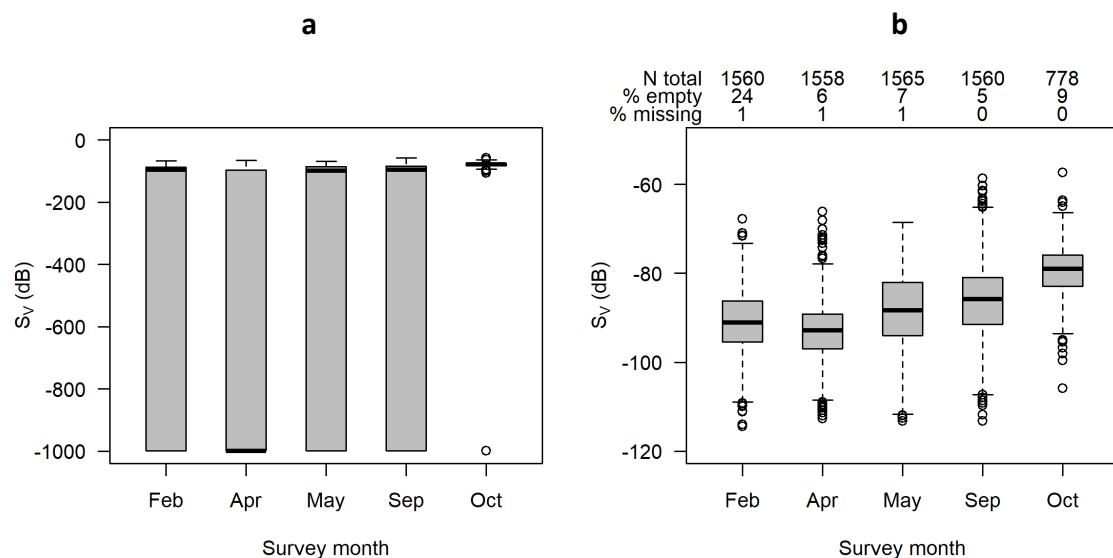


Figure 15. Summary of water column mean S_v (dB re $1 \text{ m}^2 \text{ m}^{-3}$) from the passes of transect 4 carried out in the 2018 mobile surveys. Passes are grouped by survey month. (a) Boxplot of water column mean S_v for each survey, including the samples from empty water column (dB value of -999). (b) Boxplot of water column mean S_v for each survey, excluding empty water column samples. The total number of samples, the percent of those samples that were empty water column, and the percent that were missing due to noise contamination, are shown across the top.

Water column mean S_v was similar during the day and night in the Feb and Apr surveys, but was higher at night in the May and Sep surveys (Figure 16a). Tidal stage similarly had little effect in Feb and Apr, but in May water column mean S_v was noticeably higher during the flood tide than the ebb (Figure 16b). In Sep and Oct, ebb tide backscatter appeared slightly stronger than flood tide.

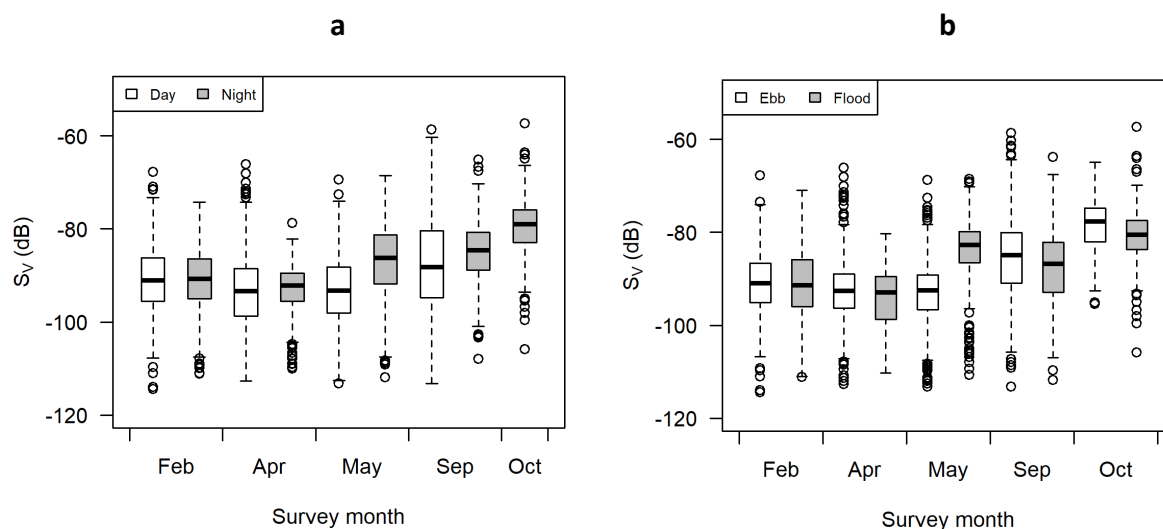


Figure 16. Summary of water column mean S_v (dB re $1 \text{ m}^2 \text{ m}^{-3}$) from the passes of transect 4 carried out in the 2018 mobile surveys. Passes are grouped by survey month and (a) diel state (day or night) and (b) tidal stage (ebb or flood). Only results from non-empty water column are shown here.

Though surveys were spread out in time, the physical conditions experienced during each pass of transect 4 were similar, based on current speed data from the ADCP on the stationary platform. This is primarily due to the fact that mobile surveys always take place during the weakest neap tide, when weather conditions are favourable. Additionally, surveys begin after a slack tide and transects are carried out in the same order nearly every time, resulting in transect 4 sampling a similar range of current speeds across surveys. Almost all passes of transect 4 occurred in current speeds of roughly 2 to 2.5 $\text{m}\cdot\text{s}^{-1}$. The largest exception was the Feb survey, in which two passes of transect 4 occurred at lower current speeds (Figure 17). This consistency was helpful in this case, as it reduced one potential source of variance and made the passes of the transects somewhat more comparable to each other.

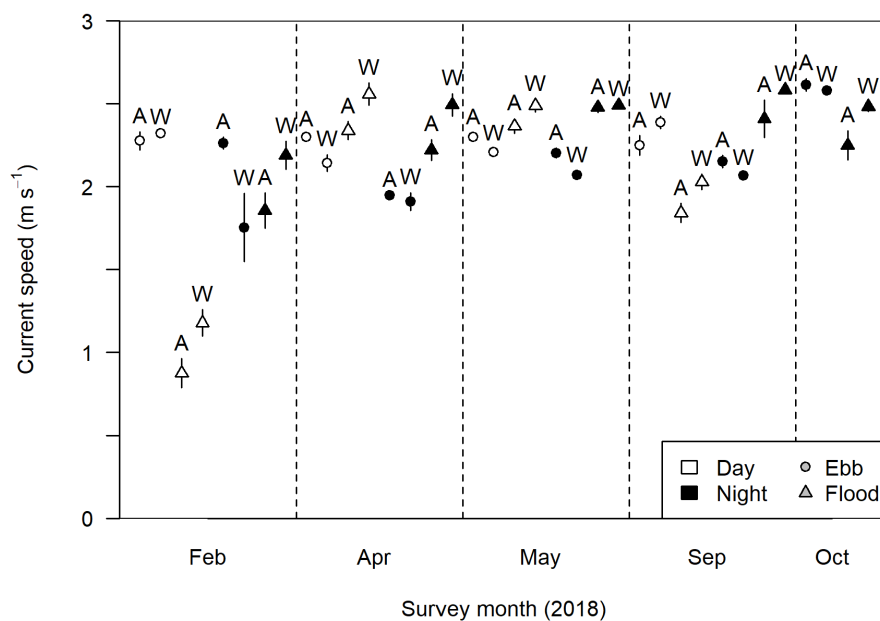


Figure 17. Current speeds during each pass of transect 4. Points are the mean current speed (± 1 standard deviation) during each pass, with diel and tidal stage indicated by point color and shape, and direction indicated by A (against current) or W (with current). Current speeds were obtained from the ADCP on the stationary platform.

Since the vessel would pass over the transect twice in a row, once moving with the current and once moving against, vessel ground speed differed substantially from vessel-through-water speed (Figure 18). This, too, was consistent across passes, despite the magnitude of the change in current speed that occurs with each tide. Transect passes moving with the tide essentially sampled less “water distance” than those moving against the tide, though the transects were approximately the same length over ground.

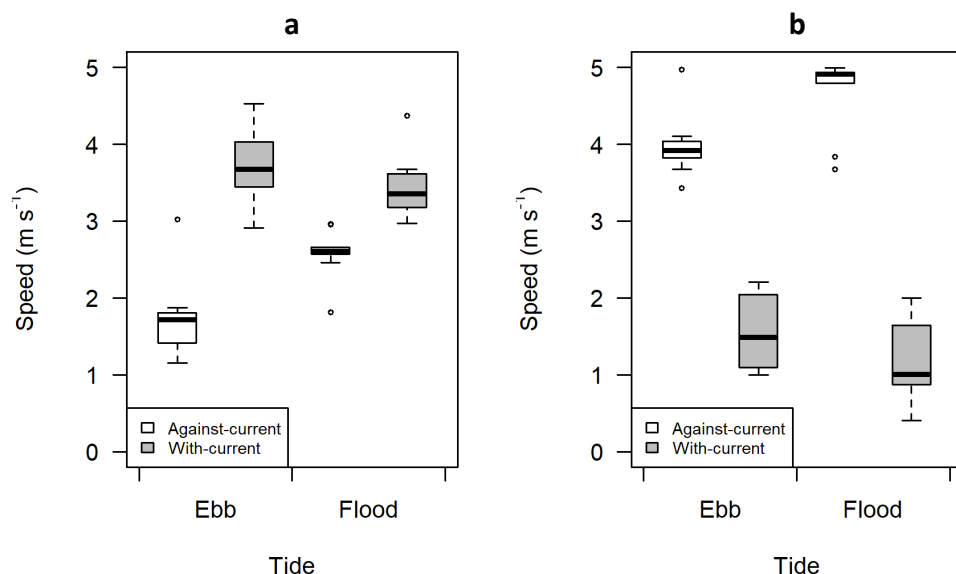


Figure 18. Vessel speed (a) over ground and (b) through water, across all passes of transect 4 in 2018, grouped by transect direction relative to flow (with or against current).

4.1.2 Stationary data

The stationary datasets spanned roughly 2 months each and captured a wide variety of backscatter from fish and other sources. Data collected from the stationary platform were noisier than data collected in the mobile surveys. This was primarily in the form of the “cascading” backscatter that appeared after slack tides, as well as the “transient noise” that would often appear at higher current speeds. Much of this noise may have simply been avoided by the mobile surveys because they occurred on the neap tides, when transient noise was rare, and during the flowing tide, when the “cascading” backscatter would not usually occur.

Another possible reason for higher noise levels in the stationary data is the pulse duration used by the echosounder. The pulse duration was shorter for the stationary echosounder than the mobile one, which increases its bandwidth and therefore potentially opens it to a broader range of unwanted backscatter [14]. The pulse duration was chosen after a test deployment which cycled through a range of operation settings; however, that deployment was closer to shore and may not have sampled the same range of conditions as the longer-term deployments mid-passage. Whether this contributes to noise in the stationary dataset could be determined with another deployment at this site, during which the echosounder cycles repeatedly through pulse length settings.

The Dec 2017 – Feb 2018 dataset had the highest levels of contamination due to entrained air, cascading backscatter, and transient noise. 57% of the recording periods were omitted, as opposed to 39% and 37% for the Mar and Sep datasets, respectively. This was potentially related to winter weather. Stronger winds were recorded during the collection of the Dec dataset than the other two (FORCE weather station data, accessible at www.oceannetworks.ca), which could have increased the amount of air entrained into the upper water column and subsequently drawn down by turbulence.

Biological backscatter was visibly different across the stationary datasets. The Dec-Feb dataset was characterized by individual targets spread throughout the water column, without much noticeable change across tides or between day and night (Figure 19). There were occasional bubbles rising from fish, possibly indicating the presence of Atlantic herring (these have been known to release swim bladder gas through the anal duct) [42].

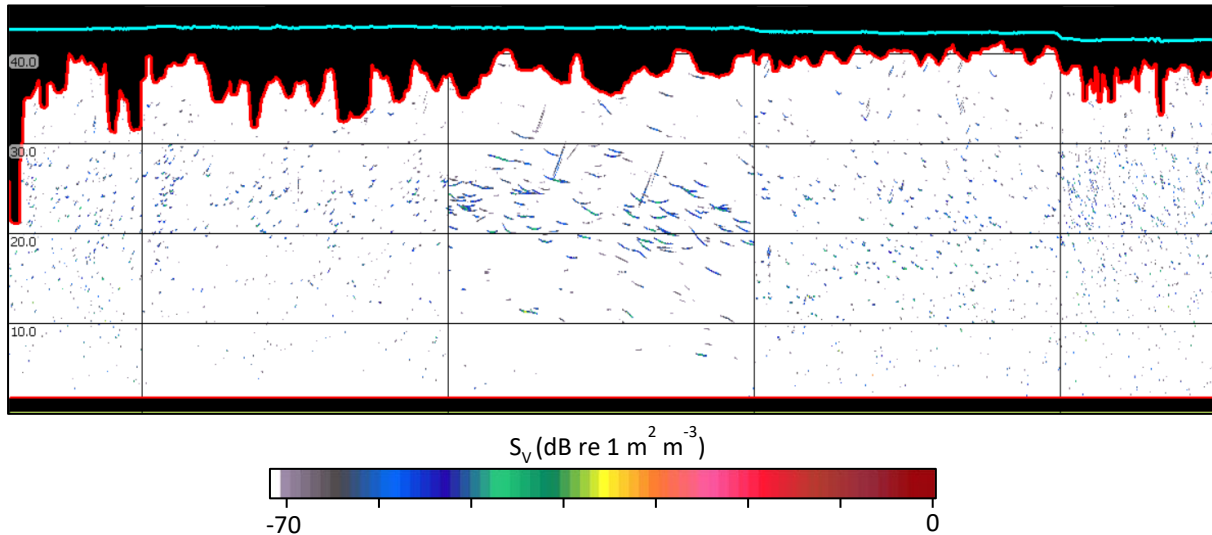


Figure 19. Example volume backscatter (S_v) data from the Dec 2017-Feb 2018 stationary, up-looking dataset, showing individual targets spread throughout the water column. In this example, slack tide occurred in the center recording period, where fish tracks are most evident and the straight angled lines potentially indicate bubbles released by fish. Vertical gridlines are the edges of each 5-minute recording period, occurring every half hour. Horizontal gridlines indicate range, measured upward from the transducer (10 m increments). Black areas are data that were omitted; e.g., contaminated by entrained air (upper red line), within the nearfield (lower red line), or above the surface (cyan line).

Backscatter in the Mar-May 2018 dataset changed noticeably from the start to the end, from more evenly-distributed individual targets at the beginning to a mix of very numerous individual targets and small, dense aggregations toward the end, with aggregations more common during the day than the night (Figure 20).

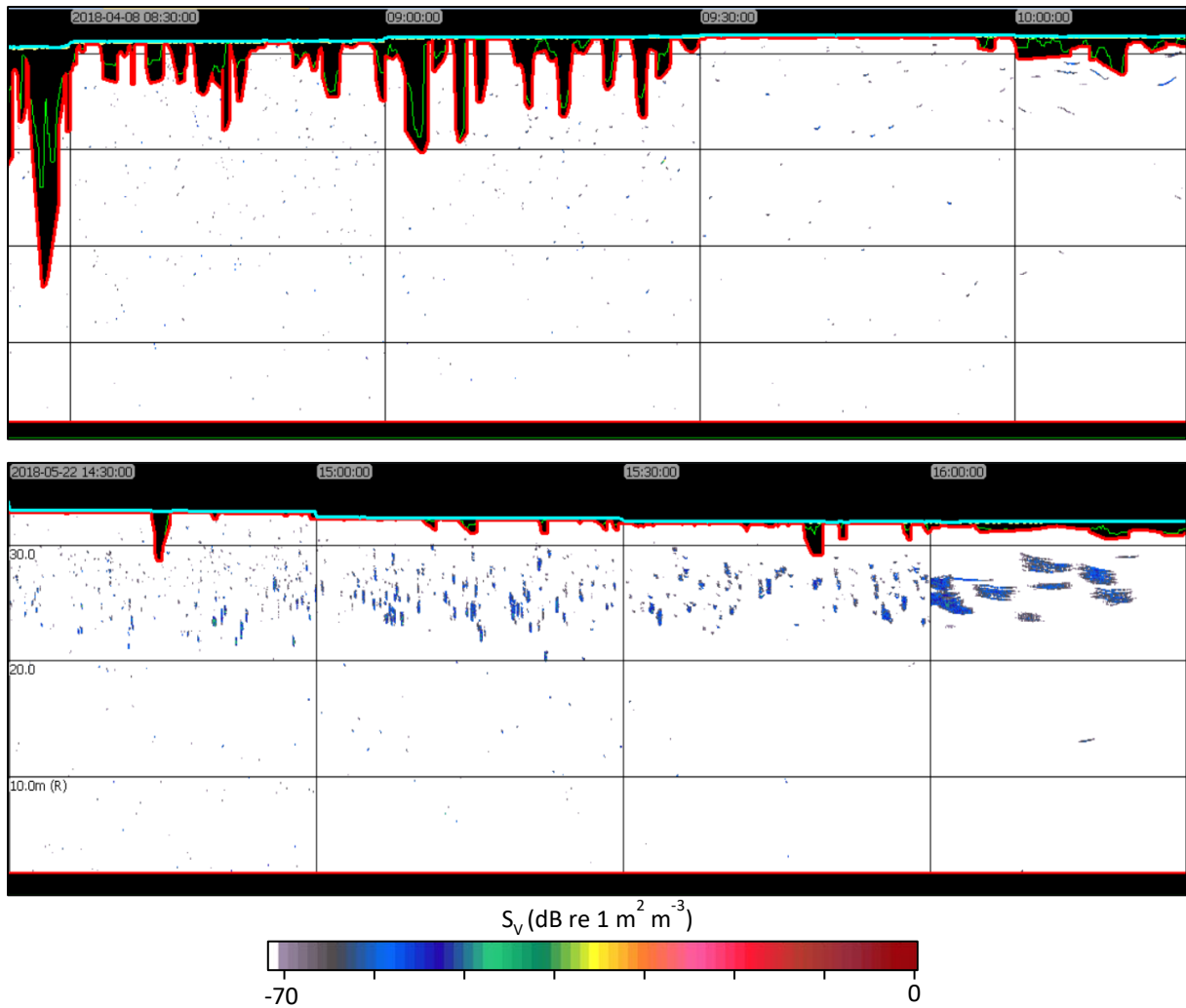


Figure 20. Example volume backscatter (S_v) data from the Mar-May 2018 stationary, up-looking dataset. Top: early April backscatter, showing individual, spread out targets. Bottom: late May volume backscatter, showing small aggregations appearing as the tide approaches low slack. Times shown are in UTC.

The Sep-Nov 2018 dataset was characterized by numerous individual targets throughout the water column, as well as numerous aggregations in the upper water column (Figure 21). These were more prevalent during the day than at night.

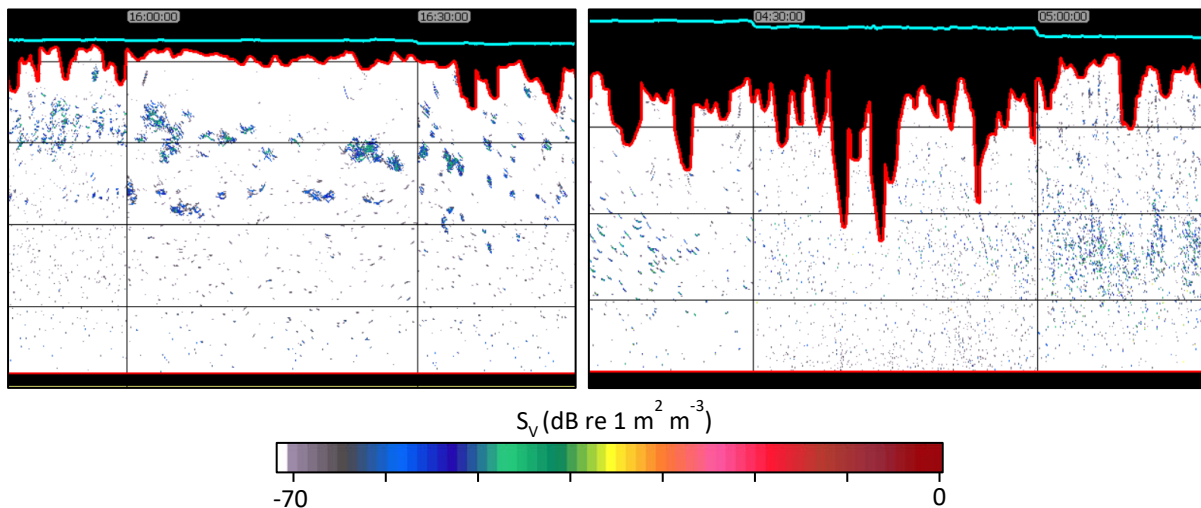


Figure 21. Example volume backscatter (S_v) data from the Sep-Nov 2018 stationary, up-looking dataset. Left: daytime example from Sep 24, showing aggregations in the upper water column and individual targets spread throughout. Right: night example from the same day, showing targets spread throughout the water column. Times are in UTC.

The changes in how fish were distributed in the water column (e.g., spread out vs. in aggregations) throughout the year are likely related to the species present, and how they are using the passage. For example, Atlantic herring are a schooling species and are present in the passage for most of the year [2,3,10,11]. However, aggregations of fish were only seen in data from the spring through fall months. This may be the result of differing behaviour based on environmental conditions, e.g. temperature, which has been found to affect the behaviour of striped bass in the passage [2]. Of course, there are other schooling species present in the passage depending on the time of year, and the presence of aggregations in the data is likely to also be related to their seasonal presence [2,3,10,11].

Overall, water column backscatter decreased from Dec 2017 through Feb 2018, increased from Apr to May 2018, and remained relatively constant from Sep to Oct 2018 (Figure 22). This trend is generally in agreement with the mobile surveys, which each sampled a much shorter period of time each. As for the mobile data, these changes in backscatter likely reflect shifts in fish abundance and community composition. Also, in both mobile and stationary datasets, variability in water column backscatter was generally larger than the change in the average from one month to the next.

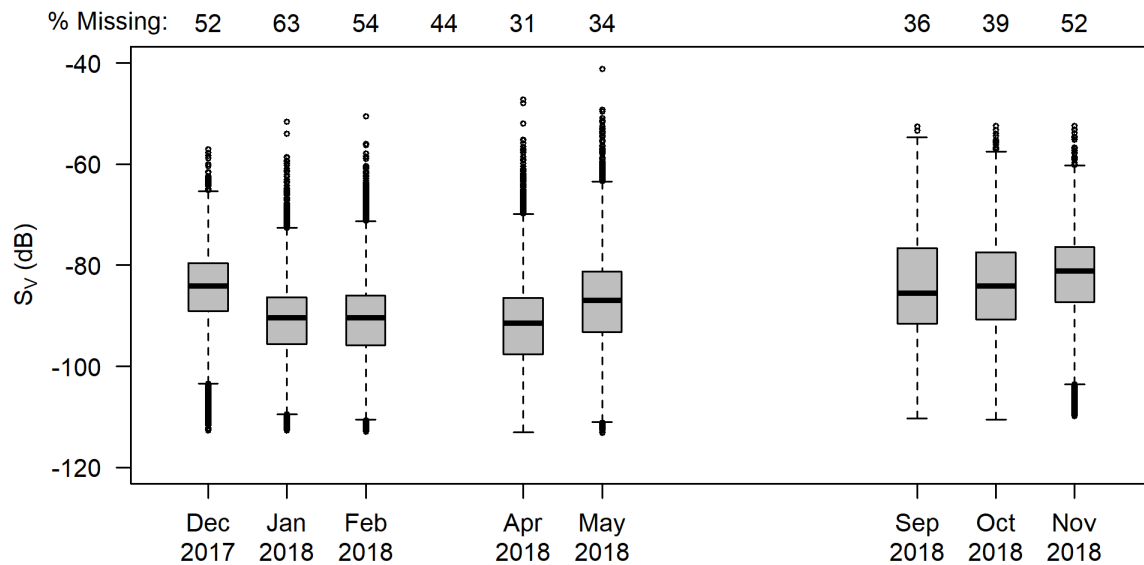


Figure 22. Water column S_v (dB re $1 \text{ m}^2\text{m}^{-3}$) for each month of data collected from the stationary platform. Each data point represents the water column mean for a 6-second time bin. The percentage of bins that were missing from each group due to noise contamination is shown at the top.

Diel differences in water column backscatter came and went throughout the three stationary datasets (Figure 23). Water column backscatter was higher during the night in December 2017, then the same during day and night until mid-April, when once again backscatter became higher at night through Nov 2018. This is likely a biological signature, as many fish change their behaviour diurnally [2,43-46]. The echograms show that this difference arises from noticeably more targets spread throughout the water column at night than during the day (e.g., Figure 21). These data cannot tell us where these fish go during the day, just that they are, apparently, not within the sampled volume at that time. The lowermost 2 m of water column, the uppermost portion (masked by entrained air), and anywhere else in the cross-section of the passage are all possibilities.

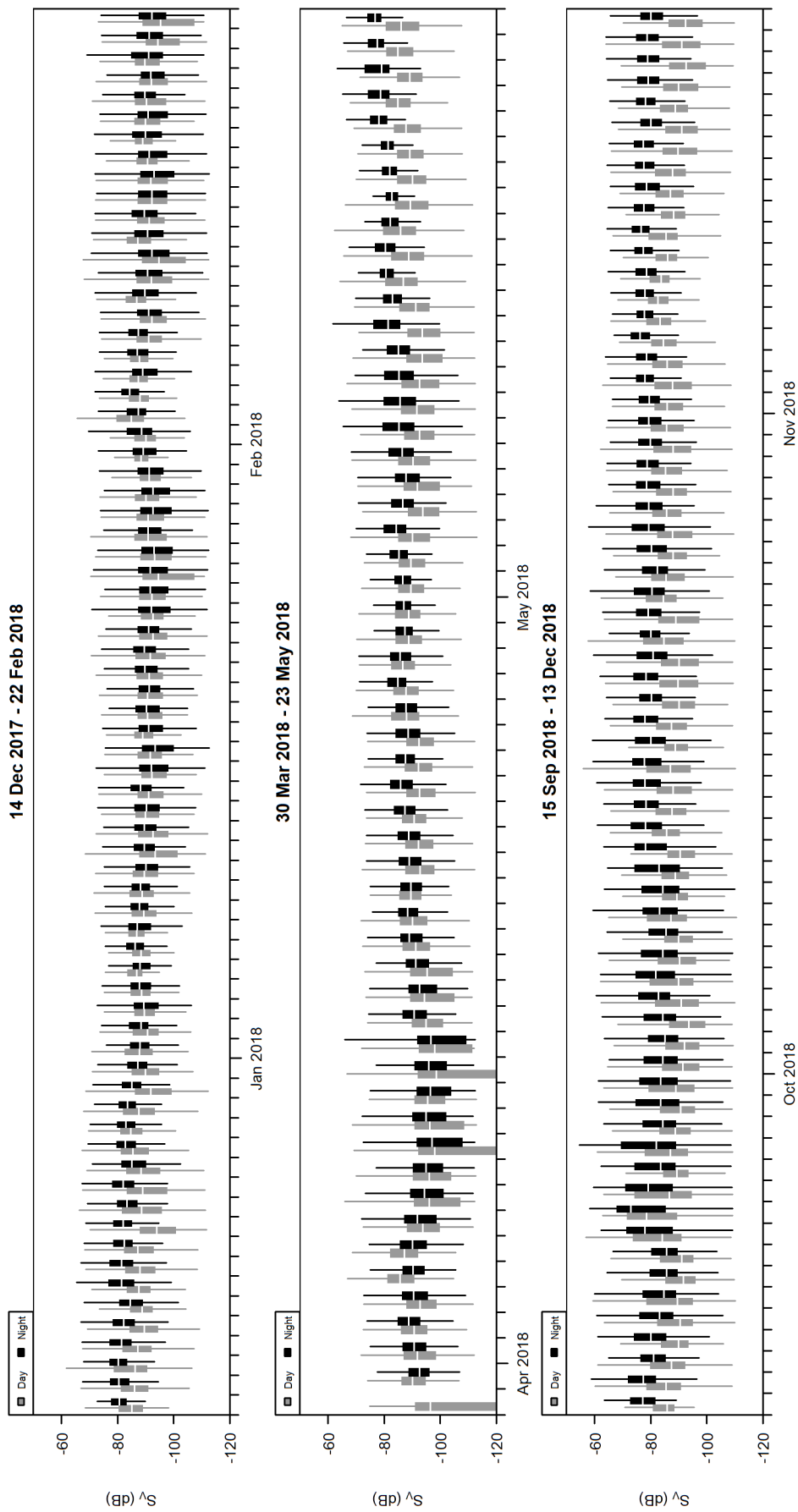


Figure 23. Water column mean volume backscatter (S_v , in dB re $1 \text{ m}^2 \text{ m}^{-3}$) for the three stationary, up-looking datasets, grouped by date and diel stage (day or night).

When volume backscatter data were grouped by tidal stage, there was not as clear a pattern as for diel stage. However, across months, low tide had consistently lower and more variable backscatter than other tidal stages, and more instances of empty water column (Figure 24).

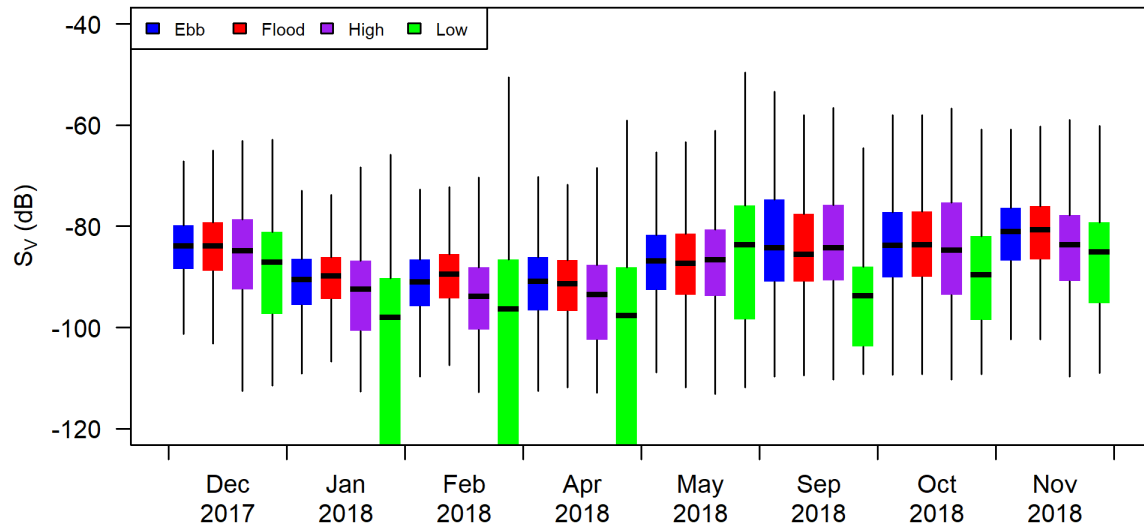


Figure 24. Water column mean volume backscatter (S_v , in dB re $1 \text{ m}^2\text{m}^{-3}$) for each month of data collected from the stationary platform, split by tidal stage. Boxes that extend beyond the lower limit of the plot are due to high prevalence of bins containing empty water column ($S_v = -999$ dB).

4.2 Spatial autocorrelation

Spatial autocorrelation was not evident in backscatter from the passes of transect 4, regardless of survey month, transect direction (with or against the current), tidal stage, or diel stage. This was clear in the empirical variograms for each pass (Figure 25), which showed almost no slope or indication of a transition point between nugget and sill. For most passes of transect 4, nearly all variogram points fell within the null envelope, indicating low likelihood of spatial dependence in water column backscatter measured along the transect.

A few passes had one or two points that fell outside of the null envelope at shorter distances, and a shape closer to what would be expected in a typical variogram (e.g., the third variogram for the Sep survey, Figure 25). This could potentially indicate some level of spatial dependency (up to 70-220 m) during these passes. However, this was not clear or consistent across transect passes, and isn't enough to draw conclusions about representative range.

The lack of correlation at the along-transect resolution tested (10 m) could occur under a few scenarios. First, the data could in fact be spatially correlated, but at a scale smaller than the 10 m resolution we were able to use. In this case, all samples would have been from the "sill" portion of the variogram, and the resolution would not have been fine enough to characterize the start of the sill. Second, the backscatter could have been spatially correlated at a scale larger than we were able to sample—that is, at distances greater than

the length of the transect. A third possibility is that both our sampling resolution and range were sufficient, and backscatter simply has no spatial structure at this site under the conditions sampled.

The echograms from the mobile surveys show an almost uniform distribution of targets along each pass of transect 4. Any spatial structure within a transect would therefore occur at quite a small scale, if present at all, and while there are no larger-scale changes obvious to the eye in the echograms (e.g. at 10's of m), it is not impossible that these could emerge if a larger distance were sampled. At the scale of our observations, the echograms and the variograms together suggest a lack of spatial correlation in the backscatter measurements made along transect 4.

Though the amount of backscatter in the water column changed over the course of the year, in accordance with the seasonally changing fish community of Minas Passage, the spatial distribution of the backscatter throughout the water column was relatively consistent in the mobile survey echograms. This is interesting, because one might expect the behaviours of different species and life stages of fish to be reflected in the echograms. Some changes were seen—for example, there were some loose aggregations visible in the daytime Sep passes of transect 4. This roughly agrees with stationary data, which show an increased presence of aggregations in May, Sep, and early Oct relative to the winter months. However, the stationary data also revealed that aggregations were most common near slack tide. During the running tide, targets appeared more dispersed throughout the water column (Figure 20). Mobile surveys all took place during the running tide, which may explain why they did not show much difference in fish distribution in the water column over time. This may also indicate that aggregation is influenced by the current speed. For example, aggregating fish species may not be forming aggregations at high current speeds, or are outside of our sampled volume (e.g., within the entrained air layer).

The apparent lack of spatial structure here contrasts with results in [16] from Puget Sound, where there was significant correlation along transects to a distance of 300+ m. Transects in that study were conducted across-current, whereas transects in this study were conducted parallel to the current. It was expected that fish biomass would show stronger correlation over distance when moving parallel to the flow than perpendicular, as the water moving through the echosounder is the same moving mass. Instead, no spatial correlation was observed in our transects at the resolution we sampled. This site is also very different from the Puget Sound site in [16]. Current speeds in Minas Passage are stronger, and mixing potentially more intense, than the Puget Sound study site, and it is possible this simply disrupts any attempt at spatial coordination by fish, at least at the scales observed here.

Given the apparent lack of spatial structure in water column backscatter at the scales observed, it is difficult to say whether data from the stationary platform (located 40 m away from the nearest point of transect 4) are directly comparable, even when collected concurrently.

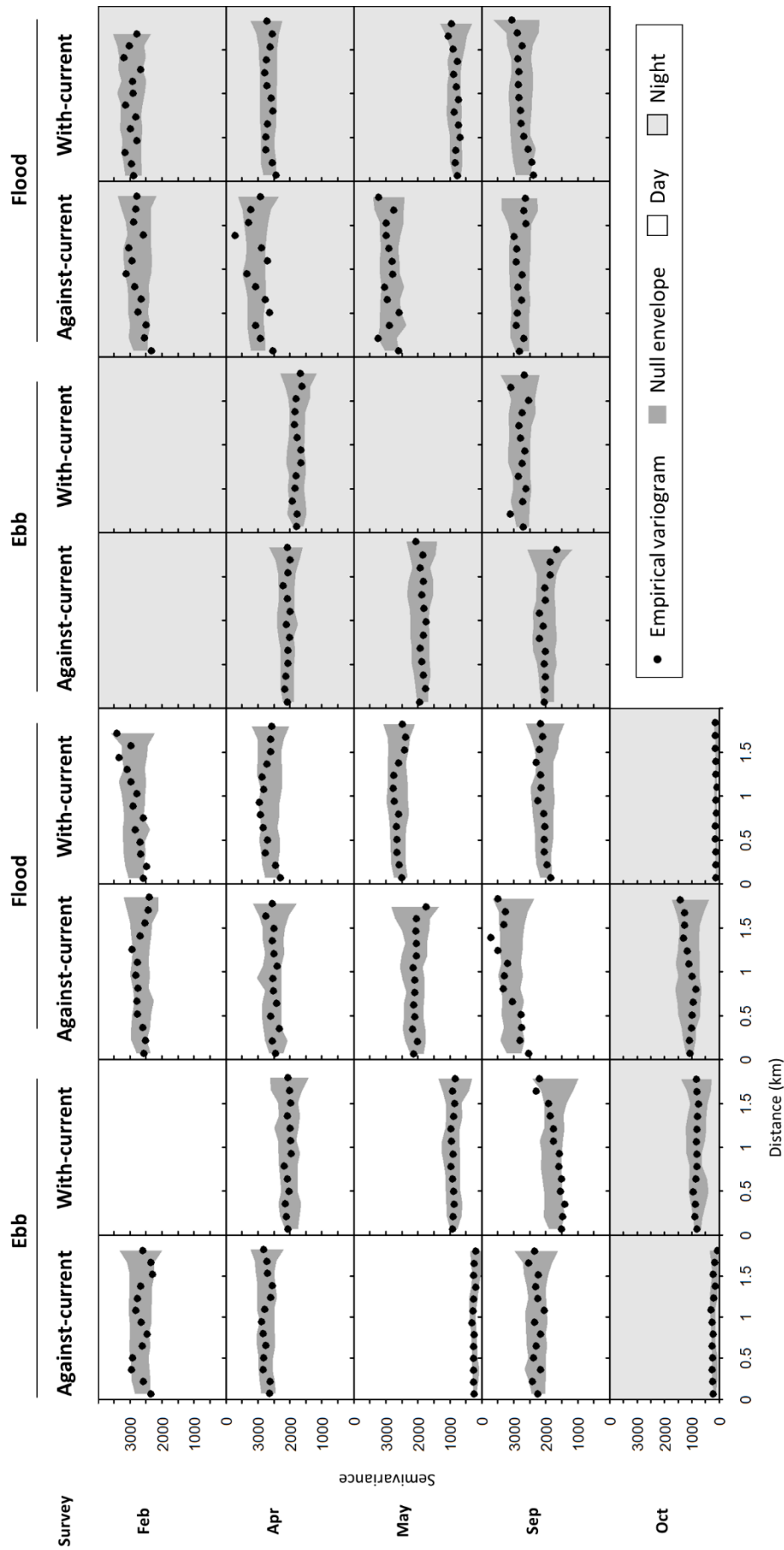


Figure 25. Variograms for repeated passes of transect 4, for mobile surveys conducted in 2018. Points are the empirical variogram, and the dark gray shaded region is the null envelope. Blank plots occur if too much of the transect was contaminated by noise to be used. Light gray backgrounds indicate data collected at night.

Analysis of data collected from all transects across the survey area, including examination of correlation with- and across- the direction of flow, would provide further insight for interpreting these results. In this example, the current regime was similar across most transect passes (Figure 17), making the individual passes more comparable to each other. When incorporating information from the other transects, which occur at different but consistent points in the tidal cycle, it will be important to account for the differing current regimes sampled by each, as this is likely to affect fish presence and distribution.

4.3 Temporal autocorrelation

Water column mean S_v measurements made from the stationary platform were found to become independent at 6 seconds for slack tide periods and at 3 seconds in ebb or flood tide periods, in all three stationary datasets (Figure 26). This makes sense, given more water passes by the transducer between pings at higher current speeds than at lower ones.

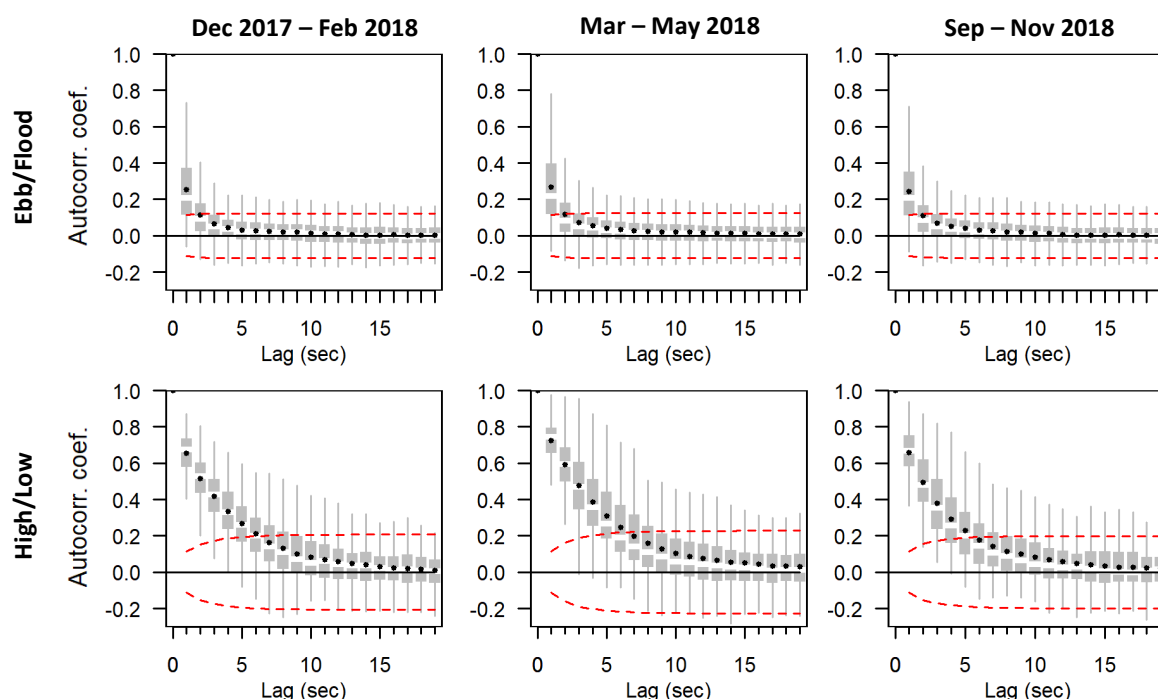


Figure 26. Autocorrelation function (ACF) for each stationary dataset at 1-second resolution. Top: running tides (ebb or flood); bottom: slack tides (high or low). The gray box plots show the distribution of the autocorrelation coefficients from each recording period, the black points indicate the average across all recording periods, and the red dashed lines are the 95% confidence interval.

Platform S_v data were subsequently binned at 6 second resolution to acquire a mean and standard deviation for each 5-minute recording period, occurring each half hour. The resulting half-hour resolution time series showed large amounts of variability on short time scales (hours), primarily related to tidal and diel periodicities in water column backscatter. This was clear in the ACF for each dataset's half-hour time series (Figure 27), with spikes in correlation aligning with 6.2, 12.4, and 24 hour lags, and at times significant correlation near larger tidal harmonics, including 13.7 and 27.6 days (particularly in the Sep-Nov 2018 data). When a 24-hour moving average was used to remove the shorter-scale variation, these peaks were removed, revealing that the underlying trend (unrelated to tidal or diel cycles)

remained autocorrelated up to approximately 3 days. The same pattern was found regardless of whether empty bins were kept in the dataset or not, and for variance estimates as well.

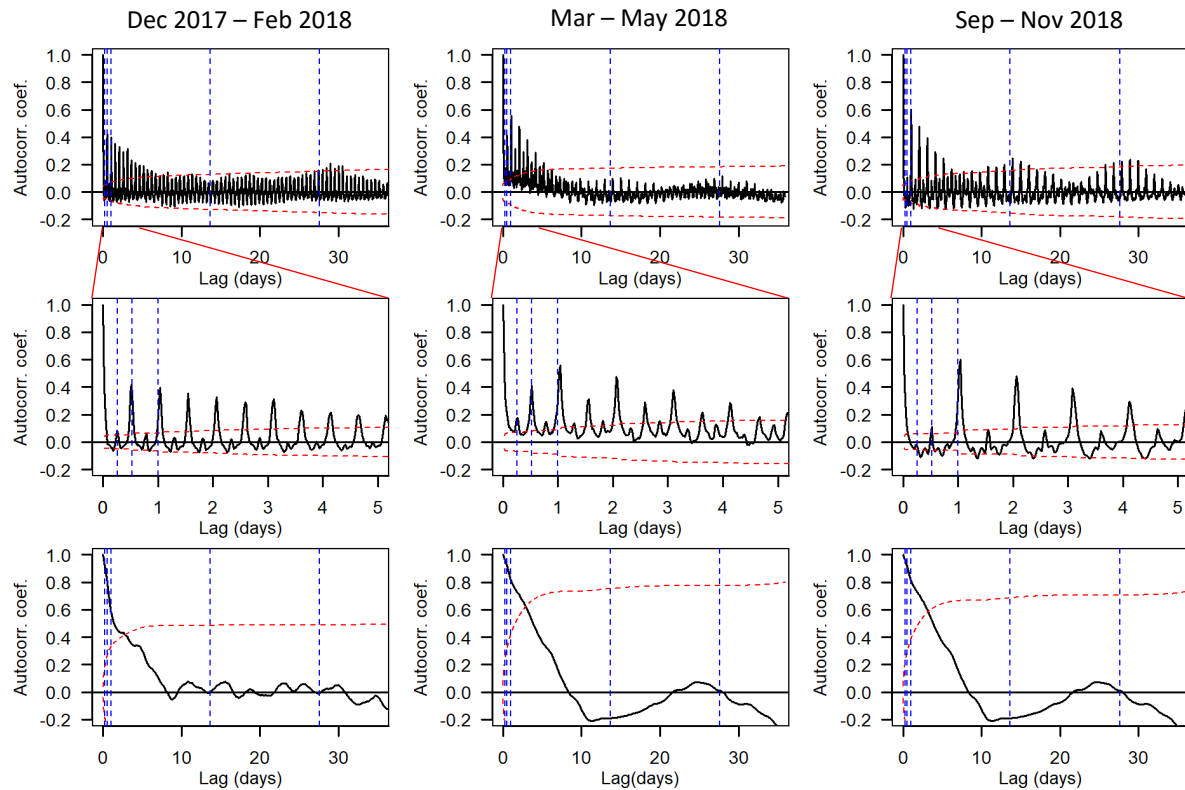


Figure 27. Autocorrelation function (ACF) for each half-hour time series of mean water column S_v generated from the stationary datasets. The black line is the autocorrelation coefficient, the red dashed line is the 95% confidence interval, and the blue vertical lines indicate relevant tidal and diel periodicities (6.2, 12.4, and 24 hrs, and 13.7 and 27.6 days). The top row shows the entire ACF, the middle row zooms in on the smaller lags, and the bottom row shows the ACF of the time series after a 24-hr rolling average filter was applied.

The cyclic variation introduced over the course of a tidal cycle or a day was often greater than the magnitude of the trend observed over the duration of the dataset. This was particularly true if bins that sampled empty water column were included when calculating the time series. For the sake of visualization, these empty points were removed, and the scale of the short-term variation can be more easily compared to the scale of the long-term changes (Figure 28).

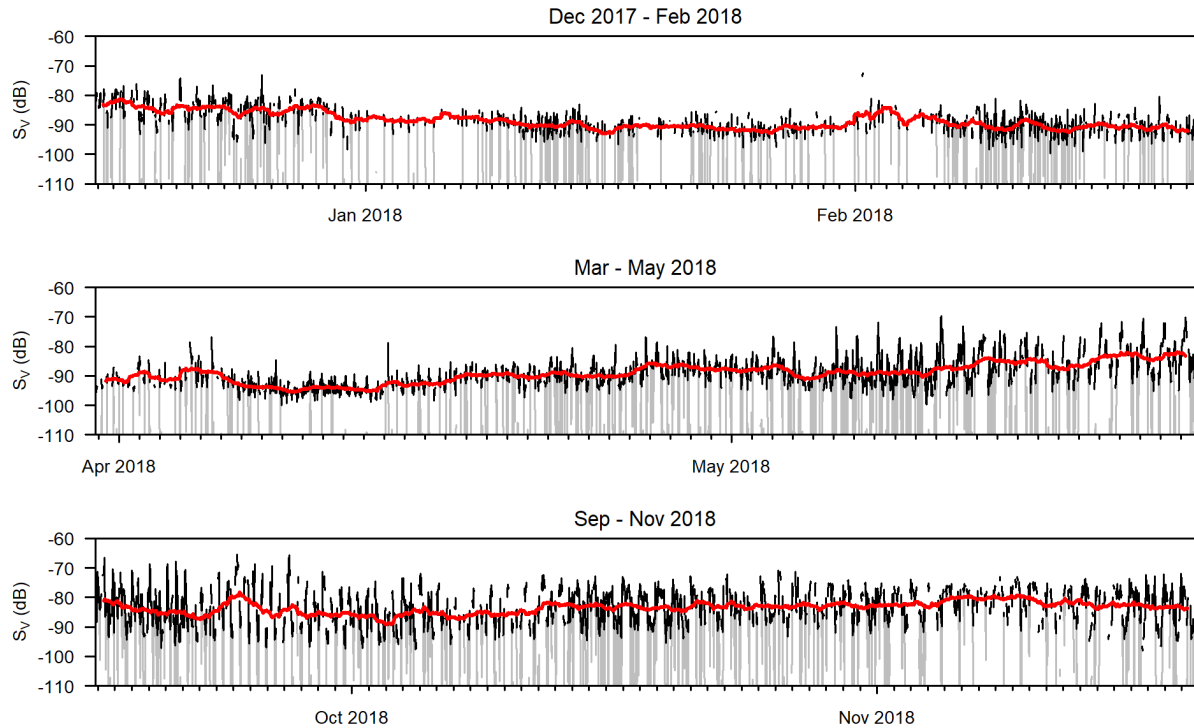


Figure 28. Water column mean S_v from stationary data, calculated for each recording period (5 minutes every half hour). Gaps exist where bins were missing more than half of their samples due to noise contamination. The gray line is the mean when empty water column bins are included in the calculation. The black line is the mean calculated without empty water, and the thick red line is the rolling mean calculated with a 24 hour window (excluding empty water).

Removing the empty water column values helps with data visualization; however, the absence of fish (the presence of empty water column) is important information that should not be eliminated from analyses. The ACF for the number of empty samples per recording period showed the same clear tidal and diel variation as the mean water column S_v (Figure 29), indicating fish presence/absence, in addition to density, is linked to these cycles.

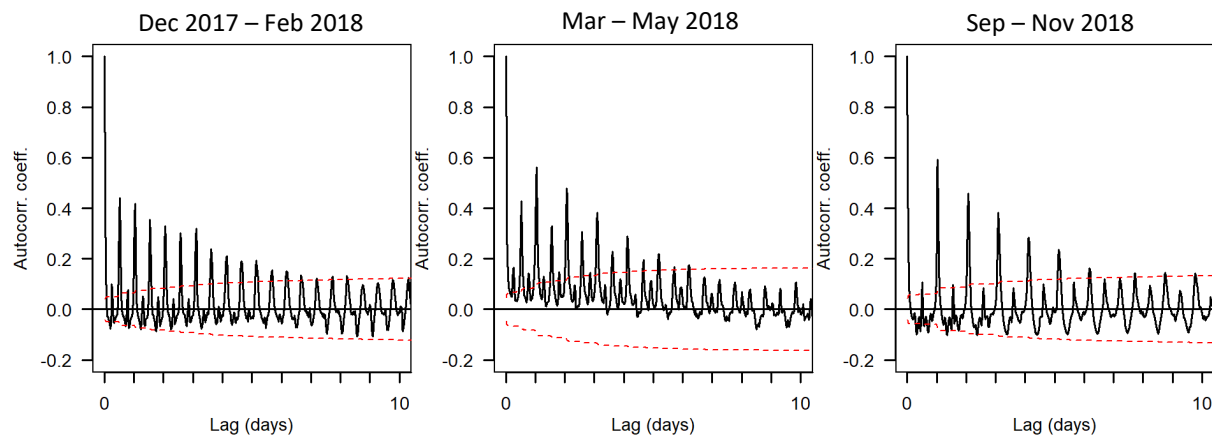


Figure 29. Autocorrelation functions for the number of empty bins per sampling period, for each of the stationary datasets.

Understanding when there are no fish present in the water column would be useful for assessing potential effects of tidal power devices. This would require a better quantitative approach for handling zero-values. One option to explore would be a two-stage model of backscatter, e.g. a delta model, which first models the probability of zero occurrence, then non-zero values [47].

The large degree of variation in fish presence and backscatter strength related to tidal and diel cycles reinforces the importance of samples spanning at least one day when seeking to monitor long-term trends with short, discrete surveys. Twenty-four hours of data allow quantification of the scale of this variation, and computation of a mean that can aid in long-term monitoring. The three stationary datasets examined here indicated that a 24 hour average may have a representative range of up to 3 days.

4.4 Comparison of mobile to stationary measurements

Direct comparison of water column mean S_v across the mobile and stationary datasets revealed differences in the results from each survey type. When just the nearest 5-minute stationary period was compared to each pass of transect 4, results were grouped but not highly correlated (Figure 30). Including empty water column segments (-999 dB) in the calculation of the mean and standard deviation for each transect (mobile data) or recording period (stationary data) strongly skewed the means toward large negative values, particularly for mobile transects, which had more empty water column segments (Figure 30a). If empty water column segments were omitted from each survey type, there was better agreement across them (Figure 30b). However, there was still a good amount of variation between the two, which appeared to be independent of tidal stage or whether the mobile transect was moving with or against the current. A linear model fit could only explain 23% of this variance ($S_{v_stationary} = -22.0 + 0.75*S_{v_mobile}$).

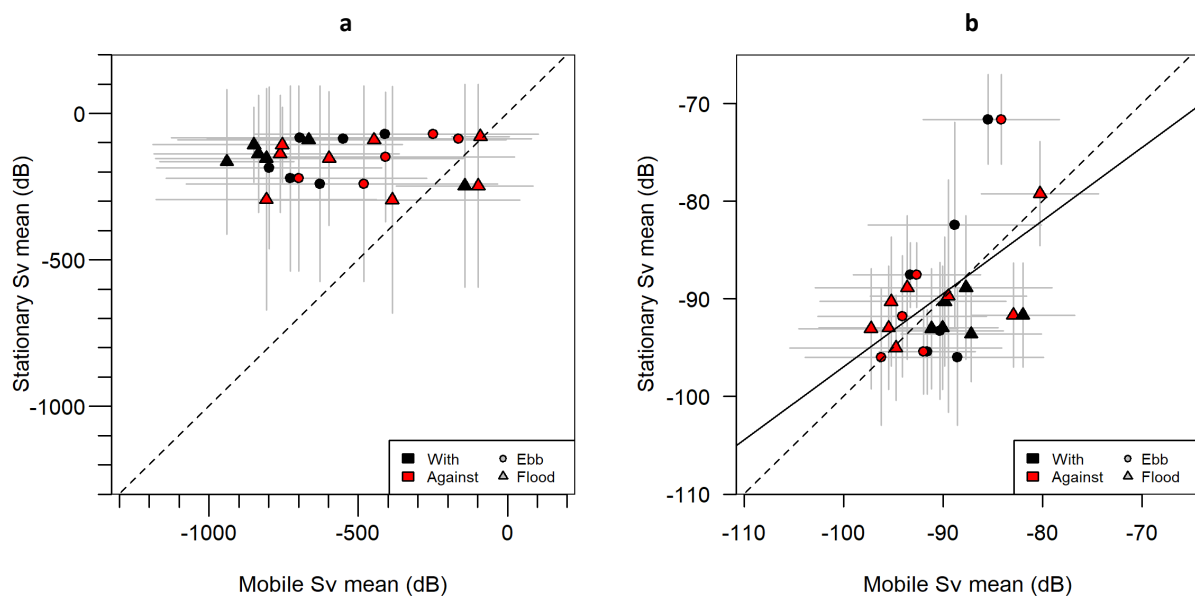


Figure 30. Average (± 1 standard deviation) water column mean S_v for stationary data vs mobile data, comparing each pass of transect 4 to the nearest 5-min stationary collection period, (a) including empty water column samples, (b) excluding empty water column samples. The dashed line is the 1:1 line, and the solid line is the linear fit.

Though the results from each survey type did not agree well when each transect pass was directly compared to the closest 5-min period from the stationary data, when data were instead grouped by day, the results agreed much more closely (Figure 31). When the empty water column bins were removed (Figure 31b), the agreement between the two was almost 1:1 ($S_{V_stationary} = -8.8 + 0.90 \cdot S_{V_mobile}$, adjusted R-squared = 0.94).

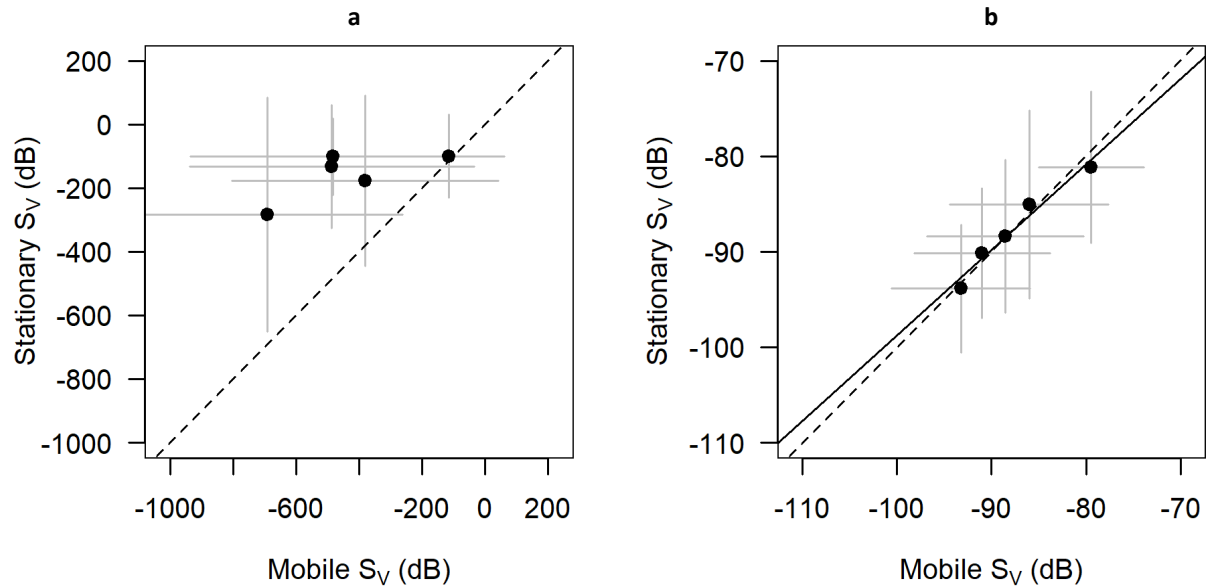


Figure 31. Average (± 1 standard deviation) water column mean S_V for stationary data vs mobile data, grouping mobile surveys by day and comparing to the corresponding 24 hours of stationary data, (a) including empty water column samples, (b) excluding empty water column samples. The dashed line is the 1:1 line, and the solid line is the linear fit.

Agreement at the scale of one day, but not at a scale of minutes, makes sense given the temporal variability described by the stationary dataset. Backscatter at this site changes drastically over shorter time scales, but a 24 hr average can provide more reliable data points for quantifying longer term trends.

Given that the two survey types agreed well when the 24 hr average was compared, it is possible that spatial variation at this scale (the platform was 40 m away from transect 4) was negligible in comparison to the temporal variability.

The vertical distributions were not, in the end, compared across sampling types, as there was simply not enough non-empty 1-m vertical bins to create a useful comparison. There is the additional issue of varying amounts of water column being sampled at any given moment due to entrained air, whether mobile or stationary, which complicates comparison of fish vertical distribution across any separation in time or space. Given that half of the water column is often missing, vertical distributions may not provide particularly useful information at this site, at least during the running tide. Proportions of fish at each layer would not be meaningful if the proportion of the water column sampled is constantly changing. One approach may be to manually isolate very clean segments of data specifically for the purpose of analysing the vertical distribution of fish. However, extrapolation of

results beyond these time periods (e.g. to times of faster speeds or rougher weather) could be difficult to justify.

5. Recommendations

Hydroacoustics is one of the best tools for examining the underwater environment at very high spatial and temporal resolutions. In tidal energy sites, it is one of the few tools that can be used to safely acquire information about fish. However, tidal energy sites also present unique challenges to acoustics sampling. The high-speed currents generate high levels of turbulence, which draw air into the water column and sometimes as far down as the seafloor. Backscatter from fish is completely masked within these contaminated areas. Much of this contamination can be identified and removed with a combination of automated steps (e.g. with the threshold offset line method in Echoview) and manual scrutiny (corrections to automated line detections). However, the appearance of this air in the echograms can change substantially, from easily defined “spikes” extending down from the surface, to nebulous clouds that appear mid-water-column. The timing and extent of entrained air contamination is difficult to predict, and thus far can only be removed by hand according to the judgement of the human observer. There is a distinct need for tools to help automate this process and reduce subjectivity, particularly in long-term datasets (e.g., the stationary dataset presented here). Machine learning is an active area of research in the acoustics community, and these techniques should be explored for applications at tidal energy sites.

Additional acoustic frequencies could also improve our ability to identify and separate fish from entrained air. In this dataset, we only had one frequency to work with, and therefore could not examine the frequency response of any of the scatterers. The frequency response could be useful for separating groups of interest—e.g., bubble clouds vs. fish schools [30]. This will depend on the size and density of the bubbles entrained into the water column and which species of fish are present, and therefore needs to be tested on site. Testing could be carried out from a vessel or a platform, as long as a wide range of noise types can be sampled concurrently (or nearly so) with the different frequencies.

Further assessment of the full mobile dataset is recommended in order to better understand the spatial structure of backscatter (fish presence and density) at this tidal energy site, and to be able to estimate the representative spatial range of acoustic data collected from a stationary platform. Data from just one transect was used here, as it was the closest to the stationary platform. However, results from this transect were inconclusive. Incorporating data from the other transects may help determine if this was an issue of resolution or span, and/or if the site simply exhibits no coherent spatial structure at the scales we are able to measure—i.e. if it is too tumultuous for fish to form any coherent spatial distribution during the running tide. At this stage, we have only scratched the surface and cannot say which is more likely.

The data from the stationary platform were incredibly useful in quantifying the temporal variability in backscatter measurements at this site. This dataset revealed a huge amount of temporal variability occurring over short time scales (seconds to hours), including strong

tidal and diel periodicities throughout the year. The magnitude of this variability was similar to or greater than the changes occurring at the seasonal scale. This finding agrees with previous assessments here and at other sites [12,26], and supports the continued use of 24-hr sampling in the mobile surveys. A 24 hr survey allows the tidal and diel variation in backscatter to be quantified, and the 24-hour average is more useful for tracking the longer term trends of interest (e.g., long-term changes in fish backscatter as an indicator of turbine effects). All three stationary datasets indicated the representative temporal range of a 24-hr mobile survey is approximately 3 days at the location sampled.

The goals of this assessment were primarily related to comparing the stationary and mobile datasets, and using their complementary information to determine the spatial or temporal applicability of the results from each. However, there is a wealth of biological information that could be extracted from these data, if challenges such as the identification and removal of noise, and the resulting varying quality and coverage of the data, can be addressed.

Budget

Please see separate MS Excel file.

Employment Summary

Please see section entitle 'Performance measures' below.

Bibliography

- [1] Copping, A., Sather, N., Hanna, L., Whiting, J., Zydlewski, G., Staines, G., Gill, A., Hutchison, I., O'Hagan, A., Simas, T., Bald, J., Sparling, C., Wood, J., Masden, E. (2016). Annex IV 2016 State of the Science Report: Environmental Effects of Marine Renewable Energy Development Around the World. Richland, WA: Pacific Northwest National Laboratory. Available: <http://tethys.pnnl.gov/publications/state-of-the-science-2016>.
- [2] Keyser, F.M., Broome, J.E., Bradford, R.G., Sanderson, B., & Redden, A.M. (2016). Winter presence and temperature-related diel vertical migration of Striped Bass (*Morone saxatilis*) in an extreme high flow site in Minas Passage, Bay of Fundy. Canadian Journal of Fisheries and Aquatic Science. DOI: 10.1139/cjfas-2016-0002.
- [3] Stokesbury, M.J.W., Logan-Chesney, L.M., McLean, M.F., Buhariwalla, C.F., Redden, A.M., Beardsall, J.W., Broome, J.E., Dadswell, M.J. (2017). Atlantic sturgeon spatial and temporal distribution in Minas Passage, Nova Scotia, Canada, a region of future tidal energy extraction. PLoS ONE, vol 11, no 7, e0158387.
- [4] Horne, J.K., Jacques, D.A., Parker-Stetter, S.L., Linder, H.L., and Nomura, J.M. (2013). Evaluating Acoustic Technologies to Monitor Aquatic Organisms at Renewable Energy Sites. National Ocean Partnership Program – Bureau of Ocean and Energy Management, Department of Energy. Final Report. 111 pp.
- [5] Viehman, H.A., Zydlewski, G.B., McCleave, J., Staines, G. (2015). Using acoustics to understand fish presence and vertical distribution in a tidally dynamic region targeted for energy extraction. Estuaries and Coasts, vol 38, suppl 1, pp S215-S226.
- [6] Staines, G., Zydlewski, G.B., Viehman, H., Shen, H., McCleave, J. (2015). Changes in vertical fish distributions near a hydrokinetic device in Cobscook Bay, Maine, USA. Proceedings of the 11th European Wave and Tidal Energy Conference. September 6-11 2015. Nantes, France.
- [7] Bradley, P.T., Evans, M.D., Seitz, A.C. (2015) Characterizing the juvenile fish community in turbid Alaskan rivers to assess potential interactions with hydrokinetic devices. Transactions of the American Fisheries Society 144: 1058-1069.
- [8] Seitz, A.C., Moerlein, K., Evans, M.D., Rosenberger, A.E. (2011) Ecology of fishes in a high-latitude, turbid river with implications for the impacts of hydrokinetic devices. Reviews in Fish Biology and Fisheries 21: 481-496.
- [9] Redden, A.M., Stokesbury, M.J.W., Broome, J.E., Keyser, F.M., Gibson, A.J.F., Halfyard, E.A., McLean, M.F., Bradford, R. Dadswell, M.J., Sanderson, B., and Karsten, R. (2014). Acoustic tracking of fish movements in the Minas Passage and FORCE Demonstration Area: Pre-turbine Baseline Studies (2011-2013). Final Report to the Offshore Energy Research Association of Nova Scotia and Fundy Ocean Research Centre for Energy. Acadia Centre for Estuarine Research Technical Report No. 118, Acadia University, Wolfville, NS. 153p

- [10] Baker, M., Reed, M., & Redden, A.M. (2014). Temporal Patterns in Minas Basin Intertidal Weir Fish Catches and Presence of Harbour Porpoise during April – August 2013. ACER, Wolfville, NS, Technical Report 120.
- [11] Dadswell, M.J. (2010). Occurrence and migration of fishes in Minas Passage and their potential for tidal turbine interaction. BioIdentification Associates. Technical Report. 35 pp.
- [12] Viehman, H.A., Boucher, T., & Redden, A.M. (2018). Winter and summer differences in probability of fish encounter with MHK devices. *International Marine Energy Journal*, vol 1, no 1.
- [13] Horne, J.K. (2000). Acoustic approaches to remote species identification: a review. *Fisheries Oceanography*, vol 9, no 4, pp 356-371.
- [14] Simmonds, J., MacLennan, D.N. (2005). *Fisheries acoustics: theory and practice*. Oxford: Blackwell.
- [15] Daroux, A. & Zydlewski, G.B. (2017). Final Report 2016-2017 Mobile Acoustic Fish Monitoring of the Fundy Ocean Research Center Crown Lease Area. Report submitted to the Fundy Ocean Research Center for Energy.
- [16] Horne, J.K., and Jacques, D.A. (2018). Determining representative ranges of point sensors in distributed networks. *Environmental Monitoring Assessment*, vol 190, no 348.
- [17] Jacques, D. (2014). Describing and comparing variability of fish and macrozooplankton density at marine hydrokinetic energy sites. M. Sc. Thesis, University of Washington.
- [18] Melvin G.D. & Cochrane, N.A. (2014). Investigation of the vertical distribution, movement and abundance of fish in the vicinity of proposed tidal power energy conversion devices. Final Report submitted to Offshore Energy Research Association (OERA), Research Project 300-170-09-12.
- [19] Shen, H., Zydlewski, G.B., Viehman, H.A., & Staines, G. (2016). Estimating the probability of fish encountering a marine hydrokinetic device. *Renewable Energy*, vol 97, pp 746-756. DOI: 10.1016/j.renene.2016.06.026.
- [20] Lieber, L., Nimmo-Smith, W.A.M., Waggitt, J.J., Kregting, L. (2018) Fine-scale hydrodynamic metrics underlying predator occupancy patterns in tidal stream environments. *Ecological Indicators*, vol 94, pp 397-408. <https://doi.org/10.1016/j.ecolind.2018.06.07>
- [21] Scherelis, C., Penesis, I., Marsh, P., Cossu, R., Hemer, M., Write, J. (2019) Relating fish distributions to physical characteristics of a tidal energy candidate site in the Banks Strait, Australia. *Proceedings of the 13th European Wave and Tidal Energy Conference*. 1-6 Sept 2019, Naples, Italy.

- [22] Fraser, S., Nikora, V., Williamson, B.J. & Scott, B.E. (2017). Automatic active acoustic target detection in turbulent aquatic environments. *Limnology and Oceanography*, vol 15, no 2, pp 184-199. DOI: 10.1002/lom3.10155.
- [23] Wiesebron, L.E., Horne, J.H., & Hendrix, A.N. (2016). Characterizing biological impacts at marine renewable energy sites. *International Journal of Marine Energy*, vol 14, pp 27-40. DOI: 10.1016/j.ijome.2016.04.002.
- [24] Wiesebron, L.E., Horne, J.K., Scott, B.E., & Williamson, B.J. (2016). Comparing nekton distributions at two tidal energy sites suggests potential for generic environmental monitoring. *International Journal of Marine Energy*, vol 16, pp 235-249. DOI: 10.1016/j.ijome.2016.07.004.
- [25] Williamson, B.J., Fraser, S., Blondel, P., Bell, P.S., Waggitt, J.J. & Scott, B.E. (2017). Multisensor Acoustic Tracking of Fish and Seabird Behavior Around Tidal Turbine Structures in Scotland. *IEEE Journal of Oceanic Engineering*. DOI: 10.1109/JOE.2016.2637179.
- [26] Viehman, H.A. & Zydlewski, G.B. (2017). Multiscale temporal patterns in fish presence in a high-velocity tidal channel. *PLoS ONE*, vol 12, no 5. DOI: 10.1371/journal.pone.0176405.
- [27] Urmy, S.S., Horne, J.K., Barbee, D.H. (2012). Measuring the vertical distributional variability of pelagic fauna in Monterey Bay. *ICES Journal of Marine Science*, vol 69, no 2, pp 184-196.
- [28] Urmy, S.S., Horne, J.K. (2016). Multi-scale responses of scattering layers to environmental variability in Monterey Bay, California. *Deep-Sea Research I*, vol 113, pp 22-32.
- [29] Demer, D.A., Berger, L., Bernasconi, M., Bethke, E., Boswell, K., Chu, D., Domokos, R., et al. (2015). Calibration of acoustic instruments. ICES Cooperative Research Report No. 326. 130 pp.
- [30] Korneliussen, R. J. (Ed.). (2018). Acoustic target classification. ICES Cooperative Research Report No. 344. 104 pp. <http://doi.org/10.17895/ices.pub.4567>
- [31] Mackenzie, K. V. (1981). Nine-term equation for sound speed in the ocean. *Journal of the Acoustical Society of America*, vol 70, pp 807-12. <https://doi.org/10.1121/1.386920>
- [32] Leroy, C. C. (1969). Development of simple equations for accurate and more realistic calculation of the speed of sound in sea water. *Journal of the Acoustical Society of America*, vol 46, pp 216-26.
- [33] Ryan, T.E., Downie, R.A., Kloser, R.J., Keith, G. (2015). Reducing bias due to noise and attenuation in open-ocean echo integration data. *ICES Journal of Marine Science*. doi: 10.1093/icesjms/fsv121.

- [34] Benoit-Bird, K. J., Southall, B. L., Moline, M.A. (2019). Dynamic foraging by Risso's dolphins revealed in four dimensions. *Marine Ecology Progress Series*, vol 632, pp 221-234.
- [35] Hartman, K.J., Nagy, B.W. (2005). A target strength and length relationship for striped bass and white perch. *Transactions of the American Fisheries Society*, vol 134, pp 375-380. DOI: 10.1577/T04-052.1.
- [36] R Core Team (2019). R: A language and environment for statistical computing. R Foundation for Statistical Computing, Vienna, Austria. <https://www.R-project.org/>.
- [37] "Water Quality Monitoring: Conductivity to Salinity Conversion." Fivecreeks.org. Friends of Five Creeks. Accessed December 2019. <<http://www.fivecreeks.org/monitor/sal.shtml>>
- [38] Francois, R.E., and Garrison, G.R. (1982). Sound absorption based on measurements. Part II: Boric acid contribution and equation for total absorption. *Journal of the Acoustical Society of America*, vol 72, pp 1879-90. <https://doi.org/10.1121/1.388673>
- [39] Fletcher, R., and Fortin, M. (2018). Spatial ecology and conservation modelling: applications with R. Switzerland: Springer.
- [40] Ribeiro Jr, P.J., and Diggle, P.J. (2018). geoR: Analysis of Geostatistical Data. R package version 1.7-5.2.1. <https://CRAN.R-project.org/package=geoR>
- [41] Holmes, E. E., Scheuerell, M.D., and Ward, E.J. (2019) Applied time series analysis for fisheries and environmental data. NOAA Fisheries, Northwest Fisheries Science Center, 2725 Montlake Blvd E., Seattle, WA 98112. Contacts eli.holmes@noaa.gov, eric.ward@noaa.gov, and mark.scheuerell@noaa.gov
- [42] Wilson, B., Batty, R.S., and Dill, L.M. (2004). Pacific and Atlantic herring produce burst pulse sounds. *Proceedings of the Royal Society of London B*, vol 271(suppl.), pp S95-S97.
- [43] Pittman, S.J., McAlpine, C.A. (2001). Movements of marine fish and decapods crustaceans: process, theory and application. *Advances in Marine Biology*, vol 44, pp 205-294.
- [44] Reeb, S.G. (2002). Plasticity of diel and circadian activity rhythms in fishes. *Reviews in Fish Biology and Fisheries*, vol 12, pp 349-71.
- [45] Huse, I., Korneliussen, R. (2000). Diel variation in acoustic density measurements of overwintering herring (*Clupea harengus* L.). *ICES Journal of Marine Science*, vol 57, pp 903-10.
- [46] Glass, C.W., Wardle, C.S., Mojsiewicz, W.R. (1986). A light intensity threshold for schooling in the Atlantic mackerel, *Scomber scombrus*. *Journal of Fish Biology*, vol 29(suppl. A), pp 71-81.
- [47] Maunder, M.N., Punt, A.E. (2004). Standardizing catch and effort data: a review of recent approaches. *Fisheries Research*, vol 70, pp 141-59.

Performance measures (NR-Can)

1. Brief summary (1/2 page) of methodology – that can be taken directly from the Final Report.

This project utilized hydroacoustic data collected during five 24-hr mobile surveys and three long-term stationary deployments of a bottom-mounted echosounder at the FORCE test site (December 2017 – November 2019) to evaluate the scientific and operational utility of individual and integrated hydroacoustic survey methods. Mobile surveys were conducted across a series of standardized transects of the FORCE test site from a vessel using a downward facing, pole-mounted Simrad EK80 WBT echosounder with a 7° circular split-beam transducer (i.e., 120 kHz in narrowband continuous wave (CW) mode). Stationary surveys included the deployment of an upward-facing Simrad EK80 Wideband Autonomous Transceiver (WBAT) with a circular beam transducer (i.e., half-power beam angle of 7°; 120 kHz in narrowband CW mode), and a Nortek Signature 500 ADCP mounted on a Fundy Advanced Sonar Technology autonomous subsea platform (i.e., FAST-3) that was deployed at the FORCE test site. Data processing was conducted using Echoview® software (version 10.0; Myriax, Hobart, Australia) and consisted of calibration, noise removal (i.e., minimum volume backscatter: -70 dB re 1 m² m⁻³), data partitioning and echo integration. After processing, data were partitioned into bins, echo integrated, and exported for analyses. Analyses of mean volume backscatter (i.e., S_V – a rough index of fish density) or the area backscattering coefficient (i.e., s_a – the summation of backscatter values over a given layer in the water column; a complementary index of fish density) was conducted using the R statistical programming language (v3.6.2; R Core Team 2019). Analyses of mean S_V was used to assess spatial and temporal trends in water column backscatter, whereas analyses of s_a was used to assess the vertical distribution of backscatter through the water column. Spatial and temporal autocorrelation in the hydroacoustic data sets was assessed to determine the distance and time frame over which information from point measurements may be considered representative.

2. Key project achievements. These can be considered relevant to tidal development in general. eg. How your research has contributed to ‘reducing uncertainty and investment risk for TEC devices and how it has contributed to further advancing the tidal energy industry; and/or contributions to building the supply chain for the sector, that could lead to global market use; reducing GHGs; etc.

This project provided the first *in-situ* assessment of the relative performance of mobile (downward-facing) and stationary (upward-facing) echosounders for monitoring fish in high-flow environments. This project demonstrated the influence of high-flow environments on the ability of current hydroacoustic technologies to monitor interactions between fish and tidal energy turbines. Specifically, the primary achievements for this project include a deeper understanding of how dynamic forces in high flow environments (e.g., flow and bathymetry, turbulence and entrained air in the water column) combine to influence the efficacy of standard, commercially available, off-the-shelf hydroacoustic technologies for monitoring fish in areas where tidal power development are sought. This is crucial for understanding the limitations of current monitoring technologies and for quantifying the risk of tidal power development to marine animals. This project also highlighted the

importance of 24-hr collection of monitoring data to capture the variability of fish density present during different tidal phases and the influence of diel migration on fish distribution.

3. Where applicable, how the key project achievements led to benefits to project 'stakeholders' and to Canada. For any 'expected benefits', how these will be achieved in the coming years; Or other benefits to the wider tidal energy community?

The achievements of this project benefit project stakeholders and Canada by broadening our understanding of how to effectively monitor the potential environmental impacts of tidal energy turbines in dynamic marine environments. This helps to ensure the continued responsible development of the marine renewable energy sector in Canada by advancing our understanding of the risk posed to marine life. Moreover, this project helps advance monitoring capabilities and protocols, and assists in quantifying risks for the regulatory community.

4. # technology and/or knowledge products generated (this can include software development); or the overarching goal of an 'ocean forecasting system'

The knowledge gained includes a deeper understanding of how to effectively monitor for interactions between tidal energy turbines and marine animals. This in turn has implications for future monitoring efforts and protocols, data analyses and reporting procedures.

5. ID key operational issues or other barriers/challenges AND how they were resolved;

Staff turnover presented a challenge for this program. Specifically, the absence of continuity – from the inception of the project until completion – by a single principal investigator generated confusion about study objectives and timelines for those who were required to take on this project while it was already underway. This project also encountered challenges in human resources required for processing raw hydroacoustic data. This specific challenge was remedied by providing training opportunities for staff (HQP development) and prioritizing and allocating dedicated blocks of time for staff to process data for analyses.

6. Listing of 'knowledge dissemination' activities undertaken over the course of the project.

Project overviews were provided in FORCE's quarterly and annual reports to regulators that are made available to the public. Further, this project was included in overviews of the suite of monitoring activities undertaken at FORCE and presented at regional, national, and international meetings, symposia, and conferences.

7. If applicable, explain how the presence of federal, provincial, or municipal policies had an impact on your project? Or impact of current and forecasted energy and/or carbon prices?

8. # codes, standards, regulations, policies impacted/implemented?

The results of this work may alter the course of fish monitoring activities at the FORCE site. However, this needs to be weighed against the value of the data collected from mobile hydroacoustic surveys that FORCE has been conducting since 2016 before a determination can be made.

9. #IPs (licenses? patents? TMs) generated?

N/A

10. How is the project expected to continue over the next 5-year period? Eg. next steps for tech development, regulatory improvement, government involvement, market development, other? And

The results of this project may alter the course of FORCE's fish monitoring program. Specifically, future fish monitoring at FORCE may move away from mobile hydroacoustic surveys to multiple stationary platforms with upward looking echosounders to quantify interactions between marine animals and tidal energy turbines.

11. Potential for replication of project in coming years?

Given the results of this study, it is reasonable to expect that it will be replicated on a larger spatial scale to confirm the findings of this project and to help guide the future of fish monitoring activities at FORCE.

12. Total number HQPs (ID. Degree level, Total #months on project, Mitacs supported?)

Dr. Haley Viehman – PhD (36 months) – MITACS supported Post-doctoral fellow (Acadia University)

Dr. Dan Hasselman – PhD (18 months)

Tyler Boucher – BSc, Ocean Technologist diploma; Nova Scotia Community College (36 months)

Jessica Douglas – Ocean Technologist diploma; Nova Scotia Community College (20 months)

Milli Sanchez – BSc (8 months)

Jeremy Locke – MSc (4 months)

13. And the following **additional metrics where applicable.....**

	At the end of project	5 yrs after project end (predicted)	In the year 2030 (predicted)	In the year 2050 (predicted)
Annual direct GHG savings (if applicable)/	N/A	N/A	N/A	N/A
Annual indirect GHG savings (if applicable)/	N/A	N/A	N/A	N/A
Technology readiness level (TRL)/	Improved	N/A	N/A	N/A
Direct economic impact (if applicable)/	N/A	N/A	N/A	N/A
Indirect economic impact (if applicable)/	N/A	N/A	N/A	N/A
Direct employment full-time equivalent - FTE (male%, female %)/	2 (50%:50%)	2 (50%:50%)	N/A	N/A
Indirect employment full-time equivalent (FTE)/	N/A	N/A	N/A	N/A